30th International Conference on "Ore Potential of Alkaline, Kimberlite & Carbonatite Magmatism ABSTRACT BOOK

Ore Potential of Alkaline, Kimberlite & Carbonatite Magmatism

30th International Conference on "Ore Potential of Alkaline, Kimberlite and Carbonatite Magmatism"

29 September - 02 October 2014
Antalya - TURKEY

ABSTRACT BOOK

Editors
Assoc. Prof. Dr. Nurdane ILBEYLI & Prof. Dr. M. Gurhan YALCIN

30th International Conference on "Ore Potential of Alkaline, Kimberlite and Carbonatite Magmatism"

ABSTRACTS BOOK

29 September - 02 October 2014
Antalya - TURKEY

Editors
Assoc.Prof.Dr. Nurdane ILBEYLI and Prof.Dr. M. Gurhan YALCIN

550.4
30th International Conference on "Ore Potential of Alkaline, Kimberlite and Carbonatite Magmatism" Abstract Book
Akdeniz University-Antalya / UCTEA Chamber of Turkish Geological Engineers-Ankara / 2014

258 pages Figure, Table

Alkaline, Kimberlite, Carbonatite, Magmatism, Ore Potential, Diamond

ISBN:

Press:

HONORARY PRESIDENT

President – Akdeniz University, TURKEY
Prof.Dr. Israfil KURTCEPHE

ORGANIZING BOARD

Akdeniz University, TURKEY
Russian Academy of Sciences, RUSSIA
Ukraine Academy of Sciences, UKRAINE
UCTEA Chember of Turkish Geological Engineers, TURKEY

ORGANIZING COMMITTEE

Chairmen of the Organizing Committee
Assoc.Prof.Dr. Nurdane ILBEYLI Prof.Dr. M. Gurhan YALCIN

Co-Chairman of the Organizing Committee
Academician RAS Lia N. KOGARKO

Organizing & Social Secretariat
Lecturer Fusun YALCIN

Logistic Secretariat
Assist.Prof.Dr. Yasemin LEVENTELI

Assistant Secretariat
Res.Asst. Ebru PAKSU

Treasurer
Assoc.Prof.Dr. Burcu DEMIREL UTKU

Logo & Flyer Design
Assist.Prof.Dr. Mehmet DEMIRBILEK

Web Design
Res.Asst. Halil BOLUK

Members
Prof.Dr. Eugenii M. SHEREMET
Academician RAS Igor D. RYABCHIKOV
Prof. Dr. David R. LENTZ
Natalia V. SOROKHTINA
Vera N. ERMOLAEVA
Victor A. ZAITSEV

SCIENTIFIC COMMITTEE

Prof.Dr. Ercan ALDANMAZ	Kocaeli University
Prof.Dr. Mesut ANIL	Cukurova University
Assoc.Prof.Dr. Faruk AYDIN	Karadeniz Technical University
Assist.Prof.Dr. Metin BAGCI	Afyon Kocatepe University
Prof.Dr. A. Feyzi BINGOL	Firat University
Assoc.Prof.Dr. Emin CIFTCI	Istanbul Technical University
Prof.Dr. Ibrahim COPUROGLU	Nigde University
Vera N. ERMOLAEVA	GEOKHI RAS
Assoc.Prof.Dr. Murat HATIPOGLU	Dokuz Eylul University
Prof.Dr. Cahit HELVACI	Dokuz Eylul University
Prof.Dr. Yusuf Kagan KADIOGLU	Ankara University
Assoc.Prof.Dr. Leyla KALENDER	Firat University
Prof.Dr. Muazzez CELIK KARAKAYA	Selcuk University
Assoc.Prof.Dr. Abdullah KAYGUSUZ	Gumushane University
Prof.Dr. Yasar KIBICI	Dumlupinar University
Dr. Serpil KILIC	Akdeniz University
Academician RAS Lia N. KOGARKO	Russian Academy of Sciences
Prof. Dr. David R. LENTZ	University of New Brunswick
Prof.Dr. Halim MUTLU	Ankara University
Prof.Dr. Ayten OZTUFEKCI ONAL	Tunceli University
Prof.Dr. Yuksel ORGUN	Istanbul Technical University
Prof.Dr. Yahya OZPINAR	Pamukkale University
Prof.Dr. Osman PARLAK	Cukurova University
Academician RAS Igor D. RYABCHIKOV	IGEM RAS
Prof.Dr. Burhan SADIKLAR	Karadeniz Technical University
Prof.Dr. Ahmet SAGIROGLU	Firat University
Prof.Dr. Sabah YILMAZ SAHIN	Istanbul University
Assoc.Prof.Dr. Ender SARIFAKIOGLU	Gen. Dir. of Mineral Res. and Exp.
Prof.Dr. Kadir SARIIZ	Osmangazi University
Prof.Dr. Mehmet SENER	Nigde University
Prof.Dr. Eugenii M. SHEREMET	Ukrainian Academy of Sciences
Natalia V. SOROKHTINA	GEOKHI RAS
Prof.Dr. Abidin TEMEL	Hacettepe University
Prof.Dr. Taner UNLU	Ankara University
Assist.Prof.Dr. Yusuf URAS	Sutcu Imam University
Assoc.Prof.Dr. Ahmet YILDIZ	Afyon Kocatepe University
Victor A. ZAITSEV	GEOKHI RAS

PREFACE

In recent years, alkaline rocks have started to attract intensive attention in both academic and practical fields. These rocks are distinguished mostly by the abundance of alkaline minerals they contain rather than their other components. They generally represent magmatic rocks which contain sodium pyroxene, sodium amphibole or feldspathoid. Alkaline magmatic rocks are produced from magmas originating from the partial fusion of the upper mantle peridotites in different types and degrees. Their role in creating rich mineral deposits increased their significance. Diamond deposits in kimberlite pipes are one of the most important examples. Carbonatites are the latest products of differentiation processes of alkaline mafic (nepheline) or ultramafic (kimberlite) magmas and they may create essential deposits (Nb, Ta, Th, Cu and other metals in addition to nonmetallic minerals such as apatite, barite, fluorite, strontianite, phlogopite, REEs, vermiculite and baddeleyite).

The 30th international conference of "Ore Potential of Alkaline, Kimberlite and Carbonatite Magmatism", previous ones of which were held in different cities in Russia and Ukraine by Vernadsky Institute of Geochemistry and Analytical Chemistry every year since 1983, will be held in Antalya, Turkey this year.

22 country representatives from Algeria, Australia, Azerbaijan, Belarus, Brazil, Canada, China, Congo, Egypt, Georgia, Germany, Hungary, Iran, Kuwait, Poland, Russia, South Korea, Switzerland, Turkey, Ukraine, UK and USA are expected to participate in the conference. There are approximately 115 statements and posters sent from the participant countries. 42 of these works are verbal statements and the rest are poster presentations. The number of guests and participants are approximately 150. The active participation shows the success rate of the conference.

On the first three days of the conference, which will be held on 29 September – 02 October 2014, scientific presentations and posters will be presented and on the fourth day, there will be a technical trip to Antalya - Tekirova area. This book contains abstracts and/or indicative abstracts of the statements and posters which will be presented in 30th International Conference on "Ore Potential of Alkaline, Kimberlite and Carbonatite Magmatism" conference which is held by Akdeniz University, Faculty of Engineering, Department of Geological Engineering and supported by Chamber of Geological Engineers of Turkey. Talks and posters to be presented in the conference involves "genesis of alkaline magmatism; genesis of kimberlites and other ultrapotassic rocks; experimental data for petrogenesis of alkaline rocks; geochemistry, petrology and ore potential of alkaline-carbonatitic, mafic and ultramafic rocks and granitoids; mineralogy, crystalochemistry of alkaline rocks and carbonatites and others" and detailed information about the subjects can be found in this book. We wish that this abstract book contributes to international science community.

Assoc.Prof.Dr. Nurdane ILBEYLI
Chairman of the Organizing Committee

Prof.Dr. M. Gurhan YALCIN
Chairman of the Organizing Committee

TABLE OF CONTENTS

GEOCHEMISTRY OF OUED AMIZOUR IGNEOUS ROCKS (BEJAIA, EASTERN ALGERIA).

Abderrahmane H., Benali H.

Laboratory of Metallogeny and Magmatism of Algeria, Department of Geology, Faculty of Earth Sciences, USTHB.
abd.houria@gmail.com

The igneous rocks of Oued Amizour are part of the North African magmatic province which belongs to the Maghrebides chain, the south part of the peri-mediterranean alpine belt. A large Zn- Pb deposit lies in the calc-alcaline volcanic rocks of this region.

The orebody is hosted in andesites of the lower unit, and sometimes in the metasomatized dacitic unit.

The geochemical study of the major elements shows a very clear separation between the rocks of lower unit and those of higher unit. This geochemical discrimination of the volcanic rocks into two groups (lower unit and higher unit) is confirmed by the study of trace elements.

Rocks of Oued Amizour show series of calc-alkaline affinity and an implement in the volcanic arc and syn-collision environments. Normalized spiderdiagrammes in the primitive mantle have a very similar and typical overall look of orogenic calc-alkaline magmatism. They show negative anomalies in Ba, Ti and P and positive anomalies in Rb, Th and Zr. Spectra normalized REE chondrite show that all the studied rocks are enriched in light rare earth elements (LREE) relative to heavy rare earth elements (HREE). They are characterized by positive Eu anomalies characteristic of adakitic magmatism.

Keywords: Oued Amizour, volcanic rocks, calc-alkaline magmatism, (Zn-Pb) mineralization

MAFIC LAYERED COMPLEXES COEVAL TO FELSIC COMPLEXES IN THE LATEA METACRATON (HOGGAR ALGERIA):AN EXAMPLE OF ALLIOUM-IN AMERTEK-OUKCEM COMPLEXES IMPLICATIONS FOR POST-COLLISIONAL IGNEOUS EPISODES IN THE PANAFRICAN OROGEN

Azzouni-Sekkal A.,[1,2] Ikhlef-Debabha F.[2], Aïdrous-Belhocine K.[2], Bonin B.,[3] Liégeois J. P.[4]

1 FSNV-STU, Université Abou Bekr Belkaïd, BP 119, 13000 Tlemcen, Algérie
asazzouni@hotmail.com
2 FSTGAT, Laboratoire de métallogénie et magmatisme de l'Algérie, USTHB, BP 32, El Alia, 16111 Bab Ezzouar, Alger, Algérie.
3 CNRS-UPS UMR 8148 "IDES", Département des Sciences de la Terre, Université de Paris-Sud, 91405 Orsay Cedex, France
4 Section de Géologie Isotopique, Musée Royal de l'Afrique Centrale, B-3080 Tervuren, Belgique

Within the Tuareg Shield, the Central Hoggar (Fig. 1) composes the LATEA metacraton (Liégeois et al., 2003).It is made up of continental terranes displaying Archean and Paleoproterozoic formations, crosscut by Neoproterozoic igneous massifs. After the ~630 Ma climax of the Panafrican collision, strain partitioning developed along kilometre-thick intra-terrane and inter-terrane shear zones. During the post-collisional stage, dominantly calc-alkaline igneous suites form extensive batholiths, which were emplaced along intra-terrane shear zones and detachment faults. Later on up to the Cambrian, transcurrent movements along inter-terrane shear zones resulted into the current configuration. They constituted the preferential sites for emplacement of alkali-calcic to alkaline granitic complexes defining the "Taourirt" suite (Azzouni-Sekkal et al., 2003). We report here the characteristics of two mafic layered complexes associated with a felsic "Taourirt" complex rooted within the same shear zone .The mafic complexes, namely Allioum (Ikhlef-Debabha, 2011) and In Amertek, were emplaced on both sides of the inter-terrane shear zone bordering Tefedest and Azrou N'Fad terranes. Moreover, the In Amertek mafic complex yields intricate contacts with the Oukcem "Taourirt" felsic complex-(Aïdrous-Belhocine, 2010), illustrating that they are coeval. The Allioum complex is composed by a pile of mafic amphibole-rich adcumulates: olivine pyroxene gabbro, ferrogabbro, amphibole gabbro and leucogabbro from base to top, capped by leucogabbro, which is likely to represent the primary liquid. The In Amertek complex is composed of more evolved rocks: olivine norite and biotite amphibole gabbro cumulates, crosscut by amphibole gabbro, amphibole gabbrodiorite and granite dykes. All rocks are tholeiitic with Fenner effect (Fig.2). By comparison with the marginal facies of the Laouni complex (Cottin et al., 1998), which displays abundant ultramafic cumulates, it is suggested that Allioum and In Amertek complexes correspond to apical parts of more extensive layered ultramafic-mafic-complexes. The coeval Oukcem felsic complex comprises alkali-calcic monzogranite, syenogranite, and alkali feldspar granite. Liquid compositions plot along the alkaline – subalkaline boundary in the TAS diagram .Low contents

of Ni and Cr as well as low Mg # indicate that no liquid compositions correspond to primitive magmas. Identical behaviors of incompatible LILE, REE and HFSE, e.g., constant Ho/Y (0.036 ± 0.002) and Zr/Hf (43 ± 7, Fig.2) ratios in all rock types, whether they occur within Allioum, In Amertek, or Oukcem complexes, argue for a single igneous suite (Fig.3)evolving by fractional crystallization of a primary magma issued from a single homogeneous upper mantle source

References

1. Azzouni-Sekkal, A., Liégeois, J.P., Béchiri-Benmerzoug, F., Belaïdi-Zinet, S., Bonin, B., 2003. The "Taourirt" magmatic province, a marker of the closing stages of the Pan-African orogeny in the Tuareg shield: review of the available data and Sr-Nd isotop evidence: Journal of African Earth Sciences, v, 37, p337-350.
2. Liégeois, J.P., Latouche, L., Boughrara, M., Navez, J., Guiraud, M., 2003**.** The LATEA métacraton (dentral Hoggar, Tuareg sheild, Algeria): behaviour of an old passive margin during the Pan-African orogeny. Journal of Africa Earth Sciences 37, 161-190.
3. Cottin, J.Y., Lorand, J.P., Agrinier, P., Bodinier, J.L., Liégeois, J.P., 1998. Isotopic (O, Sr,Nd) trace element geochemistry of the Laouni layered intrusions (Pan African belt, Hoggar, Algeria): evidence for post-collisionnal continental tholeiitic magmas, variably contaminated by continental crust. Lithos 45, 197–222.

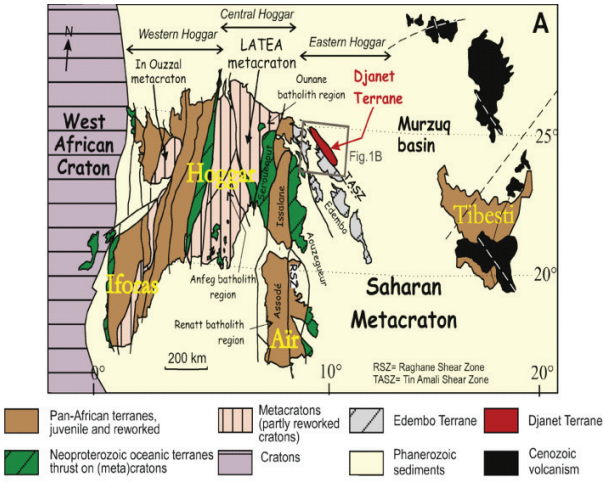

Figure 1: The different terranes of the Tuareg Shield (from Black et al., 1994; Liégeois et al, 2003);

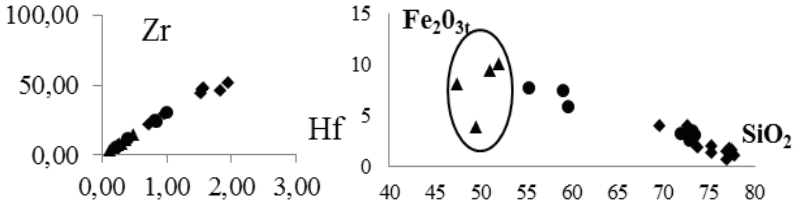

Figures 2.3: REE diagram normalized to chondrite (Taylor and Mc Lennan, 1985) for Allioum ,In Amertek mafic layered complexes and annular granitic complex of Oukcem Taourirt.

GEOCHEMICAL FEATURES OF ALKALINE MAGMATISM - RELATED FLOURITE DEPOSITS OF TURKEY

Altuncu S.,[1] Oztürk H.[2]

1 Nigde University, Department of Geological Engineering, Nigde-Turkey
saltuncu@nigde.edu.tr
2 Istanbul University, Department of Geological Engineering, Avcılar, 34320, Istanbul-Turkey

Fluorite deposits of Turkey are located mainly in Central Anatolian Crystalline Complex and its surroundings. These deposits are associated with carbonatite and alkaline magmatism and have been classified by Altuncu (2009) according to their geological settings.

Rare earth element (REE) contents of the deposits range between 30314 - 15 ppm. Average rare earth element contents of these deposits are as follows (ppm): Kızılcaören: 30314.1, Başören Kuluncak: 7469.32, Divriği: 2061.39, Keban: 553.74 , İsahocalı: 181.35, Bayındır: 179.67, Tad Deresi: 176.72 ppm, Akçakent: 152.43, Cangıllı 128.98, Yeşilyurt: 96.95, Pöhrenk: 41.85, Ovacık: 41.47 and Akkaya: 14.87 . Chondrite – normalised[1] REE patterns of the deposits are shown in Fig. 1.

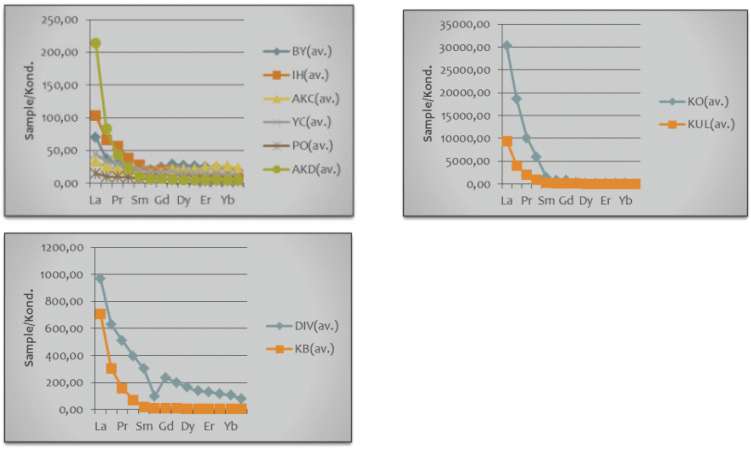

Figure 1: (a) Chondrite normalized REE patterns of Turkey fluorite deposits.

Element associations of the Kızılcaören and the Başören (Kuluncak) fluorite deposit consist of F+Ba+Th+REE+P+Ti+Nb+Ta+Cu+Mo+Sc+Be+Sr+W+Mn and F+Ba+Th+REE+P+Ti+Mn+Hf+Zr+Nb+Ta+Be, respectively. These two deposits show close relationship as geochemical character. Element associations of the Keban and Divriği flourite deposits consist of F+REE+Mg+K+Ba+ Sr+W+Mo+Cu+Pb+Zn +As+Bi+Ag+Tl+Se and F+REE+Cu+Bi+U+Sn+As+Sb+Ag+Be+Nb+Co, respectively. These two deposits are also reveals similar geochemical feature. Fluorite deposits of Kırşehir Massif, İsahocalı, Akçakent, Cangıllı, Bayındır and Tad Deresi are deplated as REE and incompatible trace elements especially as Nb+Ta+Eu+Hf+Th+Au. F and Si association is a typical feature for these deposits. Elemental association of the carbonate-hosted fluorite deposits are F+Ba+Si for the Yeşilyurt deposit whereas, F+Ba+Sr,

for the Akkaya, F+Si+Ba+Sr+Zr for the Pöhrenk and F+Ba+Sr for the Ovacık deposit. REE and the other incompatible trace element depletion is a typical feature for these deposits.

The studied fluorite deposits of Turkey occur in Anatolides related to post-collisional alkaline magmatism. The Kızılcaören, Başören (Kuluncak-Malatya), Keban and Divriği fluorite deposits with high amount of incompatible trace element, formed in a high temperature condition during volatile - rich phase of the alkaline intrusion. Bayındır, İsahocalı, Cangıllı, Akçakent and the Tad Deresi fluorite deposits formed by hydrothermal fluids with low temperature in a relatively shallow level as a fracture filling deposits with quartz. The Yeşilyurt, Akkaya, Pöhrenk and Ovacık deposits which occur in limestone, associated with hydrothermal replacement processes which are possibly related to an alkaline magmatic body, laying beneath the deposits.

Keywords: REE, Fluorite deposit, Geochemistry, Turkey

References

1. Boynton, W. V., 1984, Geochemistry of the rare earth elements: meteorite studies. In: Henderson, P., (ED). REE Geochemistry. Elsevier, pp. 63-114.(Amsterdam)

GRANITOIDS OF DIFFERENT GEOCHEMICAL TYPES OF BAIKAL AREA (RUSSIA), THEIR ORIGIN AND RARE METAL POTENTIAL

Antipin V.S., Gorlacheva N.V.

Vinogradov Institute of Geochemistry, Irkutsk, Russia
antipin@igc.irk.ru

Abundant Phanerozoic granitoids were derived within the geological structures located in the western and southern Baikal region. Their formation could be related to the Early Paleozoic collision stage and intraplate magmatism of the Late Paleozoic age of the geologic development of Baikal area. Comparative study of geological and isotope-geochemical features of the Early Paleozoic granitoids of Khamar-Daban Ridge and Olkhon region revealed their closeness in age and composition. Besides, they were referred to syncollision S-type formations derived from gneiss-schistose substratum of metamorphic sequences.

The following types of granitoids are mostly widespread in the Khamar-Daban magmatic province of the western part of Selenga-Vitim structure zone: (a) palingenic calc-alkaline granitoids (the Early Paleozoic Solzan massif, 513-516 Ma) [1], (b) subalkaline granitoids represented by a series from monzodiorite to monzonite, quartz syenite, and leucogranite (the Late Paleozoic massifs, 332 Ma) and (c) the Late Carboniferous granitoids are represented by large massifs, and intrusive-dike belts with intrusions and subvolcanic rocks of diverse compositional characteristics. The evolution of the granitoid magmatism proceeding results in the development of the rare-metal rocks united into the Urugudey-Utulik intrusive-dyke belt lying within the Precambrian metamorphic rocks. The rare-metal granitoids in Central Asia (Transbaikalia, Mongolia, Baikal area) of different ages (from the Late Carboniferous to the Cretaceous) occur in various structural zones among Precambrian and Hercynian metamorphic sequences. The rare-metal mineralization is ofen related to these series of magmatic rocks.

On the Olkhon Island (Baikal area) our field work was performed in three sizable massifs: Sharanur, Tashkiney, South-Western, as well as some small outcrops of granitoids. The granitoids of Olkhon region were classified into various geochemical types comprising formations of normal Na-alkalinity (migmatites and plagiogranites), calc-alkaline and subalkaline (K–Na granitoids, granosyenites and quartz syenites) and pegmatoid rare-metal granites. It is significant, that plagiomigmatites and plagiogranites in all elements repeat the shape of the chart of normalized contents marked for trend of K–Na granitoids, but at considerably lower level of concentrations of all elements. This general pattern of element distribution might indicate similar anatectic origin of both granitoid types, but from crustal substrata distinguished by composition and geochemical features. Melting of the Olkhon series rocks occurred at the late-collision stage of shear dislocations. The U-Pb dates obtained by SHRIMP-II indicate that the average age of central parts of magmatic zircons in K-Na calc-alkaline granitoids of the Sharanur complex equals to 505 Ma, and that of marginal part is 477 Ma [2]. The other researchers measured the age from granosyenites and quartz syenites of the Olkhon Island as 495±6 Ma [3], which is close in time of formation to K-Na Sharanur gtranitoids. Comparative geochemical analysis pointed out that the source of melts of the Early Paleozoic granitoids of the Sharanur and Khamar-Daban com-

plexes of the Baikal region could be the crustal substratum, which is obviously the criterion for their formation in the collisional geodynamic setting.

Using the Late Paleozoic subalkaline magmatism proceeding at the Khamar-Daban Range (Khonzurtay massif, 331.6 Ma) as an example, it was found that the formation of monzodiorite-syenite-leucogranite series was considerably contributed by the processes of hybridism and assimilation through mixing of the upper mantle basaltoid magma derived melts of granitic composition [4]. The involvement of the deep source is indicated by low Rb/Sr ratios and primary ratio $^{87}Sr/^{86}Sr$ (0.70592±0.00021) in rocks. Obtained data point to a profound contribution of the mantle magma to formation of intraplate syenite-leucogranite series in the middle part of the Khamar-Daban Range.

Rare-metal granite magmatism resulted in the formation of intrusive–dike belts comprising multiphase intrusions with exposed areas of approximately 10 km^2 and accompanying dikes, which are subvolcanic analogues of rare-metal granitoids. Rb-Sr formation age of granites is dated as 311-321 Ma. The early intrusive phases are made up of biotite granites (usually fluorite-bearing), which are changed during the late stage by typical rare-metal topaz-bearing amazonite–albite granites. In the subvolcanic facies, thick subalkaline dikes (monzonite porphyry, granite porphyry, and elvan) are followed by ongonite, topaz rhyolite, and topazite. The latter sometimes occurs as a cement in eruptive and fluid_explosive breccias. The development of multiphase intrusions from early biotite to late rare-metal granites with F-Li micas was accompanied by an increase in SiO_2 content and significant enrichment in Na_2O, whereas the FeO_{tot}, CaO, and K_2O contents declined. Geochemical evolution promoted an increase of F, Li, Rb, Cs, Sn, Be, Ta, and Pb and a decrease of Ba, Sr, Zn, Zr, Th, and U contents in rare-metal granites. The same evolution is common for subvolcanic rocks, which indicates the genetic relation of the entire intrusive-dike complex of the Khamar-Daban province.

To identify the indicator geochemical features of collision and intraplate granitoids the most typical varieties of the Early Paleozoic and Late Paleozoic magmatism of the Baikal region were compared. These were one type rocks with close petrographic and petrochemical characteristics. The diagram (Fig.1) presents data on the comparative geochemical analysis of granitoid rocks derived in geodynamic settings. It clearly displays that the rare-element composition of collision biotite granites and leucogranites is fairly close to the average composition of continental crust and only somewhat exceeds the average level of K, Rb, Ba, Pb, Th and U contents. The intraplate biotite granites and leucogranites with close petrochemistry and represented by rare-metal geochemical type of rocks are essentially enriched in Li, Rb, F, Sn, Nb and Ta. In contrast to the collisional leucogranites, their intraplate analogs are most highly enriched in Li, F, Sn and Ta, that reflects their formation from deeply differentiated residual magma. The Sn and W mineralization is associated with the intrusive-dyke belt of the Khamar-Daban region.

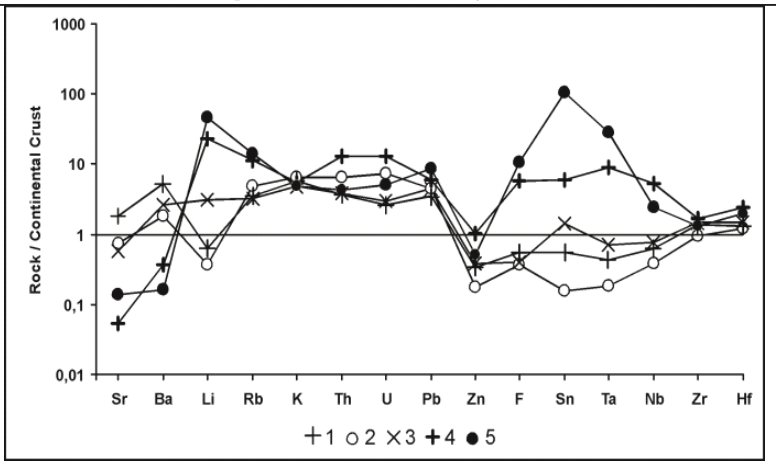

Figure 1: Spider diagram of rare-element distribution in granitoids of the Baikal region.Collisional granitoids: 1 - Bi granites, 2 - leucogranites (Olkhon Island), 3 - Bi granites (Khamar-Daban Range); intraplate granitoids: 4 - Bi-granites (Khamar-Daban Range), 5 - leucogranites (Khamar-Daban Range). Continental crust [6].

The obtained isotope characteristics of rare-metal granites of the Bitu-Dzhida massif (311 Ma), that is $^{87}Sr/^{86}Sr_{(t)}$ (0.705312-0.706187) agree with the model of formation of initial melts at the level of low horizons of continental crust. The substance of the lower crust could have the composition of biotite-bearing granulites rich in lithophyle rare elements. It is noteworthy, that the composition and isotope-geochemical features of the supposed magma-forming substratum correspond to the characteristics of the ancient Precambrian continental crust of the Southern Baikal region with the average model age T_{DM2}=1260 Ma. These conclusions agree with the results of preceding studies of rare-metal granites in the other regions of Central Asia [5].

This research was supported by the Integration project by SB RAS № 17 and Science School SS-5348.2014.5.

References

1. Makrygina V.A., Antipin V.S., Lepekhina E.N., Tolmacheva E.V., Gorlacheva N.V. Genetic features and primary data on U-Pb age of the Solzan granitoid massif, Khamar-Daban (Baikal region) // Doklady AN. 2013. v. 449. №2. pp. 210–214 (in Russian).
2. Antipin V.S., Gorlacheva N.V., Makrygina V.A. Geochemistry of the Early Paleozoic granitoids of the Baikal region and their geodynamic interpretation (Khamar-Danam Range, Olkhon Island*)* // Geology & Geophysics. 2014. v. 55. №2. pp. 228–243 (in Russian).
3. Gladkochub D.P., Donskaya T.V., Fedorovskiy V.S., Mazukabzov A.M., Larioniv A.N., Sergeev S.A. Olkhon metamorphic terrane of the Baikal region: Early Paleozoic composite of fragments of the Neo-Proterozoic active margin // Geology & Geophysics. 2010. v. 51. № 5. pp. 571–588 (in Russian).
4. Kazimirovskiy M.E. Mixing of melts and crystallization differentiation in the Early Carboniferous syenite magmas (Major Khamar-Daban). Geodynamic evolution of lithosphere of Central-Asian mobile belt (from ocean to continent). v. 1, Irkutsk, 2006, pp. 134-138 (in Russian).
5. Kovalenko V.I., Kostitsyn Yu.A., Yarmolyuk V.V. et al. (1999). Magma sources and isotope (Sr, Nd) evolution of rare-metal Li-F granites // Petrology. v. 7. № 4. pp. 401-429 (in Russian).
6. *McDonough W. F., Sun S.-s.* The composition of the Earth // Chemical Geology. 1995. V. 120: P. 223-253.

PETROGRAPHICAL AND GEOCHEMICAL PROPERTIES OF THE MAFIC (GABBROIC) ROCKS, (TURKEY, KINIK - KÜTAHYA)

Arat I., [1] **Yanık G.,**[1] **Kibici Y.,**[1] **Ilbeyli N.,**[3] **Ozkul C.**[1]

1 Dumlupinar University, Faculty of Engineering, Department of Geological Engineering, 43100 Kütahya-TURKEY

irem.arat@dpu.edu.tr
2 Akdeniz University, Faculty of Engineering, Department of Geological Engineering 07.058 Antalya -TURKİYE

The investigated area is the part of the Tavşanlı Zone. This area is located in the northern part of the Kütahya basin. The location is alingned between Torid-Anatolia Zone at the South and İzmir- Ankara Suture Zone at the north. Kınık (Kütahya) ophiolite units, located to the North of Kütahya, are composed mainly of peridotite, serpentinite, gabbro and diabase dyke. The mafic rock is gabbroic in composition and cumulate in texture. The mafic and ultramafic rocks broadly extend along the İzmir-Ankara Suture Zone.

The gabbroic rocks are both layered and massive stracture at the Kınık ophiolite. The lowest level begins with the layered gabbro at the bottom. It can be seen at the east and south-east of the Kınık (Kütahya) village. The gabbroic rocks are cut by diabasic dykes. Their widths vary from 30 cm to 1.5 meters. Plagioclase (labrador, bitownit), orthopyroxene, clinopyroxene and hornblende are the most common minerals in these rocks. Plagioclase minerals chracterize the main felsic compenent. Primary minerals such as orthopyroxene clinopyroxene, amphibole (hornblende), minor actinolite, tremolite characterize the mafic mineral association. Amphiboles have euhedral and subhedral crystals. The clinopyroxene phenocrysts are augite, aegirine-augite in composition and show pale to dark green pleochroism minor apatite, opaque minerals as primary minerals and as secondary minerals occur Kınık (Kütahya) gabbroic rocks due to the alteration such as uralitization, chloritization and carbonatization. These rocks may change into gray, grayish-green and less than black color.

Petrographical and geochemical features of these rocks show that the mafic and ultramafic rocks related to the co-magmatic differantiated tholeitic magma series. ***LIL*** elements (K, Sr, Rb, Ba) with the expection of Th show variable scatter because of ocean floor hydrothermal alteration, the ***HFSE*** (Nb; Ti, Zr, Y) and ***LREE*** (La, Ce, Nd) have been deplated relative to ***N-MORB***. The ratios of the selected trace elements (Ti/V, Zr/Y, Th/Y, Ti/Zr) and the tectonomagmatic discrimination diagrams for Ti-poor gabbros and dykes suggest that the Kınık gabbroic rocks is island arc tholeitic (***IAT***). Gabbros have high ***REE*** concentrations. This pattern is the typical of Supra -Subduction Zone (***SSZ***). The mafic-ultramafic rocks of the Kınık ophiolite were formed in the latest stages of island arc development in a supra subductional, back arc tectonic setting in the Neotethyan Ocean.

Keywords: Tavşanlı zone, Kınık Ophiolite, gabbro, geochemical features, tectonic setting. Supra-Subduction

DYKES IN THE NORTHEASTERN FENNOSCANDIAN SHIELD: A KEY FOR PALEOZOIC MAGMAS EMPLACEMENT AND ESTIMATION OF PRIMARY MANTLE MELTS COMPOSITION

Arzamastsev A. A.

Institute of Precambrian Geology and Geochronology, St. Petersburg, Russia
arzamas@ipgg.ru

The Kola part of the Fennoscandian Shield is a locus of dyke swarms among which the Proterozoic (PR) and Paleozoic (PZ) dykes are dominant. In order to systematize fragmentary information we collected available data on dyke position, geochronological age, petrography and geochemistry which are based on our own studies and were taken from reports of geological survey, scientific institutions and publications. The result is organized in a GIS form which contains data on 5740 dykes.

Trend analysis performed for dykes in different basement terrains in the Kola area, give evidence for the two main trends. The NW trending dykes are represented by PR dolerites and PZ alkaline lamprophyres, in which the former are dominant. NE trending dykes are exclusively PZ lamprophyres. These rocks are widespread throughout the whole Kola and northern Karelia and are spatially related to alkaline plutonic massifs. Within the Belomorian mobile belt and Kandalaksha Paleorift the Precambrian rocks are overcrowded by alkaline lamprophyres. By contrast, dolerite dykes in the Belomorian are uncommon. They are spread northwest off the Belomorian in the Pechenga - Imandra - Varzuga Paleorift, in the Keivy terrane and the Murmansk craton.

Geochronological data are sparse and show that dykes correlate the major episodes of igneous activity in the NE Fennoscandia. Almost all PZ dykes show the ages 388 - 362 Ma thus fitting the time span of the PZ alkaline and carbonatite intrusions (Kramm et al., 1993). Our recently obtained age determinations of the Kola (Tersky Coast) kimberlites yield the $^{40}Ar/^{39}Ar$ age 376.1±2 Ma. Similarly, north-trending dolerite dyke in the Pechenga area give the $^{40}Ar/^{39}Ar$ age 382±6 Ma. Combined with age determinations of PZ alkaline lamprophyres, which fall within the same time interval (Arzamastsev and Wu, 2014) these data give evidence for heterogeneous mantle sources for magmatism in the northeastern Fennoscandia which was initiated by the Paleozoic plume activity.

In order to calculate average weighted concentrations of trace elements we used geochemical data obtained from analyzing the samples of the main varieties of Paleozoic igneous rocks in the Kola region. Our petrochemical data set included 1070 analyzes for the Khibiny Massif, 280 analyzes for the Lovozero Massif, 360, for the carbonatite intrusions, 230 analyzes for the volcanic rocks of the Lovozero and Kontozero suites, and 350 analyzes for the Paleozoic dikes and diatremes. The mean contents of trace elements were calculated using 116 analyzes of the representative samples of rocks collected in the above mentioned sites. To improve the reliability of our estimate of the average composition of the alkaline-ultrabasic magma, we compared our average weighted composition of the alkaline-ultramafic intrusions with the compositions of the contemporaneous rocks of the province representing the most primitive mantle magmas.

The most probable candidates, compositionally resembling the primary magmas of the Kola

alkaline-ultramafic series, have been found in the Paleozoic volcanics and dikes, which were emplaced prior to and after the emplacement of the intrusions during a period of 405-360 Ma. We distinguished the following groups of rocks.

1. The alkaline-ultramafic volcanic rocks of the Lovozero and Kontozero suites, as the earliest manifestations of the Paleozoic volcanic activity in the region. The alkaline picrites and ankaramites show #mg = 0.72-0.81, Ni = 160-520 ppm, Cr = 143-1100 ppm, and Co = 21-100 ppm. Some samples were found to contain chrome diopside xenocrysts.

2. The olivine and pyroxene melteigite porphyry, found in the satellites of large carbonatite intrusions and emplaced during the main stage of magmatic activity. In spite of the extensive development of these rocks in different areas of the Kola Peninsula (Turiy Mys, Ivanovka, Ozernaya Varaka), the melteigite porphyry showed poor variations in the contents of major and trace elements. The melteigite porphyry samples yielded #mg = 67-76, Ni = 140-610 ppm, and Cr = 310-820 ppm.

3. The olivine melanephelinite dikes and diatremes are spread over the entire territory of the Kola Peninsula, commonly concentrating in the frames of the alkaline intrusions. Geological data suggest that they were emplaced during the terminal phase of magmatic activity. Most of the dikes are poorly differentiated, as indicated by the presence of xenoliths and xenocrysts of mantle origin, which could be preserved only under the condition of a relatively rapid rise of nephelinite magma from the zone of its generation. On this basis, the variety of olivine melanephelinite from the Namuaiv diatreme in the Khibiny Massif is comparable in terms of its Mg number and Ni and Cr contents with the most primitive magma.

Our calculated average weighted contents of rare earth elements in the primary ultramafic magmas of the Kola Province agree with the values reported for some varieties of the most primitive magmas of the region (Beard et al., 1998; Ivanikov et al., 1998; Rukhlov, 1997) and also with their mean contents in alkaline lamprophyres (Rock, 1987) and in the most primitive melanephelinite melts from other alkaline provinces (Le Bas, 1987; Rock, 1987). The results obtained for the other trace elements showed, as reported earlier (Kogarko, 1984), a significant enrichment of the mean composition of the Kola phonolite mantle magma in Nb, Ta, Zr, and Hf. At the same time no positive HFSE anomaly was found in the primitive alkaline-ultramafic magmas of the region. Comparison with the less differentiated rocks of the Meimecha-Kotui Province (Arndt et al., 1995, 1998) revealed that the distribution of trace elements in the Kola alkaline-ultramafic magmas resembled that in alkaline picrites and melanephelinites.

The study of the Paleozoic magmatism in the NE Fennoscandian Shield based on the geophysical and geochemical data and model calculations showed that:

(a) Primary magmas of the Kola Province could not be derived from the primitive (normal) mantle even at critically low melting degrees;

(b) Generation of alkaline magma at the PT conditions of spinel stability is highly improbable;

(c) Primitive magmas could be produced in the province as a result of the low melting degree of the rocks (0.3-0.5%), under the conditions of a garnet mantle depth, which enrichment was 3 times higher than the average contents of incompatible elements in primitive mantle;

(d) Also involved in melting were the mantle rocks with a composition of phlogopite-bearing (± amphibole) garnet lherzolite. *(Financially supported by RFBR grant 12-05-00244).*

BEHAVIOR OF ALKALI, ALKALI-EARTH AND RARE-EARTH ELEMENTS OF TRACHYBASALT-TRACHYDOLERITE AND TEPHRITE-TESCHENITE COMPLEXES OF KHOJAVEND TROUGH

Babayeva G.J., Mammadov M.N., Gasanguliyeva M.Y.

Institute of Geology and Geophysics of Azerbaijan National Academy of Sciences, Baku, Azerbaijan,
gultekin56@rambler.ru

Khojavend trough, being a part of Lok-Garabakh structural-formational zone, are located in the southern end of Agdam and in the north - Garabakh anticlinoria and has filled with Upper Jurassic and Cretaceous deposits.

The Upper Jurassic and Early Cretaceous deposits have distributed in the south-western margin and the north-western margin, but Upper Cretaceous volcanogenic and sedimentary complexes – in the axial zone of trough.

Lava-pyroclastic and subvolcanic facies of trachybasalt-trachydolerite complex relevant to early sub-stage of Santonian volcanism have localized along the south-western flange of the trough. Thin lava flows of trachybasalts are located among Early Santoinian limestones, Albian tuff-sandstones, tuff-conglomerates.

Volcanic centers have been confined to the intersection nodes of the transversal and longitudinal faults, around which volcanic breccias, different tuffs, trachybasalts have distributed. Subvolcanic formations in the form of small stock-shaped and power, as well as dyke-like bodies have been confined to linear zones and intersection nodes of the transversal and longitudinal faults.

Volcano-plutonic associations of tephrite-teschenite complex, characterizing Late Santonian development substage, have mainly developed in the axial zone of Khojavend trough. Tephrites' lava flows predominate among facial varieties of complex. Pyroclastic facies' rocks have located around volcanic centers.

Hypabyssal thin, sheet-like, laccolithic and stock-shaped teschenites have distributed among Turonian-Cenomanian limestones and Santonian tephrite flows. Dikes according to lava flows' strike have sub-latitudinal direction.

Petrographically the effusive-pyroclastic facies rocks of complex have composed of clinopyroxenic, clinopyroxene-analcime, plagioclase trachybasalts but in subvolcanic facies - trachydolerite.

Rocks of complex, being undersaturated with silica, belong to olivine-nephelinic normative type of subalkaline basaltoids, respectively.

Effusive-pyroclastic facies rocks of complex have been represented mainly by tephrite and in small amount by picrotephrite and leukotephrite (analcimite).

Picroteschenites, melano-, meso-, leukoteschenites distinguish from the bottom to top in the composition of hypabyssal differentiated intrusives. Indicated petrographic rocks types have

been cut by whitish-gray narrow veins (5-8 sm) of analcite syenites.

All rocks of tephrite-teschenite complex are olivine-normative as well.

Quantitative behavior of alkali, alkaline-earth and rare-earth elements in differentiates of trachybasalt-trachydolerite complex shows that light rare-earth elements predominate here. In this regard, La_n:Yb_n ratio (24-31) is characterized by relatively large value.

Complex's differentiates in intermediate magma chambers crystallized at volatile components loss. Therefore, crystallization of labradorite-bytownite plagioclase has occurred at relatively small lithostatic pressure whereby small maximum europium are observed in trends of REE (Rare-Earth Elements) distribution. Moreover, there is determined a compatible behavior for strontium (Kd>1). Other large-ionic elements (K, Ba, Rb) have mainly accumulated in the residual liquor. Early differentiates of tephrite-teschenite complex have also been enriched by light lanthanoids (La_n:Yb_n=23-29). However, intrusive complex rocks are appreciably depleted by lanthanum and therefore these elements ratio is reduced respectively (La_n:Yb_n=5,5-10,2).

Therefore, the revealed peculiarities of alkali, alkaline-earth and rare-earth elements behaviors show that primitive melts of the considered complexes have melted from single metasomatized amphibole-spinel peridotite.

Subalkaline olivine basalt (1-3%) melted from this substrate in the early stage. In the second stage - subalkaline picrite melt (7-10%).

RARE OCCURRENCE PLATINUM GROUP IN ESFANDAGH OPHIOLITE COMPLEX (SW OF KERMAN , IRAN)

Bagheriyan S.

Islamic Azad University, Tiran Branch, Tiran, Esfahan, 85318, I.R.Iran
siyamak.bagheriyan@gmail.com

In the Esfandagh ophiolite (south Iran) three sequences of deep mantle (homogenuse harzburgite), shallow mantle (harzburgite, dunite, orthopyroxenite, diabasic dyke) and cumulate sequence (dunite, wherlite, lehrzolite) has been recognized. the majority of the minerals of these rocks are orthopyroxen olivine and clinopyroxen and spinel. They consist of both massive and disseminated chromite. the esfandagh chromites and cumulate type and their host rocks are depleted peridotite. Which were formed in a morb environment. chromite deposits occur in 15 mineralizaed horizons. considering that some of the worid,s ophiolite complexes have worthwile resources of PGM, in addition to Cr, Ni and Co.

Some investigations and ore microscopy for identifying suifuric minerals , especially PGM, have been carried out.

So the resulte of these research, reveal the presence of PGM, in this region. PGM is found in two different parts : host rocks of the chromite deposits and also chromite lenses and layerd. The amount of PGM is very small (at most 103 ppb) and often exists the form of inclusion and fine grain in chromite and silicate gangue. As a result, the proposed models and related sampling of prospect area indicated to some potential of PGM mineralization in a close spatial association with hydrothemal systems

Keywords: PGM , Esfandaghe, ophiolite, mineralization, chromite.

A SELECTIVE AND EFFICIENT METHOD FOR THE ADSORPTION AND SEPARATION OF ARSENIC METAL ION FROM WASTE WATERS BY MAGNETIC SOLID-PHASE EXTRACTION WITH MODIFIED MAGNETIC NANOPARTICLES

Bagheriyan S.

Islamic Azad University, Tiran Branch, Tiran, Esfahan, 85318, I.R.Iran,
siyamak.bagheriyan@gmail.com

Widespread arsenic contamination of groundwater has led to a massive epidemic of arsenic poisoning in Bangladesh and neighboring countries. It is estimated that approximately 57 million people are drinking groundwater with arsenic concentrations elevated above the World Health Organization's standard of 10 parts per billion. Nanometer-sized materials have attracted substantial interest in the scientific community because of their special properties [1, 2]. These particles are super paramagnetic, which means that they are attracted to a magnetic field, but retain no residual magnetism after the field is removed. Moreover, these nanometer-sized metal oxides are not target-selective and are unsuitable for samples with complicated matrices [3].

In our work, silica coated magnetic nanoparticls, was chemically modified by aminopropyl groups and salicylaldehyde as a new solid phase extractant and this extractant was applied for preconcentration.

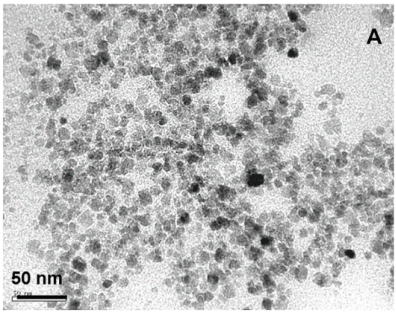

Figure 1: Right) SEM image of magnetite nanoparticles Left) Target advanced material

Under the optimal experimental conditions, The analytical curve was linear in the range 2–1000 µg/L and the detection limit was 0.18 ngr/ml and the relative standard deviation (R.S.D.) under optimum conditions was 1.98% (n = 10). Common coexisting ions did not interfere with the separation and determination of arsenic at pH 8. The sorbent exhibited excellent stability and its sorption capacity under optimum conditions has been found to be 11.7 mg of arsenic per gram of sorbent.

References

1. 1 J.P. Shukla, C.S. Kedari, J. Radioanal. Nucl. Chem. 207 (1996) 93.
2. 2 S. Mitra, Sample Preparation Techniques in Analytical Chemistry, John Wilely & Sons, Inc., Hoboken, New Jersey, 2003.
3. G.P. Rao, C. Lu, F.S. Su, Sep. Purif. Technol. 58 (2007) 224–231.

SINGULAR SYNERGISTIC EFFECTS OF EXPANDED NANOCLAY ON FLAME RETARDANT ABS/SB_2O_3/BROMINE HYBRID NANOCOMPOSITES

Bagheriyan S.

Islamic Azad University, Tiran Branch, Tiran, Esfahan, 85318, I.R.Iran,
siyamak.bagheriyan@gmail.com

It is frequently reported about the ability of polymer nanocomposites to give rise in a wide range of materials properties with the addition of only a small amount of nanofiller. Polymer matrix composite has an impressive and diverse range of applications [1, 2]. The advantages of composites over many metal alloys are dependent with the high flammability of many polymeric compounds, and consequently, improving the fire retardant behavior of polymers is a major challenge for extending their use to most applications [3].

ABS is a commercial material with relatively low cost and good mechanical properties, chemical resistance and easy processing characteristics. One of the main drawbacks of ABS is its inherent flammability [4], and therefore, there is a need to increase its thermal stability and flame retardant properties.

In this work, firstly antimony oxide nanoparticles and a novel of Schiff base halogenated compound have been synthesized and then synergistic effects between antimony oxide nanoparticles, halogenated flame retardant and expanded nanoclay were investigated carefully.

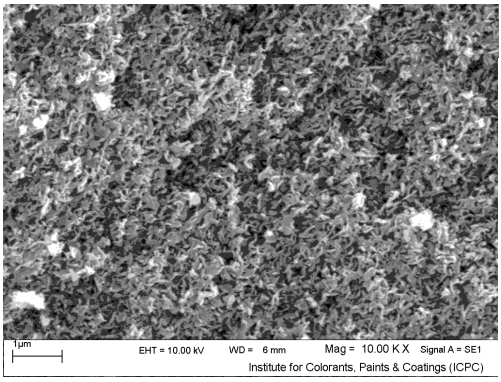

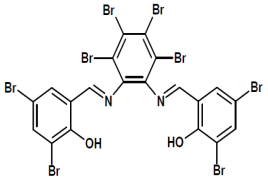

Figure 1: Left) SEM image of Sb_2O_3 nanoparticles, Right) Schiff base halogenated compound

Montmorillonite dispersion was characterized by X-ray diffraction (XRD) and transmission electron microscopy (TEM). Thermal stability and flammability properties were investigated by thermogravimetric analysis (TGA), cone calorimeter (CONE) tests and X-ray photoelectron spectroscopy (XPS) to evaluate the observed synergistic effects between nanoclay and a novel

intumescent flame retardant Sb_2O_3 in ABS nanocomposites.

The thermal decomposition of the ABS shifted towards higher temperature in the presence of the nanoparticles, montmorillonite and flame retardant additives. Improved thermal stability of composites with respect to the pure ABS can be assigned to partially altering molecular mobility of the polymer chains due to their adsorption on the surface of the montmorillonite and nanoparticles. Also, exfoliated fillers have significant barrier effect to slow down product volatilization and thermal transport during decomposition of the polymer, which assists composites with high thermal stability. Simultaneously, synergistic effect between Sb_2O_3 and halogenated flame retardant shows good improvement in thermal stability of ABS copolymer.

References

1. A. Das, KW. Stckelhuber, S. Rooj, DY. Wang, G. Heinrich, Raw Matherials and applications, 2010, 296-302.
2. Morgan AB., Wilkie CA , Flame Retardant Polymer nanocomposite Wiley Publishing CRC Press; 2007.
3. Bras ML, Wilkie CA, Bourbigot S. Fire Retardancy of Polymers. RSC 2005.
4. Dong D, Tasaka S, Aikawa S, Kamiya S, Inagaki N, Inoue Y. Thermal degradation of acrylonitrile-butadiene-styrene terpolymer in bean oil.Polym Degrad Stab 2001:73:319-326

MINERALIZATION OF QUADRANGLE OF ALIGODARZ ARIA (WEST OF IRAN) USING GEOMAGNETISM DATA OF SATELLITE IMAGES

Bagheriyan S.

Faculty of science, Tiran Branch, Islamic Azad University, Tiran, I.R. Iran,
siyamak.bagheriyan@gmail.com

The Aligodarz aria (west Iran) occupied west quadrangle of Golpayegan and located between sanandaj-sirjan zon and Zagros thrus. According to the magnetic date by using the magnetic countor maps (geomagnetic) of Golpayegan and Khoramabad (scale 1:250000) the analyzing of magnetic studding is done. So, the faults and folding are identified in the area according to the magnetic field attaching and its joining to the geology maps of the area. According to the geomagnetic finding 5 magor faults are identified which literally most of the mineralization area is mines, and deposit are taken placed by the view of the three faults of these tectonical structures. By attaching the satellite pictures and geomagnetic results by the using of RGB decomposition, 2, 4, 7, bands and geomagnetic country lines, the lines which involve the geomagnetic lines are identified and evaluated in the point view of mineralization.

Keywords: Mineralization, Aligodarz, ggeomagnetism, magnetic data

RARE OCCURRENCE PLATINUM GROUP IN ESFANDAGH OPHIOLITE COMPLEX (SW OF KERMAN , IRAN)

Bagheriyan S.

Faculty of science, Tiran Branch, Islamic Azad University, Tiran, I.R. Iran,
siyamak.bagheriyan@gmail.com

In the Esfandagh ophiolite (south Iran) three sequences of deep mantle (homogenuse harzburgite), shallow mantle (harzburgite, dunite, orthopyroxenite, diabasic dyke) and cumulate sequence (dunite, wherlite, lehrzolite) has been recognized. the majority of the minerals of these rocks are orthopyroxen olivine and clinopyroxen and spinel. They consist of both massive and disseminated chromite. the esfandagh chromites and cumulate type and their host rocks are depleted peridotite. Which were formed in a morb environment. chromite deposits occur in 15 mineralizaed horizons. considering that some of the worid›s ophiolite complexes have worthwile resources of PGM, in addition to Cr, Ni and Co.

Some investigations and ore microscopy for identifying suifuric minerals , especially PGM, have been carried out.

So the resulte of these research, reveal the presence of PGM, in this region. PGM is found in two different parts : host rocks of the chromite deposits and also chromite lenses and layerd. The amount of PGM is very small (at most 103 ppb) and often exists the form of inclusion and fine grain in chromite and silicate gangue. As a result, the proposed models and related sampling of prospect area indicated to some potential of PGM mineralization in a close spatial association with hydrothemal systems

Keywords: PGM , Esfandaghe, ophiolite, mineralization, chromite.

RARE OCCURRENCE PLATINUM GROUP IN ESFANDAGH OPHIOLITE COMPLEX (SW OF KERMAN , IRAN)

Bagheriyan S.

Faculty of science, Tiran Branch, Islamic Azad University, Tiran, I.R. Iran,
siyamak.bagheriyan@gmail.com

In the Esfandagh ophiolite (south Iran) three sequences of deep mantle (homogenuse harzburgite), shallow mantle (harzburgite, dunite, orthopyroxenite, diabasic dyke) and cumulate sequence (dunite, wherlite, lehrzolite) has been recognized. the majority of the minerals of these rocks are orthopyroxen olivine and clinopyroxen and spinel. They consist of both massive and disseminated chromite. the esfandagh chromites and cumulate type and their host rocks are depleted peridotite. Which were formed in a morb environment. chromite deposits occur in 15 mineralizaed horizons. considering that some of the worid›s ophiolite complexes have worthwile resources of PGM, in addition to Cr, Ni and Co.

Some investigations and ore microscopy for identifying suifuric minerals , especially PGM, have been carried out.

So the resulte of these research, reveal the presence of PGM, in this region. PGM is found in two different parts : host rocks of the chromite deposits and also chromite lenses and layerd. The amount of PGM is very small (at most 103 ppb) and often exists the form of inclusion and fine grain in chromite and silicate gangue. As a result, the proposed models and related sampling of prospect area indicated to some potential of PGM mineralization in a close spatial association with hydrothemal systems

Keywords: PGM , Esfandaghe, ophiolite, mineralization, chromite.

PARENTAL MELTS FROM METASOMATISED MANTLE SOURCE: CAMPTONITES IN THE DITRĂU ALKALINE MASSIF, ROMANIA

Batki A.[1], Pál-Molnár E.[1,2]

1 MTA-ELTE Volcanology Research Group, Budapest, Hungary
batki@geo.u-szeged.hu
2 Department of Mineralogy, Geochemistry and Petrology, University of Szeged, Szeged, Hungary

Camptonite dykes intrude the rift-related Mesozoic igneous body of the Ditrău Alkaline Massif, Eastern Carpathians, Romania. We present and discuss trace and rare earth element data, and the Nd isotopic compositions of the dykes in order to define the nature of their mantle source.

The Ditrău camptonites compositionally resemble basanites and trachy-basalts, and are significantly enriched in volatile elements (H_2O, CO_2), in LILE and in LREE. The small variation in trace and REE characteristics implies that the Ditrău camptonites are formed by variable degrees of partial melting of the same mantle source [1]. The depletion of Y and the HREE and the primitive mantle-normalised Sm/Yb ratios (2.1 and 4.9) in the camptonites are consistent with a garnet-bearing source region [1]. High concentrations of incompatible elements indicate a metasomatised mantle source previously enriched in LILE and HFSE [e.g. 2]. In general, a relative depletion in Nb, Ta and/or Ti is typical of arc rocks; therefore, the absence of a significant Nb–Ta negative anomaly in the Ditrău camptonites means that a subduction component was not involved in the enrichment process of the source region [1]. However, mantle metasomatism has also been attributed to partial melts and/or metasomatic fluids that migrate from the asthenospheric mantle and freeze in thin zones within the mechanical boundary layer of the continental lithosphere for long periods of geological time [3]. Re-melting of the metasomatic zone, consisting of veins enriched in volatiles and incompatible elements hybridised with variable amounts of partial melts from their less enriched peridotite wall rock, can produce alkaline magmas [e.g. 4]. Partial melting of the phlogopite-bearing mantle would generate potassic magmas with $K_2O/Na_2O>1$ [5]. High Na/K ratios of the Ditrău camptonites suggest that the metasomatic mineral in the source region was rather amphibole than phlogopite. The presence of pargasitic amphibole in the source region can account for the high Nb–Ta concentrations observed in the studied camptonites [1] since the Nb/Ta ratio in the melt is controlled by amphibole during melting, as shown by Tiepolo et al. [6].

The extremely low Zr/Hf ratio (21.0–32.2) and the positive correlation of Zr/Nb with the Zr concentration (also) indicates an enrichment process which could be produced if a constant amount of Nb is added to the variably depleted source region [7]. The low Zr/Nb ratio (0.7–5.3) confirms the strong enrichment of incompatible trace elements. High initial $^{143}Nd/^{144}Nd$ ratios (ε_{Nd} values of +4.0 to +6.1) of the Ditrău camptonites indicate that the analysed camptonite has experienced time-integrated enrichment in Sm or loss of Nd, relative to CHUR [8].

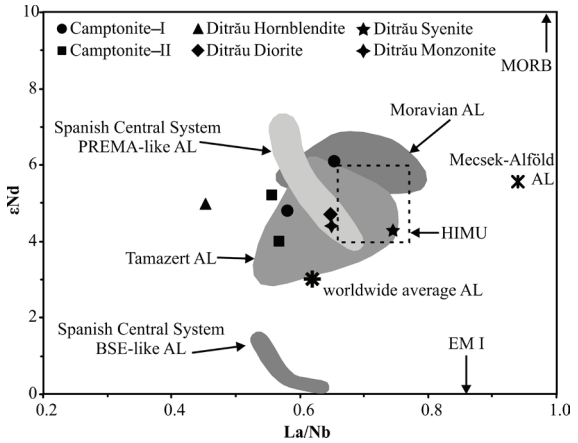

Figure 1: ε_{Nd} vs La/Nb for the Ditrău camptonites and other igneous rocks from the massif. Initial ε_{Nd} is calculated at the age of 200 Ma. Alkaline lamprophyres (AL) from Moravia [11, 12], Spanish Central System [13], Tamazert Complex [14], Mecsek-Alföld Igneous Field [12] and the worldwide average given by [8] shown for comparison as well as fields for HIMU, MORB and EM I [9, 10].

Figure 1 shows the initial ε_{Nd} values vs La/Nb ratios of the camptonites and other igneous rocks from the Ditrău Alkaline Massif, together with fields for HIMU [9, 10], alkaline lamprophyres from Moravia [11, 12], the Spanish Central System [13], the Tamazert Complex [14], the Mecsek-Alföld Igneous Field [12] and the worldwide average [8] for comparison. Ditrău camptonites are within or plot near to the fields of the alkaline lamprophyres from Moravia, the Tamazert alkaline complex and the Spanish Central System (group of PREMA-like dykes). Camptonites from the Spanish Central System are differentiated into an isotopically depleted (PREMA-like) and an isotopically enriched (BSE-like) groups [13]. The depleted isotopic signatures have been interpreted with the involvement of a sub-lithospheric source (probably asthenospheric-related) and the enriched isotopic compositions have been explained by participation of a lithospheric mantle. The close similarity to the isotopically depleted Spanish lamprophyres suggests a sub-lithospheric mantle source for the Ditrău camptonites as well. In the source region of the Moravian, Mecsek-Alföld and Tamazert lamprophyres, the HIMU OIB mantle component has been identified [11, 12 and 14]. Ditrău camptonites fall near to the field of the HIMU OIB mantle component, as well as the alkaline lamprophyres mentioned above, proposing that a HIMU-type mantle source was involved in the generation of the studied lamprophyres which is consistent with a sub-lithospheric–asthenospheric origin. The relatively homogeneous Nd isotopic compositions with slight differences can also be compatible with variable partial melting of a homogeneous mantle source as suggested by [14]. REE and Nd isotopic compositional fields for camptonite–I and camptonite–II overlap (Fig. 1), inferring that they were generated from similar mafic alkaline magma batches of the metasomatised zone in the mantle source with only slight differences in their modal mineralogy [13].

In the north-western part of the Ditrău Alkaline Massif, small ultramafic to mafic bodies occur, consisting of kaersutite peridotite, olivine hornblendite, hornblendite and gabbro. The mineral composition and chemistry of hornblendites and gabbros strongly resemble the studied camptonites [15, 16]. The ultramafic and mafic rocks are inferred to represent cumulates [15, 16] and were derived through fractional crystallisation from a basanitic parental magma [15]. Based on

the trace element, REE and Nd isotopic data (Fig. 1), in conjunction with the petrographic and mineral chemical evidence, the ultramafic and mafic bodies in the Ditrău Alkaline Massif are interpreted, with the studied camptonites, as a suite of co-magmatic and co-genetic rocks. The Ditrău lamprophyres represent the only basic melt that penetrated throughout the massif and are in close magmatic and genetic relation with the ultramafic and mafic rocks, and, as such, they are defined as parental melts to the igneous body of the Ditrău Alkaline Massif.

References

1. Batki A., Pál-Molnár E., Dobosi G., Skelton A., 2014. Petrogenetic significance of ocellar camptonite dykes in the Ditrău Alkaline Massif, Romania. Lithos. DOI: 10.1016/j.lithos.2014.04.022
2. Bouabdli A., Dupuy C., Dostal J., 1988. Geochemistry of Mesozoic alkaline lamprophyres and related rocks from the Tamazert massif, High Atlas (Morocco). Lithos 22, 43-58.
3. McKenzie D., 1989. Some remarks on the movement of small melt fractions in the mantle. Earth and Planetary Science Letters 95, 53-72.
4. Foley S., 1992. Vein-plus-wall-rock melting mechanisms in the lithosphere and the origin of potassic alkaline magmas. Lithos 28, 435-453.
5. Wilson M., Downes H., 1991. Tertiary-Quaternary extension-related alkaline magmatism in Western and Central Europe. Journal of Petrology 32, 811-849.
6. Tiepolo M., Vannucci R., Oberti R., Foley S.F., Bottazzi P., Zanetti A., 2000. Nb and Ta incorporation and fractionation in titanian pargasite and kaersutite: crystal-chemical constraints and implications for natural systems. Earth and Planetary Science Letters 176, 185-201.
7. Weyer S., Münker C., Mezger K., 2003. Nb/Ta, Zr/Hf and REE in the depleted mantle: implication for the differentiation history of the crust-mantle system. Earth and Planetary Science Letters 205, 309-324.
8. Rock N.M.S., 1991. Lamprophyres. Blackie and Son, Glasgow.
9. Zindler, A., Hart, S.R., 1986. Chemical geodynamics. Annual Review of Earth and Planetary Sciences 14, 493-571.
10. Weaver, B.L., 1991. The origin of ocean-island basalt end-member compositions: trace element and isotopic constrains. Earth and Planetary Science Letters 104, 381-397.
11. Dostal, J., Owen, J.V., 1998. Cretaceous alkaline lamprophyres from northeastern Czech Republic: geochemistry and petrogenesis. Geol Rundsch 87, 67-77.
12. Harangi, Sz., Tonarini, S., Vaselli, O., Manetti, P., 2003. Geochemistry and petrogenesis of Early Cretaceous alkaline igneous rocks in Central Europe: implications for a long-lived EAR-type mantle component beneath Europe. Acta Geologica Hungarica 46/1, 77-94.
13. Orejana, D., Villaseca, C., Billström, K., Paterson, B.A., 2008. Petrogenesis of Permian alkaline lamprophyres and diabases from the Spanish Central System and their geodynamic context within western Europe. Contributions to Mineralogy and Petrology 156/4, 477-500.
14. Bernard-Griffiths, J., Fourcade, S., Dupuy, C., 1991. Isotopic study (Sr, Nd, O and C) of lamprophyres and associated dykes from Tamazert (Morocco): crustal contamination processes and source characteristics. Earth and Planetary Science Letters 103, 190-199.
15. Morogan, V., Upton, B.G.J., Fitton J.G., 2000. The petrology of the Ditrău alkaline complex, Eastern Carpathians. Mineralogy and Petrology 69, 227-265.
16. Pál-Molnár, E., 2000. Hornblendites and diorites of the Ditrău Syenite Massif. Department of Mineralogy, Geochemistry and Petrology, University of Szeged, (Ed.), Szeged.

AGES AND SOURCES OF ALKALINE AND CARBONATITE COMPLEXES IN THE N-E PART OF THE FENNOSCANDIAN SHIELD

Bayanova T.B., Mitrofanov F.P., Serov P.A., Elizarov D.B., Nitkina E.A.

T.B. Bayanova Geological Institute of the Kola Science Centre RAS, Apatity, Russia, tamara@geoksc.apatity.ru

Alkaline complexes with carbonatites a widespread in the N-E part of the Fennoscandian Shield. The oldest massifs of alkaline granites and sienites are known in Keivy terrane - Belay Tundra, Zapadno-Keivsky, Saharjok, Ponoisky et set. with neoarhaean U-Pb ages on zircon from 2.67 – 2.61 Ga [1]. New isotope U-Pb data on zircon have been obtained for albite syenite of Panaavrsky massif and eugerin –auvgite granosyenite and Mt. Sylngyraz in Murmansk domene with neoarhaean ages from 2.67-2.65 Ga [8]. In the Central-Kola arhaean domene alkaline granite of Kanozersky massif gave U-Pb age on zircon egials 2.68 Ga [5]. The neoarchaean times have carbonatites of Siilinjarvy (Finland) yielded U-Pb ages on zircon and baddeleyite 2.61 Ga [9, 1].

Isotope-geochemical data for all alkaline and carbonatites rocks with neoarchaean ages including REE, isotope values ε_{Nd} - I_{Sr} on WR and $^{3}He/^{4}He$ investigations rock-forming minerals permit suggested the origin of magmatism such type (EM-2) of enriched mantle reservoir according to [10, 11]. For reconstruction of crustal evolution and orogenic events of neoarhaean time with alkaline and carbonatite magmatism are proposed formation of Kenorland Supercontinent [4] and ultraplate plume geodynamics.

In Paleoproterozoic time in frame in the N-E part of Fennoscandian Shield there are a lot of alkaline and carbonatites massifs with U-Pb ages on zircon and baddeleyite in interval 1.91-1.99 Ga. The main of them is potential Gremaysha-Virmes Complex in the Central-Kola Arhaean domene with 1.98 Ga. New U-Pb age on zircon and baddeleyite from carbonatite Tiksheozero massif in Karelia region have been obtained with 1999±5 Ma [2]. The same isotope ages of Kortejarvi and Laivajoki carbonatites are characterized by in Finland [6]. New results for two magmatic massifs in Murmansk domene (Elvan and Spiridon-Ty) considered as peridotite-shonkinite series have been measured on zircon with 1.58 and 1.67 Ga. Modes Sm-Nd ages of the rocks have 2.42-2.62 Ga for protolith with negative ε_{Nd} values (from -8.91 to -12.40). All $\varepsilon_{Nd} - \varepsilon_{Sr}$ isotope data are presented in (Fig 1.) together with Paleoproterozoic Tiksheozero and Gremaysha-Virmes Complex and reflect enriched mantle reservoir for the peridotite-shonkinite series [7].

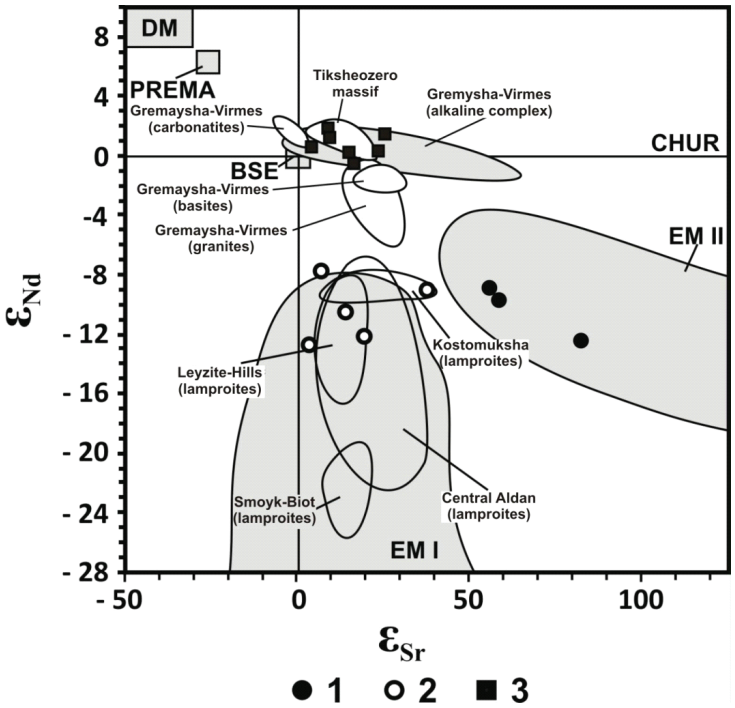

Figure 1: Isotope $\varepsilon_{Nd} - I_{Sr}$ values for alkaline rocks of Murmansk neoarhaean domene (from Petrovsky et al., 2014). 1 – peridotite-shonkinite series, 2 – lamproites and leuzitites, 3 – alkaline-ultramafic rocks of Iokanga massifs in Murmansk domene.

In Paleozoic time the main epoch of economically most important massifs were formation from 382-347 Ma [3]. Alkaline magmatism are characterized by variety of composition from kimberlites and carbonatites to agpaitic nepheline syenites and dyke complexes and in frame in $\varepsilon_{Nd} - I_{Sr}$ diagram reflects DM or HIMU reservoir. Most isotope Rb-Sr data has shown very radioactive initial I_{Sr} ($^{87}Sr/^{86}Sr$) ratios for the rocks.

Thus alkaline and carbonatites magmatism in the N-E part of Fennoscandian Shield has development from Neoarhaean to Paleozoic time and were active from EM-1, EM-2, DM and HIMU mantle reservoirs.

The studies are supported by RFBR 13-05-00493, OFI-M 13-05-12055, IGCP-SIDA 599, Department of Earth Sciences, Programs N 2 and 4.

References

1. Bayanova T.B., 2006. Baddeleyite: A Promising Geochronometer for Alkaline and Basic Magmatism. Petrology v. 14, p. 187-200.
2. Corfu F., Bayanova T., Shchiptsov V., Frantz N., 2011. A U-Pb ID-TIMS age of the Tiksheozero carbonatite: expression of 2.0 Ga alkaline magmatism in Karelia, Russia. Central European Journal of Geosciences, p.302-308.
3. Kogarko L.N., Kononova V.A., Orlova M.P., Woolley A. R., 1995. Alkaline Rocks and Carbonatites of the World. Part 2: Former USSR. Chapman and Hall, London.

4. Lubnina N.V., 2009. Earst-European craton from Neoarhean to Paleozoic time on paleomagnetic data. Abstract of doctoral dissertation. Moscow, 41 p.
5. Nitkina E.A., Apanasevich E.A., Bayanova T.B., 2004. Geochronological evidence of the complex nature of the Archaean Kanozero alkaline granites, Baltic Shield (Russia). Abstracts and Program Goldschmidt Conference Copenhagen, Denmark. June 5-11 2004. Geochimica et Cosmochimica. Acta. P. A720.
6. Nykanen J., Laajoki K., Karhu J., 1997. Geology and geochemistry of the early Proterozoic Kortejarvi and Laivajoki carbonatites, central Fennoscandian Shield, Finland. Bull. Geol. Soc. Finland v. 69, p. 5-30.
7. Petrovsky M.N., Bayanova T.B., Petrovskaya L.S., Bazai I.V., 2014. Mezoproterozoic peridotite-shonkinite series – new type of untraplate magmatism of Kola alkaline province. Doklady Earth Sciences (in press).
8. Petrovsky M.N., Mitrofanov F.P., Petrovskaya L.S., Bayanova T.B., 2009. New massif of archean alkaline syenites in the Murmansk domain of the Kola Peninsula. Doklady Earth Sciences v. 424, N 1, p. 77-81.
9. Puustinen K., 1971. Geology of the Siilinjarvi carbonatite complex, Eastern Finland. Bull. Comm. Geol. Finlande, v. 249, p. 1-43.
10. Zozulya D.R., Bayanova T.B., Eby G.N., 2005. Geology and Age of the Late Archean Keivy Alkaline Province, northeastern Baltic Shield. J. Geol. v. 113, p. 601-608.
11. Zozulya D.R., Bayanova T.B., Serov P.N., 2007. Age and Isotopic Geochemical haracteristics of Archean Carbonatites and Alkaline Rocks of the Baltic Shield. Doklady Earth Sciences v. 415, N 6, p. 874–879.

APPLICATION OF LOCAL CATALYSTS FOR CATALYTIC PROCESSES

Bentahar N.[1], Otmanine G.[2] Mimoun H.[2],

1 Département of physical, Faculty of Science M'hamed Bougara University, Boumerdes , Avenue de l'Indépendance – Algeria
2 Department of the chemical and pharmaceutical processes, Faculty of hydrocarbons and chemistry, M'hamed Bougara University, Boumerdes , Avenue de l'Indépendance – Algeria

Solid catalysts for petroleum refining and catalytic transformations have been developed starting from local Algerian materials, mainly "bentonite". These catalysts are used for the transformation of the heavy fractions and the residues of the oil by the catalytic processes leading to obtaining clean and environmentally friendly petrol (fuel) as well as petroleum fractions that are considered as important raw materials for petrochemical, pharmaceutical, and cosmetic industry. The preparation of modified catalysts using Algerian local bentonite enriched by oxides to give them a better performance for the validation of certain fractions of oil and condensate is described.

Introduction

Heterogeneous catalysis has considerably influenced the refining and petrochemical industries. The 30s of the 20th century have seen the development of three main types of processes, which were intended for primary refining, namely the catalytic cracking, alkylation and dehydrogenation. This is also valid for other important industrial process named the Fischer-Tropsch process using Co / Fe catalysts which converts coal into synthetic gas that is processed into cuts C5-C11-rich olefins and paraffins. This method is widely used in Japan, Germany and South Africa.

Nowadays heterogeneous catalysis dominates and determines the great advances in refining and petrochemical industries. It is noted that the sales of catalysts for refineries reached $ 2.7 billions in 2005 with an annual increase of 3.24% and still in progress. Taken together, the industrial catalysts are the heart of the refining processes and they determine their future. The catalytic processes are increasingly developing and the discovery of new catalysts still represents urgent need.

Heterogeneous catalysis or contact catalysis is to achieve a transformation of liquid or gaseous reagents by using a solid catalyst; the chemical process takes place at solid-fluid interface by adsorption of reagents at specific sites of the solid surface, which are capable of contracting with reactive chemical bonds more or less strong. The adsorbed species are better and strongly formed if the catalyst is properly selected for the desired reaction according to the Sabatier principle. Therefore the introduction of surface atoms or ions plays an important role. In the present work, the preparation of modified catalysts using Algerian local bentonite enriched by oxides to give them a better performance for the validation of certain fractions of oil and condensate is described [1].

Different stages of the catalytic cycle

The reaction taking place not in the whole volume of the fluid, but only at the solid-fluid interface, the formation of adsorbed species involves carriage of active molecules to the surface followed by adsorption. The surface reaction gives products followed by desorption from the

catalytic surface, then migration into the fluid. Thus we can say that a catalytic cycle takes place in the following steps:

- Transfer of reagents to the solid surface.
- Adsorption of reactants on the catalyst.
- Interaction between reactants adsorbed to the surface.
- Desorption of products from the catalytic surface.
- Transfer of products leaving the catalyst.

The importance of the catalytic processes and needs to refining are constantly changing as more and more oil is processed into fine products: fuels, base for petrochemicals, lubricants. The transport industry plays a leading role in this development: the steady progress of processes and catalysts. Due to environmental reasons, changes in fuel specifications are becoming severe challenge. In terms of processes and catalysts, the applications are shown in Table 1:

Table 1: Employment of catalysts in refining

Objective	***Processes involved***	***Targets***
Purify expenses and income	Hydrotreating	Reduction of sulfur, nitrogen, metals and asphaltens
Convert residues	Hydroconversion of vacuum residue and FCC and hydrocraking	Catalysts more active and selective in reducing their production costs
Improving the quality of products (petrol, diesel)	Catalytic reforming, FCC Increases cetane NAME NOR Reduction of benzene, sulfur, nitrogen and aromatics	A cetane NAME NOR Reduction of benzene, sulfur, nitrogen and aromatics
Lower investment and operating costs	All the existing processes, mainly hydrocracking and hydroconversions of residues	Reduced operating pressure, increased activity, selectivity and lifetime of catalyst
Improving existing processes	FCC and downstream processes Aliphatic alkylation	New catalysts decyclization of naphthenes and aromatic-naphthenics
Control emissions and reduce emissions	Claus process, purification of effluents, fumes and thermal FCC	increased sulfur recovery and conversion of SO_x and NO_x Reduced emissions of particulate
Producing Hydrogen	Partial oxidation of residues Steam reforming gas	Reduce soot, Reduce temperature, Increasing selectivity H_2

We can say that the overall objective of the use of catalysts is to produce quality products at lower cost through technologies and processes leading to emissions and discharges with minimum harmfulness

Preparation of Solid Catalysts

There are different protocols for the preparation of solid catalyst. The final properties of the catalyst depend strongly on each stage of preparation and on the purity of raw materials used. Small changes in the drying temperature, the solvent composition or the curing time can affect the performance of the catalyst. In refining we are dealing with two types of catalysts: The bulk catalysts; and the impregnated catalysts. The bulk catalysts are prepared by precipitation, hydro-thermal synthesis or fusion with mixtures of metals or metal oxides as their name implies. They consist of an active material: aluminosilicates or zeolite. Catalytic synthesis of ammonia and Raney metals belong to this class.

Impregnated Catalysts are used when one is forced to use precious metals or sensitive compounds and in this case the precursor of active metal is deposited on a porous support which may be an oxide (for example silica, alumina), activated charcoal or even a resin. The media used are themselves prepared by the same method of preparation of bulk catalysts. As examples of supported catalysts: Pd / C used in hydrogenation processes and $Pt/Sn/Al_2O_3$ for dehydrogenation processes.

Sometimes a method of preparation that combines the two previous methods is used; for example the active precursor powder is mixed with the substrate and the mixture is then agglomerated. Figure 1 shows an outline of the Key Steps for preparing a solid catalyst.

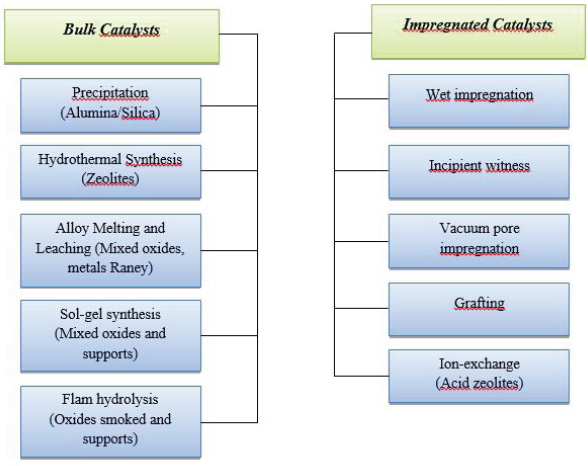

Figure 1. Key Steps for preparing a solid catalyst Methods of preparing solid catalysts

High-temperature melting technique

This technique is performed at high temperatures, it combines metal oxides and gives a good clean with a good dispersion of solids eg V_2O_5-MoO_3. The drawback of this method is the complexity of the material used because it requires special equipment in case of high temperatures required.

Technique of alloys leaching

In 1924 the American engineer Murray Raney discovered that the metal alloys used in leached hydrogenation give better results, he built a Ni / Al 50: 50 Then he removed the aluminum with NaOH and the result is called a "nickel sponge" also known as "skeletal catalyst". These catalysts are ready to use without pre-activation and have a large surface area. Figure 2 shows an outline for the preparation a Nickel sponge

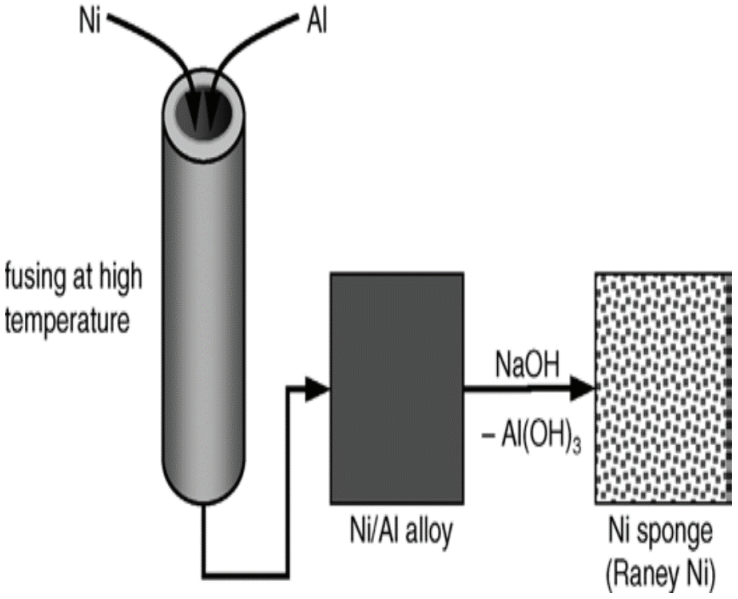

Figure 2: Preparation of nickel sponge (Raney/ Nickel)

Precipitation technique

The precipitation techniques are widely used for the preparation of several important catalysts, including silica, alumina and $Cu/ZnO/Al_2O_3$ catalyst used in the synthesis of methanol. This method produces high purity materials, but it requires solvent or precipitating agent which causes loss during the preparation of the catalyst and extra costs for the separation of the solvent compared to the previous method. This method generally comprises mixing aqueous solutions of salts and the desired salt is precipitated as a gel with the addition of a base or an acid or other precipitating agent. It passes through three stages which are super saturation, nucleation and crystal growth. Cooling the obtained material till it is matured, filtered, washed, dried and finally calcinated. For example Ni/Al_2O_3 catalysts used in steam cracking process are prepared by co precipitation of a precursor of nitrate in the presence of NaOH.

Technique for impregnating pores

It is a common method for preparing supported catalysts as the catalyst Pt/Al_2O_3 used in catalytic reforming. If impregnation of a wet 'wet impregnation' support is immersed in a solution of catalyst precursor it can be spontaneously adsorbed by the catalyst or it will precipitate by a change in pH or by the intervention of another chemical reaction and the resulting catalyst will be filtered, dried and calcinated. Taking the example of Pt/Al_2O_3 catalyst which is prepared by mixing po-

rous alumina with an acid solution chloroplatinic, the solvent is evaporated leaving 6 Pt ions on the support where they will suffer reduction using hydrogen, the reaction is illustrated below.

The disadvantage of this method is the large volume of waste liquids, but you can avoid this problem by using the method called "incipient wetness» that is to gradually moisten the powder from the support by the precursor solution until the mixture becomes slightly sticky which indicates that the pores of the support are filled with the liquid.

It can also be done by vacuum impregnation method is "Vacuum impregnation pore" where the medium is first dried and placed under vacuum to clear the air pores, then the support volume of precursor is added equivalent to pore volumes. It can happen to charge the pores by the active agent, repeating several times. Figure 3 shows photograph and schematic outline of a laboratory reactor for vacuum impregnation of the pores [4].

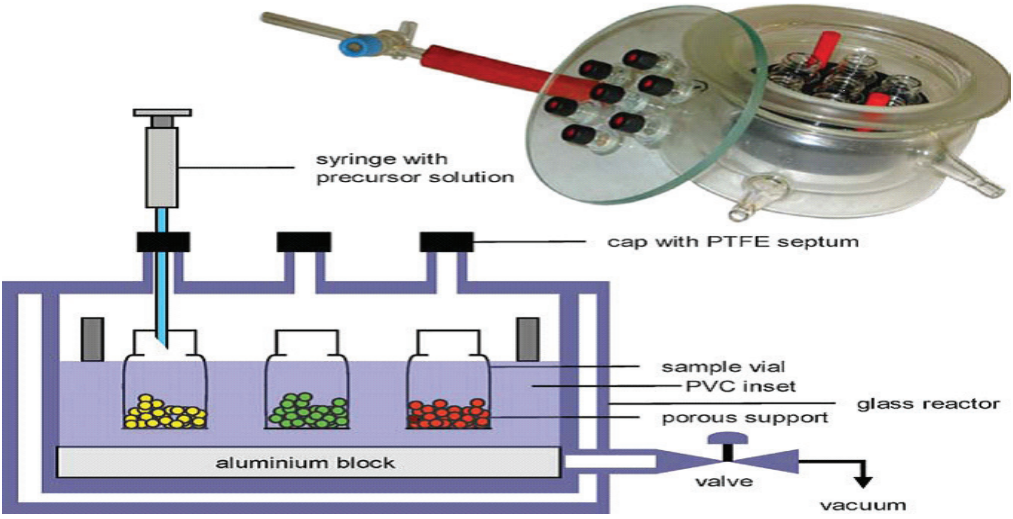

Figure 3: Vacuum impregnation of the pores.

Hydrothermal synthesis

As its name suggests it involves heating the precipitates, gels, or flocs in presence of water, this treatment is carried out in an autoclave at temperatures of 100-300 ° C, it follows from the textural and structural changes leading to a transformation from amorphous to crystalline state. This part is illustrated by the manufacture of zeolites.

Hydrothermal synthesis of zeolites

RM Barrer pioneered the synthesis of zeolites, trying to duplicate the crystallization (very slow) of natural zeolites, but he found that acceptable crystallization times (about a day) can be achieved by performing the synthesis under conditions of much more severe temperatures and alkaline mineral solutions used. The first synthesized zeolites were Al / If low (1 to 1.5) zeolite LTA, FAU type X. Subsequently zeolites average ratio (from 2-5) as the FAU zeolite Y type were synthesized. It is noted that the addition of organic compounds (structural) to the synthesis solution allowed obtaining zeolite Si / Al with very high ratio (≈ 10-100).

Milestones synthesis

The synthesis process of zeolites also called zeolitization corresponds to the transformation of a mixture of aluminum compounds and silicic, alkali metal cations, possibly of organic molecules and water in a micro-porous crystalline aluminosilicate (zeolite) using an alkaline solution super saturated. The mixture is quickly converted to an aluminosilicate hydro gel. The aging of the gel at room temperature (or slightly higher) allows slow dissolution of solid treated in the solution of monomers and oligomers silicates and aluminates in the latter leading to condense forming a crystalline phase.

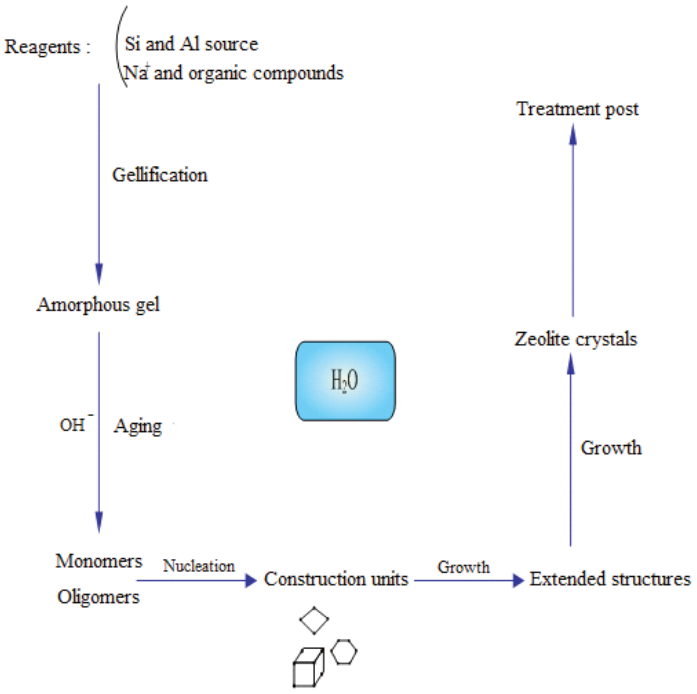

Figure 4: Stages of formation and ripening of the zeolite

The crystallization is conducted at temperatures of 60-160 ° C The zeolitization involves three stages: super saturation of the solution, nucleation and crystal growth.

a) The super saturation of the solution

One solution may be under the conditions of concentration and temperature in three forms: stable, metastable or labile. The areas of stability and metastability are separated by the curve of solubility equilibrium concentration of component C * depending on temperature. The degree of super saturation S is defined as the ratio of actual concentrations and equilibrium concentration (S = C / C *) in the field of stability or nucleation no crystal growth can occur, the crystal growth and nucleation can occur only in the field of lability, dominates in the metastability only crystal growth is possible during aging conducted at constant temperature. The concentration of aluminosilicate species increases over time by dissolving the solid amorphous phase to shift from a stable solution to a metastable solution and labile in solution [5].

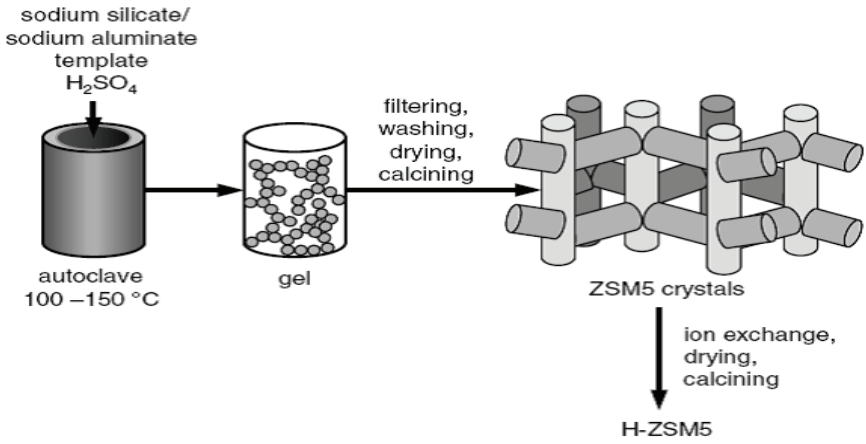

Figuer 5: Schematic diagram of the synthesis of zeolites

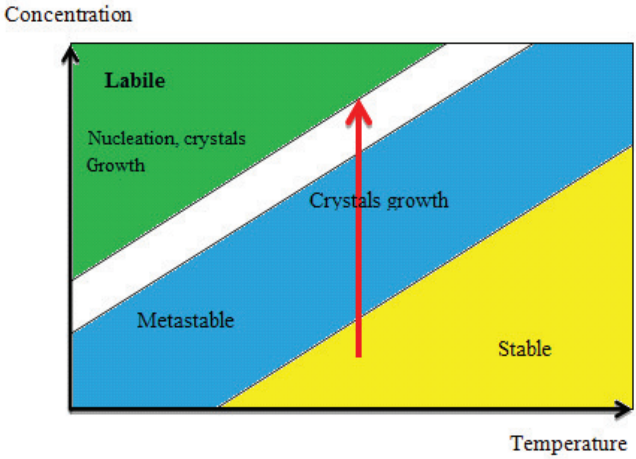

Figure 6: Solubility diagram

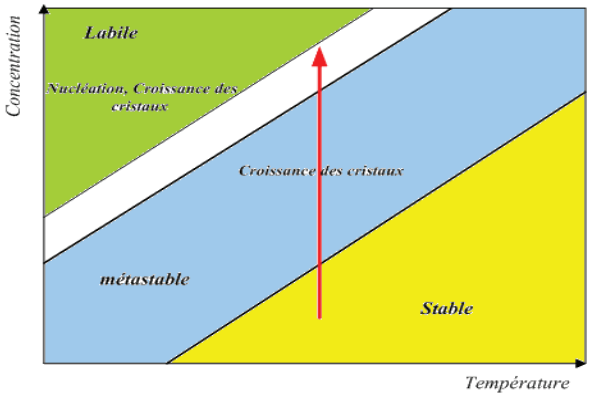

b) Nucleation:

The initial nucleation (or primary) from the labile solution may be homogeneous (spontaneous formation) or heterogeneous (induced by impurities), the secondary nucleation is induced by crystals. Nucleation is an activated phenomenon, its rate increases with temperature (by Arrhenius) as well as the degree of super saturation S. The nucleation starts for a critical value of S, the velocity reaches a maximum for a larger value, the decrease observed at high values of S from limitations in the transport of species, caused by increased viscosity of the solution.

c) Growth of crystals

The crystal growth of zeolites occurs at the interface crystal-solution by condensation of dissolved species (secondary building units or larger species). The following figure illustrates the stages of manufacture of the synthetic zeolite is the most famous H-ZSM5 (Fig.4).

Parameters determining the zeolitization

The zeolitization depends on four main factors are

The composition of the hydrogel

Each zeolite has a domain of well-defined composition, sometimes very large, sometimes very narrow, the composition of the hydrogel is a very important parameter for the synthesis of the desired zeolite. The composition of the zeolite is expressed in molar ratio of oxides: Al_2O_3: a Si_2O_2: b Na_2O: c H_2O

pH of the alkalinity of the solution

The pH of the alkaline solution synthesis (usually between 9 and 11) has an essential importance, because the OH-anions are essential to depolymerize the amorphous gel at an appropriate speed (they are mineralizing agents).

Temperature

Increasing the temperature allows for shorter times of crystallization. The temperature also determines the type of zeolite formed, leading to the growth of denser phase. There is however a limit temperature for the formation of each zeolite.

Structuring agents added to the solution

The structuring agents' role is to guide the synthesis of the wanted zeolite kinetically and thermodynamically. The oligomeric aluminosilicate organized around a particular geometry of structuring agents' molecules, precorsurs leading to species appropriate for nucleation and crystal growth.

Bentonite extracted from the region Boghni (Algeria), and processed and analyzed and the results are in the table below.

Table 2 Chemical composition of bentonite.

SiO_2	Al_2O_3	Fe_2O_3	MnO	MgO	CaO	Na_2O	K_2O	TiO_2	P_2O_5	Cr_2O_3	SO_3	Fire Los.
55,87	18,11	6,57	0,12	2,06	3,22	0,50	2,67	0,78	0,13	0,03	2,46	9,31

Four catalysts were prepared and differentiated by their chemical composition and the results of their analyses are shown in the following:

Table 3: Chemical composition of 4 prepared catalysts.

Catalyst	1	2	3	4
SiO_2	39.63	49.58	41.28	40.51
Al_2O_3	13.67	16.87	12.83	10.34
Fe_2O_3	6.82	4.03	2.51	2.47
CaO	3.87	2.87	1.97	1.76
MgO	4.36	2.66	1.66	1.63
SO_3	2.46	1.48	0.92	0.91
K_2O	2.67	1.59	0.99	0.97
Na_2O	0.50	1.90	0.17	0.17
Cr_2O_3	0.03	0.02	0.67	4.77
loss on ignition	13.56	8.29	8.88	7.81

These catalysts were used in two main treatment processes namely: cracking and isomerization; which enabled the preparation of specific species with an octane rating around 100, without additives. Moreover, the pyrolysis gasoline is highly aromatic, thereby obtaining BTX (Benzene, Toluene and Xylene) which are considered important raw material for petrochemicals [3]. Both processes have been conducted on a laboratory scale. An outline of the system is shown below and convincing results have been obtained.

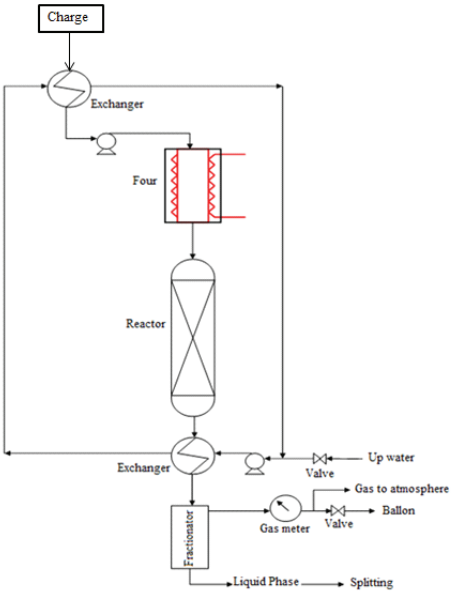

Figure 7: Catalytic cracking plant.

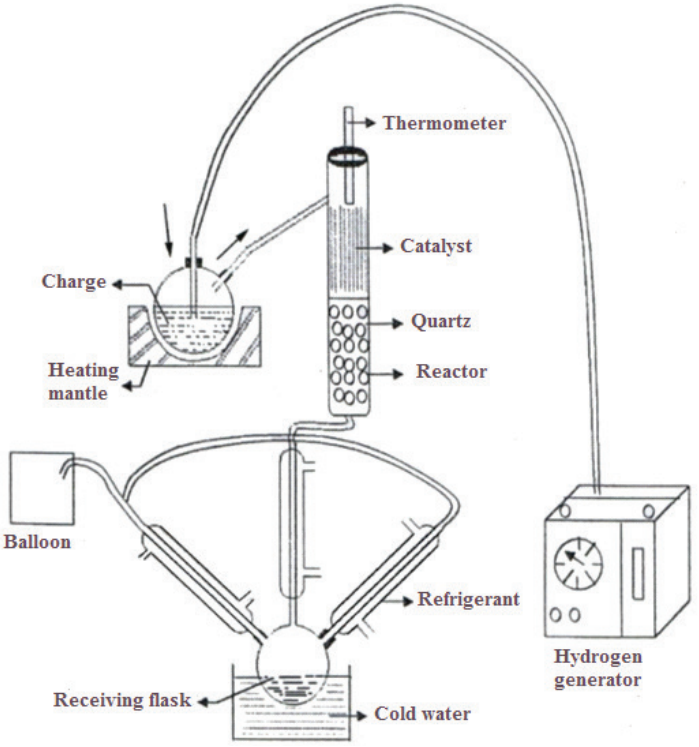

Figure 8: Installing catalytic isomerization

CONCLUSION

The catalysts prepared from local materials allowed us to conduct experiments on various charges compounding consisting of atmospheric residue and heavy diesel in the case of cracking and light fractions of condensate in the case of isomerization.
The culmination of the work is the development of local bentonite by its application in industrial processes for obtaining oil from waste and light fractions of condensate, bases clean gasoline with high octane.

In addition, the resulting gasoline is highly aromatic and can be used in the production of BTX necessary for the petrochemical industry. In addition to the catalytic cracking process produces large quantities of gases consisting mainly of unsaturated fractions BTAN-butylene-propylene and propane is also much sought after for the manufacture of high octane gasoline.

It should be noted that to improve the desired product yields it is necessary that to recycle the residuals. The gas oil obtained is possibly consistent with commercial specifications and can overcome the deficits in this product during peak periods.

The convincing results encourage us to reproduce the work in laboratory scale units before translating it to an industrial scale. In future research we recommend the use of catalysts of different compositions: for example the introduction of nickel compounds; whose properties are equivalent to the isomerizing ability of chromium.

References

1. P. Chemical Engineering Wuithier Paris 1972.
2. Michel Guisnet Ramo and Fernando Ribeiro, an Nanoworld The Zeolites Service of Catalysis, EDP Sciences, Paris 2006.
3. Technologie Oil and Gas No. 1 Moscow 2007.
4. M.Millan, Pillared clays as catalysts for hydrocraking of heavy liquids fuels. Applied Catalysis 2005.
5. Gadi Rothenberg, Catalysis Concepts and Green Applications, Wiley-VCH Verlag GmbH & Co. in Weinheim, Germany 2008

PROBLEMATIC OF THE ARTISANAL MINING EXPLOITATION AND THEIR IMPACTS ON THE ENVIRONMENT IN WALIKALE (NORTH KIVU)

Bindu L.A[1]., Byamungu M[1]., Kiro K[2].

1 Université de conservation de la nature et le developpement de Kasugho, République démocratique du Congo
2 Université de Goma., République démocratique du Congo

The artisanal mining exploitation in democratic Republic of Congo is adjusted by the article 26 of the mining Code that arranges: "without prejudice of arrangements of the article 27, only the major physical people of Congolese nationality can acquire and can detain the cards of artisanal operator and trader's cards". otherwise, the article 109 of the IV title of the mining code institutes the artisanal exploitation zone in these terms: "When the technical and economic factors that characterize some lodgings of gold, diamond or all other mineral substance don't permit to assure an industrial or semi-industrial exploitation of it, but permit an artisanal exploitation, such lodgings are erected, in the limits of a determined geographical area, in artisanal exploitation zone. The institution of an artisanal exploitation zone is made by way of decree of the minister after opinion of the direction of the Mines and the governor of the province concerned, but an activity without control. However, it includes enormous inconveniences notably on the human health but also the one of the environment and the natural resources. She/it also has some consequences on a social level. It is necessary to note indeed that the artisanal mining exploitation contributes to the deforestation, to the deterioration of soils, to the pollution of air by the dust and the monoxide of carbonic, of soil and water by the used oils of the motors and the chemicals.

This exploitation is considered like source of financing of the groups armed, it is that is to basis of the insecurity in the East of the RDC.

Keywords: Artisanal mining, environment, water, Republic of Congo

GITOLOGY STUDY OF BOUKDEMA, NORTHEAST OF SETIF (ALGERIA)

Bouchilaoune N., Abderrahmane H., Boutaleb A.

Laboratory of Metallogeny and Magmatism of Algeria, Department of Geology, Faculty of Earth Sciences, USTHB.
nabyl_b@yahoo.fr

The mining district of Guergour belongs to the allochthonous south-sétifian group

appearing in the tectonic windows of Djebels Guergour and Anini which emerge under the tellian sheets.

The sector of Guergour is dominated by many accidents, which compartmentalize the massif in various blocks conferring a structure in horsts and grabens.

This domain includes Boukdema mineralizations (Kef Gueref, El Maâden and Kef Khenoussa) and the indices of Ain Khelidj.

The gitological study reveals mineralizations of Pb-Zn and incidentally copper and barytine. These mineralizations correspond to two different styles of mineralization:

- The first consists to Pb-Zn stratabound mineralization hosted in liasic dolomites.
- The second includes cupriferous mineralization which cross cuts the first one and affects the massive cenomano-Turonian limestones.

Keywords: Mineralization; Boukdema; Lead-Zinc; Copper- Baryte

ORIGIN OF THE FLUORINE-RICH HIGHLY DIFFERENTIATED GRANITES FROM THE QIANLISHAN COMPOSITE PLUTONS (SOUTH CHINA) AND IMPLICATIONS FOR POLYMETALLIC MINERALIZATION

Chen B., Ma X., Wang Z.

Key Laboratory of Orogenic Belts and Crustal Evolution, Peking University, Beijing 100871, China
binchen@pku.edu.cn

Many composite granite plutons occur in South China, accompanied by large-scale polymetallic mineralization. Each composite pluton is composed of main-phase granite and late-stage highly differentiated granite. Traditionally, the highly differentiated granite is thought to be residual melt from the former via fractionation, and ore-forming materials and fluids are from granite magma itself. We propose a different model for the origin of the granites and related mineralization, based on petrological and geochemical studies on the Qianlishan composite plutons that host the supergiant Shizhuyuan W-Sn-Bi-Mo deposit. The main-phase granite shows features of normal granites, while the highly differentiated granite is characterized by F-rich, water-deficient, low fO_2, alkalinity, REE tetrad effect, and modified behavior of some trace elements, e.g., very high K/Ba and low K/Rb and Zr/Hf ratios. We suggest that the parent magma of the highly differentiated granite was derived from melting of dominantly granulite facies residues after extraction of the main-phase granite, triggered by underplating of a new pulse of basaltic magmas in the lower crust; the basaltic magmas and volatiles such as fluorine were involved in the source of the granite. Addition of fluorine lowered the solidus temperature and viscosity of granite magma, and thus prolonged the process of magma evolution. This resulted in extreme fractional crystallization, and intense interaction between melt and circulating waters from country rocks, forming the unusual geochemical features of the granite. The high temperature circulating waters subsequently, together with fluorine, extract ore-forming materials from country rocks through complexation, forming the polymetallic deposits.

PETROLOGY OF SARKOOBEH ALKALI GABBRO IN THE NORTH OF KHOMAIN, IRAN

Davoudian A.R., Sakhaei Z., Shabanian N.

Faculty of Natural Resources and Earth Sciences, Shahrekord University, Shahrekord, Iran
alireza.davoudian@gmail.com

The Sarkoobeh gabbroic intrusions are located 25-30 Km of the north of Khomain near to central of Iran. They are part of Sanandaj-Sirjan Zone (Fig. 1). The bodies have intruded to cretaceous limestone and therefore they have attributed to a post-late cretaceous age. Petrographic studies and whole rock geochemistry indicate that these rocks are alkali gabbro with mineralogical composition including mostly plagioclase, clinopyroxene, and opaque that they partly replaced by secondary minerals during alteration and low-grade metamorphism. They display ophitic to sub-ophitic textures.

Based on geochemical analyses that are given in Table 1, the variations of SiO_2 among the rocks are from 45.71 to 50.91 and the rocks show alkaline affinity. The strongly inclined chondrite-normalized pattern shown by REE, typical of alkali basalts, demonstrates that the primary magmatic pattern was preserved and not modified by metamorphism and alteration processes. It indicates marked LREE enrichment and significant HREE depletion, suggesting low percentages of partial melting of an enriched primitive mantle with garnet in the residue. The slightly positive Eu anomaly is clearly related to the abundance of primary plagioclase. The observed enrichment of the most incompatible elements, the positive Ta anomaly in the trace element diagram, the marked enrichment in LREE, and the positive Eu anomaly are all characteristic of alkaline rocks.

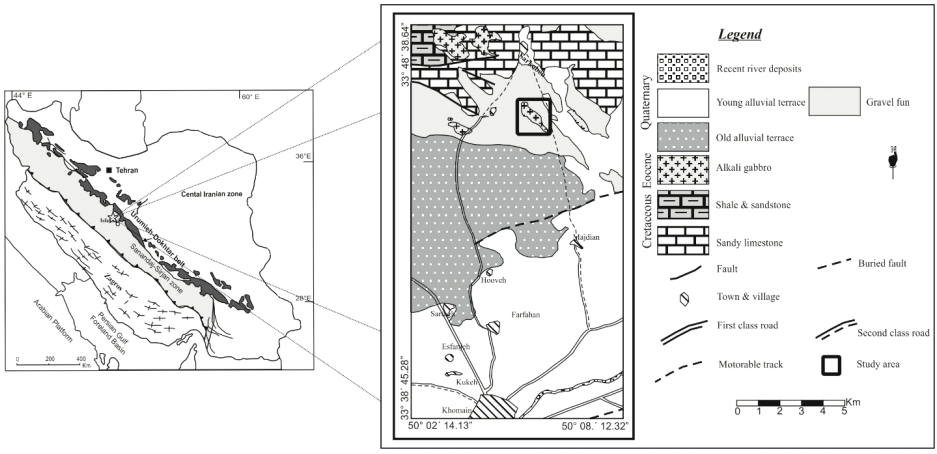

Figure 1: The simplified geological map of the study area [1] and its location in Iran.

In the Ti/100–Zr–3Y diagram [2] (Fig. 2a), all samples plot in the field of within-plate basalts. The ternary La/10–Y/15-Nb/8 diagram [3] produces the same result (Fig. 2b). A within-plate setting is also suggested by the Hf/3–Th–Ta diagram of [4] (Fig. 2c) and the 2Nb–Zr/4–Y diagram of [5] (Fig. 2d).

[6] has been proposed the Th/Yb versus Ta/Yb diagram in order to characterize the mantle source of subduction-related volcanic rocks from island arcs and active continental margins. The Sarkoobeh gabbroic rocks plots in the field of enriched-mantle source rocks (Fig. 2e). This diagram strongly supports the involvement of an OIB-like enriched mantle in the petrogenesis of the rocks. Moreover, the gabbroic rocks does not show a high Th/Yb ratio as would be indicative of crustal contamination.

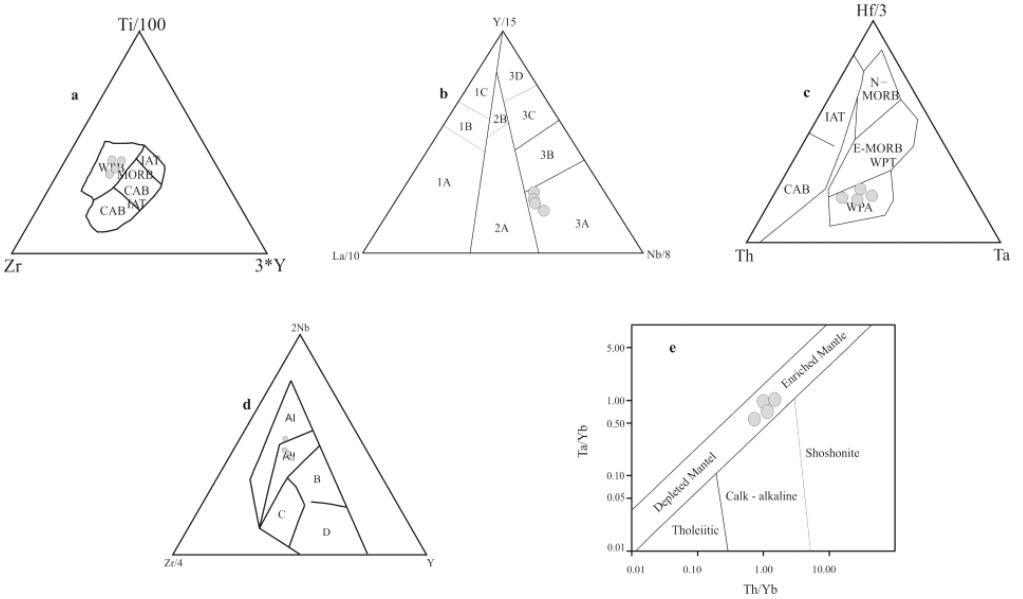

Figure 2: Geotectonic setting for the Sarkoobeh gabbro: (a) Ti/100–Zr–3Y diagram [2]; (b) La/10–Y/15-Nb/8 diagram [3]; (c) Th–Hf/3–Ta diagram [4]; (d) 2Nb–Zr/4–Y diagram [5]. d) Th/Yb versus Ta/Yb diagram from [6] for the Sarkoobeh gabbro

Table 1: Representative major (%wt) and trace (ppm) elements compositions from Sarkoobeh gabbroic intrusions.

Sample	SK-2-8	SK-2-11	SK-3-1	SK-3-5	Sample	SK-2-8	SK-2-11	SK-3-1	SK-3-5
SiO_2 (%wt)	46.59	50.91	47.45	45.71	Hf	2.0	2.2	2.8	2.1
TiO_2	1.54	1.87	1.28	1.12	Nb	14.9	15.4	25.7	14.8
Al_2O_3	15.05	19.02	15.85	14.83	Rb	74.1	17.1	17.0	47.1
Fe_2O_3	12.54	6.86	10.72	11.52	Sr	448.7	527.7	653.9	317.5
MnO	0.16	0.10	0.14	0.15	Ta	1.1	0.9	1.7	0.9
MgO	8.94	3.92	9.05	11.61	Th	1.5	1.7	1.8	1.2
CaO	8.32	8.23	7.68	7.09	Zr	80.8	84.4	112.9	84.3
Na_2O	2.74	5.48	3.41	2.35	Y	12.8	15.1	17.7	17.1
K_2O	0.99	0.47	0.49	1.55	La	10.2	10.9	15.6	9.9
P_2O_5	0.17	0.29	0.18	0.18	Ce	20.0	21.6	31.1	19.6
L.O.I.	2.6	2.6	3.4	3.5	Yb	1.09	1.46	1.70	1.55

References

1. Mohajjel M., 2002. Geological quadrangle map of the Golpayegan area, 1: 100 000, Geological Survey of Iran, Tehran, Iran.
2. Pearce J.A, Cann J.R., 1973. Tectonic setting of basic volcanic rocks determined using trace element analysis. Earth and Planetary Science Letters 19: 290–300.
3. Cabanis, B., Lecolle, M., 1989. diagrame La/10-Y/15-Nb/8: un outil pour la discrimination des series volcaniques et la mise en evidence des processys de melange et/ou de contamination crustale. Compt-es Rendus de l'Académie des Sciences-Serie II, 309.
4. Wood D.A., Joron J.L, Treuil M., 1979. A re-appraisal of the use of trace elements to classify and discriminate between magma series erupted in different tectonic settings. Earth and Planetary Science Letters 45: 326–336.
5. Meschede, M., 1986. A method of discriminating between different types of mid-ocean ridge basalts and continental tholeiites with the Nb-Zr-Y diagram. Chemical geology, 56(3), 207-218.
6. Pearce J.A., 1982. Trace element characteristics of lavas from destructive plate boundaries. In Andesites: Orogenic Andesites and Related Rocks, Thorpe RS (ed.). Wiley: Chichester; 525–548.

CRYSTALLISATION HISTORY AND SR-ND ISOTOPE GEOCHEMISTRY OF ÇIÇEKDAĞ IGNEOUS COMPLEX (ÇIC) (CENTRAL ANATOLIA, TURKEY)

Deniz K.[1], Kadıoğlu Y.K.[1-2], Stuart, F.M.[3], Ellam, R.M.[3]

1 Ankara University, Faculty of Engineering, Department of Geological Engineering, Ankara, Turkey
2 Earth Sciences Application and Research Centre, Ankara University, Ankara, Turkey
3 Scottish Universities Environmental Research Centre (SUERC), East Kilbride, Scotland, UK
kdeniz@eng.ankara.edu.tr

Calcalkaline and alkaline igneous rocks of the Central Anatolia Crystalline Complex (CACC) provide an insight into the magmato–tectonic evolution during the final closure of Neotethys Ocean. The composition, source and relative timing of the main magmatic pulses is reasonably well understood [e.g. 1]. However, there is a lack of reliable crystallization age determinations for the main magmatic rock types and no agreement regarding whether they form during or after collision of the continent continent/oceanic island arc [e.g. 2]. Further, the genesis of ophiolitic and mafic alkaline magmatism is still debated [3]. The main magmatic phases (suprasubduction zone ophiolites, calcalkaline and alkaline intrusives) are present in the Çiçekdağ igneous complex (ÇIC), along with a suite of late feldspathoid-bearing dolerite dykes that have not been reported elsewhere in the CACC. We are undertaking a detailed petrographic, geochemical, isotopic (Sr, Nd, Pb and O) and geochronological (U/Pb and Ar/Ar) study of the ÇIC igneous rocks in order to unravel the magmatic history of the CACC, and thus constrain the tectonic history. In this presentation I report new field, petrographic and geochemical data.

Ophiolitic rocks (e.g. rootless gabbros, diabase, pillow basalts and pelagic limestones) are common, and everywhere cut by later calcalkaline and alkaline intrusive rocks. The calcalkaline intrusive series is dominated by monzonites, but range from 56–67 % SiO_2 and 6–9 % Na_2O+K_2O. The later alkaline intrusives range from feldspathoid–bearing gabbro to syenites (55–65 % SiO_2, 8–14 % Na_2O+K_2O). Major oxide and trace element variations of both rock series are consistent with the removal of clinopyroxene ± plagioclase ± amphibole ± FeTi oxide minerals ± apatite during the fractional crystallisation. The high $^{87}Sr/^{86}Sr_{(i)}$ (0.7083-0.7113) and low $^{143}Nd/^{144}Nd_{(i)}$ (0.512236-0.512390) of both suites implies that they have been contaminated by continental crust. A suite of tholeiitic, feldspathoid–bearing dolerite dykes cut all the main rock units. They are typically 0.1–0.3 km wide and are oriented NW–SE consistent with other felsic dykes.

The most mafic alkaline and calcalkaline intrusives are characterised by enrichments in LILE (K, Rb, Ba, and Th) and LREE relative to HFSE (Ta, Nb, Hf, Zr and Y) and HREE indicating that they evolved from a parental magma that was derived from enriched mantle. Ta, Th, Nb, La and Yb elements indicate that the calcalkaline and alkaline rocks of the ÇIC are derived from subduction–modified lithospheric mantle. Sr-Nd isotope ratio mixing diagram suggest that calcalkaline, alkaline felsic and mafic intrusives have 46-51 %, 50-52 % and 34-37 % mixing with upper crustal component.

The origin of the late the feldspathoid–bearing dolerites is enigmatic. They differ from alkaline

gabbros especially by Nb and La element composition, but have similar trace element composition with the ophiolitic rocks. The dolerites have higher $^{87}Sr/^{86}Sr_{(i)}$ (0.7064–0.7066) and lower Ta/Yb (0.02–0.06) than the ophiolites (0.7043–0.7047; 0.02–0.18) indicative of a subduction enrichment within the dolerite source mantle. The dolerites appear to derive from melting of mantle source in spinel facies with a 10-15 % mixing of subduction sediment.

Keywords: Çiçekdağ Igneous Complex (ÇIC), alkaline basalts, feldspathoid-bearing gabbros, ophiolite, AFC, Sr-Nd isotope geochemistry.

Acknowledgement: We gratefully acknowledge The Scientific and Technological Research Council of Turkey (TUBITAK) Science Fellowships and Grant Programmes Department (BIDEB) for their supporting Miss Deniz with their International Research Fellowship Programme grant. We are also thankful to the Ankara University for financial support by Doctorate Thesis Research Project (13L4343001) and DPT (2012K120440). We are kindly grateful Earth Sciences Application and Research Centre (YEBIM) of Ankara University and Scottish Universities Environmental Research Centre (SUERC) for laboratory facility.

References

1. İlbeyli N., Pearce J.A., Meighan I.G., Fallick A., 2009. Contemporaneous Late Cretaceous calc–alkaline and alkaline magmatism in Central Anatolia, Turkey: Oxygen isotope constraints on petrogenesis. Turkish Journal of Earth Sciences, 18, p. 529–547.
2. Boztuğ D., Tichomirowa M., Bombach K., 2007. $^{207}Pb–^{206}Pb$ single–zircon evaporation ages of some granitoid rocks reveal continent–oceanic island arc collision during the Cretaceous geodynamic evolution of the central Anatolian crust, Turkey. Journal of Asian Earth Sciences, 31, p. 71–86.
3. Kadıoglu, Y.K., and Güleç, N., 1996b, Structural setting of gabbros in the Agaçören granitoid: Implications from geological and geophysical (resistivity) data. Turkish Journal of Earth Sciences, 5, p. 153–159 (in Turkish with English abstract).

CHEMICAL COMPOSITION, GEOCHEMICAL FEATURES AND GENESIS OF CHAROITE AND CHAROITE ROCKS, MURUN COMPLEX

Dokuchits E.Yu., Vladykin N.V.

Institute of Geochemistry, SB RAS, Irkutsk, Russia,
vlad@igc.irk.ru

The Murun volcanic-plutonic complex is a unique object of nature. It is the largest complex of potassic agpaitic rocks that doesn't have any analogues in the world. The complex is also unique in terms of rocks and minerals as well as deposits and ore occurrences (including those of charoite and charoite rocks).

The Murun volcanic-plutonic complex is located in the north-east part of the Irkutsk Region bordering Yakutia. The complex includes two outcrops – Big Murun and Small Murun. Further we discuss the Small Murun. The Murun complex includes a unique rock differentiation from ultramafic-alkaline rocks to alkaline granites with all intermediate varieties (Vladykin, 2001). An important process in the origin of rocks of the Murun complex is magmatic-silicate and silicate-carbonate layering. We have revealed the following scheme of the complex's magmatism:

1. **Early intrusion phase** includes a layered complex consisting of Bt-pyroxenites, K-ijolites, olivine lamproites, Fsp-schonkinites, leucitic shonkinites. Xenoliths of cumulative olivine-spinel and olivine-pyroxene-monticellite-micaceous rocks are also found.

2. **Main phase** comprises horizontally layered complex of different pseudoleucitic, Fsp-calcilitic, Bt-Py potassium feldspar syenites. Their crystallization is terminated by quartz syenites, dikes and stocks of alkaline granites.

3. **Volcanic phase** involves a layered flow of leucitic melaphonolites, leucites, leucitic lamproites, in cases with tuff-lavas and tuff-breccias. The dike complex of this phase includes leucitic tinguaites, richterite-sanidine lamproites, trachyte-porphyries, syenite-porphyries and eudialyte lujavrites.

4. **Late phase** includes a layered complex of potassium silicate-carbonate rocks of the following composition:

a) micropotassium feldspar rocks– white fine-grained rocks, containing potassium feld spar with insignificant amount of pyroxene and tinaksite;

b) quartz-calcite-pyroxene-microcline rocks; the calcite content varies from 5% to 20%;

c) pyroxene-potassium feld spar rocks with varying contents of both components;

d) calcite, benstonite and quartz-calcite carbonatites;

e) silicate charoite rocks.

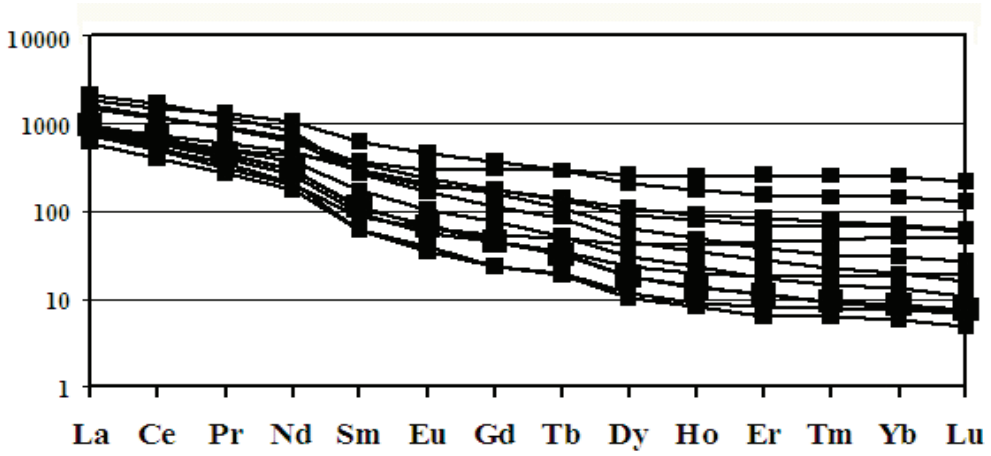

Figure 1: Spider diagram of rare-earth elements of charoite rocks.

All the above rocks are subject to intensive hydrothermal alteration through tectonic zones and fractures. The hydrothermal processes result in sulfide alteration and silicification of rocks. The hydrothermal processes are related to Cu, Pb, Zn, Au, Ag, U, Th, Mo, Nb and Ti occurrences.

The charoite rocks are composed of quartz, microcline, K-arfvedsonite, tinaksite, fedorite, apophyllite, franckamenite, pectolite phenocrysts. They are rimmed by charoite, charoite-pyroxene-tinaksite aggregate in cases with calcite A number of new minerals have been discovered in charoitic rocks. In terms of the chemical composition the charoitic rocks are similar to syenites by high contents of CaO (to 20%), alkalies (to 15 %), Ba and Sr (to 3%) and H_2O (to 5%).

Charoite contains major (K, Na, Ca, Si, H2O) and trace elements (Ba, Sr, Mn). The charoite monocrystals are not available; it forms complex polysynthetic aggregates. The scientists have quite recently deciphered the charoite structure with a common formula:

$(K,Sr,Ba,Mn)_{15\text{-}16}(Ca,Na)_{32}\ [(Si_{70}\ (O,OH)_{180})]\ (OH,F)_{4.0}.nH_2O$

The charoite consists of three Si-O radicals $[(Si_6O_{11}(O,OH)_6)_2(Si_{12}O_{18}(O,OH)_{12})_2(Si_{17}O_{25}(O,OH)_{18})_2]$ [Rozhdestvenskaya et al., 2010]. This is the most complex structure of known minerals. Charoite was firstly discovered 40 years ago, but haven't found anywhere else in the world.

Like the calcite carbonatites the charoitic rocks form schlieren- and vein-like bodies in the silicate-carbonate rocks. The bodies demonstrate as a rule insignificant thickness (5-10 m) and they are up 20 m long. The charoite matrix frequently forms structures of flow, surrounding the phenocrysts of earlier minerals. When the charoite rock is weathered its color changes to brown with different shades.

Figure 1 gives the spectrum of rare-earth elements for charoite rocks. The spectra are characterized by an insignificant slope and lack of Eu-anomaly. Figure 2 shows positive Ba, U, Pb, Sr (also Sm and Gd) and negative Th, Nb, Ta, Zr, Hf, Ti anomalies. Spectra of rare-earth elements

are close to horizontal.

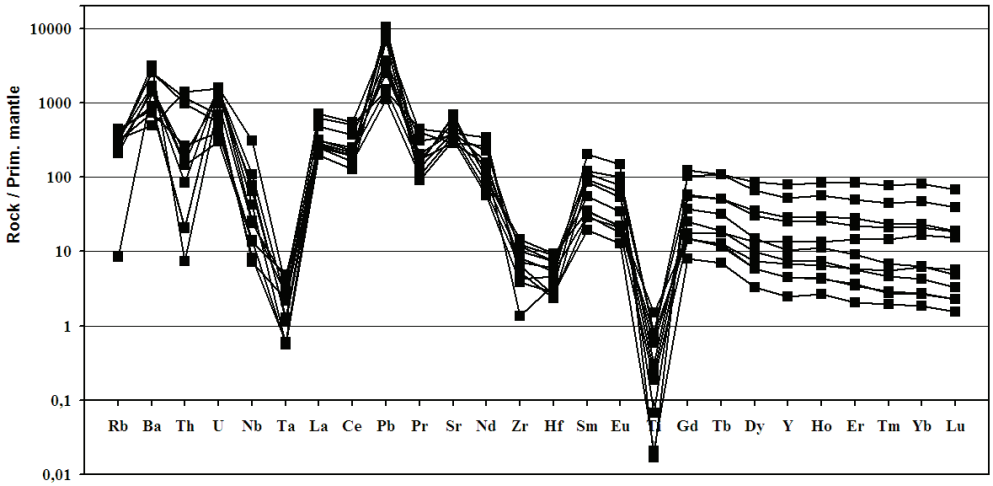

Figure 2: Spider-diagrams of charoite rocks.

The charoite rocks originate from layering of silicate-carbonate melt-fluid. The thermobarogeochemical studies of melted and fluid inclusions in charoite rocks done by A.A. Borovikov (Institute of Geology and Mineralogy, Novosibirsk) indicate that charoite rocks are crystallized from residual melt-fluid at temperatures ranging from 750 to 400^{O}C. Those studies confirmed the layering of melt-fluid into several liquids – silicate, carbonate and water. The residual silicate-carbonate melt-fluid demonstrates typical layering processes. The carbonatites show band-like separation into microcline, pyroxene and carbonate bands, while charoite rocks demonstrate drop-like separation i.e. separation of drops of pyroxene and tinaksite which form spherolites if they are fast crystallized.

STUDY OF THE PHENOMENON OF LOW RESISTIVITY RESERVOIR PRODUCER DEVONIAN (SOUTHERN ALGERIA)

Eladj S.[1], Ouadfeul S.A.[2], Mallek A.[1], Samir. M.[1], Aliouane L.[1]

1 LABOPHYT, FHC, Universite Mhamed Bougara de Boumerdes, Avenue de l`independance, 35000, Boumerdes, Algeria ,
2 Algerian Petroleum Institute, IAP, Algeria

It is generally recognized tanks porous permeable and easily saturated hydrocarbons by high resistivity along logs.Mais there are cases where reservoirs produce oil but with low resistivities.

It was recognized that a producer hydrocarbon reservoir with low resistivities reservoir is producing oil or gas with a lower or equal to Rt 5Ω.m.

For a given reservoir resistivity drop may be due to one or more factors, these factors can be grouped into two main categories, namely:

1-Factors related to the environment

2-Geological Factors influencing measures Rt

The first approach when calculating Sw is the use of resistivity values, except that in this case the saturation obtained are not reliable. At the end of solve this problem, tools have been designed in order to estimate the value of water saturation (Sw) in tanks without recourse to give resistivity (Rt) at the end affirm or reverse the presence of hydrocarbons. Such as: MDT, TDT, EPT, RST and CMR.

To overcome this problem of low resistivity, we used a tool mentioned above is the MTD, because it provides us with pressure measurements and fluid samples present in our reservoir.

MDT tool "Modular Dynamic Tester" is known for its ability to identify the nature of the fluids in place using different samples.

After measuring the pressure, pressures on the track-and depth diagram taking into account samples taken during the test, one can determine the pressure gradient for each training, and the density of the fluid in place.

Keywords: producer of hydrocarbons, low resistivity, TDS, pressure gradient, fluid density

GEOCHEMICAL AND MINERALOGICAL CHARACTERS OF THE COASTAL PLAIN SEDIMENTS OF THE ARABIAN GULF, KUWAIT

Elhabab A., Adasani I.

College of Technological Studies
Petroleum Engineering Department, Kuwait

The present study deals with detailed geochemical and mineralogical studies of the coastal plain sediments formed along the shoreline of the Arabian Gulf area, Kuwait. These deposits are mainly fluviomarine and beach sands .

The coastal plain deposits of the central Kuwait shoreline zone were found to consist of average medium-grained sand. The sand composed; on average of about 90% sand , and about 10% or less is mud, and has a unimodal distribution with a mode of medium sand (1-2 ϕ).

The sediments consists mainly quartz, Feldspar, clay minerals with carbonate minerals (detrital calcite and dolomite) and rock fragments (chert) .

The mineralogy of the clay fractions of the sediments is dominated by illite, palygorskite , mixed layer illite-montmorillonite with minor amounts of chlorite and Kaolinite

Heavy minerals are concentrated in the very fine sand fraction and are dominated by opaque minerals, and non opaque minerals which represented by amphiboles, pyroxenes, epidotes, dolomite, zircon, tourmaline, rutile, garnet and other which represented by Staurolite, Kyanite, Andalusite and Sillimenite as a trace amounts .

The chemical analysis for the detrital amphibole grains from sandstone of coastal plain sediments shows the following features; the grains which have (Na+K) <0.50 its composition ranges from actino hornblende to magnesio hornblende, but the grains which have (Na+K) >0.50 its composition have wide variation and on the (Na+K)-Al_{IV} diagram can be characterized two association: Association 1 which characterized by low amount of $Al_{IV}$and low amount of (Na+K), by comparing the chemical composition of this association and the chemical composition of amphibole grains from older basement rock, can, these association may be derived from metamorphic source rocks and association 2 which characterized by high amount of Al_{IV} and low amount of (Na+K), which may be derived from volcanic source rocks.

Keywords: Coastal area – Heavy minerals – fluviomarine sediments - clay minerals- Chemical Composition. Electro probe micro analyzer (EPMA).

CARBONATITES: GENERAL OVERVIEW AND THEIR OCCURRENCES IN TURKEY

Çiftci E.

İTÜ Maden Fakültesi Jeoloji Müh. Böl. 34469 Maslak-Sarıyer, eciftci@itu.edu.tr

Carbonatites are extraordinary igneous rocks that contain more than 50 wt. % carbonate minerals (including calcite, dolomite, ankerite, Fe-carbonates) in modal abundance. In addition pyroxenes (generaly sodic ones), alkaline amphibole, phlogopite (Mg-mica), biotite, apatite and magnetite accompany those common minerals. They typically contain silica less than 10 wt %. About 330 carbonatite occurrences in an area of about 500 km^2 have been reported upto date (some claim more than 500 occurrences). Although not all but most of the carbonatites occur in association with silica undersaturated alkaline igneous rocks.

As the carbonatites could be of mantle origin, they can also be generated within the crust through partial melting. One of the most common features of the world class occurrences is their being associated with deep rooted fractures/rifts occurring under extensional tectonic regimes and alkaline magmatism occurring within such environments. These occurrences are associated with similar tectonic setting and magmatic events in three district in Turkey. In Kızılcaören area, carbonatites were resulted as a result of late Oligocene magmatic activities, and trachitic pyroclastics, trachites, and phonolites were formed due to early Miocene volcanic activities. Trachites and phonolite domes were emplaced intruding into the serpentinites by following E-W trending major faults. REE containing major mineral phases in the area include brockite, torbaestnesite and fluorecite. While the area may have potential for Th (and U?), this investigation indicate no promising findigs for any potential for REE's.

In Çukurköy area, reported association is represented by Atdere syenite and carbonatite intruding into the crystalline basement and Eocene sediments. The Atdere foid syenite expose in the south of the village of Hayriye along both slopes of Atdere and intruding in between schists and marbles forming a dome structure. Through this investigation, besides fluorites occurring as thin and unsystematicly dispersed veins and pockets which account for Th anomalies, no other commodities were found. In Başören area, Late Cretaceous-Lower Paleocene Ardıçlı syenitoids were emplaced as small stocks cutting through Karapınar limestone along Buyunçayır fault striking NW, which it self is parallel to Düşüksöğüt fault. Mid-Late Paleocene Alibeyli carbonatites intruded into this stocks as semi circle, arc and small cones in two phases (I) early carbonatite phase and (II) late carbonatite phase. LREE-phosphate phase – britholite, fluorite and apatite were found to be associated with the carbonatites that accounting for only economic minerals of the area.

Lithological and tectonic association, ore mineral paragenesis, REE and other element contents, alteration characteristics and mineral assamblege were evaluated altogether to conclude as follows: all three occurrences are found to be associated with deep-rooted fractrure systems and alkaline magmatisms and they can only be considered to have potential for Th and REE in particular but also fluorite and phosphate if their reserves are properly outlined.

Keywords: Carbonatite, alkaline magmatism, Kızılcaören, Çukurköy, Başören Köyü, fluorite, apatite, phosphate, REE, Th, U

LEACHING OF RARE-EARTH ELEMENTS FROM __104802849 LUJAVRITE (LOVOZERO ALKALINE MASSIF, KOLA PENINSULA)

Ermolaeva V.N., Mikhailova A.V., Kogarko L.N.

GEOKHI RAS, Moscow, Russia
cvera@mail.ru

The rocks of Lovozero massif contain high concentration of rare-earth elements. We studied leaching of these elements from __104802849 lujavrite, which is rare-metal ore, with different reagents in order to determine the most effective ones. As a reagents for leaching, we used 4% solution of HCl, 2% solutions of ammonium oxalate, trilon B and ammonium difluoride, as well as mixtures (1:1) of HCl solution with 2% solutions of ammonium oxalate, trilon B and ammonium difluoride. The determination of the elements was carried out by using of ICP MS method. The results of leaching show, that *REE* from __104802849 lujavrite are leached most effective by mixtures of HCl solution with ammonium oxalate, trilon B and ammonium difluoride solutions, as well as by HCl solution. Somewhat smaller quantities of *REE* are leached by solutions of ammonium oxalate, trilon B and ammonium difluoride. Selective extraction of Ce is characteristic for ammonium difluoride solution (Ce maximum in figure 1); ammonium oxalate solution, on the contrary, extracts Ce worse than other elements (Ce minimum in figure 1). Thus, combination of HCl solution with ammonium oxalate and ammonium difluoride solutions raises enhancement of leaching as compared with pure solutions. In figure 2 are given chondrite-normalized values for __104802849 lujavrite and for solutions obtained on leaching.

This work is important from the practical point of view: the high contents of rare (including rare-earth) elements in alkaline rocks of Lovozero massif make it possible to consider it as potential object for their industrial extraction.

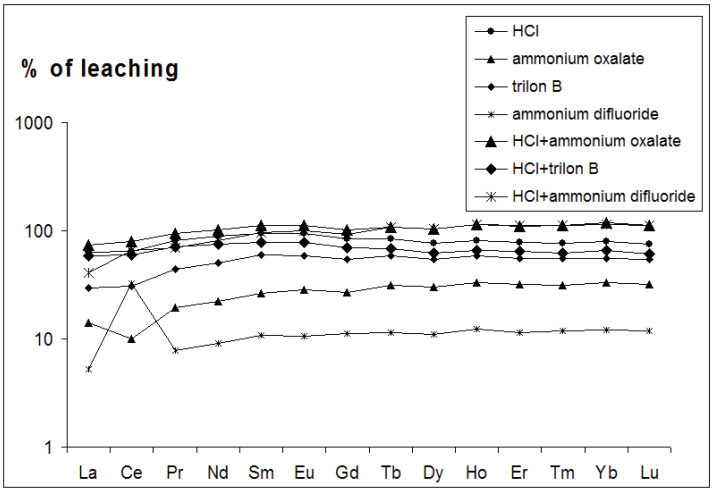

Figure 1: Results of *REE* leaching (in % from total content) from __104802849 lujavrite (Lovozero massif, Kola Peninsula).

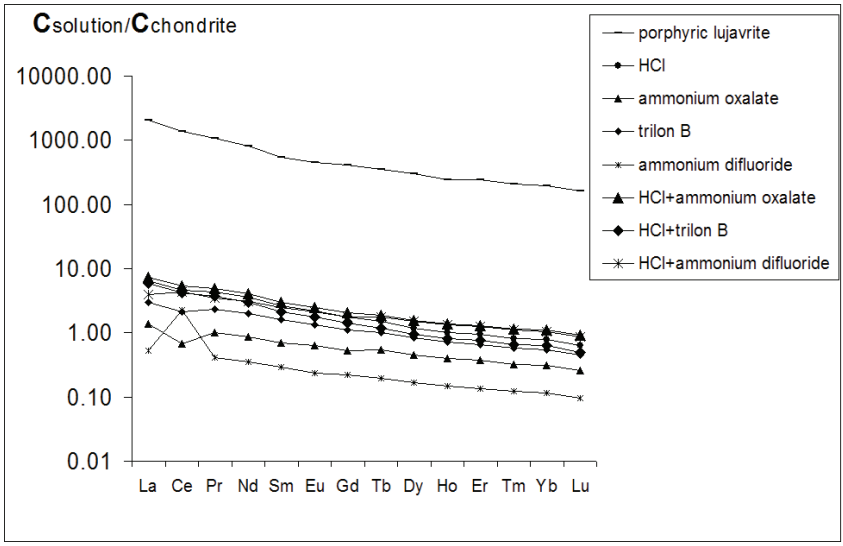

Figure 2: Chondrite-normalized values for __104802849 lujavrite and for leaching solutions.

MINERAL CHEMISTRY OF REE-RICH APATITE AT THE MUSHGAI-KHUDAG CARBONATITE-ALKALINE COMPLEX, SOUTH GOBI, MONGOLIA

Enkhbayar D.[1], Seo J.[1], Lee Y.J.[1], Choi S.G.[1], Batmunkh E.[2]

1 Department of Earth and Environmental Sciences, Korea University, Seoul, Korea (Dorjpalma.E@gmail.com)
2 Central Geological Laboratory of Mongolia, Ulaanbaatar, Mongolia

We investigated REE apatite ore and its mineral chemistry of Mushgai-Khudag carbonatite associated with alkaline complexes located at South Gobi, Mongolia. Four different main mineralization zones are found in the study area: 1) REE enriched in carbonatite called as main zone (MZ), 2) REE enriched in fluorapatite and hydroxyl-flourapatite called as apatite hill zone (AHZ), 3) LREE + Fe enriched in magnetite called as Tumurtui zone (TZ), and 4) LREE enriched in fluorapatite, and hydroxyl-fluorapatite with monazite, called as high grade zone (HGZ). It is found that REE mineralization occurs along with the peripheries of alkaline massive consisting of porphyry syenite, micro syenite and quartz syenites. REE-rich apatite are mainly found within phlogopite-apatite, brecciated-apatite, celestine-apatite, and monazite-rich apatite in the AHZ and HGZ. Among of these zones, high REEs are shown within the apatite. It is also found that the ores are classified as metasomatized apatite, showing that grade is greater than 10 wt. % REEs.

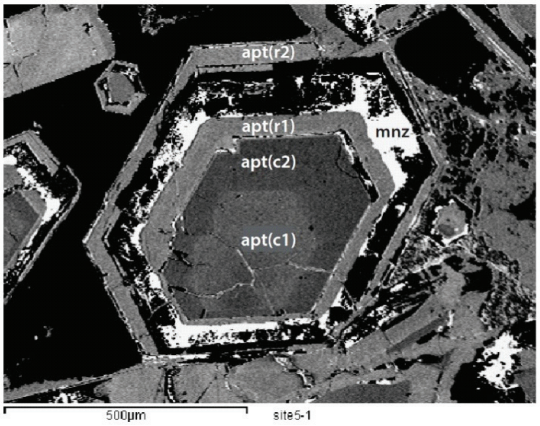

Figure 1: BSE image of apatite and monazite in the high grade zone, Mushgai-Khudag deposit. The apatite show the alterative zonation with monazite band.

A particular interesting of REE minerals is an individual sulfatian-monazite grain having high REEs, and these minerals occurs along with the rim of compositional zoning fluorapatite and hydroxyl-fluorapatite grains. The compositional zoning of the apatite in the back scattered electron image can be discerned to mostly core1 (c1), core2 (c2), and rim1 (r1), rim2 (r2) areas in the HGZ (Fig.1). The bright area such as c1, r1, and r2 have range of (11.7~18.5 wt. % Ce_2O_3+-La_2O_3+Nd_2O_3), whereas dark part of apatite (c2) contains depleted LREE contents (about 10~11 wt. % Ce_2O_3+La_2O_3 +Nd_2O_3)

The REE-bearing apatites from the Mushgai-Khudag deposit are mostly pure fluorapatite to hydroxyl-fluorapatite with variable REE content (Fig. 2). The composition of monazite ranges show 60~98 mol. % monazite $(LREE)PO_4$, and contains 2~40 mol. % anhydrite and celestine $(Ca,Sr)SO_4$ (max.14 mol. % $ThSiO_4$, Fig. 3).

The more strong depletion of LREE at the core 2 than core1, is well matched by depletion in Si and Na, indicating the coupled substitution reactions; (1) $Si^{4+}+(Y+REE)^{3+}=P^{5+}+Ca^{2+}$ and (2) $Na^{+}+(Y+REE)^{3+}= 2Ca^{2+}$. At the rim1, show extremely enrichment of Ce and La than core 2. Enrichment of LREE and P is accompanied with depletion in Si, Na and S, implying operation of two different coupled substitution reactions; (3) $2P^{5+}=Si^{4+}+S^{6+}$ and (4) $2P^{5+}+LREE^{3+}=2S^{6+}+Na^{+}$ (Harlov et al., 2003).

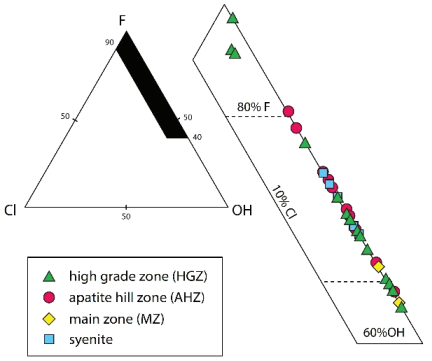

Figure 2: Apatite solid solution amaong F-OH-Cl end-members (Fleet and Pan, 1995). The apatites mostly show fluorapatite in Mushgai-Khudag deposit, Mongolia.

At the monazite zone, individual sulfatian-monazite was formed due to Si and Na leaching out from apatite structure and sulfatian-monazite structure (Y+REE) are charge balanced through coupled substitution reaction (1) and (2). The monazite are charge balanced by the complex substitution reactions; (5) $Ce^{3+}+P^{5+} = (Ca, Sr)^{2+}+S^{6+}$ (Chakhmourdian and Mitchell, 1999). Note that the high grade REE within the apatite depend on the metasomatized fluorapatite and hydroxyl-fluorapatite with high REE content of sulfatian-monazite inclusions or individual grains, suggesting that the Mushgai-Khudag deposit is affected by a variety metasomatism of sulfate-rich fluid complexes with REE in the last stage of mineralization.

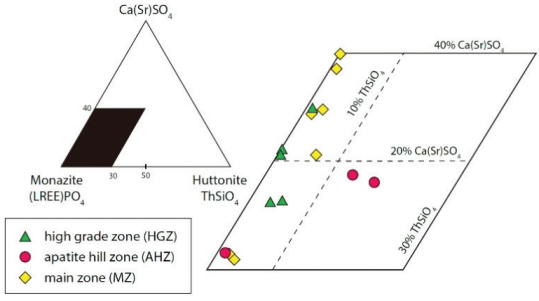

Figure 3: The composition of monazite expressed in mol. %, anhydrite+celestine, monazite, and huttonite (after Erwin et al., 2011).

References

1. Erwin K., Hubert P., Fritz, F. 2011. Sulfur-rich monazite with high common Pb in ore-bearing schists from the Schellgaden mining district (Tauern Window, Eastern Apls). Miner Petrol. v. 102, p. 51–62.
2. Chakhmouradian, A.R., Mitchell, R.H. 1999. Niobianilmenite, hydroxylapatite and sulfatian monazite: Alternative hosts for incompatible elements in calcite kimberlite from internatsional'naya, Yakutia. The Canadian Mineralogist. v. 37, p. 1177–1189.
3. Fleet M.H., Pan, Y. 1995. Site preference of rare earth elements in fluorapatite. American Mineralogist. v. 80, p. 329–335.
4. Harlov, D.E., Forster, H.J, Schmidt, C. 2003. High P-T experimental metasomatism of a fluorapatite with significant britholite and fluorsellestadite components: implications for LREE mobility during granulite-facies metamorphism. Mineralogical Magazine. v.67, p. 61–72.

GENESIS OF THE WEISHAN LREE DEPOSIT IN THE SHANDONG PROVINCE, EASTERN CHINA: EVIDENCES FROM RB-SR ISOCHRON AGE, LA-MC-ICPMS ND ISOTOPIC COMPOSITION AND FLUID INCLUSION

Fan H.R., Lan T.G., Hu F.F., Yang K.F.

Key Laboratory of Mineral Resources, Institute of Geology and Geophysics, Chinese Academy of Sciences, Beijing 100029, China
fanhr@mail.iggcas.ac.cn

Weishan LREE deposit, a pegmatite-type REE deposit related to alkaline rocks and the third largest LREE deposit in China, is located at Luxi Block, southeastern North China Craton. According to muscovite Rb-Sr isochron, it formed at the age of 119.5 Ma, which belonged to the early Cretaceous large-scale mineralization in the North China Craton. LA-ICPMS Nd isotopic compositions of bastnaesite and monazite indicate that the source of the REE minerals is the enriched lithospheric mantle. Observation of fluid inclusions in quartz, fluorite and barite shows that four types of inclusions can be identified, including (1) H_2O inclusions, (2) pure CO_2 inclusions, (3) H_2O+CO_2 inclusions and (4) H_2O+CO_2+daughter mineral inclusions. The H_2O inclusions are secondary inclusions while others are primary inclusions. The daughter minerals in H_2O+CO_2+daughter mineral inclusions include thenardite, barite, celestine, calcite, aphthitalite and glauberite. The homogenization temperature and capture pressure of H_2O+CO_2 and H_2O+CO_2+daughter mineral inclusions range from 205 °C to 433 °C and 120 MPa to 200 MPa, respectively. Coupled with the existence of abundant daughter minerals and sulphur stable isotopic compositions, it can be deduced that the initial ore-forming fluids were high-temperature, moderate-pressure and high-concentration orthomagmatic fluids, which were characterized by enrichment of HCO_3^- /CO_3^{2-}, SO_4^{2-} and F^- and multicomponent (e.g., Na^+, K^+, Ca^+, Ba^{2+}, Sr^{2+} and REE^{3+}). The coexistence of C, HC and HCD inclusions and the wide range of liquid/vapour ratios between these inclusions suggest that fluid unmixing may have occurred during ore-forming process. REE were most probably transported as $REEF^{2+}$ and precipitated through fluid boiling. Fluids mixing, which contributed little to the REE precipitation, also happened in the late stage of the ore-forming process.

PETROLOGY OF META-ULTRAMAFIC ROCKS IN THE KHOY OPHIOLITIC COMPLEX, NW IRAN

Faridazad M.

Sahand University of Technology, Sahand New town, Iran
Faridazad@sut.ac.ir

The study area is part of Khoy Quadrangle which is located between eastern longitudinal 44° 36′ 02″ to 44° 57′ 01″ and northern latitude 38° 37′ 22″ to 38° 54′ 16″. The Khoy quadrangle is in the northwest of Iran and with regard to divisions of Iranian units of sedimentary and structure, belongs to colored mélange and Alborz-Azarbaijan (Central Iran) that are divided to two structural subarea: Zurabad (from colored mélange zone) and Ishgasu (Alborz-Azarbaijan). In this region crops out sedimentary, metamorphic basement, volcanic and plutonic rocks from late Precambrian to Holocene with NW-SE trend.

Petrographically the study rocks are the vast rage of metamorphic and igneous rocks that are: serpentinized ultramafics, serpentinites, talc-schists, amphibolits, chlorite-schists, epidote-schists, actinolite-schists, chloritites, greenstons, actinolities, epidosites, phyllites, schists, calcschists, meta-diabases, meta-gabbros and granitoids. These rocks are metamorphosed under Greenschist to Upper Amphibolite facies during seafloor and dynamothermal metamorphism (Faridazad, 2010).

According to mineral chemistry studies in serpentinized perdotites, the composition of olivines is from $Fo_{89.46}$ $Fa_{10.37}$ $Tp_{0.17}$ to $Fo_{89.86}$ $Fa_{10.0}$ $Tp_{0.14}$ and Mg number ($Mg^{\#}$ = Mg/(Mg+Fe^{2+})) all of analyzed points is 0.90 and the composition of olivines is forsterite type. The composition of orthopyroxenes is from $En_{86.022}$ $Wo_{2.491}$ $Fs_{9.368}$ $Ac_{0.0}$ to $En_{87.314}$ $Wo_{6.719}$ $Fs_{10.474}$ $Ac_{0.319}$ and Mg number ($Mg^{\#}$ =Mg/(Mg+Fe^{2+})) all of them is 0.90 and the composition of orthopyroxenes is enstatite type. Prominent character of this orthopyroxens is having relatively high Cr (Cr_2O_3=0.59-0.82). The composition of clinopyroxenes is from $En_{44.159}$ $Wo_{46.910}$ $Fs_{4.323}$ $Ac_{1.459}$ to $En_{46.803}$ $Wo_{49.589}$ $Fs_{4.786}$ $Ac_{2.081}$ and Mg number ($Mg^{\#}$ = Mg/(Mg+Fe^{2+})) them is 0.91. The studied clinopyroxenes are high Cr-rich (Cr_2O_3=0.87-1.21) and are diopside type. Cr-rich orthpyroxenes and clinopyroxens indicate low partial melting of peridotites. Mineral chemistry studies show the relation of these peridoties to oceanic environment and as a result the oceanic environment can be considered tectonic setting of them. As well as high Mg number of above mentioned minerals and high forsterite in olivines indicate tectonite origin for them (Faridazad, 2010).

Whole rock studies on serpentinized peridotites indicate that they are tectonite type. As well as classification of these rocks according to Norm calculation indicate that they are Lherzolite, Harzburgite and Dunite and form in both MOR and SSZ setting. According these studies the studied peridotites were suffered low partial melting (less than 15%) in redox conditions. Therefore they probably have formed in development time of tensional basin of Khoy sialic back arc in late Jurassic (Faridazad, 2010).

Different models are presented for explanation of geotectonic development of this area that among of them tectonic model of Moayyed (1381) is considered acceptably. In this model the basin of Khoy is considered back arc extensional basin. In this model with regard to lack of outcrops of sediments of passive margin type in southwest of Khoy basin and forming of colored mélange he believe that Khoy complex is formed in a sialic back arc extensional basin. With

accord to his opinion, observation of island arc and active continental margin characteristics in basic metamorphites in this area are indication of effects of continental crust in geochemical characteristics of eruptive basalts in this basin.

References

1. Faridazad M., 2010. Petrology and petrography of metamorphosed ultramafic and mafic rocks in the Khoy ophiolitic complex (NW Iran), PhD thesis, University of Tabriz. 205p. (in Persian)
2. Moayyed M., 2002. New insight for creation and development of Neotethys and its relation to Urmia-Dokhtar and western alborz-Azarbaijan magmatism, proceedings of 6th symposium of geological survey of Iran, Shahid Bahonar University, Kerman, 374-378. (in Persian)

PETROLOGICAL AND GEOCHEMICAL INVESTIGATION ON A CARBONATE-DYKE FROM THE VAL MASTALLONE (IVREA-VERBANO ZONE): EVIDENCE OF A CUMULATE CARBONATITE IN THE LOWER CRUST?

Galli A., Grassi D.N., Schwab L., Schenker F.

Department of Earth Sciences, ETH Zurich, Sonnegstrasse 5, 8092 Zurich, Switzerland
andgalli@hotmail.com

The Ivrea-Verbano Zone (NW Italy / S Switzerland) represents one of the best exposed mantle-crust sections worldwide. Its geological evolution has been controlled by the underplating of large volume of mantle-derived basic magmas ("Mafic Complex") into the amphibolite to granulite facies metamorphic basement of the Southern Alps ("Kinzingite Formation") in Permian time.

Widespread in the Ivrea-Verbano Zone, marbles and calcsilicates occur as concordant lenses and bodies intercalated with paragneisses and micaschists of the Kinzingite Formation, or as up to 40 m thick, grey-brownish, partly discordant carbonate-dykes through upper amphibolite to granulite facies paragneisses and micaschists, mafic granulites, gabbros and ultramafic rocks. Commonly, these carbonate-dykes are composed of calcite, diopside, scapolite, sphene and contain up to 50 cm large, in part disrupted and altered, rounded or angular xenoliths of the host rocks. The dykes display sharp contacts to the host lithologies without any evidences of extensive zones of alteration.

However, in Val Mastallone (western Ivrea-Verbano Zone) an up to 40 m thick carbonate-dyke with different characteristics occurs within garnet-opx-cpx-bearing mafic granulites. This dyke is exclusively composed of coarse-grained calcite and clinopyroxene clasts. No scapolite is observed. The dyke cut across the high-grade main foliation of the host rock. The contacts to the host granulite are characterized by a 1.5 m thick, greenish zone of alteration constituted of actinolite, chlorite, clinozoisite, plagioclase, calcite, apatite, sphene, biotite, quartz and opaques. Up to 10-15 cm thick carbonate-apophyses intrude the host granulite. The dyke displays numerous, up to 2 m large xenoliths of black, coarse-grained, spinel-bearing clinopyroxenite. This rock type is not outcropping elsewhere in the proximity of the carbonate-dyke, suggesting that the clinopyroxenite was transported from a significant distance. Rare host mafic granulite inclusions are found exclusively in the marginal part of the dyke (ca. < 50 cm). Cross-cutting relationship, fluidal textures and the occurrence of xenoliths suggest that the investigated carbonate-dyke were intrusive into the host granulite.

Geochemical investigations on the carbonate-dyke from Val Mastallone yield an average major-element composition of SiO_2 = 7.9 wt%, TiO_2 = 0.27 wt%, Al_2O_3 = 2.38 wt%, FeO = 1.82 wt%, MnO = 0.04 wt%, MgO = 2.29 wt%, CaO = 50.12 wt%, Na_2O = 0.05 wt%, K_2O = 0.02 wt%, P_2O_5 = 0.02 wt%. Considering the trace-element composition, the carbonate displays Sr and Ba contents of 1457 ppm and 447 ppm, respectively. The dyke shows an enrichment of LREE over HREE ((La/Yb)N = 14), with a Σ REE = 338 and Y/Ho ratio of 27 close to the primitive mantle composition. On the chondrite-normalized REE abundances diagram, no Eu anomaly is observed. Mantle-normalized pattern shows strong negative anomalies at Rb, K, Zr,

Hf and Ti and a less pronounced negative Pb anomaly. The above described characteristics have strong similarities with the "world average carbonatites" but, in comparison with them, the Val Mastallone dyke shows lower absolute trace element concentrations. Nevertheless, the measured concentrations are significantly higher than typical limestone compositions and similar to cumulate carbonatites found elsewhere in the world (e.g. India, China and Brazil).

The enclosed clinopyroxenites have the following average composition: SiO_2 = 43.23 wt%, TiO_2 = 1.75 wt%, Al_2O_3 = 14.37 wt%, FeO = 9.08 wt%, MnO = 0.11 wt%, MgO = 8.55 wt%, CaO = 21.92 wt%, Na_2O = 0.43 wt%, K_2O = 0.006 wt%. Except for the concentration of alkalis, which may have been partly removed through reactions with the host carbonate, the pyroxenites are geochemically very similar to Triassic alkaline hornblendite-dykes and gabbroic pipes occurring widespread in the Ivrea-Verbano Zone.

Several field observations including i) cross-cutting relationship and metasomatic reactions at the contact to the country rock, ii) fluidal texture and iii) the occurrence of clinopyroxenite xenoliths with a strong compositional similarity to alkaline dykes from the Ivrea-Verbano Zone, together with the geochemical characteristics explained above, strongly suggest that the carbonate-dyke from Val Mastallone may be a cumulate carbonatite (sövite) crystallized within the lower crust. This carbonatitic magmatism is most probably related to the Triassic CO_2-bearing alkaline magmatism and metasomatism occurred in the Ivrea-Verbano Zone during the early stage of the opening of the Thetyan Ocean.

DIAMONDS FROM RUSSIA

Garanin V.K.[1], Garanin K.V.[2], Kriulina G.Y.[2]

1 A.E. Fersman Mineralogical Museum, Russia
vgaranin@mail.ru
2 M.V. Lomonosov Moscow State University, Russia,

The first documented discovery of diamond in Russia dated 5th of June, 1829. It was in Perm Area (Ural Mountains, Central Russia). The 0.5 carat diamond was recovered by P. Popov who was washing heavy minerals concentrate for gold. The unusual stone was detected as a diamond by the geologist F. Schmidt. Later diamonds have been recovered from sediments in large area, and exploration of placer diamond deposits was started at western flank of Ural Mountains in1937. Since 1942 mining was started. Only placer diamond deposits have been recognized in Ural and its primary source is still undiscovered.

In 1897 first diamond was discovered near Eniseysk town (Western Siberia, Eastern Russia). After 50 years first diamonds have been recovered from stream sediment samples collected in Sokolinaya bar in 1947 (Western Yakutia). Intensive exploration allowed discovering first primary deposit – Zarnitsa kimberlitic pipe in 1954. Pipe was found by L. Popugaeva and N. Sarsadskikh. Since that time many rich placer deposits and unique primary deposits have been recognized in large area of northern Yakutia. Presently it is the main diamondiferous province in Russia where more than 1200 pipes of kimberlitic and related rocks are known.

In 1904 peasant and enthusiast-miner I. Popov sent a parcel to the Mining Department of Russia where he put identified himself stone as a diamond and description book. Thus, he informed the Department about first discovery of diamond near his village Lebskaya, Mezenskaya Area (Archangelsk Region, Northern-Western Russia) and asked funds for exploration works. However he did not receive any answer. Only after 50 years in 1955 during exploration works first documented diamond was discovered near Mezenskaya Pizhma River in Archangelsk Region. Long time the local sources of diamonds could not be recognized and only in 1977 several diamonds have been recovered from sediments. In 1980 first kimberlitic pipe Pomorskaya was discovered. Presently more than 150 pipes of kimberlites and related rocks have been recognized in Archangelsk province including industrial ones. The placer deposits are absent in Archangelsk province.

The all mined Russian kimberlitic deposits are Devonian-Carbonic age and content of mostly ancient Archaean diamonds. The total diamond reserves are 1 billion carats. More than 77% of reserves and 88% of resources are located in Yakutian province. By the date more than 1500 kimberlitic and related rocks pipes have been discovered, but there are only 22 economical ones (1.5 % of total) with total production of all recovered diamonds in the country. The averages grade of kimberlitic deposits is varying from 0.8 to 8.8 carats per ton. Kimberlitic pipes have been mined mostly by open pits, but according to complexity of geological environment underground mining was started. Some pipes were mined totally, some are in exploration stage, but running mines produce 94% of total diamonds. The quality and range of color of diamonds from Russian deposits are significantly high compare to the other World's deposits. The 342.57 carats crystal was the biggest diamond recovered in Russia, but some authors mentioned discoveries even bigger diamonds.

44 industrial discovered placers put together only 6% of total national diamond reserves now. 37.9 million carats of diamonds have been recovered in 2013.

Russia is one of the major producers of diamonds both by their value and quantity. The total value of exported diamonds (26.8 million carats of gem quality and 8.5 million carats of industrial diamonds) was 4.4 billion US$. The average price of exported Russian diamond was 88 US$ per carat (Ministry of Finance undervaluation), though gem quality diamonds exported by ALROSA Company have been estimated as 176 US$ per carat.

Diamonds are presented as phenocrysts in groundmass and mantle rock xenoliths of kimberlitic rocks. The size of diamonds is varying from microns to several centimeters. Every year individual diamonds with weight >50 carats recovered in Russia.

More than 12,000 carats of diamonds from Yakutian and Archangelsk provinces have been investigated in Diamond Deposits Laboratory of M.V. Lomonosov Moscow State University and A.E. Fersman Mineralogical Museum of Russian by microscopy and IR-spectrometry techniques. There were diamonds in following size categories: -8+4, -4+2, -2+1 mm. Yakutian diamonds have been collected from industrial diamond deposits: Mir, Internatsionalnaya, Dachnaya pipes (Mirniskoe field, Malobotuobinsky Area); Yubileynaya and Komsomolskaya pipes (Alakit-Markhinskoe field, Daldyn-Alakitsky Area); Udachnaya pipe (Daldyn field, Daldyn-Alakitsky Area); Nurbinskaya and Botuobinskaya pipes (Nakynsky field, Sredne-Markhinsky Area). Archngelsk diamonds have been collected from industrial deposits: V. Grib pipe (Chernoozerskoe field); Archangelskaya and Karpinskogo-1 pipes (M.V. Lomonosov deposit, Zolotitskoe field). Some of Archangelsk diamonds have been collected from uneconomical pipes: Snegurochka, Pervomayskaya and Koltsovskaya (Zolotitskoe field).

88-98% of Yakutian and 60-87% of Archangelsk diamonds refer to I^{st} group of Y. Orlov classification (1973). For instance 98-99 % of Ural placers diamonds are related to I^{st} group. Yakutian diamonds are mostly presented by octahedrons. Dodecahedrons are prevailing among Archangelsk diamonds, but the ratio between different habitus forms is varying for individual pipes (Palazhchenko, 2008).

Diamonds of II^{nd}, III^{th} groups are rarely and V^{th} group are very rarely occurring in Yakutian pipes (≤3% of total), while there are quite many V^{th} group diamonds in M.V. Lomonosov deposit and V. Grib pipes (mostly grey and black crystals of dodecahedron or combinational habitus). Cubic crystals are distributed in Zolotitskoe field (10-15% of total) and V. Grib (6%) pipes. Diamonds of IV^{th} group are very rare in kimberlites of Zolotitsky and Chernoozerskoe fields of Archangelsk province, but presented in pipes of Nakynskoe (10%) and Alakit-Markhinskoe fields (2-8%) of Yakutian province (Palazhchenko, 2008).

Yakutian diamonds have high N_{tot} (≤1000 ppm) and N_B (50-95%) content, H and platelets concentrations are significantly lower than in diamonds from Archangelsk province (Palazhchenko, 2008). Thus, Yakutian diamonds are showing the evidences of longer post-crystallizing annealing compare to Archangelsk diamonds.

Archangelsk diamonds have bimodal distribution of N-impurities, with domination of A-centers. There are bimodal- and trimodal-distribution of H and platelets impurities. The content of N_{tot} is higher for macro-diamonds compare to micro-diamonds.

4 general populations of diamonds have been distinguished for Archangelsk diamonds: nitro-

gen-free, moderately nitrogenous, middle nitrogenous and high-nitrogenous (Kopchikov, 2009).

Yakutian diamonds also presented by 4 general groups distinguished (according to N-, H-defects, and their ratio) based on morphogenetic analyze and IR-spectroscopy data.

Totally 7 groups of diamonds have been distinguished for Yakutian and Archangelsk provinces (Fig. 1) based on their characteristics (N and H concentrations and their ratios). These diamonds present different petrochemical types of kimberlites separated by titanium-content.

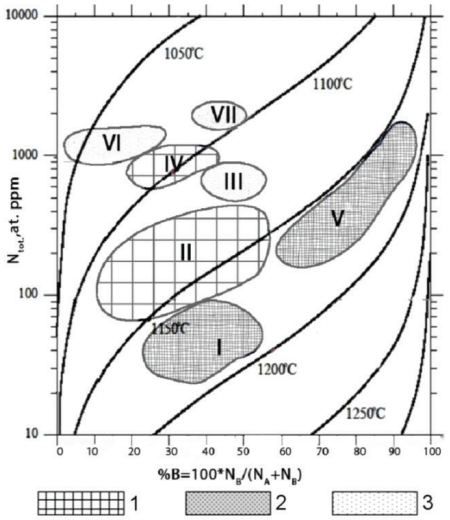

Figure 1: N-concentrations for Archangelsk and Yakutian diamonds (type IaAB) with adaptation on Taylor W.R. and Milledge H.J. graph (1995). Calculated diamond age – 3 billion years.

Groups of diamonds: 1. Low-titanium (≤ 1 wt.% TiO_2) and moderate titanium (1<TiO_2<2.5 wt.%) kimberlites, 2. Typical for low-titanium kimberlites, 3. Typical for moderate titanium kimberlites.

Morphogenetic groups of Archangelsk and Yakutian diamonds: I. Nitrogen-free, II. Low nitrogenous, III. Moderate nitrogenous, IV. Middle nitrogenous low-aggregated, V. Middle nitrogenous highly-aggregated; VI. High nitrogenous low-aggregated, VII. High nitrogenous moderately aggregated

Thus, it was possible to conclude the diamonds from diamonds deposits (fields, areas, and provinces) present special morphogenetic groups, which may be distinguished according to the differences in physicochemical and PT-conditions, and also duration of diamond genesis and formation.

The diamond grade, quality, its morphological features are generally correlated with petrochemical composition of kimberlites: higher Mg and Cr content is in higher diamondiferous kimberlites, while higher content of Ti, Al, Fe and Mn in kimberlites indicates lower grade, smaller size of diamonds, and such diamonds have higher dissolution and corrosion grade.

There are several genetic types of diamonds in Russia, but only kimberlites build up the industrial deposits including its residual placers. However, the huge volume of diamonds has been discovered in Popigay impact structure.

The Popigay structure is giant meteoritic crater with 100 km in diameter. It is located in Northern part of middle Siberia, 900 km east of Norilsk town and was discovered at the beginning of 1970th. The age of cryptoexplosion structure is 35,7±2 million years. The diamond grade is significantly high, sometimes several tens carats per ton. Accoding to V.L. Masaitis opinion: "The total resources of impact diamonds at that area is more than total resources of diamondiferous provinces all over the World".

Diamonds of Popygay are presented as polyphase aggregates. As usually there are lonsdaleite with impurities of graphite; diamond, lonsdaelite and graphite; or diamond and lonsdaelite. The quality of Popigay diamonds is significantly poor and in spite of huge resources of diamonds the deposit is not mined.

Thus, Russia has unique diamond deposits located in Yakutian, Archangelsk and Ural provinces. Significant reserves and resources of diamonds allow predicting successful mining of diamond deposits in future. But diamond is not only industrial material, but also it is a source of precious knowledge about our planet.

References

1. Kopchikov, M.B. 2009. Typomorphic features of diamond from Archangelsk diamondiferous province. PhD thesis, Moscow: M.V. Lomonosov Moscow State University, 17 p. In Russian
2. Orlov, Y.L. 1973. Mineralogy of diamond. Moscow: Nauka, 264 p. In Russian
3. Palazhchenko, O.V. 2008. Diamond from the deposits of the Archangelsk diamondiferous province. Ph. D. Thesis. Moscow: M.V. Lomonosov Moscow State University, 24 p. In Russian
4. Taylor, W.R., Milledge, H.J. 1995. Nitrogen aggregation character, thermal history and stable isotope composition of some xenolith-derived diamonds from Roberts Victor and Finch // Extended Abstr. of the 6-th Int. Kimberlite Conf. Novosibirsk. P. 620–622.

ALKALINE-ULTRAMAFIC MAGMATISM IN DIAMONDIFEROUS AREAS IN THE WESTERN URALS (PERM REGION)

Lukianova L.I., Goloburdina M.N.

Russian Geological Research Institute (VSEGEI), St. Petersburg, Russian Federation
marina_goloburdina@vsegei.ru

Rare potassic alkaline-ultramafic rocks were studied in the western slope of the Middle Urals (Perm Region) in the multiphase Blagodatsky Massif [1]. They are represented by olivine-sanidine lamproite and kimberlite. Based on materials of bore-hole sections of up to ~ 500 m deep and trenches (~ 3.5 m x 2 km), it was identified that thin alkaline-ultramafic rock bodies consist of pipe-like, vein and dyke intrusions. Alkaline-ultramafic rocks are associated in the massive with essexite-dolerite, trachydolerite (PZ_2) and trachybasalt (V_2). Rock contacts between one another and with terrigenous rocks (V_2) and sandstone (D_1) are tectonic or intrusive.

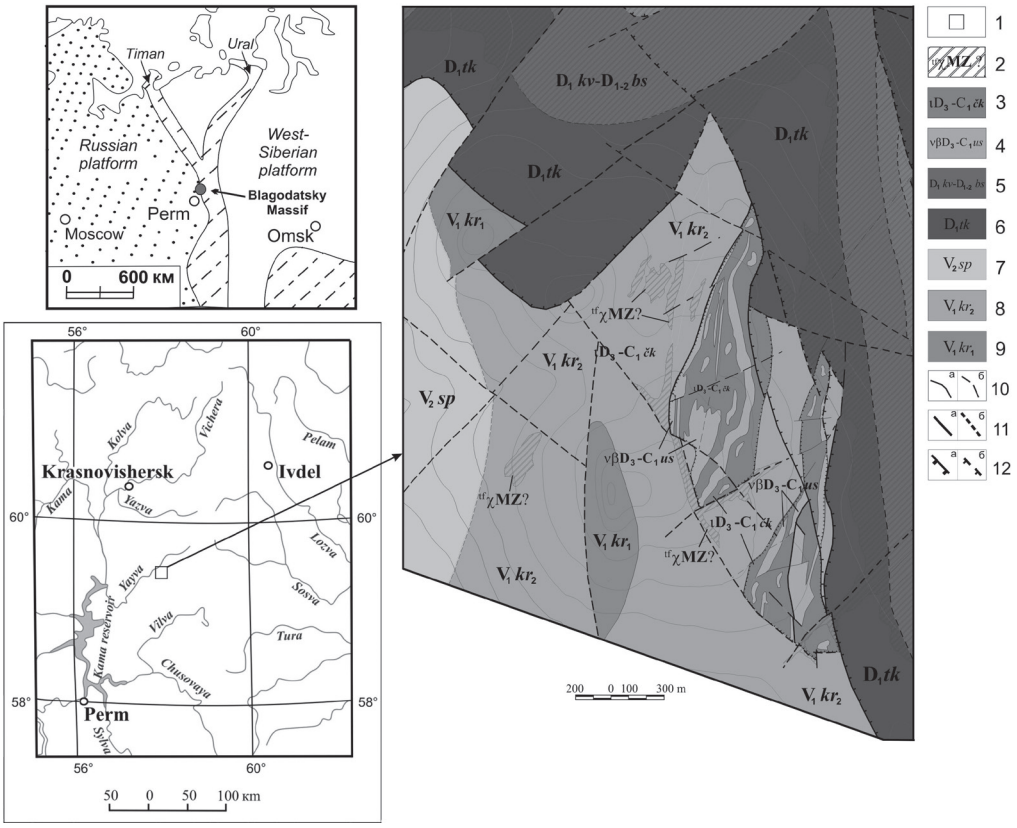

Figure1: Location of potassic alkaline ultramafic rocks and geological map of the Blagodat mountain north site

[Based on "Diamondiferous fluid-explosive formations Perm Cisurals", 2011].

Legend: 1 - Blagodftsky Massiv; 2 – clayed fluid-explosive rocks of kimberlite-lamproite type; 3 – kimberlites; 4 – dolerites-trachydolerites; 5,6 - carbonate-terrigenous rocks (D); 7,8,9 - igneous-sedimentary rocks (V); 10 – geological boundaries: a - certain; b – assumed on geophysical investigations; 12 – thrusts: a – certain; b – assumed.

Rock-forming minerals of the studied rocks are represented by pseudomorphically substituted olivine, leucite, melilite, and mica and diagnosed on the basis of characteristic crystallographic shape and composition of their substitution products. Kimberlite are represented of melilite-beraing and leucite- melilite-bearing varieties. Probably, leucite- melilite-bearing rocks are an extreme member of Group II kimberlites. Such kimberlites are known in the Kroonstad area, South Africa (Besterskraal North, Voorspoed Mine) [2]. The kimberlites are dominated by breccias of diatreme facies. They are composed of altered, including carbonated kimberlites containing xenoliths of deep (mantle) rocks, rock debris of the basemen, sedimentary cover, including trachybasalt (V). Microprobe analysis showed the presence of low content of sodium (Na2O~ 0,52 and 1,85 %) admixture in sanidine of the olivine-sanidine lamproites (?) that is chemically typical of the sanidine from lamproite (Mitchell, Bergman, 1991). Accessory minerals of rocks are rare pyrope of lherzolite paragenesis, diopside, chrome-spinelide, picroilmenite and large zircons similar to those of kimberlite. Single diamonds of dodecahedroid shape have been found in bulk samples of the breccia of melilite-bearing kimberlites. They are typical of alluvial diamond occurrences and deposits of the Urals.

Chemical composition of the rocks varies widely due to superimposed transformations expressed in chloritization, silicification, carbonatization, micatization, hematitization, leucoxenization, albitization. Distribution of rare elements and rare earth elements in alkaline-ultramafic rocks are similar to those in kimberlites of the of Mid-Timan, and Zolotitsky and Nakynsky fields (Fig. 2).

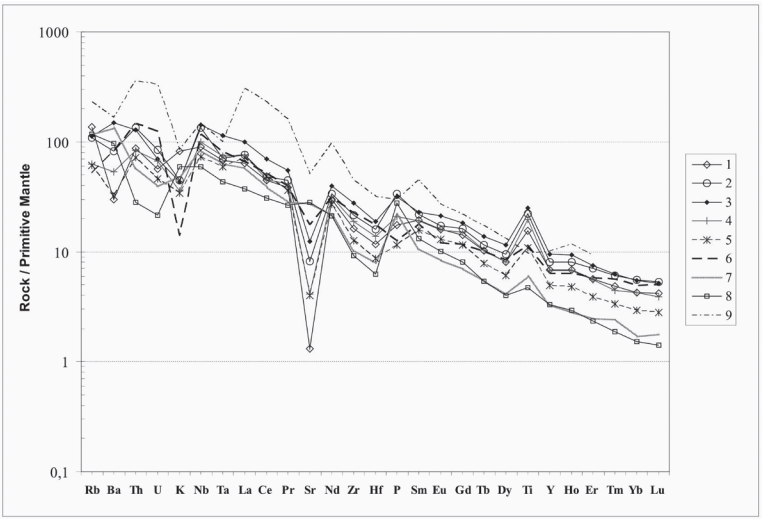

Figure 2: Distribution of rare and rare earth elements in alkaline-ultramafic rocks of the Blagodatsky Massif as compared to the kimberlites of Mid-Timan, ADP, YDP and South Africa (Kroonstad area).

Legend: alkaline-ultramafic rocks of Mount Blagodat: 1 – breccia of melilite-bearing kimberlites; 2 – leucite-melilite-bearing kimberlites; 3 – melilite-bearing kimberlites; 4 – olivine-sanidine lamproites (?); 5 - carbonatized kimberlite breccias; kimberlites in different areas of the world: 5 – pipe Umbinskaya, Mid-Timan [Bogatikov, Kononova et al, 2004]; 6 – pipe Pionerskaya of the Zolotitsky field ["Arkhangelsk Diamond Province", 1999]; 7 – pipe Nyurbinskaya of the Nakyn field [Bogatikov, Kononov, Golubeva et al, 2004]; 8 – pipe Voorspoed, South Africa [2]. Normalization is according to Taylor&McLennan (1988).

Rare (Nb, Zr, Ta, etc.) and rare earth elements grades are sharply decreased in carbonatized breccia of melilite-beraing kimberlites (Fig. 2). Therefore, carbonatization of the studied rocks is a superimposed hydrothermal metasomatic process resulted from the presence of host carbonate strata in the section as evidenced by isotopic data (Table 1).

Table 1. Isotopic data C, O, $^{87}Sr/^{86}Sr$ of carbonates of Blagodatsky Massiv rocks

№ п/п	$\delta^{13}C$, ‰, $_{VPDB}$	$\delta^{18}O$, ‰, $_{VSMOW}$	$^{87}Sr/^{86}Sr$
1	-1,7	19,3	-
2	-4,7	23,9	0,709006±14
3	-1,4	27,1	-
4	-5,4	26,8	0,708435±21
5	2,9	31,4	-

Note: № 1-3 – carbonatized kimberlite breccias; № 4 – chlorite–calcite-dolomite rock;

№ 5 - xenolit of spinel peridotite. Centre of Isotopic Research of VSEGEI.

Isotopic dating of zircons (SRIMP-II) yields the age of the alkaline-ultrabasic rocks corresponding to the Middle Paleozoic (D_3-C_1) and shows that these occurrences are confined to the tectonomagmatic stage of kimberlite magmatism of the East European platform.

Thus, such formations could be a bedrock source of diamonds in the western slope of the Urals.

References

1. Goloburdina M.N., Lukianova L.I., Lepekhina E.N. 2014. Alkaline-ultramafic rocks of the Blagodat mountain (western slope of the Middle Urals). Regional geology end metallogeny. № 59. (in Russian).
2. Howarth G.H., Michael E., Skinner W., Prevec S.A. 2011. Petrology of the hypabyssal kimberlite of the Kroonstad group II kimberlite (orangeite) cluster, South Africa: Evolution of the magma within the cluster. Lithos. v.125 (1-2), p. 795-808

THE POTENTIAL FOR REE DEPOSITS ASSOCIATED WITH ALKALINE AND CARBONATITE MAGMATISM IN EUROPE

Goodenough, K.M.[1], Deady, E.A.[2], Shaw, R.A.[2] and the EURARE Work Package 1 Team

1 British Geological Survey, West Mains Road, Edinburgh, UK
kmgo@bgs.ac.uk
2 British Geological Survey, Keyworth, Nottingham, UK

The rare earth elements (REE) are a group of 17 chemically similar metallic elements, including the 15 lanthanides (lanthanum-lutetium) together with yttrium and scandium. They are used in a wide range of emerging technologies, particularly those required for the low carbon economy. Both the light rare earth elements (LREE) and the heavy rare earth elements (HREE) have been identified as critical raw materials in a recent report [1]. They are of vital economic importance to the European economy and yet the European Union (EU) is almost entirely dependent on imported supplies of the REE because of a lack of domestic production [1].

The EURARE project (www.eurare.eu) aims to establish a basis for the development of a sustainable European rare earth industry. This includes a review of all REE resources and occurrences in Europe, including both primary and secondary types. Primary resources are those formed by igneous and hydrothermal processes, whereas secondary resources are those resulting from the weathering and/or erosion of primary resources. This talk will focus on primary resources, and specifically the metallogenetic provinces associated with alkaline magmatism in Europe.

The largest European REE deposits are associated with alkaline magmatism in rift-related tectonic settings. Major rift systems in Europe are generally younger southwards, although there are some exceptions. Meso- to Neoproterozoic alkaline magmatism occurred around the margins of Archaean cratons in Greenland, Norway and Sweden. The northern part of the Baltic Shield hosts the major Devonian Kola alkaline province. Permo-Carboniferous rifts contain alkaline magmatism around craton margins in Norway and the UK, with subsequent Meso- to Cenozoic rifting in western Europe associated with opening of the Atlantic Ocean. Cenozoic rifts associated with alkaline magmatism arc across central and southern Europe from Spain to Turkey, including the Rhine Graben and the Massif Central. All these rift systems have the potential to host REE resources, but whereas the older provinces of northern Europe are deeply exposed, exposures in southern Europe are largely at the supracrustal level.

The currently most advanced REE projects are in intrusions associated with Mesoproterozoic alkaline provinces, these include Kringlerne and Kvanefjeld in the Gardar Province in Greenland, and Norra Kärr in Sweden. Carbonatites of a range of ages also represent potentially important European REE resources; these include Fen in Norway, Alnö in Sweden, Qaqarssuk (Qeqertaasaq) and Sarfartoq in Greenland, and Storkwitz in Germany. In Southern Europe, the shallower erosion level of the rift systems means that plutonic rocks are not exposed and potential REE resources may well exist at depth. In these areas, secondary deposits are currently of greater importance in terms of identified resources.

References

1. European Commission 2014. Report on Critical Raw Materials for the EU. http://ec.europa.eu/enterprise/policies/raw-materials/files/docs/crm-report-on-critical-raw-materials_en.pdf

DISTRIBUTION OF RARE AND RARE EARTH ELEMENTS BETWEEN GRT, CPX AND CB AT MANTLE PT (EXPERIMENTAL DATA).

Gorbachev N.S., Kostyuk A.V., Osadchy E.G.

Institute of Experimental Mineralogy RAS, Chernogolovka, Russia
gor@iem.ac.ru

Carbonatite melts play an important role in the upper mantle metasomatism, enriching its volatile and incompatible elements. To clarify the behavior of trace elements in the process of melting of carbonated mantle the distribution of trace and REE elements between Cpx, Grt and carbonate Cb were studied at P = 4 GPa, T in the range 1100-1350°C.

Experiments were carried out in Au and Pt capsules on an anvil-with-hole apparatus by a quenching technique. Products of experiments were studied and analyzed by electron microprobe and by ICP MS.

Distribution coefficients D of trace elements between Cpx, Grt and carbonatite melt Cb at P = 4 GPa, T=1100-1350°C showed broad (2.5-3 order) variation. High affinity for carbonate (D silicate / carbonate <1) have P, LREE, Sr, Ba, U, Th, Ta, and to silicates (D silicate / carbonate > 1) - Sc, Ti, Cr, Mn, Co, Ni, Cu, Zn (Fig. 1).

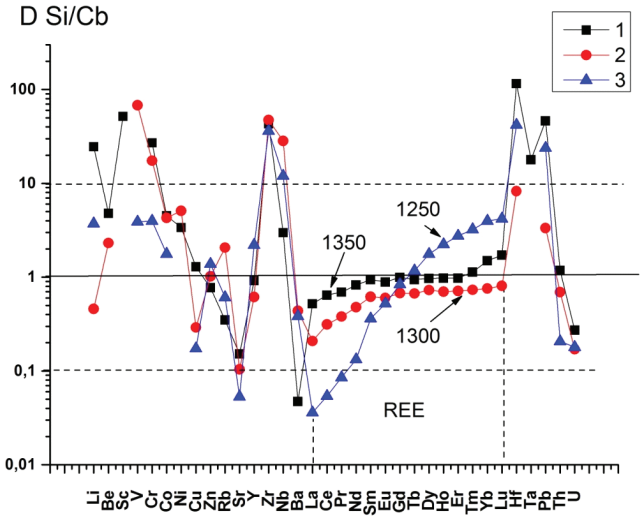

Figure 1: Distribution coefficients of trace elements between Cpx, Grt and Cb. P=4 GPa. 1-D Cpx/Cb, 1350ºC, 2-D Cpx/Cb, 1300ºC, 3- D Grt/Cb, 1250ºC.

In association with carbonate Grt is more efficient concentrator of trace elements than Cpx. Trend of D REE Si / Cb is positive. With increasing N D REE Grt / Cb increases from $n \times 10^{-2}$

at La to10 or more for Lu. D REE Cpx / Cb varies from n × 10^{-1} to 2 respectively. Effect of temperature on D REE Cpx / Cb is positive, on D REE Grt / Cb - negative (Fig. 2).

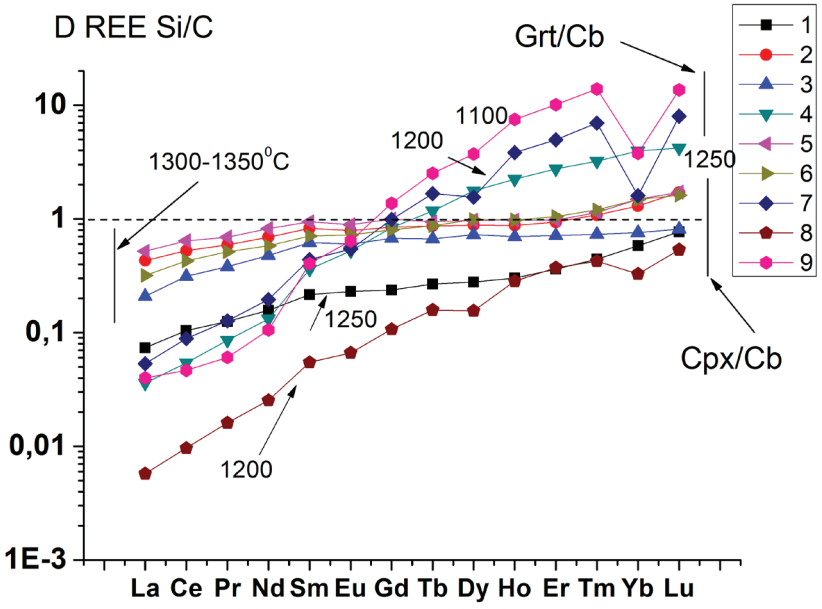

Figure 2: Distribution coefficients of REE between Grt, Cpx and Cb. 1 – Cpx/Cp T=1250°C; 2 - Cpx/Cp T=1300°C; 3 - Cpx/Cp T=1300°C; 4 - Grt/Cp T=1250°C; 5 - Cpx/Cp T=1350°C; 6 - Cpx/Cp T=1350°C; 7 - Grt/Cp T=1200°C; 8 - Cpx/Cp T=1200°C; 9 - Grt/Cp T=1100°C.

Significant (2.5-3 order) variation of the distribution coefficients D trace elements between Grt, Cpx and Cb indicate their effective fractionation in silicate-carbonate systems. The experimental data allow us to quantitatively model and predict the formation of deposits trace and REE in carbonatites.

Supporting by grant RFBR № 12-05-00777a

TRACE AND RARE EARTH ELEMENTS IN CARBONATES AND SILICATES OF CARBONATITES FENNOSCANDIAN SHIELD

Gorbachev N.S., Shapovalov Y.B., Sultanov D.M.

Institute of Experimental Mineralogy RAS, Chernogolovka, Russia.
gor@iem.ac.ru

Carbonatites of alkaline-ultrabasic igneous complexes are source of trace and rare earth elements. Their formation is connected with melting of enriched metasomatized mantle [1]. Explore of geochemistry peculiarity of carbonate (Cb) and silicate (Si)-containing component of carbonatite-bearing complexes is interest to understanding of genetic relationships among them. For this purpose carbonatites Fennoscandian Shield of three formation types and different age were studied:

Cb and granatitite Grt of carbonatite dikes from Caledonian cover Tromso area, Norway, (UHPC). Age ~ 452 ml years [2];

Cb and Cpx from carbonatite – alkaline - ultrabasic massif Kovdor (Kv), Kola Peninsula, Russia. Age ~ 440-360 million years [2] ;

Cb and pyroxenite Pxt from carbonatite – alkaline - basic masive Tiksha - Lake (TO), North Karelia, Russia. Age ~ 1800-1900 Ma [3].

Samples have been collected during fieldwork and scientific visits and were studied and analyzed by electron microprobe. Trace elements were determined by ICP MS in IPM RAS, Chernogolovka.

On spidergrams C_N (on the primitive mantle normalized concentrations REE and other trace elements) of Cb KV and TO characterized by similar negative trend. The general background trend highlighted negative anomalies C_N K, Li, Rb, Th, U, Nb, Zr. Cb UHPC different from Cb KV and TO, Cb UHPC have positive trend C_N LREE and lower their concentrations. Trend C_N HREE of Cb UHPC similar to Cb KV and TO. C_N REE in Cb of magmatic complexes of Kv, TO and UHPC Tromse are similar to carbonatite-bearing igneous complexes of the world, the sources of which are associated with mantle plumes (Fig. 1) .

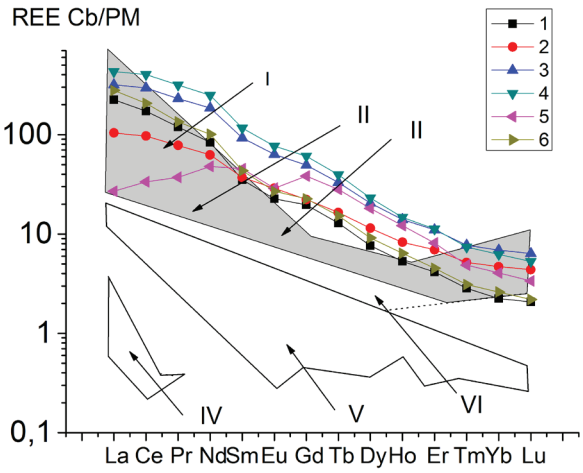

Figure 1: C_N REE in carbonatites : 1-4 - TO, 5 - UHPC, 6 - KV. I - Kergulen , II - Mongolia , II – S. Africa , IV- Spitsbergen, V- Tanzania, VI - Yakutia [3, with change].

Distribution of C_N trace elements in Si component of KV and TO differ from its Cb components. C_N of the most incompatible elements (from K to La) observed positive trend with maximum C_N at La, from Ce to Lu observed negative trend C_N REE. Ratio of the C_N trace elements between Si and Cb components (R_{Si} / Cb) of carbonatites UHPC, KV and TO is characterized by heterogeneous spectrum. Comparison of R_{REE} Grt, Cpx / Cb in UHPC, KV and TO with experimental distribution coefficients REE D_{REE} Grt, Cpx / Cb showed, that R_{REE} Grt / Cb UHPC differ from the experimental D_{REE} Grt / Cb, and R_{REE} Cpx / Cb in KV and TO massives are similar to the experimental D_{REE} Cpx/Cb.

Unlike R_{REE} Grt / Cb UHPC from experimental D_{REE} Grt / Cb shows lack of equilibrium between Grt and carbonatite melt UHPC. Similarity R_{REE} Cpx / Cb KV and TO and experimental D_{REE} Cpx /Cb can be regarded as evidence of a genetic link between silicate and carbonate magmas at their formation. This similarity is hereby confirms magmatic genesis of carbonatites.

Supporting by grant RFBR 12-05-00777

References

1. Kogarko L.N. New concept of genesis carbonatites. 1999. Carbonatites of Kola peninsula. StPet:Nauka, p. 72-90. (In Russian)
2. Gorbachev N.S. Ravna E. et al. Phase composition and geochemistry of carbonatites Tromse area, Norvai. Ore potential of alcalic, kimberlitic and carbonatitic magmatism. Moscov, Geokhi, (In Russian)
3. Metallogeniya of magmatic complexies intraplate geodynamic situation. 2001. M.Geos. 639p
4. Tschegg C, Ntaflos T., et all., 2012. Carbonate-rich melt infiltration in peridotite xenoliths from the Eurasian-North American modern plate boundary (Chersky Range, Yakutia). Contrib. Mineral Petrol. v. 164, N. 3, p. 441-455.

AS A GREEN ENERGY RESOURCE; TURKEY'S THORIUM POTENTIAL

Gungor A.

Akdeniz University, Department of Mechanical Engineering, Antalya, Turkey
afsingungor@akdeniz.edu.tr

Thorium is a chemical element with the symbol Th and atomic number 90. A thorium atom has 90 protons and 90 electrons, of which four are valence electrons. Thorium metal is silvery and tarnishes black when exposed to air. Thorium is weakly radioactive: all its known isotopes are unstable, with the six naturally occurring ones (thorium-227, -228, -230, -231, -232, and -234) having half-lives between 25.52 hours and 14.05 billion years. Thorium is estimated to be about three to four times more abundant than uranium in the Earth's crust, and is chiefly refined from monazite sands as a by-product of extracting rare earth metals.

The development of a nation is highly dependent on its energy sector. The energy sector of an economy interacts with demand, supply, technological progress, a technology′s market potential, the environment and the society. Good energy planning takes into consideration of all these variables and parameters. Energy is utilized in all sectors of the economy, broadly taken as industrial, commercial, agricultural and residential. Hence, energy plays a role in production in the industrial sector. From this point of view, Thorium which is a source of nuclear energy is a green raw material for nuclear power plants. Turkey has the %11 of the total Thorium reserve of the world. Thus, with that much of a very valuable reserve, careful use of the material may provide Turkey with a convenient, environmentally friendly and efficient energy source as the result of thorough scientific investigations.

Keywords: Thorium, green energy, nuclear energy, environment, energy resource.

PETROLOGICAL CONSTRAINTS ON THE QUATERNARY ALKALINE LAVAS IN CEYHAN - OSMANIYE AREA, SOUTHERN TURKEY

Güçtekin A., Aldanmaz E.

Department of Geological Engineering, Kocaeli University, TR-41380 Izmit, Turkey
guctekin@kocaeli.edu.tr

The Quaternary alkaline volcanic province of Southern Turkey is characterized by intra-continental plate-type magmatic products, exposed to the north of the Iskenderun Gulf along a NE-SW trending zone between Ceyhan and Osmaniye. The alkaline rocks are mostly classified as basanites and alkaline basalts with their low-silica contents ranging between 43 and 48 wt.%. The microphyric texture of these rocks is defined by the presence of numerous euhedral and resorbed olivine phenocrysts accompanied by lesser amount of plagioclase, clinopyroxene and titano-magnetite in a fine-grained groundmass. The volcanic rocks are characterized by Ocean Island Basalt (OIB)–type trace element patterns characterized by significant enrichment in LILE, HFSE and L-MREE, and a slight depletion in HREE, relative to N-MORB.

Quantitative trace element modelling of fractionation-corrected data indicates that mafic alkaline magmas formed by variable degrees of partial melting of a single mantle that is enriched in all incompatible elements relative to depleted MORB mantle (DMM) and/or Primitive Mantle (PM) compositions. Using dynamic melting inversion method and a set of selected parameters the average degree of partial melting has been identified to be 2% for the basanites and 8% for the alkaline basalts. The modeling based on relative abundances of trace elements suggests that the melting took place within a range of depth from garnet- to spinel-stability field. The negative anomalies in K and Rb can most likely be explained by existence of hydrous phase(s) such as phlogopite and/or amphibole in the mantle source region, which might, in turn, indicate the metasomatic nature of the source.

PETROGENESIS OF EL-KAHFA RING COMPLEX EASTERN DESERT, EGYPT

Hegazy H. A.

Geology Department – Assiut University, Egypt
hhegazy4451@yahoo.com

El kahfa Ring Complex (ERC) is a member of an alkaline province including complexes of similar size, structure and composition which crop out along the western margin of the Red Sea in Egypt. ERC (5x6 km) occurs as oval intrusion, rising up to 1018 m.a.s.l. at the intersection of latitude 24^0 08\ 18\\ and longitude 34^0 38\ 55\\, belongs to the youngest group of Phanerozoic ring complexes having an emplacement age of 92±5 Ma (Serecsists et al. 1981; lutz et. al. 1988). It is related to structural lineament trending N 30 W parallel to the Red Sea and was controlled by pre-existing deep crustal lines of weakness in the basement complex.

Field investigation revealed that ERC is composed of two intrusive phases, i.e. oldest one represented by essexite gabbros, intruded later by syenitic rock. The latter formed of inner zone of undersaturated syenites (i.e. Litchfieldite and cancrinite syenites), while the outer ring massif is composed of silica oversaturated syenites. The extrusive rocks of trachyte, basalt and rhyolite form plugs, sheets and ring dykes.

The mineralogical and chemical features show that these rocks belong to anorogenic interplate A-type alkaline suite (i.e. enriched in alkalis and HFS elements, Nb, Ta, Zr, Hf, Y, HREE). The Y/Nb and Ce/Nb ratios suggest fractional crystallization of primary source of picritic-like basaltic magma in the asthenospheric mantle. Oversaturated liquid is an excellent demonstration of the strong fractionation of saturated magma, while undersaturated magma may evolve in a rather similar way dominantly by fractionation of feldspar until the nepheline feldspar coetectic is reached. Later iron-rich sodic (amphibole and pyroxene) and potassic (micas) minerals are of intercumulus origin and the result of magmatic differentiation ; they appear often as subsolidus assemblages, sensitive to oxygen fugacity and to the water content of vapor phase. Simplified modeling of magma evolution within Petrogeny's Residue System demonstrates the ability of ACF processes to cause a critically undersaturated magma to evolve across the feldspar join and produce oversaturated rocks.

TYPOCHEMISM OF THE APATITE SUPERGROUP MINERALS FROM DEVONIAN ULTRABASIC ALKALINE ROCKS FOUND IN THE BRAGINSKY AND LOEVSKY SADDLE (BELARUS)

Ignatkevich E.S.[1], **Varlamov D.A.**[2]

1 Belarusian scientific research and designed institute of oil, Gomel, Belarus
e.ignatkevich@beloil.by
2 Institute of Experimental Mineralogy RAS, Chernogolovka, Rassia

Braginsky and Loevsky saddle is the western segment of Pripyat-and-Donetsk aulacogene located within the ancient East European platform. Devonian alkaline magmatism is associated with tectonic and magmatic cycles of intracratonic rifting of Paleozoic Pripyat-and-Donetsk rift belt. On the territory of Belarus it is expressed in the form of buried pipes of explosions, dikes, volcanic structures and sills; the scale of its manifestation offers prospects for searches of primary sources of diamonds, industrial clusters of rare metals and rare earth elements.

Work to identify the composition and typochemism of the apatite supergroup minerals of alkaline ultrabasic rocks of Braginsky and Loevsky saddle (as for the whole Devonian magmatic complex of Belarus) was held for the first time. The data are obtained by microanalysis of polished thin sections of alkaline picrite from Vasilyevskaya 1 drill-hole core (1785-1788 m depth) and nephelinite from Yastrebovskaya 3k drill-hole core (957-1207 m depth). Compositions of minerals were studied with a scanning electron microscope Tescan VEGA-II XMU with energy dispersive spectrometer INCA Energy 450 at the Institute of Experimental Mineralogy (Chernogolovka, Russia).

In alkaline picrite and nephelinite of the apatite supergroup minerals are contained in the amount of 1-2% of the total volume of the rock, they form small idiomorphic crystals (up to 0.1 mm in length), zoned crystals up to 0.1–0.3 mm of the long axis, and also microinclusions (up to 20 microns) in the clinopyroxene phenocrysts. In the studied rocks the composition of the phosphate glass (observed in some samples) is approximate to the composition of apatite. The apatites represent species containing fluorine and strontium (up to the composition of fluorcaphite), Ba, Th, REE concentrate as impurities. The BaO content reaches 5 wt. %, ThO_2 – 0.5 wt. %, TR_2O_3 – 1.8 wt. % (Table). Entering of REE in the apatite structure occurs according to heterovalent isomorphism $REE^{3+} + Si^{4+} = Ca^{2+} + P^{5+}$. Evidence of this is the presence of silicon in REE-bearing apatite (0.4-1.6 wt. % SiO_2) [1, 2].

Table - Chemical compound of the apatite supergroup minerals (wt. %)

	CaO	P_2O_5	F	SiO_2	SrO	BaO	Na_2O	Y_2O_3	La_2O_3	Ce_2O_3	Nd_2O_3	ThO_2	As_2O_3	Fe_2O_3	MgO	Total
Ap I	48.86	40.89	4.79	1.03	2.32	-	-	-	0.43	0.94	0.46	-	-	-	-	99.72
ApII (c)	52.32	41.50	1.08	0.48	3.08	-	-	-	-	-	-	-	*0.22*	-	-	98.68
ApII (r)	50.17	37.92	2.66	0.68	5.47	-	-	0.44	*0.23*	0.88	0.36	0.49	*0.23*	-	-	99.53
ApII (r)	43.27	39.48	3.61	0.38	11.97	-	-	-	*0.03*	*0.17*	-	-	*0.38*	-	-	99.29
ApII (r)	38.29	37.49	2.95	1.18	17.11	-	-	-	-	-	-	-	-	0.66	*0.10*	97.78
ApII (r)	39.69	35.69	1.28	1.03	13.76	5.30	1.30	0.44	-	-	-	0.06	*0.22*	-	-	98.77
ApII (r)	33.36	35.67	2.40	1.58	25.87	-	-	-	-	0.54	-	-	-	-	-	99.42
ApII (i)	36.90	31.84	1.39	2.04	13.23	5.27	1.53	-	-	-	-	-	-	0.59	0.50	93.29
ApII (g)	51.99	39.47	1.79	0.91	5.02	-	-	-	-	*0.18*	*0.06*	-	-	-	-	99.42

Note: italics gives definitions with values of concentration of an element more low 2 θ (a root-mean-square error of the analysis); r - the grain rims, c - the grain centre, i - inclusion, g - glass.

Apatites of the studied rocks show significant similarity in the outward look and composition, and are generally zoned for strontium. It made possible to distinguish among them the same species formed at different stages of evolution of melts. Less strontium apatite-I contains up to 2-3 wt.% SrO, forms automorphic small crystals, and also composes the core of strontium zoned crystals. High strontium apatite-II forms a micro-inclusions in clinopyroxene phenocrysts (Fig.1), forms rims of strontium zoned crystals, it is probably the source of phosphate glass; contains from 5 to 26 wt.% SrO, its composition is approximate to fluorcaphite [3].

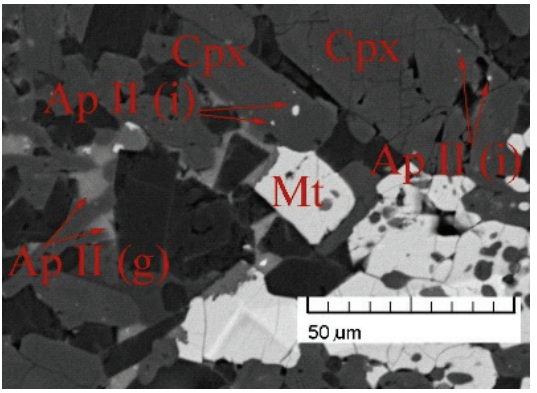

Figure 1: Alkaline picrite from Vasilyevskaya 1 drill-hole core.

In the study of "kindred" alkaline ultramafic platform rocks the composition of the apatite supergroup minerals is involved to solve formation problems. The examples of the Khibiny Massif and the Massif of Inagli proved a direct correlation between the amount of strontium in apatites and alkaline environment of their formation [4]. Apatites from kimberlites contain up to 3-4 wt.% SrO and a similar amount of fluoride, from lamproites – to 7 wt.% SrO. BaO content in the apatite supergroup minerals of these rocks sometimes reaches 1-2 wt.%. In carbonatites' apatites the content of these elements is much higher, up to the formation of independent mineral phases [5,6]. So fluorcaphite, fluorstrophite, stronadelphite are found only in abnormally enriched with strontium ultragpaitic rocks (the Khibiny Massif on the Kola Peninsula, the Massif of Inagli in South Yakutia) [4,7].

The content of strontium and barium in the apatite supergroup minerals of the studied ultrabasic rocks of Braginsky and Loevsky saddle significantly exceeds the number of those in kimberlites' and lamproites' apatites, reaching the values inherent to the apatite supergroup minerals of carbonatites (up to 5 wt.% BaO, and to 13-26 wt .% SrO). In the studied rocks thepresence of the apatite supergroup minerals containing REE, fluoride, barium and high strontium (up to the composition of fluorcaphite) indicates high-alkali conditions of mineral formation, the enrichment of melts with incoherent rare metal and rare earth elements and suggests a possible association of alkaline ultrabasic rocks of Braginsky and Loevsky saddle with rare metal carbonatites.

This research was carried out with financial support from the Belarusian Republican Foundation of Fundamental Investigations (grant № X14M-088)

References

1. Arzamastcev A.A., Arzamastseva L.V., Bea F., Montero P., 2008. Elements-impurities in minerals as indicators of the evolution of the alkaline ultrabasic dyke series: LA-ICP-MS data for magmatic

provinces of North East Fennoscandia and Germany // Petrology. V.16. № 6, p. 1-28. (in Russian)

2. Roeder P.L., MacArthur D., Ma X.P., Palmer G.R., 1987. Cathodoluminescence and microprobe study of rare-earth elements in apatite // Am. Mineral. V.72, p. 801-811.
3. Pasero M. & etc., 2010. Nomenclature of the apatite supergroup minerals. Eur. J. Mineral. № 22, p. 163-179.
4. Homiakov A.P., 1990. Mineralogy of ultraagpaitic alkaline rocks. M.: Nauka, 196 p. (in Russian)
5. Olejnikov O.B., 2001. Features of a chemical composition of the apatite from intrusive kimberlites of Yakutia. Domestic geology. № 5, p. 13-15. (in Russian)
6. Mitchell R.H., 1995. Kimberlites, orangeites and related rocks. – New York: Plenum Press.
7. Pekov I.V., 2001. Lovozerskiy Massif: the history of the study, pegmatites, minerals. M.: Zemlya, 432 p. (in Russian)

PETROLOGICAL AND GEOCHEMICAL FEATURES OF ENCLAVES IN THE SOGUT PLUTON (ESKISEHIR-BILECIK, TURKEY)

Ilbeyli N.[1], Demirbilek M.[2], Kibici Y.[2]

1 Akdeniz University, Faculty of Engineering, Department of Geological Engineering, 07058 Antalya-TURKEY
ilbeyli@akdeniz.edu.tr
2 Dumlupinar University, Faculty of Engineering, Department of Geological Engineering, 43100 Kütahya-TURKEY

The Sakarya Zone is > 1500 km long and 120 km wide (Okay, 2004). The basement of the zone is made up of Devonian plutonic rocks, Carboniferous plutonic and metamorphic rocks, and Triassic accretionary complexes with blueschists and eclogites (Okay et al., 2006). The basement was overthrust from the south by the Karakaya Complex (Tekeli, 1981; Okay et al., 1996). In the zone, the complex is overlain unconformably by an upper Mesozoic sequence in the west and passes directly up into a Jurassic sequence in the east (Okay, 2000).

There are few Late-Paleozoic-aged plutons in the basement of the Sakarya Zone. The Carboniferous Sogut pluton is one of them (Cogulu, 1967; Ustaomer et al., 2012).

These rocks are quartzdiorite-granodiorite, granodiorite and granite in composition. The quartzdiorite-granodiorite and granodiorite are cut by pegmatitic and aplitic dykes. Enclaves are widespread in these rock types. The granites are grey- and medium- to coarse-grained with light pink K-feldspar crystals.

Two types of enclaves have been recognized in the Sogut pluton (I) xenoliths and (ii) igneous enclaves. The latter is defined as (a) fine-grained and (bi) medium-grained to porphyritic with feldspar megacrysts. Most abundant types are igneous enclaves.

Major minerals in the host rocks and enclaves are plagioclase, K-feldspar, quartz, biotite and hornblende. Accessory phases include titanite, zircon, apatite and opaques.

The origin and evolution of the enclaves are mainly linked to those of their host rocks. For example, igneous enclaves, originated from magma mixing/mingling, in the plutonic rocks may indicate the existence of some interaction between silicic magmas and mantle-derived melts.

Keywords: Söğüt pluton, Sakarya zone, Late Paleozoic, igneous enclaves, geochemistry

Acknowledgment:This research was supported by the Akdeniz University Research Fund and grant no. 2013.01.0102.

References

1. Çoğulu, E., 1967. Sarıcakaya-Eskişehir pegmatitlerinin jeolojik ve petrolojik etüdü. General Directorate of Mineral Research and Exploration (MTA), Report no. 1535 (in Turkish).
2. Okay, A.İ., 2000. Was the Late Triassic orogeny in Turkey caused by the collision of an oceanic pla-

teau? In: Bozkurt, E., Winchester, J.A., Piper, J.A.D. (Eds.), Tectonics and Magmatism in Turkey and Surrounding Area. Geological Society, London Special Publications 173, pp. 25-41.

3. Okay, A.İ., 2004. Tectonics and high pressure metamorphism in northwest Turkey: Field trip guide book-P01. 32nd International Geological Congress, APAT, Italy, 56 pp.
4. Okay, A.İ., Satır, M., Maluski, H., Siyako, M., Monié, P., Metzger, R., Akyüz, S., 1996. Paleo- and Neo-Tethyan events in northwestern Turkey: Geologic and geochronologic constraints. In: Yin, A., Harrison, M. (Eds.), Tectonics of Asia. Cambridge, Cambridge University Press, pp. 420-441.
5. Okay, A.İ., Satır, M., Siebel, W., 2006. Pre-Alpide Palaeozoic and Mesozoic orogenic events in the Eastern Mediterranean region. In: Gee, D.G., Stephenson, R.A. (Eds.), European Lithosphere Dynamics. Geological Society, London Memoirs 32, pp. 389-405.
6. Tekeli, O., 1981. Subduction complex of pre-Jurassic age, northern Anatolia, Turkey. Geology 9, 68-72.
7. Ustaömer, P.A., Ustaömer, T., Robertson, A.H.F., 2012. Ion probe U-Pb Dating of the central Sakarya Basement: A periGondwana Terrane intruded by late Lower Carboniferous subduction/collision related granitic rocks. Turkish Journal of Earth Sciences Vol. 21, 905-932.

PETROLOGICAL STUDIES OF ROCKS FROM CATANDA CARBONATITIC MASSIF (W ANGOLA) – PRELIMINARY RESULTS

Jackowicz E., Wolkowicz K., Wolkowicz S., Bojakowska I.

Polish Geological Institute-National Research Institute
Warsaw, Poland
stanislaw.wolkowicz@pgi.gov.pl

Erosional relics of a huge carbonatite complex, including those of volcanic necks and fissure eruptions, may be traced in area of about 80 km^2 in the vicinities of Catanda (Cuanza Sul province, Angola). These carbonatites have penetrated Precambrian basement built of granites, migmatite-granite gneisses, quartz schists and diabases and are directly overlain by eluvial-aluvial sediments.

The carbonatite complexes from Catanda and other regions of Angola form a lithological unit seated at the crossing of four fault systems of the NE-SW oriented Lucapa transcontinental rift structure (Lapido-Loureiro, 1973). Radiometric datings made for alkaline rocks co-occurring with the carbonatites range from 138-109 My (Filho, 1990) to about 92 My (Silva, 1973), making it possible to assume Cretaceous age of this structure and the whole lithological unit. This unit belongs to the Parana-Angola-Namibia igneous province, in which carbonatites representing intrusive bodies related to central parts of alkaline complexes are much more common than those resulting from extrusive and effusive volcanic processes.

The Catanda carbonatites remain poorly known in comparison with the remaining complexes of the Lucapa structure. This is the case despite of the fact that they appears very attractive from the scientific point of view as the example of an extrusive carbonatite, comprising both pyroclastic rocks and lavas. Up to now, only 14 out of 49 extrusive carbonatite complexes hitherto identified in the world were found to represent such mixed type (Woolley, Church, 2005).

The studies covered rock samples taken at outcrops of relics of volcanic cones which nowadays form the Chimbala, Ngonge, Viallala and Conjomba hills. This paper presents preliminary results of petrographic-mineralogical analysis of the studied material.

The studied rocks were found to be represented mainly by porphyric lavas and finely stratified lapilli, lapilli-ash and ash tuffs as well as tuffs characterized by graded bedding. The tuffs are usually composed of varying amounts of spherical lapilli and similar ash particles or, sometimes, lapilli cauliflower-like in shape.

Lavas representing material of lava flows were identified in some samples only. Components of lava phenocrysts include here pyroxenes (ordinary augite, diopside), hornblende, olivine, phlogopite, apatite, calcite, ore minerals (magnetite, titanomagnetite and chromite), pyrochlore and feldspars at least partly of the xenocryst character (phagioclases, K-feldspars), biotite and quartz. Rock groundmass is crypto- to microcrystalline, with carbonates and lumps of ore minerals as the only identifiable components identified so far. Small enclaves formed of amphibole and phlogopite often with admixture of apatite, magnetite and calcite and sometimes pyroxene, as well as xenoliths of granite occur in subordinate amounts.

Two types of interrrelated lavas were identified. They are characterized by presence of mineral assemblages similar in composition but differing in volume relations and size of main compo-

nents. Lavas of the type 1 differ from those of the type 2 in definitely higher share and larger size of phenocrysts of mafic and opaque minerals. Lavas of the type 2 are impoverished in these components at the advantage of calcite phenocrysts and xenocrysts of light minerals as well as smaller variability in size of grains.

Lavas also form juvenile clasts of lapilli and ash fraction present in tuffs. A special attention should be paid to spherical to ellipsoidal clasts called as spinning droplets (Junqueira-Brod et al., 1999). They are formed of nuclei represented by phenocrysts or xenoliths, surrounded by lava material with concentrically arranged microphenocrysts. Several features of the studied lapilli suggest that nucleation of some of them has taken place in upper parts of continental crust and the remaining ones – possibly even at depths close to the Earth mantle but this hypothesis needs further confirmation. The studied lapilli sometimes shows some underdevelopment in relation to those genetically related to CO_2 diatresis, typical of diatreme facies as represented by tuffisite or chimney breccia or their subaerial equivalents – pyroclastic currents which form maars and tuff rings around diatremes (Lloyd, Stoppa, 2003).

Spinning droplets form local concentrations in lapilli-ash tuffs with graded bedding, being rather rare in other tuffs. The spinning droplets also cooccur with lapilli known as frozen droplets (op. cit.), that is forms rounded and without nuclei nor concentric texture. Such co-occurrence may suggest volcanic activity of the strombolian type whereas the mode of fracturing of lapilli and other clasts seems to indicate an overprinting of phreatomagmatic factor on effects of an eruption.

The phreatomagmatic nature of eruptions is further supported by the presence of tuffs with accretionary lapilli, both of the lapilli-ash and lapilli types. The former are mainly built of clasts derived from walls of a volcanic chimney and armoured lapilli, made of large crystaloclats (carbonatite lava phenocrysts) or xenoliths with a thin rim of lava or ash or at first lava and later ash.

Lapilli tuffs are characterized by predominance of various accretionary lapilli with small admixtures of ash and carbonate cement and clearly subordinate share of lithic components. The lapilli sometimes display small ovate voids infilled with calcite. In some samples the accretionary lapilli form subspherical agglutinates of frozen droplets and amoeba-like brownish particles of carbonatite lava. Other samples yield lapilli with finely-crystalline interior and a cryptocrystalline brownish-greenish rim of clay minerals. Their interior is built of clay-carbonate matrix with small clasts of calcite, quartz, opaque minerals, biotite and feldspars, often concentric to spiral in arrangement. Some lapilli have nuclei represented by feldspar, phlogopite or ash lumps.

Products of phreatomagmatic erosions may also include ash tuffs with effects of vesiculation traceable throughout the whole rock mass of particles resembling frozen droplets and sintered to a various degree, and numerous fine crystalloclasts. Vesicles are most common in tuffs with cauliflower-like lapilli, characteristic of lava fragmentation in the course of eruptions of the strombolian type.

It is still not possible to decipher sequence of eruptive processes because of insufficient knowledge of vertical and lateral succession of the facies types identified in the studied volcanic unit. Microtextures of pyroclastic rocks make it possible to assume that origin of tuffs with accretionary lapilli and ash tuffs was related to pyroclastic flows and surges whereas lapilli-ash tuffs with graded bedding may represent effects of accompanying falls of airborne pyroclastic material. It may be concluded that the eruptions were of the phreatomagmatic, magmatic-phreatomagmatic

and magmatic (strombolian) character. Subordinate content of pyroclastic material of the ash fraction shows that the dynamics of these eruptions was moderate.

Difficulties in explaining the origin of carbonatite laves and related pyroclastic deposits are due to an overprint of effects of alterations by post-volcanic activity and weathering on their original composition. These processes resulted in origin of a several generations of calcite which heals fractures and fills voids that occurred due to trapped volcanic gases, and replaces original rock components (pyroxenes, amphiboles, plagioclases, biotite and phlogopite) to a various degree. The activity of mineralizing solutions is better marked in tuffs than in lavas which may be explained in terms of higher susceptibility of poorly compact deposits (especially soon after their origin) and the presence of accidental components which could be an additional source of elements involved in mineralization processes. The tuffs were also found to be enriched in REE and Nb, the carriers of which include primary minerals as well as the secondary ones (LREE phosphates, oxides and carbonates, titanite and leucoxene, secondary pyrochlore, baddaleyite, zirconolite and others).

Acknowledgements: Studies were conducted as a part of Grant no. 61.2814.1401.00.0 financed by the Ministry of Science and Higher Education.

References

1. Issa Filho A., Dos Santos A. B. R. M. D., Riffel B. F., Lapido-Loureiro F. E. V., Mc Reath I., 1991. Aspect of the geology, petrology and chemistry of some Angolan carbonatites. In: Rose A. w., Taufen P. M. (Editors), Geochemical Exploration 1989. J. Geochem. Explor., 40: 205-226
2. Junqueira-Brod T. C., Brod J. A., Thompson R. N., Gibson S. A., 1999. Spinning droplets – a conspicuous lapilli-size structure in kamafugitic diatremes of southern Goiás, Brazil. Rev. Braz. Geosci., 20 (3):437-440
3. Lapido-Loureiro F. E. 1973. Carbonatitos de Angola, t. HYPERLINK "http://www.google.pl/search?hl=pl&tbo=p&tbm=bks&q=bibliogroup:"11HYPERLINK "http://www.google.pl/search?hl=pl&tbo=p&tbm=bks&q=bibliogroup:": Memórias e Trabalhos, Instituto de Investigação Científica de Angola, Instituto de Investigação Científica de Angola, 242 p Lloyd F. E.,
4. Silva, M. V. 1973. Estrutura vulcânica-carbonatitica de Catanda (Angola). ServoGeol. Min. Angola, 24, pp. 5-14.
5. Stoppa F., 2003. Pelletal lapilli in diatremes – some inspiration from the old masters. GeoLines
6. Woolley A. R., Church A. A., 2005. Extrusive carbonatites: A brief review. Lithos, v.85, 11-12: 1–14

PETROLOGY AND GEOCHEMISTRY OF POTASSIC FOID- SYENITES OF EAST AZARBAIJAN, NW IRAN

Jahngiri A.[1], Ashrafi N.[2]

1 Dept of Earth Sciences, University of Tabriz, Tabriz, Iran
2 Dept of Geology, Payame Noor Universit, Tehran, Irany
A_jahangiri@tabrizu.ac.ir

The studied foid-syenites include the Bozqush, Kaleybar and Razgah intrusions; which belong to the Paleogene alkaline magmatism of NW Iran. These intrusions are intruded the Cretaceous and Eocene volcanic and sedimentary rocks. The dominant lithologies are nepheline syenite, pseudoleucite syenite, nepheline-bearing gabbro (alkali-gabbro), nepheline-bearing monzo-diorite and pseudoleucitolite. Based on whole rock geochemistry, the foid-syenites and associated rocks classify as potassic alkaline (shoshonitic) and transitional alkaline series; commonly they are metaluminous and vary from magnesian through ferroan. Almost all of the rocks display similar spider-diagram profiles, with LILE and LREE enrichment and Ta, Nb, Ti (TNT) depletion, which are typical of subduction-related magmas. The Nb/Ta and Zr/Hf ration of studied samples plot in the range of mantle chondrite ratios (Nb/Ta =17, Zr/Hf = 40). The present geochemical features suggest that the studied rocks were formed from similar parental magmas which have undergone different degree of fractionation and crustal contamination. Felsic magmas forming the foid-syenites may be final liquids resulting from extensive fractionation of mafic parents (e.g. olivine alkaline basalt) in which olivine, clinopyroxene, and plagioclase were the main fractionating phases. The REE patterns and the partial-melting model diagrams indicate that garnet was not a significant phase in the source rocks. Therefore we suggest a phlogopite spinel lherzolite source for the studied rocks. Based on the temporal and spatial association of the alkaline and calc-alkaline rocks in NW Iran and geochemical characteristics, it can be suggested that the simultaneous local extension with subduction of Neo-Tethys oceanic crust, have probably caused invasive magmatism during Eocene.

THE ROLE OF MELT INCLUSIONS STUDY IN CLARIFYING JACUPIRANGITE PETROGENESIS, KERIMASI (TANZANIA)

Káldos R.[1], Guzmics T.[1], †Dawson J.B.[2], Szabó Cs.1, Milke R.[3]

1 Lithosphere Fluid Research Lab, Eötvös University Budapest, Hungary
2 School of Geosciences, University of Edinburgh, United Kingdom
3 Free University Berlin, Germany
tibor.guzmics@gmail.com

Carbonatites and associated silicate rocks are one of the most exciting and complex branch to examine petrographically and geochemically. The study of these igneous rocks deserve much attention as they are important mineral sources of rare earth elements (REE+Y) and such high field strength elements (HFSE) as Zr, Nb and Ta. Because of intensive alteration (e.g. weathering) of some phases of these exceptional rocks, their origin is still unclear. Thus examination of the bulk rock chemistry solely of these rocks gives uncertain results about the composition of their parental magma. However, detailed melt inclusion study in several host minerals of carbonatites and associated silicate rocks is a powerful method to determine the magma composition and evolution [1][2][4][5].

Jacupirangite, like other plutonic rocks in Kerimasi volcano, occur as blocks in the volcanic agglomerates [3]. The jacupirangite consists of dominantly clinopyroxene (diopside) and magnetite with lesser amount of calcite, phlogopite, apatite, forsterite, and pyrrhotite. Diopside and magnetite are rich in crystal and irregular shaped, randomly distributed melt inclusions (10-50 μm). SEM and HR-Raman spectroscopic measurements proved that diopside contains magnetite, apatite, calcite, phlogopite, badelleyite and alkali carbonates, whereas magnetite contains apatite, phlogopite, calcite, dolomite, badelleyite, perovskite and alkali carbonates as crystal inclusions. HR-Raman spectroscope was also applied to determine the alkali carbonates (nyerereite, shortite) and other water soluble phases such as nahcolite and sulphohalite within the inclusions of magnetite and diopside. However alkali carbonates are not present in the bulk rock possibly because of their quick alteration due to secondary processes, Raman spectroscopy is a suitable tool to recognize the presence of these phases in unexposed inclusions. This suggests that during formation of carbonatites, an alkali rich carbonate melt exists, similarly to that observed at Oldoinyo Lengai [1]. Based on microtermometric measurements, the homogenization of the diopside hosted melt inclusions occurred at 800-950 ˚C with the homogenization of the fluid bubble into the melt phase. Furnace technique was applied on diopside and magnetite separate grains to reproduce the melt phase at the time of entrapment. In the furnace, statistically significant (n=180) homogenized carbonate melts were produced in the inclusions of magnetite and diopside (Figure 1). These were exposed and analyzed by SEM and EMPA.

Magnetite and diopside hosted melt inclusions are both Ca and alkali rich, P, Cl, F bearing carbonate melts. With increasing alkali content of the carbonate melt the CaO and P_2O_5 showing a decreasing trend resulting in calcite and apatite fractionation. Based on petrographic and geochemical results, we assume that during crystallization, an alkali rich carbonate melt was present and entrapped in magnetite during its formation when diopside was already crystallized. Carbonate melts in diopside were entrapped after its formation, forming secondary melt inclusions.

The composition of the trapped carbonate melt is very similar to the parental melt of the Kerimasi calciocarbonatite [4] suggesting that silicate-carbonate liquid immiscibility most probably

plays important role during formation of jacupirangite. Compared the mineral data and the composition of the carbonate melt with those in Kerimasi afrikandite [5] and calciocarbonatite, the jacupirangite represents an intermediate stage of magma evolution between the formation of afrikandite and calciocarbonatite. Jacupirangite was formed after the silicate-carbonate liquid immiscibility happened when the carbonate melt did not yet separated completely from the system.

Our study clearly demonstrated that examination of melt inclusions in carbonatites and associated alkaline series coupled with Raman spectroscopy is essential to determine their magmatic composition and petrogenesis.

This research was granted by the Hungarian Science Foundation (OTKA PD, 105364 to T. Guzmics). Part of these results has been carried out in the framework of the REG_KM_INFRA_09 Gábor Baross Programme and KMOP project nr.4.2.1/B-10-2011-0002 by the European Union and the European Social Fund.

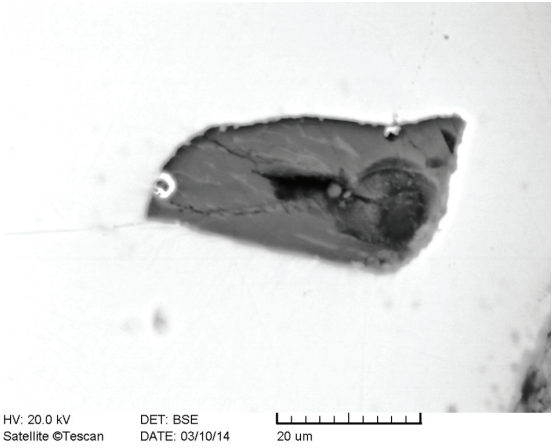

Figure 1: Representative quenched carbonate melt inclusion in magnetite after heating 1000˚C. Hole represents the fluid phase in the inclusion that was present before exposure. BSE image.

References

1. Mitchell R.H. (2009) Peralkaline nephelinite-natrocarbonatite immiscibility and carbonatite assimilation at Oldoinyo Lengai Tanzania. Contrib Mineral Petrol 158:589-598
2. De Moor M.J., Fischer T.P., King P.L., Botcharnikov R.E., Hervig R.L., Hilton D.R., Barry P.H., Mangasini F., Ramirez C., (2013) Volatile-rich silicate melts from Oldoinyo Lengai volcano (Tanzania): Implications for carbonatite genesis and eruptive behavior. Earth Planet. Sci. Lett. 361, 379-390.
3. Dawson J.B. (2008) The Gregory rift valley and Neogene-recent volcanoes in Northern Tanzania. Geol Soc London 33:64–66
4. Guzmics T, Mitchell R.H., Szabó Cs., Berkesi M., Milke R., Abart R. (2011) Carbonatite melt inclusions in coexisting magnetite apatite and monticellite in Kerimasi calciocarbonatite Tanzania: melt evolution and petrogenesis. Contrib Mineral Petrol 161:177-196
5. Guzmics T., Mitchell R.H., Szabó Cs., Berkesi M., Milke R., Ratter K. (2012) Liquid immiscibility between silicate carbonate and sulfide melts in melt inclusions hosted in co-precipitated minerals from Kerimasi volcano (Tanzania): evolution of carbonated nephelinitic magma. Contrib Mineral Petrol 164:101-122

OXYGEN, CARBON AND SULPHUR ISOTOPE STUDIES IN THE KEBAN PB–ZN DEPOSITS, EASTERN TURKEY; AN APPROACH ON THE ORIGIN OF HYDROTHERMAL FLUIDS

Kalender L.

Firat University, Department of Geological Engineering, 23119 Elazig, Turkey.
leyakalender@firat.edu.tr

Pb–Zn deposits are widespread and common in various parts of the Taurus Belt. Most of the deposits are of pyrometasomatic and hydrothermal origin. The Keban Pb-Zn deposits are located along the intrusive contact between the Paleozoic – Lower Triassic Keban Metamorphic Formation and the syenite porphyry of the Upper Cretaceous Keban igneous rocks. Various studies have already been carried out; using fluid inclusion studies on fluorite, calcite and quartz on the pyrite-chalcopyrite bearing Keban ore deposits. This study focuses on the interpretation of stable isotope compositions in connexion with fluid inclusion data. Sulfur isotope values ($\delta^{34}S$) of pyrite are within the range of -0.59 to +0.17 ‰ $_{V\text{-}CDT}$ (n=10). Thus, the source of sulphur is considered to be magmatic, as evidenced by associated igneous rocks and $\delta^{34}S$ values around zero"0". Oxygen isotope values $\delta^{18}O$ of quartz vary between +10.5 and +19.9 ‰ $_{(SMOW)}$. However, $\delta^{18}O$ and $\delta^{13}C$ values of calcite related to recrystallized limestone (Keban metamorphic formation) reach up to +27.3 ‰ $_{(SMOW)}$ and +1.6 ‰ $_{(PDB)}$, respectively. The $\delta^{34}S$, $\delta^{13}C$ and $\delta^{18}O$ values demonstrate that skarn-type Pb-Zn deposits formed within syeno-monzonitic rocks and calcschist contacts could have developed at low temperatures, by mixing metamorphic and meteoric waters in the final stages of magmatism.

Keywords: Stable isotopes, contact pyrometasomatic type, East Anatolian, Keban, Turkey

Acknowledgement: I thank Mr. Prof. Dr. Bernard Bonin for reading and his constructive advise to improve the manuscript.

References

1. Arni, P., 1937. Report about Geology of the Keban Mine MTA Report No: 564, Ankara.
2. Asutay, H.J., 1988. Geologic and petrografic studies around of Baskil (Elazig). MTA Bulletein v.107, p.38-60.
3. Barnes, H.L., 1979. Geochemistry of hydrothermal ore deposits. 2nd edition, John Wiley, New York.
4. Boni, M., Balassone, G., Iannace, A., 1996. Base metal ores in the Lower Paleozoic of southwestern Sardinia. In: D.F. Sangster (Ed.), Carbonate-Hosted Lead–Zinc Deposits. Society of Economic Geologist Special Publication v.4, p.18–28.
5. Borthwick, J., Harmon, R. S. 1982. A Note Regarding ClF3 as an alternative to BrF5 for Oxygen Isotope Analysis, Geochimica et Cosmochimica Acta v.46, p.1665-8.
6. Calagari, A.A., 2003. Stable isotope (S, O, H and C) studies of the phyllic and potassic–phyllic alteration zones of the porphyry copper deposit at Sungun, East Azarbaidjan, Iran. Journal of Asian Earth Sciences v.21, p.767-780.
7. Çağlayan, H., 1984. Die Vererzung der fluorit-molybdanglanzführenden blei-zink-lagerstâtten von Keban-Elazığ im Südost-Taurus (Türkei): Ph. D. Thesis Univ. Vienna (in Italy).
8. Çelebi, H., H anelçi, Ş., Seyrek, A., 1997. Sanidine geochemistry from Keban Magmatic rocks. Çukurova University, Geology Engineering 20. Annual Symposium, pp.64. Adana.

9. Choi, S.G., Kim, S.T., Lee, J.G., 2003. Stable isotope systematic of Ulsan Fe-W skarn deposit, Korea, Journal of Geochemical Exploration v.78-79, p.601-606.
10. Clark, I., Fritz, P., 1997. Environmental isotopes in hydrogeology. Lewis Publishers, pp. 328, New York.
11. Degans, E.T., Epstein S., 1964. Oxygen and carbon isotope ratios in coexisting calcites and dolomites from recent and ancient sediments. Geochimica et Cosmochimica Acta v.28, p.23-44.
12. Dickson J.A.D., Coleman, M.L., 1980. Changes in carbon and oxygen isotope composition during limestone diagenesis. Sedimentology v. 27, p.107-118.
13. Eastoe, C.J., Nelson, S.E., 1988. A Permian Kuroko-type hydrothermal system, Afterthought-Ingot Area, Shasta Country, California: Lateral and vertical section, and geochemical evolution. Econimic Geology v.83, p.588-605.
14. Eldridge, C.S., Williams, N., Walshe, J.L., 1993. Sulphur isotope variability in sediment-hosted massive sulphide deposits as determined using the ion microprobe SHRIMP: II. A study of the HYC deposit at Mc Artur River, Northern Territory, Australia. Economic Geology v.88/1, p.1–26.
15. Epstein, S., Graf D.L., Degens E.T., 1963. Oxygen isotope studies on the origin of dolomites. In: H. Craig, S.L. Miller, G.T. Wasserburg, (Ed.), Isotopic and Cosmic Chemistry - Dedicated to H.C. Urey 70 th Birthday. pp.188., Amsterdam (in North Holland).
16. Goldfarb, R.J. Newnerry, R.J. Pickthom, W.J. Gent, C.A., 1991. Oxygen, hydrogen and sulphur isotope studies in the Juneau gold belt, southeastern Alaska: constraint on the hydrothermal fluids. Economic Geology v.86, p.66-71.
17. Hanelçı, Ş., 1991. Studies of ore deposits around the Zeryan Stream and Siftil. PhD Thesis, Istanbul University, pp. 200. Istanbul (in Turkey).
18. Hitzman, M.W., Beaty, D.W., 1996. The Irish Zn–Pb–(Ba) orefield. In: D.F. SANGSTER (Ed.), Carbonate-Hosted Lead–Zinc Deposits. Society of Economic Geologist Special Publication v.4, p.112–143.
19. Hoefs, J., 1997. Stable isotope geochemistry. Springer (Ed), NewYork.
20. Kalender, L., 2000. Geology, origin and economic importance of the copper mineralization of Keban (Elazig), East Euphrates Kebandere area, Ph.D. Thesis, Firat University, pp.100. Elazığ, Turkey, (in Turkish).
21. Kalender, L., Hanelçi, Ş., 2001. Mineralogical and petrographical features of Nalliziyaret Tepe (Keban-Elazığ) copper mineralization. Istanbul University Earth Sciences, v.14, p.51 (in Turkish, with English abstract).
22. Kalender, L., Hanelçi, Ş., 2002. General Features of Copper Mineralization Nalliziyaret Tepe (Keban–Elazıg): An Approach to its Genesis. Geosound v.40/41, p.133–149 (in Turkish).
23. Kalender, L., Hanelçi, Ş., 2004. General features of copper mineralization in the Eastern
24. Euphrates, Keban-Elazığ Area, Turkey. Journal of the Geological Society of India v.64, p.655-666. Kalender L., Sağıroğlu A., Kişman, S., 2009. Fluid inclusion studies in the different origin Quartzs associated with Cu, Pb, Zn mineralizations at Kızıldağ and Köprücük-Harput, East Anatolian District, Turkey. Ozean Journal of Applied Sciences v.2(1), p.128-138.
25. Kalender, L., Akgül, M., Akgül, B., Sağıroğlu, A., 2010. Türkiye. (C, O, S Isotope
26. Studies of Late Cretaceous Magmatits relationship mineralizations in East Taurus, Elazığ, Turkey). Seventh International Symposium on Eastern Mediterranean Geology, Abstract, 18-22 October Adana / Turkey, pp. 117-118.
27. Kesler, S.E., 1996. Appalachian Mississippi valley-type deposits: paleoaquifers and brine provinces. In: D.F.SANGSTER, (Ed.), Carbonate-hosted lead–zinc deposits. Society of Economic Geologist Special Publication (4), 29–57.

28. Kineş, T., 1969. The geology and ore mineralization of the Keban area, Eastern Turkey. PhD. Thesis. Istanbul University, pp. 213. Istanbul (in Turkey).
29. Kipman, E., 1976. Geological and petrological features of the volcanic rocks in Keban. Associated Prof. Thesis. Istanbul University, pp 200, Istanbul (in Turkey).
30. Kipman, E., 1981. Geology and thrust fault of Keban. İstanbul University-Geo-science Bulletin v.1-2, p.75-81.
31. Kipman, E., 1982. Petrology of Keban volcanic roks. Geo-science Bulletin, Istanbul University v.4, p.203-230.
32. Koksoy, M., 1972. Element distribution of the associated with Keban ore deposit: Etibank Report, Number: 983, pp. 88, Ankara.
33. Koptagel, O., Ulusoy, U., Efe, A., 2005. A study of sulphur isotopes in determining the genesis of Goynuk and Celaldagi Desandre Pb-Zn deposits, eastern Yahyali, Kayseri, Central Turkey. Journal of Asian Earth Sciences v.25,p.279-289.
34. Köksoy, M., 1972. Distrıbution of elements associate with mineralizations around Keban. Etibank Report. Report Number: 983, pp 88. Ankara.
35. Kovenko, V., 1941. Feasibility report about Keban ore deposits. MTA Report Number: 1255. pp.113. Ankara.
36. Kuşçu, I., Erler, A., 1999. Using of piroxenes to classification of some skarns in the middle Anatolian: Akçakışla and Akdağmadeni skarns. TJK Symposium Book. 10-12 May, pp. 183. Ankara.
37. Marquillas, R., Sabino, I., Sial, A.N., Papa, C.del, Ferreira, V., Matthews, S., 2007. Carbon and oxygen isotopes of Maastrichtian-Danian sallow marine carbonates: Yacoraite Formation, north-western Argentina. Journal of South American Earth Sciences v.23, p.304-320.
38. Mc Crea, J.M., 1950. The isotopic chemistry of carbonates and a paleotemperature scale. Journal of Chemical Physics v.18, p.849.
39. Moucher, A., 1938. Über die Erzvorkommen Keban-Maden (Turkei). Zeitschr. Für Prakt. Geol. (46/5), 79-98.
40. Ohmoto, H., Rye, R.O., 1979. Isotopes of sulphur and carbon, In: H.L. Barnes, (Ed.), Geochemistry of hydrothermal ore deposits. Wiley-Intersci, New York.
41. Perinçek, D., 1979. Guidebook for excursion (B), interrelations of the Arab and Anatolian plates: First Geology Congress on Middle East Tecknical University, Ankara.
42. Rouxel, O., Shanks, W.C., Bach, W., Edwards, K.J., 2008. Integrated Fe and S isotope study of seafloor hydrothermal vents at East Pacific Rise 9-10ºN. Chemical Geology v.252, p.214-227.
43. Sakai, H., 1968. Isotopic properties of sulphur compounds in hydrothermal process. Geochemical Journal v.2, p. 29-49.
44. Seeliger, T.C., E. Pernicka, G.A. Wagner, F. Begemann, S. Schmitt-Strecker, C. Eibner, Oztunali O, Baranyi I., 1985. Archaometallurgische untersuchungen in nord- und ostanatolien. Jahrbuch des Romisch-Germanisches Zentralmuseums Mainz v.32, p.597-659.
45. Shepherd, S.M.F., 1976. Identification of the origin of ore forming solutions by the use of stable isotopes. Volcanic Processes in Ore Genesis, 25-41, The Institution of Mining and Metallurgy, London.
46. Shimazaki, H., Yamamoto, M., 1979. Sulphur isotope ratios of some Japanese skarn deposits. Geochemical Journal v.13, p.261-268.
47. Taylor H.P.Jr., 1974. The application of oxygen and hydrogen isotopic studies to problems of hydrothermal alteration and ore deposition. Economic Geology (69), 843–883.
48. Ueda, A., Krouse, H.R., 1986. Direct conversion of sulphide and sulphate minerals to SO2 for isotope analyses. Geochemical Journal v.20, p. 209-212.
49. Wada, H., 1978. Carbon isotopic study on graphite and crbonate in the Kamioka mining district, Gifu

Prefecture, central Japan, in relation to the role of graphite in the pyrometasomatic ore deposition. Mineralium Deposita v.13, p.201-220.

50. Wagner, T., Boyce, A.J., Fallick, A.E., 2002. Laser combustion analysis of δ34S of sulfosalt minerals: determination of the fractionation systematic and some crystal-chemical considerations. Geochimica et Cosmochimica Acta v.66, p.285-2863.
51. Ziserman, A., 1969. Geological and mining study of Keban Mine: Etibank Archive Number: 123, Ankara.

NEW CONTRIBUTION TO THE THE DIAMOND-BEARING REE-GOLD-SILVER MINERALIZATION AT KASR EL- BASSEL AREA, SOUTH EL-FAYOUM, UPPER EGYPT

Kamel O. A.[1], **Niazy E. A.**[2]

1 Geology Department, Faculty of Science, Minia University, Minia, Egypt
2 National Research Centre, Egypt
omar_ali_kamel@hotmail.com

The studied mineralization is represented by silicified picrite porphyry, kimberlite semi-ring dykes and associated carbonatite-bearing rocks. Banded skarn sheets and lenses were formed during a contact-metamorphic process. This rock assemblage is commonly altered by hydrothermal veins, pockets and stockworks. The host rocks are Quaternary Protonile and Prenille sediments and other Middle- Eocene limestones.

The mineralized bodies comprise REE minerals, native gold, electrum, Au-bearing pyrite, krennerite, native silver, argentite, cerargyrite, proustite, chrysocolla and dioptase. REE minerals are represented by common monazite, xenotime, and weinschenkite. While, rutile, chromite, pyrrhotite, niccolite, cobaltite are the associated ore minerals. The described mineralization is mostly related to the effect of nearby Quaternary volcanics that comprise porphyritic trachyte, phonolite porphyry and siliceous tuffs.

In the northern part of the area, a black silicified Middle Eocene limestone rich with graphite forms a circular stock, and is accompanied by the ultrabasic-basic bodies. These rocks are commonly brecciated, amygdaloidal and associated with REE-rich carbonatite-bearing rock. Southwards, the black rock is covered by the mineralized skarn bodies, particularly where siliceous volcanics are exposed. While, at the north-eastern part, the area is mainly covered by dunite rock with abundant chromite pods and lenses, and laterally grades to serpentinite rock and asbestos.

Aggregates of spherical and separate diamond crystals are associated with the altered kimberlite, picrite porphyry and chromite-rich dunite, particularly where the garnet mineral pyrope is present. This mineral assemblage is accompanied by the REE minerals (monazite, xenotime, bastnasite and weinschenkite), in addition to zircon, baddeleyite and less commonly phlogopite and omphacite.

Keywords: Diamond- bearing, REE, gold, silver, mineralization, Egypt.

STRONTIUM AND BARIUM BEHAVIOR IN POTASSIC-ALKALINE AND SUB-ALKALINE BASALTOID COMPLEXES OF THE TALYSH ZONE (AZERBAIJAN)

Kerimov V.M.[1], Purmuxtari M.B.[2]

1 Azerbaijan State Oil Academy, Baku, Azerbaijan
2 Institute of Geology and Geophysics of Azerbaijan National Academy of Sciences, Baku, Azerbaijan

The Talysh zone is situated in the southeastern part of Azerbaijan. Eocene alkaline and sub-alkaline volcanic formations are developed here. Early-Middle Eocene absarokite-shoshonite-alkali-basaltic and Upper Eocene latite-phonolitic complexes are distinguished according to formation time and petrographic composition.

The first complex has mainly developed in the Kosmolyan trough and Astara uplift, and the second – in Lerik trough and Burovar uplift.

Olivinic absarokite, shoshonite, tephrites, leucitic, analcite, aegirine, sanidine trachybasalts, trachydolerites, essexites take part in the composition of first complex in different distribution area.

In the mentioned rocks the strontium content varies from 450 g/t up to 900 g/t. However it is mainly concentrated in subdolerite ground mass in absarokite. Therefore the distribution coefficient is less than unity (Kd <1). A similar behavior pattern is also determined for barium.

However, compatible behavior of strontium is characterized for shoshonite, tephrite, trachybasalt, trachydolerite and essexite (Kd>1). Labradorite- bytownite plagioclase and apatite have crystallized in early magmatic stage, because they are the carrier and concentrator of strontium. Strontium content decreases significantly in glassy ground mass.

Strontium concentration is 1100-1400 g/t in the latites of megaplagioporphyritic andesite-labradorite plagioclase, and in hyalopilitic ground mass - 300-350 g/t. Undoubtedly, there is determined compatible behavior pattern of strontium as well.

Barium has mainly concentrated in the ground mass (Kd<1) in mentioned differentiates of subalkaline and alkaline series of Talysh. The most concentrations of barium were determined in epileusite phonolite (1450-1560 g/t). K-feldspar is the main barium concentrator here.

Melting fraction of metasomatized phlogopite peridotite is 7-11% according to Ba/Ca:Sr/Ca ratio.

Primitive subalkaline olivine-mafic melt has developed its composition from olivine absarokite up to epileusite phonolite during graben-like structures control.

INVESTIGATING IRON MINERALIZATION IN CHOGHART AND CHADORMALU IRON DEPOSITS, BASED ON MINERALOGICAL AND GEOCHEMICAL CHARACTERISTICS OF APATITE IN BAFQ MINING DISTRICT, YAZD PROVINCE, IRAN

Khorshidian F. [1], **Asadi S.**[2]

1 M.S. of economic geology, Shiraz university, Shiraz, Iran,
farid_sun94@yahoo.com
2 Assistant professor of economic geology, Shiraz university, Shiraz, Iran

Chadormalu iron deposit occurs 65 Km north of Bafq town, 180 Km northeast of Yazd city; and Choghart iron deposit is located 12 Km northeast of Bafq town, 130 Km southeast of Yazd city. Both deposits occur in central Iran zone and are Infracambrian (late Proterozoic- early Paleozoic) in age. The genesis of the Bafq iron deposits is very debatable and in the last 100 years many geologists who studied the area have proposed different genetic models, including: magmatic, sedimentary, volcanic, metamorphic, hydrothermal and exhalative models. In this study magnetite and apatite geochemistry and geothermometric measurements of fluid inclusions in apatite are used to determine geological processes related to ore deposition. the obtained results along with field observations and petroghraphic evidences in Choghart and Chadormalu show that both deposits are similar to Kiruna type and magmatic- hydrothermal deposits such as El Laco iron deposit in chily. Recently, Kiruna type deposits are classified as IOCG deposits. REE content of apatites and magnetites in Choghart and Chadormalu are very high and ∑REE ranges between 5781- 16460 in apatites, and between 22- 774 in magnetites. Distribution of REE, major and minor elements in apatite and magnetite reveal that similar geochemical processes have operated in Choghart and Chadormalu, and show the similarity of genesis of these deposits with those of Kiruna type IOCG. However, clear evidences emphasis the important role of hydrothermal activity, and ore replacements from high salinity and temperature fluids. Salinity of fluid inclusions ranges between 15 and 56 wt % NaCl equivalent, homogenization temperature varies between 310 and 475 °C and estimated pressure using Baker software is between 2.6- 3.4 Kb. Salinity and homogenization temperature of ore forming fluids is similar to magmatic fluids and brines. The result of this study show that both hydrothermal and magmatic processes are responsible for ore formation in Choghart and Chadormalu deposits.The origin of Choghart iron deposit and other similar iron oxide deposits in the Bafq mining district, like their counterparts in the rest of the world, has been the subject of continuing controversy for local geologists with the difference that the controversy has been fueled by the lack of absolute agedeterminations, accurate isotopic and fluid inclusion studies, and reliable analytical data.

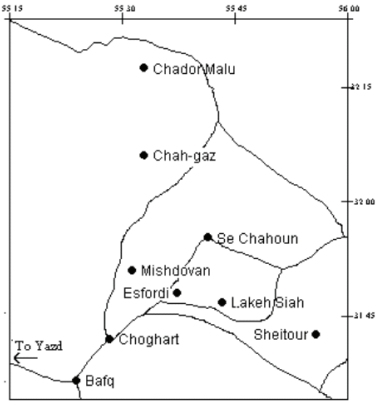

Figure 1. Geographic map showing the location of Choghart iron oxide deposit in the Bafq mining district of Iran.

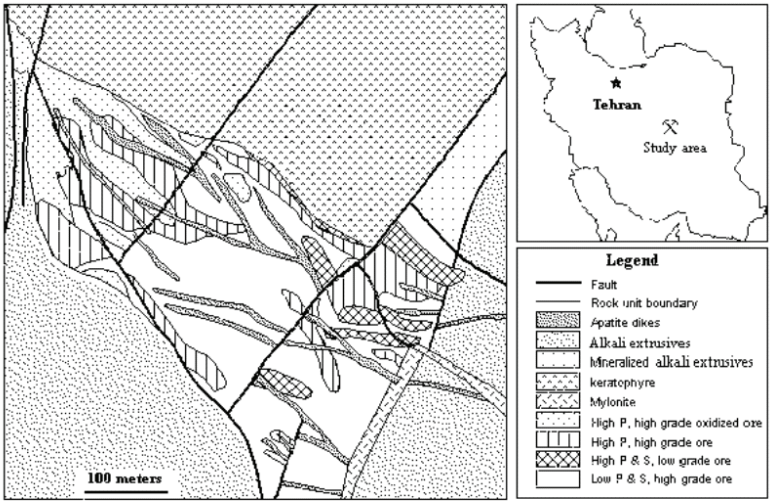

Figure 2. Geological map of Choghart deposit.

References

1. Moore F., Modabberi S., "Origin of Choghart Iron Oxide Deposit, Bafq Mining District, Central Iran: New Isotopic and Geochemical Evidence", Journal of Sciences, Islamic Republic of Iran, (2003),14(3): 259-269 University of Tehran, ISSN 1016-1104.
2. Williams P. J., Barton M. D., Johnson D. A., Fontbote L., De Haller A., Mark G., Oliver N. H. S., and Marschik, R., ″Iron Oxide Copper-Gold Deposits: Geology, Space-Time Distribution, and Possible Modes of Origin″, Society of Economic Geologists, Inc. Economic Geology 100th Anniversary Volume. (2005).
3. Wilkinson J. J., ″Fluid inclusions in hydrothermal ore deposits″. Lithos, (2001), Vol. 55, pp. 229-272.
4. Hitzman M. W., Oreskes N., and Einaudi M. T., ″Geological characteristics and tectonic setting of Proterozoic iron oxide (Cu–U–Au–REE) deposits″, Precambrian Res, (1992), Vol. 58, pp. 241–287.

CHEMICAL CONTENT AND STATISTICAL CORRELATION OF RARE EARTH ELEMENTS (REE) BETWEEN BOGACAYI (ANTALYA) RIVER SEDIMENT AND ALANYA-MANAVGAT (AKDENİZ) BEACH SAND

Kilic S.[1], Yalcin F.[2], Kilic M.[1], Yalcin M.G.[3], Paksu E.[3]

1 Akdeniz University, Food Security and Agricultural Research Center, 07058, Antalya, Turkey
2 Akdeniz University, Deparment of Mathematics, 07058, Antalya, Turkey
3 Akdeniz University, Deparment of Geological Engineering, 07058, Antalya, Turkey

Rare earth elements are a group containing Yttrium and Scandium with the lanthanides of which atomic numbers are between 57 and 71, and consisting of chemically similar elements. They are named as "rare" because they rarely exist compared to other minerals on the earth's crust. Mineralization of Rare Earth Elements is related with their main stratums, alkali rock complexes, carbonatites and placers, and they are observed generally together in secondary pegmatites and various metamorphic rocks' structure. Rare Earth Elements are generally used in glass and ceramic industry, the metallurgical industry, laser production, magnet production, oil catalyst and the production of high-tech devices. Rare Earth Elements actualize hybrid cars, electric vehicles, vehicles, wind turbines, solar energy panels, MRI machines and many clean energy technology. Due to Rare Earth Elements are needed in many green energy technologies, they are also known as "green elements".

The study area in which river sand of Bogacayı is examined flows in the basin which is approximately 25 kilometers in length. On the creek sand located in this line, La (Lanthanum), Ce (Cerium), Y (Yttrium) and Sc (Scandium) of Rare Earth Elements were analyzed. Maximum and minimum values obtained from analyses of 25 samples collected from the area are; Lanthanum (9.1-23.3), Cerium (15-40), Yttrium (7.7-15.5) and Scandium (5-11), and their average values respectively were calculated as 15.81, 27.84, 11.95 and 8.64. The maximum values for Lanthanum, Cerium and Yttrium are observed in 15 numbered location, for Scandium in 20 numbered location. The average values of samples collected from this area were calculated as Lanthanum 8.39, Cerium 16.07, Yttrium 8.60 and Scandium 2.60 (Table 1,2. Fig.1).

Considering the average of the results of chemical analysis, the REE values observed in Bogacayı creek sediments are higher than the REE values belonging to coast sand between Alanya-Manavgat. In both of the working area (Bogacayı and Alanya-Manavgat coastline), in 15 numbered location, Lanthanum and Cerium elements show the highest value together and it is observed that Yttrium and Scandium elements show behavior which is independent of this association. In Manavgat coast line, Yttrium has the highest value with Lanthanum and Cerium but Scandium has the highest value in a different location and shows an independent behavior.

Table 1: Chemical analysis contents

REE	La	Ce	Y	Sc
1	9,1	15	7,7	5
2	14,0	25	11,0	9
3	13,6	25	10,9	8
4	13,7	23	11,3	9
5	10,0	17	9,4	8
6	15,2	28	11,6	8
7	17,2	30	12,4	8
8	15,4	26	11,0	8
9	17,8	31	12,1	8
10	16,0	28	12,4	10
11	16,7	29	12,2	9
12	15,5	27	11,8	9
13	18,0	33	13,0	8
14	16,0	29	12,0	8
15	**23,3**	**40**	**15,5**	7
16	16,9	32	13,1	8
17	18,7	33	13,3	9
18	15,3	27	11,9	9
19	15,6	28	11,7	8
20	15,9	27	12,6	**11**
21	15,4	27	11,4	9
22	17,9	32	13,1	10
23	16,6	29	13,2	9
24	15,5	27	12,6	11
25	16,0	28	11,5	10

Table 2: Statistic data of chemical analysis contents.

		La	Ce	Y	Sc
N	Valid	25	25	25	25
	Missing	0	0	0	0
Mean		15,81200	27,84000	11,94800	8,64000
Median		15,90000	28,00000	12,00000	9,00000
Mode		16,000	27,000	11,000[a]	8,000
Std. Deviation		2,698969	4,930179	1,438784	1,254326
Variance		7,284	24,307	2,070	1,573
Skewness		-,113	-,490	-,645	-,483
Std. Error of Skewness		,464	,464	,464	,464
Range		14,200	25,000	7,800	6,000
Minimum		9,100	15,000	7,700	5,000
Maximum		23,300	40,000	15,500	11,000
Sum		395,300	696,000	298,700	216,000
Percentiles	25	15,25000	26,50000	11,35000	8,00000
	50	15,90000	28,00000	12,00000	9,00000
	75	17,05000	30,50000	12,80000	9,00000

a. Multiple modes exist. The smallest value is shown

Figure 1: correlations between Bogacayi creek sediments and Alanya-Manavgat coast sand REE contents.

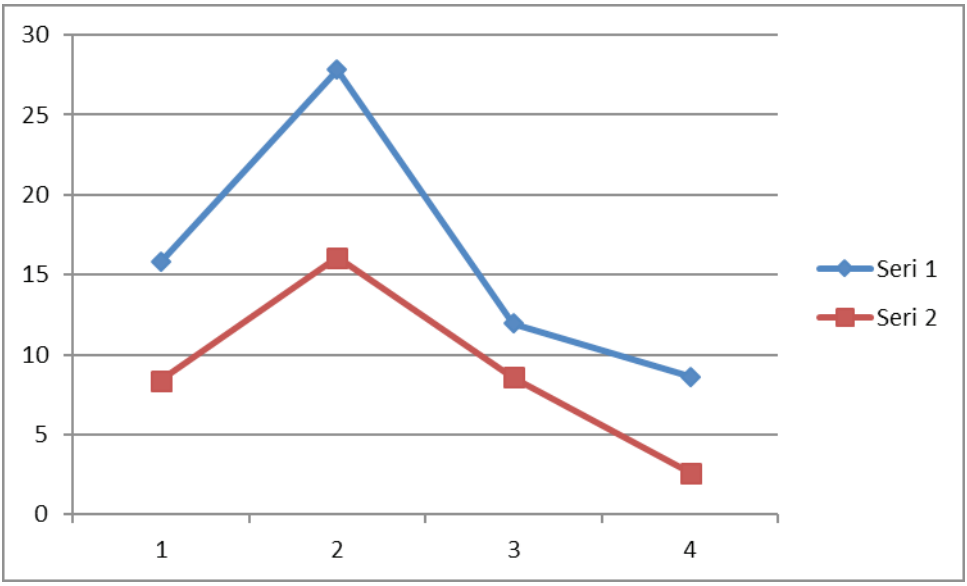

Seri 1. Bogacayi; Seri 2. Alanya-Manavgat

SUPER-LARGE ZIRCONIUM-HAFNIUM-RARE EARTH DEPOSIT OF KOLA PENINSULA (RUSSIA) ISOTOPIC ND, SR, HF, PB SIGNATURE, GEOCHEMISTRY, HIDDEN LAYERING, ORE FORMATION

Kogarko L.N.

V.I. Vernadsky Institute of Geochemistry and Analytical Chemistry, Russian Academy of Sciences, ul. Kosygina 19, Moscow, 119991 Russia
kogarko@geokhi.ru

At present the interest to alkaline rocks and carbonatites has grown significantly due to the increasing consumption of strategic metals in industry. This is well illustrated on an example of rare earth elements during the last several years. This is related to the extension of the utilization of REE in nuclear industry, in the production of high precision weapons and in the productioon of pure energy.

In the Kola Peninsula (Polar Russia) there are three superlarge REE deposits related to peralkaline nepheline syenites-Khibina (apatite deposit) and Lovozero complexes. The Lovozero massif, the largest of the Globe layered peralkaline intrusion,comprises super-large loparite (Na, Ce, Ca)$_2$ (Ti, Nb)$_2$O$_6$) rare-metal (Nb, Ta, REE) deposit and eudialyte (Na$_{13}$(Ca,Sr,REE)$_6$Zr$_3$(Fe,Nb,Ti)$_3$(Si$_3$O$_9$)$_2$[Si$_9$O$_{24}$(OH,Cl,S)$_3$]$_2$ ores-the valuable source of zirconium, hafnium and rare earth.Khibina apatite and Lovozero loparite had been mined during many years and constitute a world class mineral district. The Lovozero Pluton [1] (Fig. 1) consists of three intrusive phases: (1) medium-grained nepheline and hydronosean syenites; (2) differentiated complex of urtites, foyaites, and lujavrites; and (3) eudialyte lujavrites. Zirconium-hafnium-rare-earth deposit is saturated in the upper part of Lovozero intrusion as horizontal lentiform bodies.The amount of Zr in eudialyte is very hight -up to 14 wt %and total REE up to 4 wt %. (Fig.4) In contrast to other REE minerals of Lovozero eudialyte is enriched in HREE in a larger extend. Our investigations, [2] demonstrated, that the mantle source of these world's largest deposits exhibit significantly depleted signatures (ε_{Nd} +5 - +2.5, $^{87}Sr/^{86}Sr$- 0.70336-0.70400).

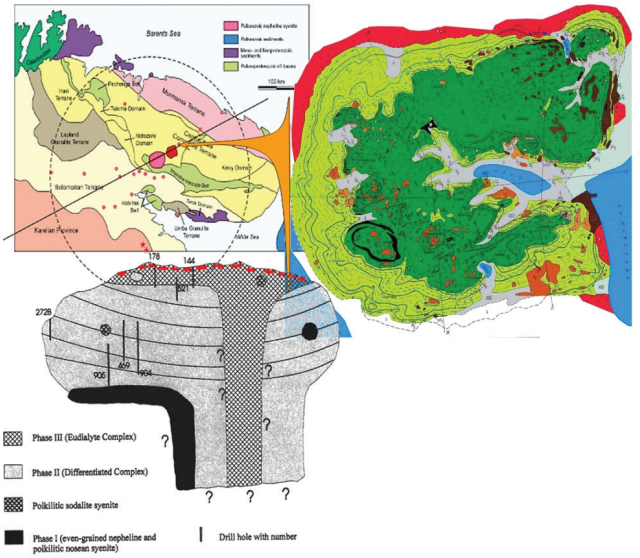

Figure 1: Lovozero massif

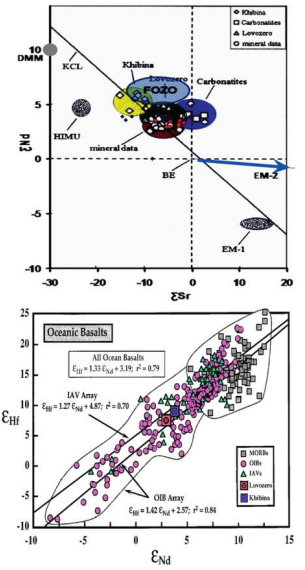

Figure 2: Isotopic signature of Lovozero and Khibina rare metal ore

Average ε_{Nd} for eudialyte ore of Lovozero is equal to 8. [3] (fig. 2) The plotting of the obtained data on the mantle correlation diagrams ε_{Nd} - ε_{Hf}, $^{87}Sr/^{86}Sr$ - ε_{Nd} demonstrates that the alkaline rocks and ores of the Lovozero rare metal deposits have depleted mantle sources similar to OIB. Alkaline rocks of the Kola Peninsula are the most enriched in rare elements, and they were generated due to the partial melting of the depleted material. This is possibly explained by the rapid development of mantle metasomatism, which resulted in the transport of rare elements and alkalis to the zone of magma generation.

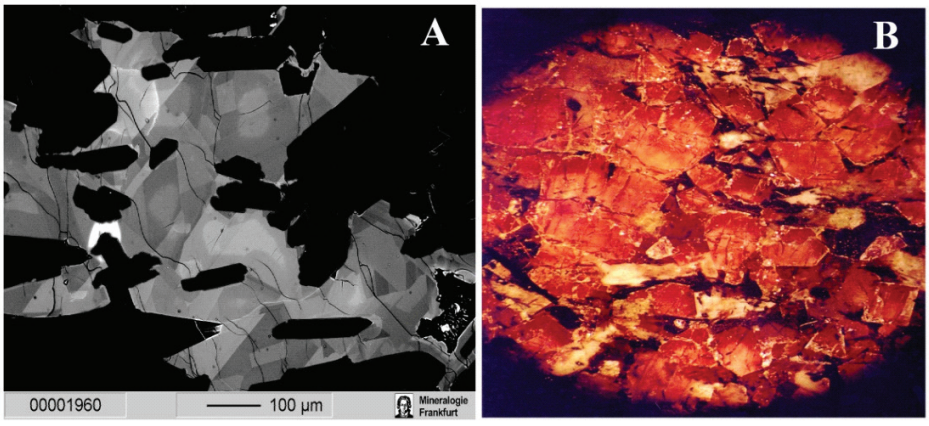

Figure 3: A – Interstitial eudialyte; B – Eudialyte ore

Morfology of eudialyte grains is changed with depth of Lovozero intrusion. (Fig. 3) In the lower part of the intrusion eudialyte forms anhedral interstitial crystals and crystallised when rock-forming minerals generated well-developed framework when convection ceased and accumulation of eudialyte is impossible. In the upper part of Lovozero stratigrafic section eudialyte forms euhedral grains which were formed at the early stage of crystallization. Thus the initial magma of Lovozero complex was undersaturated with this mineral. The melt became saturated with eudialyte after the approximately two-third of the volume of the massif solidified. Compositional evolution of eudialyte has been investigated through a 2.35 km section of the Lovozero massif using CAMECA microprobe and LA-ICP-MS. There is hidden layering in eudialyte in the crossection of the intrusion.The composition of cumulus eudialyte changed systematically upward through the third intrusion with an increase in Na, Sr,Nb,Th ,Mn/Fe Nb/Ta , U/Th and decrease in REE, Zr,V,Zn,Ba and Ti.The specific gravity of eudialyte is much higher then initial alkaline melt.Nevertheless eudialyte accumulated in the .very upper zone of Lovozero intrusion We suggest that eudialyte formed very small crystals (nanoctystals) (Fig. 5) which were stirred in melt and under the conditions of steady-state convection eudialyte emerged upward. Later eudialyte crystals recrystallized and increased in size. (Fig. 5)

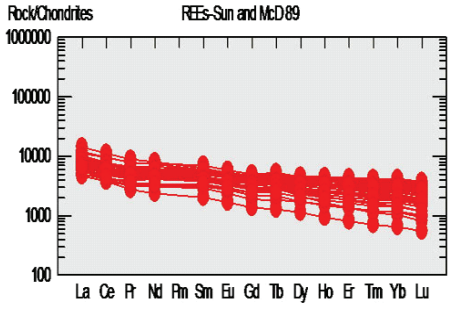

Figure 4: REE pattern of eudialyte

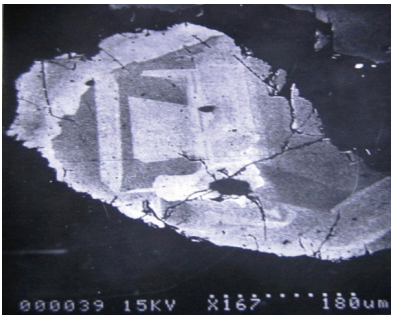

Figure 5: recrystallized eudialyte

Our investigation indicates that the formation of eudialyte ore was the result of several factors including the chemical evolution of high alkaline magmatic system and mechanical accumulation of eudialyte in the upper part of the intrusion. This work was supported by Arctica Program RAS.

References

1. Kogarko L.N., Kononova V.A., Orlova M.P., Woolley A.R., 1995. Alkaline rocks and carbonatites of the world: Part 2. Former USSR. Chapman and Hall, London, p. 225
2. Kramm U., Kogarko L.N., 1994. Nd and Sr isotope signatures of the Khibina and Lovozero agpaitic centers, Kola Alkaline Province, Russia. // Lithos, 32, 225-242 p.
3. Kogarko L. N. & Lahaye Y. & Brey G. P., 2010. Plume-related mantle source of super-large rare metal deposits from the Lovozero and Khibina massifs on the Kola Peninsula, Eastern part of Baltic Shield: Sr, Nd and Hf isotope systematic. Miner Petrol 98, 197-208 p.

SUPERLARGE STRATEGIC-METAL DEPOSITS IN THE PERALKALINE COMPLEXES OF EASTERN PART OF BALTIC SHIELD (AGE, ISOTOPIC SOURCES, GEOCHEMISTRY, MECHANISMS OF ORES FORMATION)

Kogarko L.N.

V.I. Vernadsky Institute of Geochemistry and Analytical Chemistry, Russian Academy of Sciences, Moscow, Russia
kogarko@geokhi.ru

At present the interest to alkaline rocks and carbonatites has grown significantly due to the increasing consumption of strategic metals in industry. This is well illustrated on an example of rare earth elements during the last several years. This is related to the extension of the utilization of REE in nuclear industry, in the production of high precision weapons and in the production of pure energy. In the center part of Kola Peninsula (Russia) there is ultramafic alkaline province comprising carbonatites, ultramafic rocks and two largest of the Globe layered peralkaline intrusion Khibina and Lovozero (370 Ma age [1,2]) (Fig. 1).

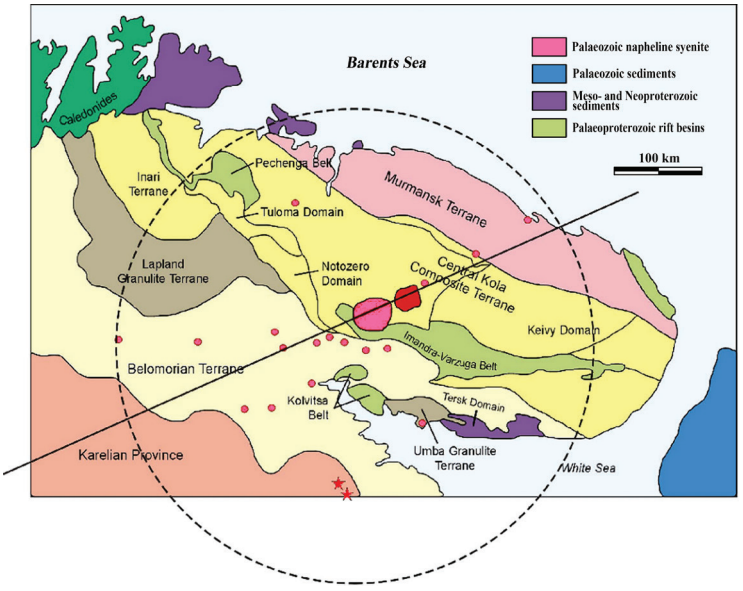

The Lovozero massif, contains super-large loparite $(Na, Ce, Ca)_2 (Ti, Nb)_2O_6$) rare-metal (Nb, Ta, REE) deposit and eudialyte $(Na_{13}(Ca,Sr,REE)_6Zr_3(Fe,Nb,Ti)_3(Si_3O_9)_2[Si_9O_{24}(OH,Cl,S)_3]_2$ ores-the valuable source of REE,Nb, Ta,Zr,Hf..Khibina apatite and Lovozero loparite had been mined during many years and constitute a world class mineral district. The Lovozero Pluton [1] consists of three intrusive phases: [1] medium-grained nepheline and hydronosean syenites; [2] differentiated complex of urtites, foyaites, and lujavrites; and [3] eudialyte lujavrites [1].

The main ore mineral is loparite $(Na, Ce, Ca)_2 (Ti, Nb)_2O_6$ (Fig 2). In the deepest zone of the intrusion loparite forms anhedral grains confined to interstitial spaces. Above 800m in stratigraphic section loparite makes up euhedral crystals which were formed at the early stage of crystallization. Therefore the initial magma was undersaturated with loparite. After the formation of approximately one-third of the volume of the Lovozero intrusion, the melt became saturated with loparite and this mineral accumulated in ore layers. The composition of cumulus loparite changed systematically upward through the intrusion with an increase in Na, Sr, Nb, Th, U and decrease in REE, Zr, Y, Ba and Ti. Our investigation indicates that the formation of loparite ore was the result of several factors including the chemical evolution of high alkaline magmatic system and mechanical accumulation of loparite as a heaviest phase at the base of convecting unit.

Zirconium-hafnium-rare-earth deposit is saturated in the upper part of Lovozero intrusion as horizontal lentiform bodies. The amount of Zr in eudialyte is very hight -up to 14 wt % and total REE up to 4 wt % (Fig. 4)

Morfology of eudialyte grains is changed with depth of Lovozero intrusion. In the lower part of the intrusion eudialyte forms anhedral interstitial crystals and crystallised when rock-forming minerals generated well-developed framework when convection ceased and accumulation of eudialyte is impossible. In the upper part of Lovozero stratigrafic section eudialyte forms euhedral grains which were formed at the early stage of crystallization. Thus the initial magma of Lovozero complex was undersaturated with this mineral. The melt became saturated with eudialyte after the approximately two-third of the volume of the massif solidified. Compositional evolution of eudialyte (Fig. 3) has been investigated through a 2.35 km section of the Lovozero massif using CAMECA microprobe and LA-ICP-MS.

There is hidden layering in eudialyte in the cross-section of the intrusion. The composition of cumulus eudialyte changed upward through the third intrusion with an increase in Na, Sr, Nb, Th, Mn/Fe, Nb/Ta, U/Th and decrease in REE, Zr, V, Zn, Ba and Ti. The specific gravity of eudialyte is much higher then initial alkaline melt. Nevertheless eudialyte accumulated in the very upper zone of Lovozero intrusion. We suggest that eudialyte formed very small crystals (nanocrystals) which were stirred in melt and under the conditions of steady-state convection eudialyte emerged upward. Later eudialyte crystals recrystallized and increased in size. Our investigations, [2,3] demonstrated, that the mantle source of these deposits exhibit depleted signatures (ε_{Nd} +5, $^{87}Sr/^{86}Sr$- 0.70336-0.70400, εHf+6) (Fig. 5, 6).

The Khibina alkaline massif (Kola Peninsula, Russia) hosts the world's largest and economically most important apatite deposit. The Khibina massif is a complex multiphase body built up from a number of ring-like and conical intrusions. The apatite bearing intrusion is ring-like and represented by a layered body of ijolitic composition with a thickness of about 1-2 km. The upper zone is represented by different types of apatite ores.This rocks consists of 60-90% euhedral very small (tenths of mm) apatite crystals. The lower zone is mostly ijolitic composition. The lower zone grades into underlying massive urtite consisting of 75-90% large (several mm) euhedral nepheline. Our experimental studies of systems with apatite demonstrated the near-eutectic nature of the apatite-bearing intrusion, resulting in practically simultaneous crystallization of nepheline, apatite and pyroxene.

The mathematical model of the formation of the layered apatite-bearing intrusion based on the processes of sedimentation under the conditions of steady state convection taking account of crystal sizes is proposed. Under the conditions of steady-state convection large crystals of nephe-

line continuously had been settling forming massive underlying urtite when smaller crystals of pyroxenes, nepheline and apatite had been stirred in the convecting melt. During the cooling the intensity of convection decreased causing a settling of smaller crystals of nepheline and pyroxene and later very small crystals of apatite in the upper part of alkaline magma chamber.

References

1. Kogarko L.N., Kononova V.A., Orlova M.P., Woolley A.R., 1995. Alkaline rocks and carbonatites of the world: Part 2. Former USSR. Chapman and Hall, 225 p. (London)
2. Kramm U., Kogarko L.N., 1994. Nd and Sr isotope signatures of the Khibina and Lovozero agpaitic centers, Kola Alkaline Province, Russia. Lithos. v. 32, p. 225-242.
3. Kogarko L. N., Lahaye Y. & Brey G. P., 2010. Plume-related mantle source of super-large rare metal deposits from the Lovozero and Khibina massifs on the Kola Peninsula, Eastern part of Baltic Shield: Sr, Nd and Hf isotope systematic. Miner Petrol. v. 98, p. 197-208.

ABOUT ORIGIN OF KIMBERLITES

Kostrovitsky S.I.

Institute of Geochemistry SB RAS, Irkutsk 664033, Russia
serkost@igc.irk.ru

When developing the model of kimberlite formation of the 1st group the following features of rock composition should be taken into account:

1. Kimberlites of different provinces, fields and pipe clusters may be considerably distinguished in the contents of such oxides as FeO_{total}, TiO_2 and K_2O. Within the Yakutian Province there are both high-Mg kimberlites (FeO_{total} < 8 wt. %, TiO_2 <1 wt.%) forming highly-diamondiferous deposits (e.g. International, Aikhal, Njurbinsky, etc.), and Mg-Fe kimberlites (8-12 wt. % FeO_{total}l 1-2 wt.% TiO_2) producing sizable deposits Mir, Udachnaya, Yubileinaya, and eventually Ti-Fe kimberlites (10-15 wt. % FeO_{total}l 2-6 wt.% TiO_2) occurring in the north of Yakutia and forming no significant deposits of diamonds.
2. Kimberlites are ultrabasic rocks with unusually abundant incompatible elements. Regarding the distribution of incompatible elements kimberlites seem to be close to the rocks of alkaline-basaltoid composition.
3. Irrespective of location and varying chemical composition kimberlites have close isotope and geochemical characteristics pointing to the involvement of the same source, supposedly asthenosphere.
4. Kimberlites are characterized by the presence of carbonate component, which widely varies in composition from 1-3 to 20 %.
5. Kimberlites are typified by the presence of low-Cr, high-Ti megacryst association of minerals, but high-Mg kimberlites, its heavy fraction dominated by pyropes and chrome spinel, the low-Cr mineral association practically not available. The genetic relationship is existent between megacrysts and hosting kimberlites, which is indicated by affinity of isotope characteristics and dating (Nowell et al, 2004; Agashev et al., 2006; Kostrovitskiy et al., 2007, 2013).
6. Kimberlites contain clastic material of the lithosphere mantle available as xenoliths and xenocryst minerals.

The critical goals in recognizing the nature of kimberlites are to find out: (1) the primary composition of melt of these rocks and (2) the principal processes of evolution of primary composition of kimberlites while ascending from the mantle depth towards the earth surface.

The hybrid nature of kimberlites, which is acknowledged by practically all researchers is due to both mechanic capture of clastic material of the lithosphere mantle and its inevitable partial assimilation (Russel et al., 2012), which results in the further change of primary melt composition towards magnesium coefficient rise. Therefore, any efforts to determine the composition of primary melt from the composition of kimberlites, even hypabyssal facies are doomed to failure (Mitchell, 2008).

The role of hybridism in kimberlite emplacement is evident in the composition of breccias and massive kimberlites composing pipe and dyke bodies of the Kuoiksky field, in particular Ob-

nazhennaya pipe. The former compared to massive varieties of kimberlites show much higher contents of SiO_2, MgO and much lower CaO and CO_2; the massive varieties of kimberlites are more ferriferous and titaniferous. The onset of breccias formation should evidently be attributed to the time of passing kimberlite melt-fluid through the lithosphere mantle. It is triggered by the processes of disintegration and capture of its rocks.

Diverse assumptions concern the primary composition of kimberlite melt. Many researchers based their evaluation of data on the composition of hypabyssal kimberlites of aphanite structure bearing minimum amount of unknown olivine macrocrysts (Kopylova et al, 2007). In the recent years some researchers tend to believe that the carbonate component was role-defining in the formation of kimberlites of carbonate component. The other group inferred on the insignificant contribution of olivine which crystallized from kimberlite melt (Arndt et al , 2010; Brett et al, 2009). The model of kimberlite formation (Russell et al., 2012) assumes that the primary source of kimberlite formation is the carbonatite fluid, which disintegrated and assimilated its fragments in ascending through the lithosphere mantle, gradually being transformed into a kimberlite melt.

In our view, the Russell's model (2012) disagrees with the material available in the composition of kimberlites. It does not explain a wide variety of petrochemical composition common for kimberlites. Second, this model does not account for the presence in kimberlites of genetically-linked megacryst low-Cr high-Ti association of minerals.

Suppose that the primary composition of kimberlite melt-fluid was in fact the composition of asthenosphere melt being close to alkaline-basalt one saturated with high CO_2. The genetic relation of kimberlites with basaltoids is indicated by a spatial and temporal affinity of their formation (Carlson et al, 2006; Chalapathi, Lehmann, 2011; Lehmann et al, 2010; Tappe et al, 2012), similarity of the pattern of incompatible elements distribution, presence of megacryst minerals in alkaline basaltoids, Pyr-Alm garnet included, and finally, model calculation of parent melt composition for low-Cr megacryst minerals; it showed this composition to be typical for the alkaline basaltoid (Jones, 1980).

P-T conditions of crystallization of low-Cr megacrysts evaluated by geothermobarometers correspond to the zone of asthenosphere layer transition into lithosphere mantle (Moore et al, 1992; Hops et al, 1992). While crystallizing minerals of relatively ferriferous megacryst association, the Mg# of residual asthenosphere melt raised thus transforming its composition from alkaline-basaltoid into the one close to ultrabasic (kimberlite).

We assume that prior to crystallization (or in time of crystallization) of the low-Cr megacryst association of minerals at the level of asthenosphere the differentiation of primary melt causing formation of parts with varying met/fluid ratio and possibly with different content of alkalis (K_2O).

The outbreak of asthenosphere substance through lithosphere mantle proceeded by different scenarios:

(1) With a noticeable dominance of fluid component kimberlites were formed by the capture and contamination of high-Mg, high-Cr rocks of lithosphere mantle that caused formation of high-Mg kimberlites.

(2) With a considerable proportion of melt phase depending on its ratio with fluid phase there formed magnesium-ferriferous and ferriferous-titaniferous petrochemical types of kimberlites. There is no doubt that in formation of these kimberlite types the contamination of lithosphere material was the case, however at the much lower level than in formation of high-Mg kimberlites.

In fact, the model derived by Russel et al. (2012) fits the 1st scenario and thus it is a particular case of our model which logically explains steady differences in the chemistry of kimberlites making up clusters of different pipes, fields and even provinces. The model clarifies presence or absence of low-Cr, high-Ti megacryst mineral associations, with its crystallization proceeding in the melt phase of asthenosphere source of kimberlites.

References

1. Agashev A.M., Pokhilenko N.P., Malkovets V.G., Sobolev N.V. (2006) Sm-Nd-isotope system in garnet megacrysts from kimberlite pipe Udachnaya (Yakutia) and problem of kimberlite genesis. Dokladi RAN. V. 407. N 6. P. 806-809 (on Russian).
2. Arndt, N. T., Guitreau M., Boullier, A. M., le Roex A., Tommasi A., Cordier P., and A. Sobolev. (2010). Olivine, and the origin kimberlite. Journal of Petrology. V. 51. N. 3. P. 573-602.
3. Brett, R. C., Russell, J. K. & Moss, S. (2009) Origin of olivine in kimberlite: phenocryst or imposter? Lithos. V. 112. P. 201–212.
4. Carlson, R.W., Czamanske, G., Fedorenko, V., Ilupin, I. (2006) A comparison of Siberian meimechites and kimberlites: implications for the source of high-Mg alkalic magmas and flood basalts. Geochem. Geophy. Geosys. V. 7. 755 doi:10.1029/2006GC001342
5. Chalapathi Rao N.V., Lehmann B. (2011) Kimberlites, flood basalts and mantle plumes: New insights from the Deccan Large Igneous Province. Earth-Science Reviews, V. 107, Issues 3–4. P. 315-324.
6. Lehmann B., Burgess R., Frey D., Belyatsky B., Mainkar D., Chalapathi R., Heaman L.M. (2010) Diamondiferous kimberlites in Central India synchronous with Decan flood basalts. Earth and Planetary Science Letters. V. 290. P. 142-149.
7. Hops J.J., Gurney J.G., Harte B. (1992) The Jagersfontein Cr-poor megacryst suite – towards to motlel for megacryst paragenesis. Journal of Volcanology and Geothermal Researches. V. 50. P. 143-160.
8. Kopylova, M.G., Matveev, S., Raudsepp, M. (2007). Searching for parental kimberlite melt. Geochimica et Cosmochimica Acta. V. 71. P. 3616-3629.
9. Kostrovitsky S.I., Morikiyo T., Serov I.V., Yakovlev D.A., Amirzhanov. (2007) Isotope-geochemical systematics of kimberlites and related rocks from the Siberian Platform. Russian Geology and Geophysics. V. 48 P. 272–290.
10. Kostrovitsky S. I., Solov'eva L. V., Yakovlev D. A., Suvorova L. F., Sandimirova G. P., Travin A. V., and Yudin D. S. (2013) Kimberlites and Megacrystic Suite: Isotope_Geochemical Studies. Petrology. V. 21, No. 2. P. 127–144.
11. Mitchell, R. H. (2008) Petrology of hypabyssal kimberlites: relevance to primary magma compositions. J. Volcanol. Geotherm. Res. V. 174. P. 1–8.
12. Moore R.O., Griffin W.L., Gurney J.J., Ryan C.G., Cousens D.R., Sic S.H., Surer G.F, (1992) Trace elements geochemistry of ilmenite megacrysts from the Monastery kimberlite, South Africa. Lithos. V. 29. P. 1-18.
13. Nowell G.M., Pearson D.G., Bell D.R., Carlson R.W., Smith C.B. and Noble S.R. (2004) Hf isotope systematics of kimberlites and their megacrysts: new constraints on their source regions. J. of Petrology. V. 45. N. 5. P. 1583-1612.
14. Russell J. K., Porritt L.A., Lavallee Yan, Dingwell D.B. (2012) Kimberlite ascent by assimilation – fuelled buoyancy. Nature. V.481, No. 19, 352-356.
15. Tappe, S., Simonetti, A., 2012. Combined U-Pb geochronology and Sr–Nd isotope analysis of the Ice River perovskite standard, with implications for kimberlite and alkaline rock petrogenesis. Chem. Geol. 304-305, 10-17.

GEOCHEMICAL DATA IN GEOTECHNICS: ECEMIS FAULT ZONE

Leventeli Y.

Akdeniz Univ., Geological Eng. Dep., Antalya/TURKEY
leventeli@akdeniz.edu.tr

The Ecemis Fault Zone is located between Adana and Niğde, in the south of Turkey with numerous huge landslides. The main cause of geotechnical problems in the zone; especially huge landslides with several billions cubic meters have been formed by trinity of water-discontinuity-clay. Water is an important factor in geotechnical problems. So, the geochemical analyses used to determine the origin of water can be used to explain the landslide mechanism. The analysis indicate how and where the water comes from. In this study, the geochemical anaysis showed that the origin of water is meteoric and water is one of the main causes of the landslide in the study area.

Keywords: Ecemiş, fault, landslide, water, geochemistry

References

1. Canik, B., 1998. Investigation, operation and chemistry of groundwater. Ankara University, Faculty of Science, Geological Engineering Departmen, s.286, Ankara (in Turkish).
2. Craig, H., 1961. Isotopic variations in meteoric water. Science 133, 1702-1703.
3. Leventeli, Y., 2002. The Importance of geology and geotechnic in engineering projects: Ecemis Fault Zone, Adana – Nigde. Cukurova University., PhD Thesis, Adana, (in Turkish).
4. Leventeli, Y., Yilmazer, I., 2003. Geotechnical approach for Ecemis Valley. Journal of Engineering Geology, Volume: 27, No:1, 45-57 (in Turkish).
5. Mathewson, C.C., 1981. Engineering Geology. Bell&Howell Company, pp. 450.
6. M.T.A (1987), 1:100 000 Geological map of Turkey, KOZAN-J 20 , 17 s., Ankara (in Turkish)
7. M.T.A (1990), 1:100 000 Geological map of Turkey, KOZAN-J 19, 28 s., Ankara (in Turkish).
8. Sahinci, A., 1991. Geochemistry of Natural Water. Akdeniz Univesity Isparta Engineering Faculty, P.548, İzmir. (in Turkish)
9. Yetis, C., 1978. Geological investigation of Çamardı (Niğde) and properties of Ecemiş Fault Zone between Maden Boğazı-Kamışlı. Istanbul University, Faculty of Science; PhD, 164 s., Istanbul (in Turkish)
10. Yilmazer, I., 1995. Significance of discontinuity surveying in motorway alignment selection, southern Turkey. Engineering Geology 40, 41-48.
11. Yilmazer, I., Yilmazer, O., Dogan, U., 1997. Significance of water-discontinuity-clay (WDC). Proceedings International Symposium on Engineering Geology and the Environment, 457-462, Athens.

REE, Y, ZR, NB CONTENTS IN HAINITE FROM DIFFERENT ALKALINE ROCKS

Lyalina L., Zozulya D., Savchenko Y., Selivanova E.

Geological Institute, Kola Science Centre, Russian Academy of Sciences, Apatity, Russia
lialina@geoksc.apatity.ru

Hainite belongs to the minerals of rosenbuschite group together with rosenbuschite, götzenite, seidozerite, kochite and grenmarite. The rosenbuschite group minerals are Na-, Ca-rich titanosilicates with layered type of structure. It is known that titanosilicates are remarkable for their cation exchange properties and thereby the study of their crystallization conditions is of great practical importance.

Rosenbuschite group minerals normally occur in alkaline rocks and related Si-undersaturated rocks. The group shows a wide compositional variability hosting a large number of elements. Besides Si the main elements are Na, Ca, Y, Mn, Fe, Ti, Mg, Zr, Nb, and REE, which occur in various concentrations. Hainite $(Na(Na,Ca)_2Ca_2(Ca,Zr,Y)_2Ti(Si_2O_7)_2F_2F_2)$ and götzenite $(NaCa_6Ti(Si_2O_7)_2OF_3)$ are closely related in composition and structure [3].

By today hainite is known from the five occurrences. Hainite was originally described in phonolites and tinguaites vugs from Northern Bohemia [2, 5]. The next description of hainite was made in phonolites vugs from Minas Gerais, Brazil [1, 4]. The following discoveries of hainite were made from pegmatites related to nepheline syenite of Langesund Fjord, Norway [3] and pulaskite of Ilímaussaq alkaline complex, Greenland [6]. The last finding of hainite is made during this study. It is revealed in nepheline syenite pegmatite of Sakharjok massif, Kola Peninsula, NW Russia. Mineral occurs as disseminated individual crystals up to 2 mm length and agglomerations of several tens grains in unhomogeneous aggregate of leucocratic minerals (hydrated muscovite, analcime, albite, nepheline).

Comparison of hainite compositions from different localities revealed the follow distinctions. Noteworthy that hainite from all previously known occurrences has the differences in chemical composition. Only Ce and La are indicated for hainite from type locality in Northern Bohemia (suggesting the Y and other REE are negligible). Y and REE contents for Minas Gerais hainite are relatively low (0.01-0.07 and 0.08-0.24 apfu). Hainite from Langesund and from Ilímaussaq have more elevated Y and REE contents (0.3 and 0.25, 0.22 and 0.32 apfu, respectively). The Sakharjok mineral is distinguished by extremely high Y (average values 0.66 apfu) and elevated REE (0.20 apfu). Chondrite-normalized REE pattern for Sakharjok hainite (Fig. 1) is characterized by strongly prevailing HREE (average Ce/Y_n is 0.07). Otherwise, Ce/Y_n ranges from 7 to 49 for Minas Gerais, 2.6 to 2.8 for Ilímaussaq, 1.1 for Langesund. Sakharjok hainite differs from all previously studied minerals by two-, five-fold depletion by light REE (in some samples La and Ce contents are below detection limit). These peculiarities of REE distribution in hainite worldwide might explained by HREE-Y enrichment of parental melts/fluid for Sakharjok pegmatite.

Zr content in previously studied hainite comprises 0.14-0.41 apfu, and Sakhrjok hainite mostly falls in this range. At the same time the Sakharjok hainite is strongly richer in Nb (up to 0.20 apfu, average value 0.13), which is significantly higher than that for hainite from Ilímaussaq, Langesund and Minas Gerais (0.06-0.08 apfu, Fig. 2).

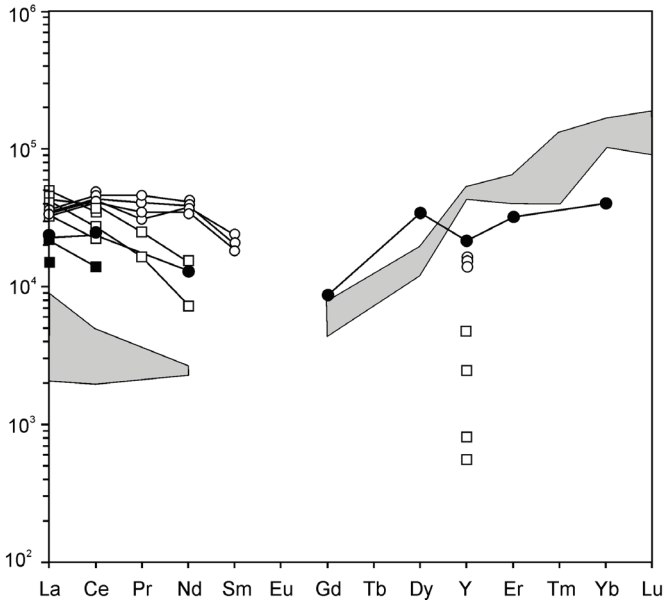

Figure 1: Chondrite-normalised REE patterns for hainite (shaded area – Sakharjok; filled squares – Nortern Bohemia; squares – Minas Gerais; filled circles – Langesund; circles – Ilímaussaq).

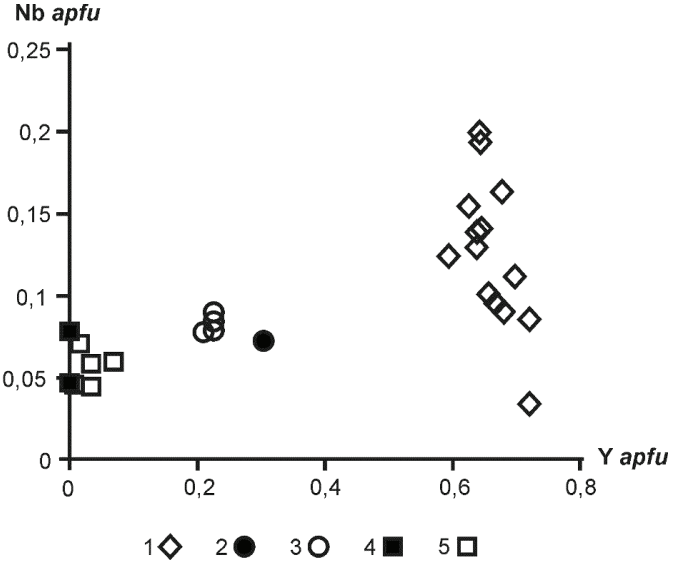

Figure 2: Chemical composition of hainite from different occurrences on Y-Nb (apfu) diagram (1 – Sakharjok, 2 – Langesund, 3 – Ilímaussaq, 4 – Northern Bohemia, 5 - Minas Gerais).

Thus, hainite is capable to incorporate the significant amounts of Zr, Nb, REE and Y. Hainite is of late- and post-magmatic origin, as it occurs in pegmatites and volcanic vugs. The relatively higher contents of Nb, HREE and Y in hainite from pegmatite occurrences (and extremely for Sakharjok) comparing to volcanic rock occurrences can be explained by different PT conditions and fluid composition of crystallization media.

The study is supported by the Earth Science department of Russian Academy of Sciences (Program 9).

References

1. Atencio D., Coutinho J.M.V., Ulbrich M.N.C., Vlach S.R.F., Rastsvetaeva R.K., Pushcharovsky, D.Yu., 1999. Hainite from Poços de Caldas, Minas Gerais, Brazil. Canadian Mineralogist, 37, 91-98.
2. Blumrich J., 1893. Die phonolithe des Friedländer Bezirkes in Nordböhmen. Tschermaks Mineralogische und Petrographische Mitteilungen, 13, 465-495.
3. Christiansen C.C., Johnsen O., Makovicky E., 2003. Crystal chemistry of the rosenbuschite group. Canadian Mineralogist, 41, 1203-1224.
4. Guimarães D., 1948. The zirconium ore deposits of the Pogos de Caldas plateau, Brazil, and zirconium geochemistry. Instituto de Tecnologia Industrial, Boletim 6.
5. Johan Z., Čech F., 1989. New data on hainite, $Na_2Ca_4[(Ti,Zr,Mn,Fe,Nb,Ta)_{1.50}\square_{0.50}](Si_2O_7)F_4$ and its crystallochemical relationship with götzenite, $Na_2Ca_5Ti(Si_2O_7)_2F_4$. C.R. Acad. Sci. Paris, 308, series II, 1237-1242
6. Rønsbo J.G., Sørensen H., Roda-Robles E., Fontan F., Monchoux P., 2014. Rinkite-nacareniobsite-(Ce) solid solution series and hainite from the Ilímaussaq alkaline complex: occurrence and compositional variation. Bulletin of the Geological Society of Denmark, 62, 1-15.

SEISMICITY OF THE REGION OF ALGERIERS ANALYSIS AND SYNTHESIS OF CURRENT KNOWLEDGE

Mabrouk D.

Physics laboratory of the Earth
M'Hamed Bougara University, Boumerdes Algeria

The Algiers region is linked to the geodynamic context of the western Mediterranean consequence of the collision between the Eurasian-African plates. It 'is one of Algeria or deformation regions are slow and most active and where the activity diffuse and moderate seismic magnitude is often not exceeding V degrees but sometimes produces rare strong earthquakes Thus, from the XIV th century, several strong earthquakes of high intensity occurred (Algiers and its surroundings in 1365,1541,1673, 1716,1755,1924 ... Blida region in 1825 and 1716, Boumerdes region in 2003 ...)

This seismic activity is mainly localized on the edges of the basin Mio-Pliocene - Quaternary Mitidja and offshore Many research in geosciences (seismotectonic, seismic etc. ...) have identified the existence of some potentially major seismogenic faults (fault Thenia, Boumerdes fault, fault Kair Eddine fault Atlas blidéen, F goes to Chenoua etc. ...) of which the actual knowledge of their geodynamic evolution, their depth extension etc. ... are inadequate and require further multidisciplinary research. These reverse faults and generally not particularly inclined concealed type are capable of generating earthquakes in the Algiers region.

Keywords: Algiers region, seismicity, slow deformations seismogenic faults, basin Mitidja

ENRICHMENT OF RARE EARTH ELEMENTS (REE) DURING THE MAGMATIC EVOLUTION OF THE ALKALINE TO PERALKALINE ILÍMAUSSAQ COMPLEX, SOUTH GREENLAND

Marks, M.A.W., Markl, G.

Universität Tübingen, Mathematisch-Naturwissenschaftliche Fakultät, FB Geowissenschaften, Wilhelmstrasse 56, D-72074 Tübingen, Germany
michael.marks@uni-tuebingen.de

The Ilímaussaq igneous complex in South Greenland is a Mesoproterozoic composite intrusion that mainly consists of syenitic and nepheline syenitic rocks. Some Ilímaussaq rocks have economically very attractive levels of REE, Zr, Nb, Be and U. The complex has therefore a long prospection and exploration history and recent developments on the REE market as well as political changes in Greenland has led to increased exploration activity in the complex. In the northwestern part of the Ilímaussaq complex, the Kvanefjeld project hosts the second-largest deposit of REEs and the sixth-largest U deposit world-wide. Kvanefjeld differs from many other emerging REE projects in that it is a multi-commodity project that is also expected to produce U and Zn. Several new target areas (Steenstrupsfjeld, Sørensen Zone and Zone 3) have also been identified as potential economic deposits. To date, these deposits are owned by Greenland Minerals and Energy Ltd (GMEL) and have an estimated resource of 956 Mt containing 575 Mlbs U_3O_8, 10.33 Mt total RE_2O_3 and 2.2 Mt Zn (May 2014).

Several major intrusive phases can be distinguished: The oldest and least evolved unit of the complex is a metaluminous augite syenite, followed by minor amounts of peralkaline granite and quartz syenite. Peralkaline nepheline syenites represent the largest volume of the complex and most of them contain eudialyte-group minerals, classifying them as agpaitic rocks for which the Ilímaussaq complex is the type locality. They are subdivided into coarse-grained roof series (pulaskite, foyaite, sodalite foyaite, naujaite) and floor series (kakortokite) cumulate rocks and several types of mostly fine-grained and melanocratic rocks (lujavrites), many of which possess strong magmatic fabrics.

To date, it is believed that such rock types form by fractional crystallization processes of alkali basaltic and nephelinitic parental magmas derived from lithospheric mantle sources. In that sense, the Ilímaussaq rocks are some of the most extreme products of magmatic differentiation processes known. Because of its exceptionally long crystallization interval and the major changes in the mineralogy of the successive rock units, the complex offers a unique possibility to study the stability relations and compositional evolution of rock-forming minerals in alkaline to peralkaline magmas and the parameters governing the enrichment of Na, Fe, halogens, and economically important elements such as REE such systems.

Detailed investigations of mineral assemblages and their compositional evolution trends within and between the various rock types provide detailed insight in the magmatic evolution of the Ilímaussaq system: The mafic mineral assemblage changes from olivine + augite + Fe-Ti oxides + apatite + baddeleyite in the augite syenite towards sodic amphibole + eudialyte ± sodic pyroxene ± aenigmatite in the agpaitic rocks. Felsic minerals during the augite syenite stage are

alkali feldspar and minor amounts of nepheline. In the agpaitic rocks, alkali feldspar, nepheline and sodalite are very abundant and in some lujavrites, albite and microcline form separate crystals and alkali feldspar is not present. The formation of sodalite, fluorite and villiaumite in the agpaites clearly reflects the unusual Cl- and F-rich composition of the agpaitic melt and because of the high solubility of REE, Zr and other HFSE in such alkali- and halogen-rich melts, their concentration reaches high values and eudialyte is eventually stabilized as a magmatic phase.

In some of the latest and most evolved lujavrites, so-called hyper-agpaitic mineral assemblages formed, which mark an even more evolved stage compared to the agpaites in general. The most important mineralogical changes compared to the earlier agpaites include the formation of naujakasite and steenstrupine at the expense of nepheline and eudialyte. The latter attracted increased interest as they contain the highest concentrations of REE, Zn, U, Be, Nb and Sn, resulting in the formation of various Be-silicates (e.g., tugtupite and chkalovite), Nb-minerals (pyrochlore) and the extremely rare Sn-Be silicate sørensenite. In these final products of the Ilímaussaq evolution several water-soluble minerals like villiaumite, trona, thermonatrite and natrophosphate are stable.

In all, during the long-lasting differentation history of the complex, the major REE carriers change from apatite in the augite syenite, via eudialyte in the agpaitic rocks to steenstrupine in the hyperagpaitic rocks. The major factors causing the extreme differentiation trends and the substantial enrichment of REE, Zr, Nb and U are low oxygen fugacity and silica activity as well as very low water activity in the melts. These inhibit the early exsolution of aqueous NaCl-bearing fluids and thereby facilitate the enrichment of alkalis and halogens in the melts, thereby increasing the solubility of HFSE. The unusually long crystallization interval of these rocks and the suspected continuous transition from melt to fluid result in extensive (auto) metasomatism and hydrothermal overprint. Primary mineral assemblages are therefore partially resorbed in most rock units and replaced by secondary minerals to various extents.

STRUCTURAL-COMPOSITIONAL EVOLUTION AND ISOTOPIC AGE OF THE ILMENY-VISHNEVOGORSKY COMPLEX, THE SOUTH URALS, RUSSIA

Medvedeva E.V.[1], Rusin A.I.[2], Krasnobaev A.A.[2], Baneva N.N.[2], Valizer P.M.[1]

1 Ilmeny State Reserve UB RAS, Miass, Russia.
mev_62@inbox.ru
2 Institute of Geology and Geochemistry UB RAS, Yekaterinburg, Russia.

The Ilmeny- Vishnevogorsky complex forms a narrow longitudinal zone elongated for more than 100 km from the Ilmeny to Vishnevye Mountains. This zone is considered as a deep fragment of a regional postcollision shear, which includes the blocks of the various metamorphosed sedimentary and alkaline igneous rocks [10].

The primary rocks of the shear zone were the rocks of the platform crystal basement:

various migmatite gneisses, amphibolites, two-pyroxene schists and magnetite quartzites combined into Selyankino Group. The isotopic-geochronological study indicates that the rocks of the Selyankino Group underwent high-temperature amphibolite retrograde metamorphism about 2 Ga [5]. They keep the relict minerals assemblages of the granulite facies, but the period of the progressive metamorphism is not supported by geochronological data. The age values calculated by the lower interceptions of Discordia with Concordia are characterized by significant variations (from 250 to 540 Ma) and it is difficult to interpret their geological meaning because of the absence of petrographic evidence of transformation in this period. All blocks of metamorphosed sedimentary and igneous rocks in shear zone are characterized by the tectonic contacts and are longitudinally oriented that points to the secondary origin of the structure related to the formation of the postcollision shear.

The mafic-ultramafic association includes individual large ultramafic massifs associated with metamafic rocks and by numerous lens-shaped or block-like bodies. Recently, these rocks were excluded from consideration on the Ilmeny-Vishnevogorsky complex that led to erroneous conclusion on the absence of relation of the alkaline rocks with the deep mantle magmatism [2,6]. Our studies showed [10] that the mafic-ultramafic rocks of the Ilmeny-Vishnevogorsky zone are the fragments of desintegrated alkaline-ultramafic intrusion. The volumetric proportions of these rocks inside the intrusion are still enigmatic, but they may be surely distinguished and this allows us to confirm that the alkaline-carbonatite association of the Ilmeny-Vishnevogorsky zone is the derivative of the deep mantle magmatism. The metafoidolites are similar in petrochemical composition with the rocks of the ijolite-jacupirangite series, are strongly enriched in rare and rare earth elements, and contain such minerals as pyrochlore and tetraferriflogopite. Their mineral assemblages indicate the extremely deep (up to 30 kbar) conditions of generation of the parental melts [9] that is well in agreement with new finding of the high-pressure assemblage of omphacite, glaucophane, and phengite microinclusions in rutile [1], and also with Nd and Sr isotopic composition.

The age of the alkaline-ultramafic association based on the age of single zircons from metafoidolites of the Lipovaya Kur'ya area is characterized by two values: 662 ± 14 and 543 ± 7.1 Ma. The early age is interpreted as a period of endogenic formation of zircons and the late age

corresponds to the transformation and decompression uplift of the mantle block. Similar Sm-Nd age (602 ± 24 Ma) of the rocks of the Buldym massif, which includes both olivine-richterite and dolomite-calcite carbonatites, was obtained by I.L. Nedosekova. These data allow suggestion that the alkaline-ultramafic association was formed before the opening of the Urals Ocean and was related to the Vendian activation of rift-related processes.

The miaskite-carbonatite association is developed in the Ilmenogorsky and Vishnevororksy massifs and also by a series of bed-like bodies, which occurs in the axial zone of the shear. The rocks of this association more or less underwent plastic (brittle-plastic) deformations, which may be observed in small and large massifs. This peculiarity of miaskite is known for long and may indicate the diapiric displacement of massifs to the upper crust that agrees with their internal structure [7] and the geological-petrological data. The detailed characteristic of the miaskite-carbonatite association and related deposits of rare and REE deposits are given in (Levin et al., 1997). This work suggests the palingenic-metasomatic origin of the association related to the transformation of the crustal substrate under influence of the mantle fluids. Such an interpretation contradicts the results of isotopic compositions of O, C, and Sr, which indicate the mantle genesis of miaskites and carbonatites [3,8].

Currently, most researchers relate the formation and metamorphic transformation of the miaskite-carbonatite association of the Urals to the Ordovician rifting and Hercynian orogenesis, respectively. Such ideas are based on Rb-Sr age of nepheline syenites of the Ilmenogorsky (446 ± 13 and 245 ± 24 Ma) and Vishnevogorsky (440 ± 43 and 244 ± 8 Ma) massifs and interpretation of results in the frame of two-stage model, which does not reveal the geological sense of the lower Discordai interception. Relatively close values of the U-Pb age of zircons from miaskites (423 ± 10 and 261 ± 14 Ma) and carbonatites (432 ± 12 and 261 ± 6 Ma) of the Ilmenogorsky massif [11] are constantly cited and are commonly accepted. Numerous SHRIMP II ages of zircons from all rock varieties of the alkaline-carbonatite association were recently obtained. Majority of ages of zircons from miaskites group in a range of 400-420 Ma. Zircons with age of 240-270 Ma are found in all groups of the rocks, as well as in the alkaline-ultramafic association. We may assume that the formation of the Permian zircon was related to the formation of the regional shift, but no evidences of this event are found in mineral assemblages of the miaskite-carbonatite association. Similar conclusion may be drawn for individual intermediate ages (280-380 Ma), the geological sense of which is still unclear. The maximum ages (439 ± 28 Ma, early generation of zircon from calcite carbonatites of the Vishnevogorksy massif; 489 ± 18 Ma, zircon from amphibole miaskites of the Ilmenogorsky massif) are probably rejuvinated. The formation of genetically related alkaline-ultramafic and miaskite-carbonatite associations, which composed the complex intrusion of the central type, could be caused only by rift activation related to the pulsation operation of the mantle plumes. The duration of the plume magmatism in trap provinces is estimated as hundreds or first millions of years. On the basis of this, it may be suggested that all rock associations of the alkaline-carbonatite intrusion were formed in the Vendian-Cambrian.

The isotopic-geochronological study of zircons from phenitized granitic blastomilonites, which are most widespread in the shear zone, showed extremely broad range of ages [4]. The maximum values (2119 ± 38 Ma) coincide with the age of amphibole diaphthoresis of the Selyankino complex. These relict ages are not related to the evolution of phenitization. It is interesting that no evidences of phenitization are found in gneisses of the headwaters of the Selyanka River and a widespread opinion that contact phenites occur precisely in this range is erroneous. The

phenitization of the granitic blastomilonites were related to the formation of the regional shear zone and are expressed along its whole extension. The age of zircons from phengites is discrete: the major ages belong to the Lower Proterozoic and Mesoproterozoic. No Neoproterozoic to Devonian ages are determined for zircons. It is difficult to define the geological sense of the Devonian zircons (409 ± 7 and 374 ± 19 Ma), because no mineralogical evidences, which register the endogenic events of that period, are known. The age of 286 ± 8 Ma is of special interest. Similar age values determined in all types of rocks of the shear zone clearly register the strong impulse of endogenic activity probably related to the formation of the regional shear zone in the Late Permian-beginning of the Triassic. The final shear deformations (180-220 Ma) were accompanied by the formation of the latitudinal faults and crystallization of various pegmatite veins with rich semiprecious stones. It is probable that they are derivative of the remnant high-pressure fluid originated during the evolution of the postcollision shear.

Conclusions. The assemblage of the available data, in our opinion, shows the evolutionary direction and temporal consequence of the structural-compositional transformations of the Ilmeny-Vishnevogorsky regional shear zone. The strongly metamorphic rocks of the crystal basement are the primary substrates of this zone. In the Neoproterozoic, due to the activation of the rift-related process, this basement was intruded by the complex alkaline-carbonatite intrusion of the central type, which includes the alkaline-ultramafic and carbonatite-miaskite associations. In Permian-beginning of the Triassic, this intrusion was disintegrated and extended along the zone of the postcollisional shear. Plastic deformations, which led to the formation of the granitic blastomilonites, occurred under the medium-temperature conditions (400-550 °C) at increased pressures of fluids (up to 10-13 kbar) and was accompanied by intense development of metasomatic processes (acid leaching, phenitization, etc.). The relict fluid enriched in alkaline, rare, and rare earth elements, caused the crystallization of various pegmatite veins with unique semiprecious mineralization at the final stage of formation of shear and development of the cross-cutting faults.

This study was supported by the Interdisciplinary project of the Urals Branch of RAS no. 12-C-5-1011 and the project no. 12-II 5-2035 jointly conducted with Siberian and Far East Branches of RAS.

References

1. Valizer P.M., Rusin A.I., Krasnobaev A.A., Baneva N.N. 2014 Microinclusions of omphacite, glaucophane, and phengite in rutile from ultramafites of Buldym massiv (South Ural) Vestnik of IG of Komi SC of the UB RAS №2 P.7-10
2. Ginzburg A.I.,Samoylov V.S. To the problems of the carbonatites 1983 Zapisky VMO V.2 P.112 P.164-176
3. Kononova V. A., Kramm U., Grauert B. The age and the source of the matter of miaskites… 1983 DAN USSR V.273 №5 P. 1226-1230
4. Krasnobaev A.A., Valizer P.M., Rusin A.I., Busharina S.V., Medvedeva E.V. 2011 Zirconology of the fenites from Ilmeny maintains DAS V.440 №1 P. 100-104
5. Krasnobaev A.A., Cshulkin E.P. Davydov V.A., Cherednichenko N.V. 2001 Zirconology of the Selyankinsky block from Ilmeny mauntains DAS V.379 №6 P. 807-811.
6. Levin V.Y., Roneneson B.M., Samkov V.S., Levina I.A., Sergeev N.S., Kiselev A.P. 1997 The alkali carbonatites complexes of the Ural/ Yekaterinburg 274 p.
7. Makagonov E.P., Bazhenov E.A., Valizer N.I., Novokresheniva L.B., Plochich N.A., Varlakov A.S.

Deep building of the Ilmenogorsky miaskite massiv 2003 Miass.180 p.

8. Nedosekova I.L., Belyazkyi B.V., Belousova E.A., Bayanova T.B. The Geochronology.the isototy geochemistry and the source of the matter of the Ilmeno-Vishnevogorsky complex in the new dates Sm-Nd, U-Pb, Lu-Hf (Ural) 2010 XXVII Internatonal conference «Geochemistry of magmatic rocks» Koktebel P.125-127
9. Rusin A.I., Valizer P.M., Krasnobaev A.A., Baneva N.N., Medvedeva E.V., Dubinina E.V. The origin of the garnet-anortite-clinopyroxene-amphibolic rocks of the Ilmenogorsky complex (S.Ural) 2012 Lithosphere №1 P. 91-109
10. Rusin A.I., Krasnobaev A.A., Valizer P.M, Medvedeva E.V. 2006 The alkali ultramafic association from the Ilmencky and Vishnevy maintains Geochemistry, petrology, mineralogy and genesis of alkali rocks. Miass:UB RAS P.222-227
11. Chernyshov I.V., Kononova V.A., Kramm U., Grauert B., Isotopic geochronology of the alkali rocks from the Ural the dates U-Pb metod 1987 Geochemistry №3 P. 323-338

TRACE ELEMENT AND ISOTOPES HF AS A SIGNATURE OF ZIRCON GENESIS DURING EVOLUTION OF ALKALINE-CARBONATITE MAGMATIC SYSTEM (ILMENY-VISHNEVOGORSKY COMPLEX, URALS, RUSSIA)

Nedosekova I.L.[1], Belousova E.A.[2], Belyatsky B.V.[3]

1 Zavaritsky Institute of Geology and Geochemistry UB RAS, Ekaterinburg, Russia, vladi49@yandex.ru
2 GEMOS ARC National Key Centre, Macquarie University, Sydney, Australia
3 VSEGEI . St. Petersburg, Russia

Local analysis of zircon in the study of the isotopic and trace element compositions has made this mineral is widely used tool not only for datin g rocks and minerals, but also to address the question of the genesis of the zircons, as well as the origin of the source. Along with the morphological characteristics and zircon cathodoluminescence properties for these tasks can now be used geochemical data (trace element composition, including REE distribution), and the results of U-Th-Pb and Lu-Hf isotope systems study.

To study the source and the patterns of distribution of trace elements in zircons that crystallized at various stages of operation of the alkaline-carbonatite magma system, we have investigated zircons of Ilmeny-Vishnevogorsky Alkaline-Carbonatite Complex (IVAC) by laser ablation (LA-ICP MS) in GEMOS ARC National Key Centre, Macquarie University, Sydney, Australia. We have studied Hf isotopic composition accompanying by U-Pb-age and the content of trace elements in zircons of the different stages of crystallization from different IVAC rock – miaskites, miaskite-pegmatites and carbonatites (sovite I and sovite II).

IVAC zircons presented earlier (zircon I) and late (zircon II) generations, which crystallize in different stages of operation of the alkaline-carbonatite magma system. The early zircon (I) is a brownish, fairly transparent grains, with weak or no emission in monochrome cathodeluminescence (CL), which is probably due to the high content of trace elements and, above all, U. Usually, they form prismatic crystals, occasionally zircon I are characterised by oscillatory zoning. Zircon II forms a light brown bipyramidal crystals and irregular grains. Zircon II has a light gray tint in CL, sometimes with oscillatory zoning. Some zircon I relics can observed in crystals of zircon II, sometimes with traces of dissolution and emulsion disintegration. Zircon II occurs in carbonatites and miaskite-pegmatites, and his formation, probably, was connected with the final stage of alkaline carbonatite melt crystallization.

Furthermore, in all IVAC rocks present newly formed "metamorphic" zircon which forms rounded and wedge-shape grains, sometimes with multiple facets typical for metamorphic origin zircon (zircon III) and overgrowths over the early generations zircon I and II (zircon IV). Transparent zircon III grains have a light colors in CL.

The early generations of IVC zircon I and II form a single concordant age cluster (individual grain U-Pb-ages are in the range of 410–428 Ma). Concordant age for zircon from carbonatites equals to 417.3 ± 2.8 Ma at MSWD = 0.21 and n = 20. The outer zones of the early zircon are characterised by encreased age discordance (D), and much of the IVAC zircon grains are highly

disturbed isotope systems (15% < D < 35%), illustrating the varying degrees of the early zircons transformation. The IVAC late zircon III has an age T = 250-360 Ma and is characterized by a high degree of discordance (D = 18–60%). Much of the newly-formed transparent zircon grains (zircon IV) has completely destroyed U-Pb isotopic system (D > 50–90%).

The trace element contents of the studied IVAC zircons correspond to the compositions of zircons from alkaline rocks and carbonatites of the world-wide [2]. The IVAC early zircons I and II have a wide range of REE contents and a pattern of element distributions with a well defined Ce anomaly and the degree of REE fractionation (Yb/Gd_n = 8 – 40), in general, is close typical for magmatic zircons [3, 4]. A specific feature of the IVC zircon is a poorly defined Eu minimum (*Eu/Eu = 0.8 – 0.98), which is charactestic signature for zircons from carbonatites [2] and syenite [1]. Zircon III has lower REE contents, but keeps the patterns of the REE distributions characteristic for the magmatic IVAC zircons. The composition of zircon IV (with completely disturbed isotopic systems, D > 35–90%) is a relatively flat, unfractionated REE distribution without Ce anomaly typical one for the "hydrothermal" zircons [3].

Trace element composition of the IVAC zircon is characterized by existance of linear covariance many of the above elements (U-Y, Y-Hf, Y-Th, Nb-Ta, Zr-Hf, U-Th), which are previously known for magmatic zircon [2] and mainly determined by parental melts magmatic evolution. Linear trends in the binary composition diagrams show the predominance of the crystallization factor in the trace element distribution in the IVC zircon and reflect the sequence of zircon formation, which is in the final stages of the complex formation crystallized along with rare-metal minerals (U-pyrochlore and Ti-pyrochlore). The formation of these minerals results not only in the residual melt concomitant trace elements depletion (U, Th, Nb, Ta, etc.) but crystallizing the later zircon also. Similar trends also probably related to the co-crystallization U-pyrochlore and zircon have been observed for zircons from Kovdor carbonatites (Russia) and nepheline-syenite and syenite pegmatites from Oslo (Norway) [2].

The early zircon I and II from carbonatites and miaskites of the IVAC (with individual U-Pb ages T = 410 - 428 Ma and D < 5%) have a moderately depleted isotopic hafnium composition ($(^{176}Hf/^{177}Hf)_{420}$ = 0.282841 – 0.282662, εHf = +11.3 – +4.7). Considerable variations in the initial Hf isotope ratios in these zircons are likely to reflect the heterogeneity of primary magmatic source and may be indicative of the participation in the crystallization of IVAC zircon new portions of melts with different isotopic composition determined by mixing materials at their source.

The later newly-formed zircons II dated at 250–360 Ma (frequently D > 50–90%, $(\varepsilon Hf)_{250}$= -5 to +11) often exhibit some depletion in the radiogenic Hf relative to the early generations of zircon. However, recalculation of the initial Hf isotope ratios to the age of the IVAC carbonatite crystallisation (417 Ma) shows the correspondence of the initial signatures ($^{176}Hf/^{177}Hf$) in the early (I and II) and late (III and IV) zircon generations. This argues in favor of the later zircons were formed during recrystallization of the early zircon without substantial additional supply of trace elements (particularly REE and Hf) during the later (~ 250 Ma) metamorphic event.

The study is supported by Program of UD RAS, projects № 12-S-5-1031 and № 12-P-5-2015.

References:

1. Fedotova A.A., Bibikova E.V., Simakin S.G., 2008. Geochemistry of zircon (ion microprobe data) as an indicator of the Genesis of mineral with a geochronological studies. Geochemistry. № 9, p. 980-997. *(in Russian)*

2. Belousova E.A., Griffin W.L., O'Reilly S.Y. et al., 2002. Igneous zircon: trace element composition as an indicator of source rock type. Contrib. Mineral. Petrol. v.143, p. 602-622.
3. Hoskin P.W.O., 2005.Trace-element composition of hydrothermal zircon and the alteration of Hadean zircon from Jack Hills, Australia. Geochim. et Cosmochim. Acta. v. 69. № 3, p. 637-648.
4. Hoskin P.W.O., Ireland R., 2000. Rare earth element chemistry of zircon and its use as a provenance indicator. Geology. v. 28. № 7, p. 627-630.

KIZILCAÖREN ORE- AND CARBONATITE-BEARING COMPLEX: FORMATION TIME, MINERALOGY AND SR-ND ISOTOPE GEOCHEMISTRY OF THE ROCKS (NORTHWESTERN ANATOLIA, TURKEY)

Nikiforov A.V.[1], Oztürk H.[2], Altuncu S.[3], Lebedev V.A.[1]

1 Institute of Geology of Ore Deposits, Petrography, Mineralogy, and Geochemistry, Russian Academy of Sciences
nikav@igem.ru
2 Istanbul University, Department of Geological Engineering, Avcilar Campus, Istanbul, Turkey
3 Nigde University, Department of Geological Engineering, Nigde, Turkey

The results of isotop-geochronological [1], mineralogical [1] and isotope-geochemical studies of the rocks making up the Kizilcaören fluorite–barite–REE deposit, Northwestern Anatolia, Turkey are discussed in the presentation. The ore is a constituent of the subvolcanic complex localized in a large fault zone. The complex includes (from earlier to later rocks): (1) phonolite and trachyte stocks, (2) dike-like carbonatite and carbonate–silicate bodies; and (3) fluorite–barite–bastnaesite ore in the form of thick homogeneous veins and cement in breccia. The K–Ar dating of silicate igneous rocks and carbonatites shows that they were formed during the Chattian age of the Oligocene (25–24 Ma).

Mineralogical observations show that the ore is the youngest constituent in the rock complex. Supergene alteration deeply transformed ore-bearing rocks, in particular, resulting in leachingof primary minerals, presumably Ca–Mn–Fe carbonates, and in cementation of the residual bastnaesite–fluorite framework by Fe and Mn hydroxides. Most of the studied rocks contain pyrochlore, LREE fluorocarbonates, Nb-bearing rutile, Fe–Mg micas, and K-feldspar.

The Sr-Nd isotope studies have testified that phonolites, carbonatites, and fluorite-barite-bastnaesite ores are characterized by similar isotope parameters ($^{87}Sr/^{86}Sr_{(T=24Ma)}$ - 0.70591-0.70608; $^{143}Nd/^{144}Nd_{(T=24Ma)}$ - 0.512545- 0.512574: eNd ~ -1). So, all these formations had the single source for Sr and REEs.

The formation of Kizilcaören deposit rocks took place at the earliest stages of post-collisional magmatism (24-0.1 Ma) which has been manifested within western and Central Turkey. Isotope compositions for the rocks generated during aforementioned time span vary wide in ranges of: $^{87}Sr/^{86}Sr_{(T)}$ - 0.7031-0.7091, $^{143}Nd/^{144}Nd_{(T)}$ - 0.51230-0.51299 [1, 2]. The strict dependence of rock isotope composition vs. their age is absent. Isotope composition of the studied rocks has intermediate values among regional magmatic formations and close to composition of andesites, trachyandesites, rhyolites, and ignimbrites from Afyon-Suhut–Sandikli, Seyitgazi, and Bigadic-Sindigri volcanic fields.

The Kizilcaören deposit represents a variant of postmagmatic mineralization closely related to carbonatite magmatism associated with alkaline and subalkaline intermediate rocks.

This study was financially supported by the Russian Foundation for Basic Research.

References

1. Nikiforov A.V., Öztürk H., Altuncu S., Lebedev V.A., 2014. Kizilcaören Ore- and Carbonatite-Bearing Complex: Formation Time and Mineralogy of Rocks, Northwestern Anatolia, Turkey. Geology of Ore Deposits, 2014, Vol. 56, No. 1, pp. 35–60 (in English).
2. Dilek Y., Altunkaynak S., 2010. Geochemistry of Neogene-Quaternary alkaline volcanism in western Anatolia, Turkey, and implications for the Aegean mantle. International Geology Review Vol. 52, N. 4-6, p. 631-655
3. Chakrabarti R., Basu A.R., Ghatak A, 2012. Chemical geodynamics of Western Anatolia. International Geology Review, Vol. 54, p.227-248

PETROLOGY OF THE VAKIJVARI SYENITE INTRUSIVE COMPLEX AND THEIR OREFIELD CHARACTERISTIC (LESSER CAUCASUS, GURIA REGION, GEORGIA)

Okrostssvaridze A.V.[1], Bluashvili D. I.[2], Chung S.L[3]

1 Institute of Earth Sciences , Ilia State University, Tbilisi , Georgia, okrostsvari@gmail.com
2 Department of ore deposits, Georgian Technical University, Tbilisi, Georgia
3 Department of Geosciences, National Taiwan University, Taipei, Taiwan

The Caucasus represents a Phanerozoic orogen formed along the Euro-Asian north continental margin, in a NW-SE direction, between the Black and Caspian seas. Currently, it is an expression of continental collision between the Arabian and Eurasian lithospheric plates. Three major units are distinguished in the Caucasian construction: 1) the Greater and 2) the Lesser Caucasus fold-thrust- systems and 3) the Inner Caucasian microplate [1]. The Lesser Caucasus is the southern most expression of the Caucasus orogen, which in SW part is constructed of Paleogene-Neogenian the Achara-Trialeti fold-thrust belt and which is considered as a back-arc rift trough [2].

Guria subtropical region is situated in the west part of the Achara-Trialeti fold-thrust belt across the Black See and built up by Eocenenian volcanogenic-sedimentary and intrusive formations. Vakijvari syenite intrusive complex is located in the central part of the region, near the Vakijvari village and represents one of the largest plutonic body of the Achara-Trialeti fold-thrust belt. The biggest outcrop of this complex is exposed in the r. Bjuja gorge, which occupies 15 km^2 area on the modern erosional level. Comparatively smaller bodies crop out in the gorges of the tributaries of this river. Erosional outcrops of the mentioned bodies are separated from each other by Middle Eocene volcanogenic-sedimentary country rocks (dated faunistically). As for the age of this intrusion rocks, it was recently dated by U-Pb method in the Department of Geosciences of Taiwan National University and it corresponds to 46.77+0.81 Ma (Middle Eocene). Based on this age, it turns out that volcanic activity was at once followed by plutonic activity, though so far it has been considered that the injection of plutonic magma took place in Upper Eocene [2].

Vakijvari intrusive complex is mainly of subalkaline syenetic composition and comprises pyroxene–biotite and hornblende-bearing varieties, though biotite-pyroxene monzonites are observed as well. These are mainly coarse-grained rocks, which contain pyroxene (egirin-avgit), horn blende, potassium feldspar, oligoclase, biotite and magnetite. Accessory minerals are apatite and sphene. Pyroxene–biotite syenites are constructed the major part of Vakijvari intrusive complex are mainly alkaline rocks. Their chemical composition is changeable and varies on average within the following limits: SiO_2 = 56.5-61.5%, Al_2O_3 =16.2-17.7%, Fe_2O_3 =2.5-4.3%, FeO = 2.2 - 4.8%, CaO = 4.2 - 6.7%, Na_2O = 3.4 – 5.1%, K_2O = 3.8- 5.9%. It should be mentioned, that in contact with volcanogenic-sedimentary rocks of Vakijvari intrusive complex, strong postmagmatic hydrothermal alteration zones are developed. On some areas of these zones ore mineralization occurrences are observed, forming Vakijvari orefield in combination.

Vakijvari orefield (70 km^2) within their boundaries are represented by 10 gold containing ore occurrences, which could be united into three groups according to their spatial position and composition. In particular, Shemokmedi (Gonebis-kari, Jakhua, Gvarda tions), Pampaleti (Pampaleti, Tsikhisubani, Lashisgele), Vakijvari (Chachuasgele, Chkhikva, Nasakhlebi, Koris-bude) groups. Result of analyses of conducted geological activities in Vakijvari ore field show that, gold-bearing ore manifestations are singled out quartz-copper-polimetallic, iron ore–pegmatitic, sulphur-pyrite, copper-molybdenum-porphyry and low sulfidation ore occurrences. All ore occurrences in this ore field are spatially and genetically related to endo and exocontact areas of Vakijvari intrusive complex.

Prognostication of total resources of Vakijvari ore field was made by Z.Chkhikvishvili and his colleagues [3]. According to these data iron reserves of P_2 category is 11.8 mln.t., P_2+P_1 is 13.2 mln.t. In this ore field prognostic resources for P_3 category gold is 136 t, silver – 430 t, copper – 2322 thousand tones, lead – 750 thousand tones, zinc -1135 thousand tones, molybdenum – 20.000 tomes, cobalt – 5 thousand tones, bismuth - 25 thousand tones. It's difficult to make comments on other metals, but the fact that Vakijvari ore field contains giant reserves of iron, is proved by the Guria coast of the Black Sea. Here beaches are totally covered by iron bearing sand e.g. magnetite beach of the famous resort Ureki.

By us in Vakijvari orefield group were carried out special investigations of radioactive elements in the Acme Analytical Laboratories (Vancouver, Canada) by ICP-ES analysis, using 1F15 method. In this ore field anomalous contents of uranium haven't been found, though tree significant anomalies of thorium were exposed : Nasakhlebi-1 (Th-185 g/t), Nasakhleb-2 (Th-237 g/t) and Chkhikva (Th-428 g/t). As it is known, like uranium and plutonium, it can be used as fuel in nuclear reactors. However, compared with these elements, thorium has quite a number of priorities: is more widely spread; in comparison with uranium its extraction is rather cheap; is less radioactive; full annihilation of its waste is possible; produces 2-3 times more energy than uranium. Due to such unique properties and the present complicated energy situation, thorium is considered as the green energy of the future [4]. Nowadays the world's developed countries, including India and China, are working on a project for modernized nuclear reactor and it is planned that in the nearest 10 years thorium reactors will fully replace uranium reactors.

Thus, as we can see Vakijvari orefield is complex ore element bearing and if we take into consideration its scales, developed infrastructure and favourable natural conditions, then we should consider it as perspective economic object, requiring further detailed investigation.

References

1. Okrostsvaridze A., Tormay D., 2013, Phanerozoic Continental Crust Evolution of the Inner Caucasian Microplate. J. "Episodes", v. 36, no. 1, pp. 31-39.
2. Lordkipanidze M., Zakariadze G., 1986. Evolution of the Alpine volcanism of the Caucasus and its relations to tectonics. Piri Reis International Contribution Series, İzmir, Turkey 2, pp. 415–435.
3. Chkhikvishvili Z. et al, 1973. Report of gold exploration-revision party according to activities held during 1968–1972 years. Fund material of Georgian geological department, Tbilisi, 137p.
4. Martin R., 2009. "Uranium Is So Last Century - Enter Thorium, the New Green Nuke" Wired magazine, Dec. 21.

K-AR AND SEM RESULTS OF THE ALKALINE PORPHYRITIC STOCKS IN THE ŞEKEROBA BARITE DEPOSIT, KAHRAMAN-MARAŞ,TURKEY

Oztürk H.[1], Cansu Z.[1], Nikiforov A.E.[2], Zhukovsky, V.M.[2]

1 Istanbul University, Department of Geology Enginering, Avcılar Campus, 34320 Avcılar-Istanbul, Turkey
zeynep.oru@istanbul.edu.tr
2 Russian Academy of Sciences, Staromonetny per., 35 IGEM RAS, 119017, Moscow-Russia

The Şekeroba Barite Deposit is the biggest barite deposit in Turkey which is located 40 km southwest of Kahramanmaraş, SE Turkey. The barite mineralization occurs within the Ordovician aged Seydişehir formation, which mainly consists of sandstone shale alternation. Barite veins are accompanied by extensively quartz veins and cut by black colored alkaline magmatic rocks. These porphyritic rocks are only seen in the underground gallery of the mining site and they should be associated with barite mineralization.

This alkaline hypabysal rocks named as kersantite which mainly consist of plagioclase (bitownite), titanaugite, olivine, alkali amphiboles, magnetite and secondary calcite and barite in amygdaloidal cavities. SEM datas were processed on pyroxene minerals of kersantite by WinPyrox programme (Yavuz, 2013), 901 ^{O}C mean temperature and 3,2 kbar pressure conditions were calculated.

K-Ar age determination studies were carried out by isotope dilution method with ^{38}Ar spike in Isotope Lab. of Russian Academy of Sciences (IGEM RAS) and alkaline rocks' age is measured as 13.2 ± 0.5 and 15.8 ± 1.0 Ma ±2σ.

This 13- 15 Ma of hipabisal stock result indicate a very young mineralization stage - epoc in Anatolia during Miocene. Such Miocene aged necks and associated iron ore formation was defined by some geologists around the Malatya -Hekimhan region. On the other hand, This Miocene aged relatively young hipabisal intrusion also indicates quick reagional uplifting-erosion phenomena from Miocene to present.

References

1. Yavuz F, 2013,. "WinPyrox: A Windows program for pyroxene calculation classification and thermobarometry". American Mineralogist, Vol. 98, No. 7, s. 1338-1359.

LA-ICP MS ZIRCON DATING, GEOCHEMICAL AND SR-ND-PB-O ISOTOPIC COMPOSITIONS OF THE EOCENE I-TYPE KILIÇKAYA GRANITOID, EASTERN PONTIDE, NE TURKEY

Oztürk M., Kaygusuz A.

Department of Geological Engineering, Gumushane University, TR-29000 Gumushane, Turkey
met_121@hotmail.com

In this study, petrographical, geochemical and petrological characteristics of Kılıçkaya Granitoid in the Kılıçkaya (Bayburt) area were determined, and the evolution and origin of plutonic rocks were investigated. The age of Kılıçkaya Granitoid by U-Pb method ise 46.75 ± 0.79 Ma [1]. The granitoid rocks are medium to coarse grained, and composed of orthoclase, plagioclase, quartz, hornblende, biotite, apatite, zircon and opaque minerals [2].

The Kılıçkaya Granitoid is elipse shaped, and settled approximately in an area of 18 km^2. It consists of diorite, granodiorite and tonalite, and includes abundant wall-rock xenoliths and dioritic mafic magmatic enclaves (MME). The Kılıçkaya Granitoid shows disequilibrium textures showing magma mixing. The Kılıçkaya granitoid is generally I type, high K calc-alkaline character, and has high SiO_2 (58-67 wt.%) contents. The samples has metal**u**minous characters and enriched in large ion lithophile elements. Chondrite normalized REE patterns are concave shaped (La_N/Yb_N=17.14-8.72), and show slightly negative Eu-anomalies (Eu_N/Eu^*=0.64–0.91). Major and trace element variations indicate significant role of plagioclase, hornblende and Fe-Ti oxide fractionation during the evolution of rocks. Primitive εNd values are between -0.02 and 0.72 and $^{87}Sr/^{86}Sr_{(i)}$ ratios range from 0.70451 to 0.70564. Depleted mantle Nd model age are between 0.70 and 0.86 Ga. $^{206}Pb/^{204}Pb_{(i)}$, $^{207}Pb/^{204}Pb_{(i)}$ and $^{208}Pb/^{204}Pb_{(i)}$ contents of samples change from 18.43 to 18.79, 15.58 to 15.62 and 38.44 to 38.76, respectively. $\delta^{18}O$ values of samples are between ‰ 6.6 and 6.9.

All these properties, low $(Al_2O_3)/(MgO+FeOT)$, $(Na_2O+K_2O)/(FeOT+MgO+TiO_2)$, $(Al_2O_3)/(FeOT+MgO+TiO_2)$, K_2O/Na_2O, ASI and high $(CaO+FeOT+MgO+TiO_2)$, $(Na_2O+K_2O)/(FeOT+MgO+TiO_2)$, $(Al_2O_3+FeOT+MgO+TiO_2)$ values indicate that magma generation by dehydration melting of an amphibolite-type lower crustal component with additional input of a subcontinental lithospheric mantle component.

This work was financially supported by the Research Foundation of Gümüşhane University (Grant No: 2013.F5114.02.1).

References:

1. Kaygusuz A., Öztürk M., 2014. Kılıçkaya (Bayburt) ve civarındaki granitik kayaçların petrografisi, jeokimyası ve petrolojisi, GÜ Araştırma Fonu Project No: 2013.F5114.02.1, Final Report (Turkish with English Abstract, 98 pp.)
2. Öztürk M., 2014. Kılıçkaya (Bayburt) Granitoyidi'nin petrografik, jeokimyasal ve petrolojik özelliklerinin incelenmesi. PhD Thesis, GÜ Gümüşhane, (Turkish with English Abstract, 94 pp.)

OPHIOLITES AND OCEANIC CRUST: A TETHYAN PERSPECTIVE

Parlak O.

Çukurova University, Geology Department, Adana, Turkey
parlak@cukurova.edu.tr

Ophiolites have been recognized as on-land fragments of oceanic crust since the advent of plate tectonics. Incorporation of ophiolites into continental margins is a significant component of the tectonic evolution of orogenic belts. Ophiolites display variable internal structure, pseudostratigraphy and chemical composition and feature in many different orogenic belts of different age. They are interpreted to have formed in a wide range of tectonic settings, including mid-ocean ridge, nascent arc, fore-arc and back-arc. Numerous models exist for oceanic crust generation, tectonic emplacement and hydrothermal ore genesis. The commonly associated metamorphic soles provide evidence of intra-oceanic convergence prior to tectonic emplacement onto continental lithosphere. A typical "Penrose Type" ophiolite pseudostratigraphy includes mantle tectonites, ultramafic to mafic cumulates, isotropic gabbros, sheeted dike complex with plagiogranite, volcanic complex and associated sediments. The Mesozoic Tethyan ophiolites of the Alpine-Himalayan orogenic belt include the Mid-Late Jurassic ophiolites of the Dinarides, Albanides and Hellenides in the western region and the Late Cretaceous ophiolites of Turkey, Troodos, Baer-Bassit, Khoy, Kermansah, Neyriz, and Oman in the eastern region. The Mid to Late Jurassic ophiolites in the western region formed in a transitional tectonic settings from MORB to SSZ, whereas the late Cretaceous ophiolites in the eastern region, from Turkey to Oman, are supra-subduction zone (SSZ) type.

Neotethyan ophiolites in Anatolia are located along several east-west trending suture zones separated by continental blocks, metamorphic core complexes and the sedimentary basins. These suture zones are marked by the ophiolites, the ophiolitic melanges and the ophiolite-related metamorphic rocks. These tectonic units were emplaced in the late Cretaceous as a result of series of collisions of intraoceanic arc-trench systems with the continental margins.

The ophiolites in the northern Anatolia were originated from the İzmir-Ankara-Erzincan suture. These ophiolites crop out in western, central and northeastern Anatolia. The ophiolites are incompletely to completely preserved and crustal units display suprasubduction zone geochemical character. In western Turkey, the ophiolites emplaced over a subducted and exhumed passive margin of the Tauride-Anatolide platform in the Campanian. The Late Cretaceous dismembered ophiolites above the Kırşehir/Niğde metamorphic massifs and within the Ankara Melange are interpreted mainly as remnants of SSZ-type ophiolites formed in the Late Cretaceous within a northerly Neotethyan oceanic basin. The Ankara-Erzincan suture zone includes large bodies of ophiolites and ophiolitic melanges in the northeastern Anatolia. The ophiolitic units display well-preserved oceanic lithospheric sections and accretionary melanges with local blueschist assemblages. Southward-emplacement onto the Tauride passive margin and northward emplacement onto the Pontide active margin have been proposed during Late Cretaceous-Early Tertiary. These ophiolitic units are unconformably overlain by Campanian-Maastrichtian sediments that were, in turn, imbricated with the ophiolitic rocks. However, Early-Middle Jurassic isotopic ages were reported from the Ankara mélange in central Anatolia and from the Refahiye complex in the Eastern Pontides.

The Tauride belt ophiolites start with the Lycian nappes to the west and end with the Divriği ophiolite to the east. These ophiolites (Lycian nappes, Antalya, Beyşehir-Hoyran nappes, Mersin, Pozantı-Karsantı, Pınarbaşı and Divriği) are situated either on the northern or on the southern flank of the E-W trending Tauride carbonate platform axis. They mainly consist of three tectonic units namely, in an ascending order, ophiolitic mélange, sub-ophiolitic metamorphic sole and oceanic lithospheric remnants. The plutonic sections and the metamorphic soles of the Tauride ophiolites are crossed by numerous isolated diabase dykes at different structural levels. The dikes are not deformed, indicating that they were emplaced after the deformation of metamorphic soles, but they do not extend into the underlying melanges. Sheeted dike complex and volcanic section are rarely present in some of the ophiolites such as Antalya, Mersin and Pozantı-Karsantı. Geochemitry of crustal rocks displays SSZ origin.

Two subparallel, NE-SW-trending belts of Upper Cretaceous ophiolitic rocks transect southeastern Turkey, extending through northern Syria, Cyprus and intervening offshore areas. The southern belt includes the Troodos ophiolite (Cyprus), the Baer-Bassit ophiolite (northern Syria) and the Antalya (Tekirova and Gödene), Hatay, Amanos and Koçali ophiolites (southern Turkey). These ophiolites originated within the Southern Neotethys. Regional comparisons show that the Kızıldağ ophiolite has similar petrological and geochemical features to the Baer-Bassit and Troodos ophiolites. The extrusive rocks in these ophiolites are mostly depleted and exhibit the geochemical features of island arc tholeiites (IAT) to boninites. The more northerly belt includes the North Berit (Göksun) ophiolite, the İspendere ophiolite, the Kömürhan ophiolite, the Guleman ophiolite and the Killan ophiolite. These ophiolites originated from an ocean basin, located between the Malatya-Keban platform to the north and the Bitlis and Pütürge continental units to the south. The SE Anatolian ophiolites are tectonically overlain by the Malatya-Keban platform and intruded by late Cretaceous granitoids. These ophiolites were thrust over the Maden Group at the end of Middle Eocene time. They include differentiated rock units in both the plutonic (quartz diorites) and the volcanic sections (i.e. basalt to rhyolite). They are also overlain by volcanic arc units (i.e. Elazığ Unit, Yüksekova Complex), suggesting that SSZ-type crust evolved into an ensimatic island arc as subduction continued. All of the evidence suggests that the Göksun, İspendere, Kömürhan, Guleman ophiolites and the North Berit (Göksun) ophiolite were related to the northern margin of the southern Neotethys (i.e. the Malatya-Keban Platform), whereas the Kızıldağ (Hatay) ophiolite was attached to the southern margin (i.e. the Arabian Platform) of the southern Neotethys in the latest Cretaceous time.

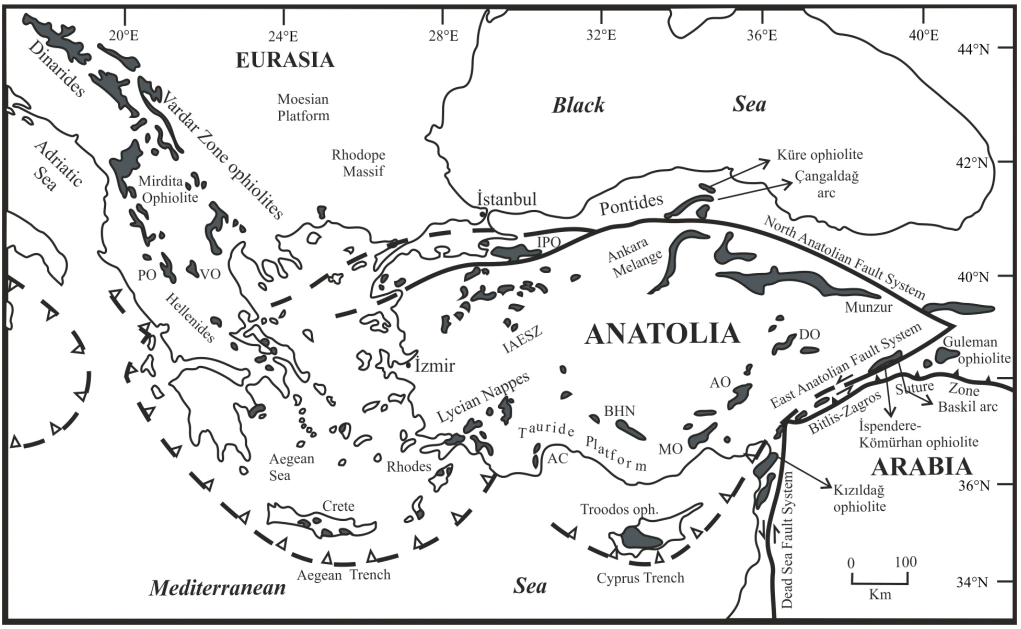

Figure 1. Distribution of the Neotethyan ophiolites and major tectonic features in the eastern Mediterranean region. AC: Antalya Complex; IPO: Intra Pontide Ophiolites; BHN: Beyşehir-Hoyran Nappes; İAESZ: İzmir-Ankara-Erzincan Suture Zone; MO: Mersin Ophiolite; PO: Pindos Ophiolite; VO: Vourinous Ophiolite; AO: Aladağ Ophiolite; DO: Divriği Ophiolite.

Keywords: Suture zones, Inner Tauride Suture, İAE Suture, Bitlis-Zagros Suture, Anatolia, ophiolite, mélange.

POLYMICT BRECCIA XENOLITH FROM NOYABRSKAYA PIPE (YAKUTIA)

Pokhilenko L.N., Afanasiev V.P., Pokhilenko N.P.

V.S. Sobolev Institute of Geology and Mineralogy, Siberian Branch, Russian Ac. Sc., 3 Koptyuga Avenue, Novosibirsk, 630090, Russia
lu@igm.nsc.ru

Mantle xenolith of unusual composition from the kimberlite pipe Noyabrskaya (Yakutia) has been studied. The sample was taken from the collection by the late Cherenkova Lyudmila Ivanovna and kindly provided for research by our Moscow colleague from FGUNPP "Aerogeologiya" Cherenkov V.G. To determine the chemical composition of minerals and their relationship cut off the sample surface was polished and coated with carbon film. Studies were conducted using a scanning electron microscope TESCAN MIRA3 LMU (IGM SB RAS) at an accelerating voltage of 20 kV, counting time at each point 20 c.

The sample is a polymict breccia - a complex rare type of deep mantle rocks. Such non-equilibrium complex rocks were previously described in some papers: 1) Lawless et. al. (1979) - four polymict peridotites from the Bultfontein and De Beers Mines, Kimberly, South Africa, 2) Zhang et al. (2001, 2003) - polymict mantle xenoliths from the Bultfontein kimberlites, South Africa and 3) Pokhilenko N.P. (2009) - one xenolith of polymict breccia from the Premier Mine, South Africa, and one xenolith of polymict peridotite from the Sytykanskaya Pipe, Siberia. Each polymict breccia is unique, and the sample described in our work has its own characteristics as compared with the above. In fact it is a conglomeration of contrasting composition rock fragments and minerals of the same name. Minerals are often zoned. Composition of the same mineral in rocks varies within a fragment.

The sample can be observed the following associations (wt%):

	mineral	SiO2	TiO2	Al2O3	Cr2O3	FeO	MnO	MgO	CaO	Na2O	K2O	Mg#	Ca#	Total
1)	garnet	41.43	1.3	21.66	0.76	10.14	0.25	19.43	5.03			77.35		100
	opx	56.19	0.31	1.35		8.46		32.69	1.01			86.47		100
	cpx	55.3		1.93	1.26	2.5		16.56	20.54	1.71		91.93	47.14	100
	phlogopite	44.01	2.37	9.73	0.77	5.64		25.56		0.65	6.77	88.98		95.5
	ilmenite		55.02	0.74	0.9	30.18		12.7				42.85		100
	магнетит	2.93		0.77	0.37	86.47		0.74	1.4					100
2)	garnet	41.27		21.17	3.63	8.16	0.55	19.59	5.63			81.05		100
	opx1	57.71		0.72	0.29	5.38		35.58	0.32			91.99		100
	opx2	56.8		1.23	0.3	6.99		33.92	0.77			89.17		100
	phlogopite	38.89	4.74	14.23	0.88	5.28		21.23		0.34	9.92	87.75		95.5
	ilmenite		53.04	0.54	2.71	31.69	0.39	11.63				39.54		100
	olivine1	40.8				8.24		50.59				91.55		100
	olivine2	40.64				12.06		47.3				87.48		100
3)	garnet	41.6		20.37	4.44	8.05	0.48	19.3	5.76			81.03		100
	opx	57.9		0.79	0.28	5.29		35.35	0.4			92.25		100
	cpx	55.53		1.95	1.15	2.3		16.76	20.82	1.5		93.9	47.18	100
	phlogopite	40.57	4.15	13.64	1.18	4.36		21.61		0.39	9.6	89.82		95.5
	spinel	0.44	2.7	17.32	41.85	24.41		12.45	0.47			47.61		100
	olivine	40.61				10.9		47.91	0.24			88.68		100
4)	garnet	41.16	1.13	20.56	1.69	10.42	0.4	18.53	6.1			76.01		100
	opx	56.2		1.66	0.31	8.48		32.49	0.86			86.96		100
	ilmenite1		48.88	1.68	7.26	30.5		11.68				40.92		100
	ilmenite2		50.94	0.74	4.96	31.22		12.14				40.93		100
	phlogopite	38.59	4.52	15.14	1.29	5.7		20.43		0.66	9.16	86.47		95.5
	chromite		0.54	10.67	50.59	27.89		10.3				39.69		100
	olivine	40.55				11.91		47.53				87.67		100

Dedicated associations - only a small part of various combinations of the above minerals, ranging in composition, size, position. The vast majority of minerals are found as rock-forming, and as inclusions in other minerals, as well as small fragments in the intergranular space.

Zoning from center to edge in garnet was found in parageneses with chromospinelide:

	SiO2	TiO2	Al2O3	Cr2O3	FeO	MnO	MgO	CaO	Mg#	Total
centre	41.71		21.09	3.56	7.97	0.61	19.42	5.63	81.28	100
intermediate zone	41.63		20.48	4.17	8.26	0.56	20.25	4.65	81.37	100
rim	40.96	0.59	19.32	5.32	8.56		18.82	6.43	79.67	100

Regions consisting of fine-grained olivine and orthopyroxene with variable composition were observed; sometimes they contain chromite with high content of TiO2 (up to 4.5 wt%) and ilmenite riched by Cr2O3 (up to 12.3 wt%). Close intergrowth of similar chromite and ilmenite with exsolution structures were observed.

Cracks and intergranular space are filled with serpentine, chlorite and sulphides (pyrrhotite, pentlandite).

Large orthopyroxene grains have exsolution structures - separate or fused lamellae of cpx and chromite:

mineral	SiO2	Al2O3	Cr2O3	FeO	MgO	CaO	Na2O	Mg#	Ca#	Total
opx (host)	57.86	0.83	0.37	5.11	35.51	0.32		92.53		100
cpx (lam)	55.39	1.85	1.49	2.71	17.39	19.69	1.48	91.96	44.88	100
chromite (lam)	0.48	11.34	52.64	22.56	12.98			50.62		100

Iron and nickel sulfides of various compositions are frequent in the low chromium ilmenite as inclusions, chalcopyrite is rare. Djerfisherite, formed under the influence of kimberlitic melt, never been revealed in the intergranular space, either in the form of adhesions with sulfides included in other minerals.

Some garnets have kelyphitic rims similar to those for pyrope peridotite assemblages containing high-Al pyroxenes of variable composition, Al-spinel.

In general, such a huge variety of mineral compositions and chemical compositions of minerals of the same name, the presence of fine-grained olivine and orthopyroxene (similar to the bulk of olivine from sheared peridotites) along with large secretions of these minerals, the absence of signs of melting in the cracks, zoning minerals, exsolution structures, kelyphitic rims - all this testifies to the highly non-equilibrium conditions and the rapid formation of the studied rock actually received by mixing contrasting compositions in the mantle before the introduction of the kimberlite melt.

This work was supported by RFBR grant 12-01-043a.

References

1. Lawless, P.J., Gurney, J.J., Dawson, J.B.,1979. Polymict peridotite from the Bultfontein and De Beers Mines, Kimberly, South Africa. In: Boyd, F.R., Meyer, H.O.A. (Eds.), The Mantle Sample: Inclusions in Kimberlite and Other Volcanics. American Geophysical Union, Washington, pp. 145–155.
2. Zhang, H.-F., Menzies, M.A., Mattey, D.P., Hinton, R.W., Gurney, J.J., 2001. Petrology, mineralogy and geochemistry of oxide minerals in polymict xenoliths from the Bultfontein kimberlites, South Africa: implication for low bulk-rock oxygen isotopic ratios. Contributions to Mineralogy and Petrology 141, 367–379.

3. Zhang, H.-F., Menzies, M.A., Mattey, D.P., 2003. Mixed mantle provenance: diverse garnet compositions in polimict peridotites, Raapvaal craton, South Africa. Earth and Planetary Science Letters 216, 329–346.
4. Pokhilenko N.P., 2009. Polymict breccia xenoliths: Evidence for the complex character of kimberlite formation. Lithos 112S, pp. 934-941.

PLACEMENT PRINCIPLES OF POTENTIALLY DIAMANTIFEROUS MIDDLE-LATE TRIASSIC MAGMATIC ROCKS (HYDROEXPLOSIVE TUFFS OF KIMBERLITES, LAMPROITES, CRUSTAL CARBONATITES) OF TAIMYR-OLENEK REGION

Proskurnin V.F., Petrov O.V., Lukyanova L.I., Gavrish A.V., Saltanov V.A., Stepunina M.A., Gromov P.A.

A.P. Karpinsky Russian Geological Research Institute (VSEGEI), Saint-Petersburg, Russia
vasily_proskurnin@vsegei.ru

Taimyr-Olenek region, perspective for discovering of new diamantiferous areas, is located in joint zone of Siberia platform and Early Cimmerian Byrranga and Late Cimmerian East Taimyr-Olenek fold belts. This tectonic position distinguishes Taimyr-Olenek region from central parts of platforms – areas of diamantiferous kimberlite magmatizm manifestation.

General geological potentially diamantiferous process is early Cimmerian tectono-magmatic deformations in the border of Ladinian-Carnian ages of late Triassic, accompanied by formation of diamantiferous Carnian tuffites [3] and hydroexplosive tuffs of kimberlites [9], lamproites, explosive pipes of alkaline syenites [10], non-traditional type of crustal carbonatites [8].

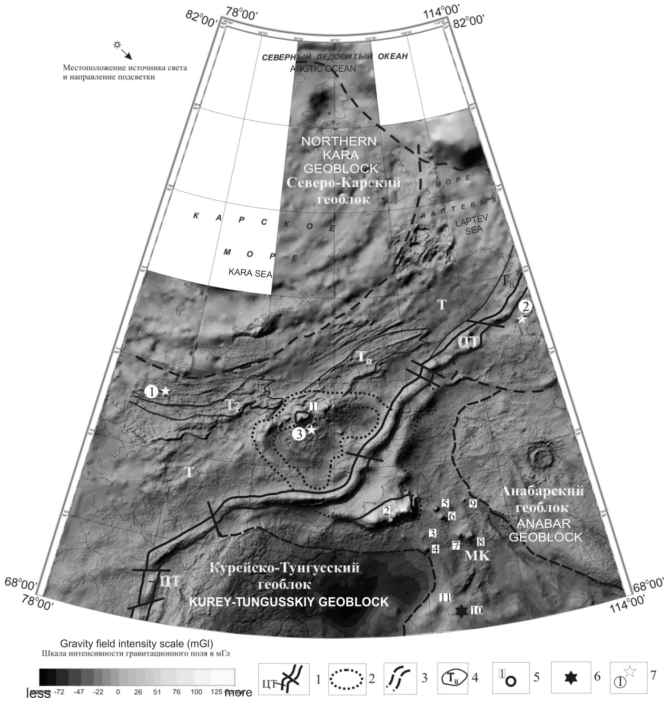

Figure 1: Distribution of potentially diamantiferous rocks of Taimyr (T) and Maymecha-Kotuy (MK) province relative to position of Fadjukuda-Kotuy hot area, on the map of gravity field

Buge reduction, density of intermediate layer 2,67 g/sm^3. Relative level (grayscale pseudorelief).

1 – Central-Taimyr suture; 2 - Fadjukuda-Kotuy hot area; 3 - carbonatite provinces Taimyr (T) and Maymecha-Kotuy (MK); 4 – Taimyr carbonatite areals: TB – Eastern Taimyr, TC – Central Taimyr, T3 – Western Taimyr; 5 – intrusive massifs: Dumtaley (1), Guli (2); 6 – Haramayskoe kimberlite field; 7 – predictable diamantiferous field related with lamproites.

According to structural geological, petrographic, mineralogical and isotopic geochemical data on areas of distribution of diamantiferous terrigenous rocks of Carnian horizon, upper Triassic, in the northeastern part of Siberian platform and Eastern Taimyr, there are diamantiferous volcanic rocks lying in the base part of this secondary Triassic collector and in form of transgressive bodies in older deposits. Angardamtasskyi volcanic diamantiferous hydroexplosive-clastic rock association was assigned inside the Carnian horizon [9]. It is composed by lapilli tuffs, xenotuffs, tuffites of ultrabasic and kimberlitic composition, which were formed with active participation of freatomagmatic processes.

Early Cimmerian potentially diamantiferous lamproites and carbonatites of Taimyr are located north of biggest post-trap gravimetric and magnetic ring structure (fig. 1) of middle-late Triassic (Fadjukuda-Kotuy), south of which alkaline-ultrabasic with rare-metal bearing carbonatites volcano-plutonic rocks of Maymecha-Kotuy province are spread. Its northern part outcrops in Central Taimyr, where great Dumtaley differentiated ferrogabbro-troctolite-verlite intrusion is located [4]. Southeastern part of structure in the northern ending of Siberian platform is characterized by outcrop of unique Guli volcano-plutonic body of clinopyroxenite-dunite, picrite-melanefelinite and ijolite-carbonatite composition [2]. By treatment of mantle convection cells of first order and hot spots, existing before Pangea breakup, ring structure can be placed in post-trap position, in the North of Euroasian platform, and corresponds to hot spot or area of lower mantle Triassic plume [5, 11].

A lateral mineragenical zoning relative to the hot area position is outlined. It was already noted by Egorov [2]. At 150-250 km distance to south and southeast from rare metal and platinum-bearing Guli massif intrusions Magan, Yraas, Essei acquire alkaline-salic bias and are completed by forming Haramayskoye kimberlite field. In Byrranga mountains (north border of ring structure) presence of early-middle Triassic volcanic rocks of trachyandesite-trachyte formation (Ajatari formation) and middle-late Triassic ring intrusions of ferrogabbro-monzonite-granosyenite (Dikarabigay rock association), nepheline-syenite (Fadjukuda rock assotiation) formations assotiated with carbonatitic bodies of crustal type (Taimyr-lake rock association) is noted. On river Gorbita one of the intrusive bodies of the areal of hot spot is related to alnoites by Sobolev [12] and to micaceous kimberlites by Moor [7], where later 3 diamonds were found.

On Western and Eastern Taimyr at a distance from hot spot areals of small intrusions and crustal carbonatites are spread. Western Taimyr magmatism is finished by dyke fields of potassic lamprophyres, potentially diamantiferous lamproites and explosive pipes of alkaline syenites. Eastern Taimyr magmatism is finished by carbonatites with polymetallic mineralization and potentially diamantiferous rocks with unrounded crystals of pyrope, chrome spinellid and picroilmenite, located on Tsvetkova cape. We interpret some of these rocks as hydroexplosive tuffs and kimberlitic xenotuffs by analogy with region of Olenek branch.

Adduced data requires additional verification. However, discovery of two diamond deposits of non-traditional type in Priuralie [6] exposure of diamantiferous crustal carbonatites in Uz-

bekistan in the region of South Nurutau range in collision situation of Tien Shan system [1], appearance of new data on diamond mineralization of explosive tuffs, tuffites and tuffisites of Eastern Taimyr-Olenek fold system, signs of diamond mineralization of Taimyr lamproites and carbonatites requires a new approach to diamond and ore mineralization of platform marginal parts and zones of their joint with mobile fold belts.

References

1. Divaev F.K., 1996. Chagayskiy carbonatite association – a new type of magmatic rocks of Uzbekistan. Uzb. Geol. Journal., v. 6, p. 32-41. (in Russian)
2. Egorov L.S., 1985. Alcaline-ultrabasic magmatism and its minerageny. Geology of ore deposits, v. 4, p. 24-40. (in Russian)
3. Grakhanov S.A., Smelov A.P., Egorov K.N., Golubev U.K., 2010. Vulcano-clastic nature of basis of Carnian age – the source of diamonds in the North-east Siberia platform. National geology, v. 5, p. 3-12. (in Russian)
4. Komarova M.Z., Kozyrev S.M., Kokorin N.I., Knauf V.V. 1997. Differentiated intrusion of river Dumptaley. Petrology, mineralisation. Taimyr subsoil, Norilsk: VSEGEI, v. 3, p. 42-68. (in Russian)
5. Kravchenko S.M., Hain V.E. 1996. Global structures of lithosphere and mantle convection. Rep. of RAN., v. 347, #3, p. 368-371. (in Russian)
6. Lukjanova L.I., Ostroumov V.R., Rybalchenko A.Ya. et al., 2011. Diamantiferous fluid-explosion rocks of Perm Priuralye. Moscow, Saint-Petersburg: GEOKART, GEOS, VSEGEI, 2011. 240 p. (in Russian)
7. Moor G.G., 1941. About micaceous kimberlites in the North of Central Siberia. Rep. AN USSR, v. 31, #4, p. 261-363. (in Russian)
8. Proskurnin V.F., Petrov O.V., Gavrish A.V. et al., 2010. Early Mezozoic carbonatite belt of Taimyr peninsula. Lithosphere, v. 3., p. 95-102. (in Russian)
9. Proskurnin V.F., Vinogradova N.P., Gavrish A.V., Naumov M.V., 2012. Signs of explosiveclastic genesis of diamantiferous Carnian horizon of Ust-Olenek region (petrographic and geochemistry data). Geology and geophisic, v. 6. (in Russian)
10. Romanov A. P., 1994. Taimyr lamproites and their index minerals in Mesozoic-Cenozoic collectors. Geology of intermediate diamond collectors . Novosibirsk: Nauka, p. 105-108. (in Russian)
11. Sazonov A. M., Zviagina E. A., Leontiev S. I. et al, 2001. Platinum-bearing alkaline-ultrabasic intrusions of Polar Siberia. Tomsk: TsNTI. 510 p. (in Russian)
12. Vakar V.A., 1958. Toward probably of diamant mineralisation of Taimyr. Inform. Bull. NIIGA. Leningrad: Nedra, v. 8, p. 49-51. (in Russian)

NEW ARCHEAN TERRANES WITH THICK LITHOSPHERE OF ARCTIC REGIONS OF SIBERIAN AND NORTH AMERICAN ANCIENT PLATFORMS: ARE THEY PROSPECTIVE FOR DIAMONDIFEROUS KIMBERLITES?

Pokhilenko N.P. [1,2], **Afanasiev V.P.** [1], **Agashev A.M.** [1], **Malkovets V.G.** [1], **Pokhilenko L.N.** [1]

1 VS Sobolev Inst. Geology and Mineralogy, Novosibirsk, 630090, Russia
chief@igm.nsc.ru
2 Novosibirsk State University, Novosibirsk, 630090, Russia

Arctic areas both Siberian and North American ancient platforms (SP and NAP, respectively) are not studied geologically in detail and are not reliably explored for diamonds as well. Thus, an estimation of a real perspective of these areas for discovery of a new clusters or fields of diamondiferous kimberlites requires of serious additional geological studies combined with intensive exploration work.

Alluvial sediments and some terrigene secondary collectors of large areas of arctic regions of the SP (~120,000 km^2, area between Anabar River and lower part of Lena River), and NAP (~150,000 km^2, areas to N, NW from the Slave Craton and to W from Great Bear Lake) were sampled for kimberlite indicator minerals (KIM) during the diamond exploration programs (field seasons of 2002-2013). Cr-pyropes, magnesian ilmenites and chromites as well as multiple diamond crystals were found in many hundreds of samples, and over 70,000 of KIM grains from these samples were studied and analyzed using optical microscopes, SEM and EMP methods at Analytical Center of V.S. Sobolev Institute of Geology and Mineralogy, SB RAS, Novosibirsk, Russia, and zircon grains U-Pb isotopes were analyzed using LAM-ICP-MS at laboratories of UM, Sydney, Australia and Tokyo University, Japan.

A comparative analysis of composition features of KIM from the sampled area showed that: 1) there are variable and often high proportions of Cr-rich varieties of pyropes (>7 wt.% of Cr_2O_3) among the most of pyrope bearing samples; 2) several hundred of samples contain high-Cr subcalcic knorringite-rich ($Mg_3Cr_2Si_3O_{12}$ up to 32 mol. %) garnets (G10 group), and in several tens of these samples together with significant number of G10 garnets were found diamond crystals of kimberlitic morphological types up to 2 ct in weight; 2) magnesian ilmenites have all the compositional features of typical kimberlite ilmenites (MgO – 5,2-15,8 wt.%; Cr_2O_3 – 0.1-10,1 wt. %; hematite - Fe_2O_3 – 3-29 mol.%); 3) chromites also have all the compositional features typical for kimberlite chromites (Cr_2O_3 – 14-67 wt.%; MgO – 9.8 – 29.4 wt.%; TiO_2 – 0.01-8.5 wt.%).

KIM were found both in samples taken from modern alluvial sediments of many hundreds of rivers inside sampled areas and in samples taken from terrigene secondary collectors of the basal horizons of Paleozoic and Mesozoic ages. Very high concentrations of KIM were found in Cretaceous secondary collector of Blue Fish River, Canada, and in Triassic and Lower Carboniferous secondary collectors developed inside NE part of SP. Some of analyzed metamorphic zircons from samples taken from terrigene rocks (North of SP and NAP) and kimberlites of

Mesozoic age (North of SP) have Archean U-Pb ages. It is especially important for large Birektinsky Terrain (SP) proposed earlier as terrain of Proterozoic age of stabilization, because follow the Clifford rule this result very significantly change and improve a perspective of this area for discovery of new diamondiferous kimberlites of Middle Paleozoic age of emplacement.

So, all the obtained data both mineralogical and geological suggest that it is very likely that there are some new terrains presented by craton-sized blocks of the Archean age inside arctic parts both SP and NAP. A presence of diamonds and high pressure varieties of KIM (high-Cr subcalcic pyropes and high-Cr chromites) is a robust and reliable evidence of thick lithosphere (> 200 km) for this blocks at time of kimberlite emplacements and of presence inside them multiple kimberlite bodies including diamond-bearing ones. These results improve and support significance of both studied areas for successful diamond exploration.

This study was also supported by RAS Presidium Program #27 (SB RAS Project 27.1) and RFBR (Grant 13-05-00907).

REDOX DIFFERENTIATION IN DEEP MANTLE AND OXYGEN FUGACITY OF DIAMOND-FORMING PROCESSES, KIMBERLITES AND ALKALINE-ULTRAMAFIC MAGMAS

Ryabchikov I.D.

Russian Academy of Sciences, IGEM RAS
iryab@igem.ru

Reducing environment of sublithospheric mantle is caused by the experimentally established disproportionation of FeO into Fe^0 and Fe_2O_3 at super-high pressures.

The thermodynamic analysis of phase equilibria of rock-forming minerals of pyrolitic lower mantle with carbon-bearing crystalline compounds demonstrated that the field of diamond stability is separated from that of Fe-rich metallic alloy by the field of co-existence of iron carbides with prevailing silicates and oxides (Fig. 1). It implies that the formation of diamond in lower mantle requires more oxidizing conditions by comparison with the predominant part of this geosphere.

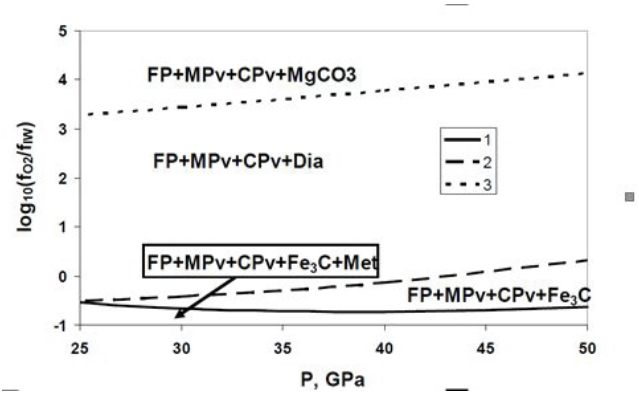

Figure 1: Stability fields of lower mantle mineral assemblages (oxygen fugacity is normalized by iron wuestite buffer). FP is ferropericlase, MPv is Mg-rich silicate perovskite, CPv is Ca-rich silicate perovskite, Dia is diamond and Met is Fe-rich metallic alloy.

The absence of metallic phase among the minerals of low-mantle diamond-bearing paragenesis is consistent with the high (about 1% - Fig. 2) Ni contents in ferropericlases trapped by diamond (Ni should be intensely extracted by Fe-rich alloy). The elevated redox-potential is confirmed by the findings of carbonate phases among the mineral inclusions in sublithospheric diamonds.

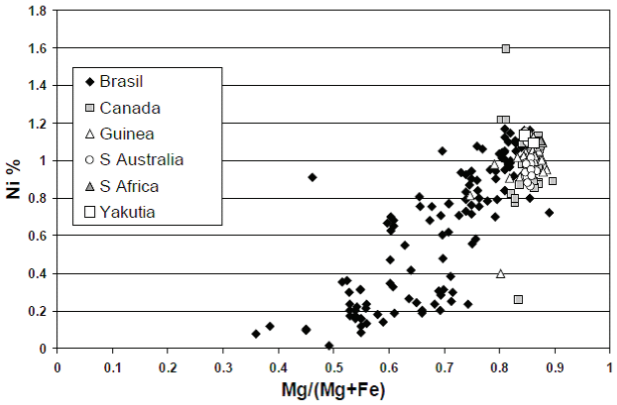

Figure 2: *FP* inclusions in diamonds of lower mantle origin with Mg-numbers appropriate for metaperidotite bulk composition all cluster around 1 % of Ni. Some outliers may correspond to lower fO_2 values.

The most likely cause of increasing oxygen fugacities is the displacement of redox equilibria with the growing temperature towards the decreasing amount of Fe-rich alloy and finally its complete disappearance (Fig. 3). An important role in the genesis of diamonds may be played by the appearance of carbonate-phosphate and silicate melts their migration and interaction with the surrounding rocks.

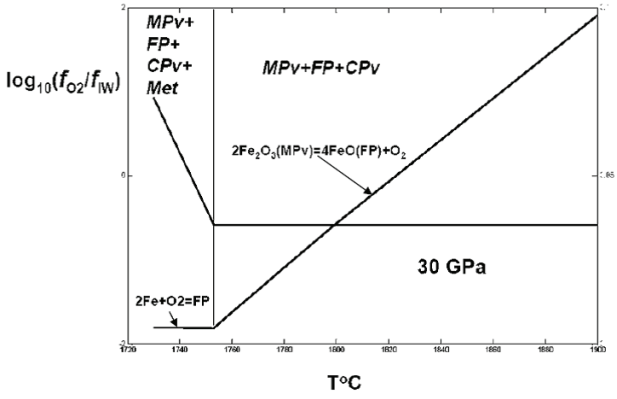

Figure 3: Effect of temperature on redox equilibria in lower mantle of pyrolitic composition.

The link of sublithospheric diamond formation with high temperature conditions follows from the confinement of such processes and to mantle plumes. Kimberlites are also related to the mantle plume environment.

Relatively oxidizing conditions related to mantle plumes are also manifested in the high level of oxygen fugacitiy typical for some ultramafic-alkaline magmatic rocks such as meimechites and intrusive rocks of the Maimecha-Kotuy Province (Polar Siberia).

EVIDENCES OF REE MINERALIZATION IN A QUATERNARY HIGHLY POTASSIC VOLCANIC COMPLEX WITH CARBONATITE AFFINITIES, CENTRAL IRAN

Saadat, S.,[1] Stern, C. R.[2], Moradian, A.[3]

1 Department of Geology, Mashhad Branch, Islamic Azad University, Mashhad, Iran
2 Department of Geological Sciences, University of Colorado, UCB 399, Boulder, CO
3 Department of Geology, Shahid Bahonar University, Kerman, Iran
Saeed.Saadat@colorado.edu

The Quaternary Qaleh Hassan Ali's (QHA) maars (1,2) occur within the convergent orogen between the Arabian, Eurasian and Indian plates connecting the Alpine and Himalayan orogenic systems. These highly potassic basanite tephrite maars are located in central Iran at the intersection of the north-south Nayband fault and a system of northwest-southeast trending faults (Fig. 1). The NW-SE fault system trends towards the 11 Ma leucite-bearing ultrapotassic Saray volcano (3), and to the SE into the Makran arc (4), which continues to the east into Pakistan and to the northeast towards the Quaternary Khanneshin Carbonatite Complex in Afghanistan (5,6; Fig. 1).

The country rocks of the QHA maars are Eocene calc-alkaline volcanic and plutonic rocks and belong to the Urumieh–Dokhtar magmatic belt (UDMB; Fig. 1) generated by the subduction of the Neotethys ocean below the Eurasian continental crust of central Iran (7,8). All the QHA extrusive samples plot on a silica versus total alkali diagram as basanaite tephrites in the alkalic field and plot on the K_2O versus Na_2O diagram in the high K-series field. They have high La/Yb ≥100 (Fig. 2) and low Nb and Ta contents relative to large-ion-lithophile elements (Ba, Rb, Sr, K and La), distinct from OIB or intra-plate alkali olivine basalts and more similar to convergent plate boundary volcanic arc magmas formed in post-collisional continental areas which had previously experienced subduction-related arc volcanism (1; Fig. 2).

Tephrite coated plutonic xenoliths found within the tuff rims of the maars are interpreted as cogenetic with the tephrites because of their similar mineralogy and isotopic compositions. Some of the xenoliths contain up to >20% modal calcite. The calcite is interpreted as magmatic because of (a) its grain size, which is similar.

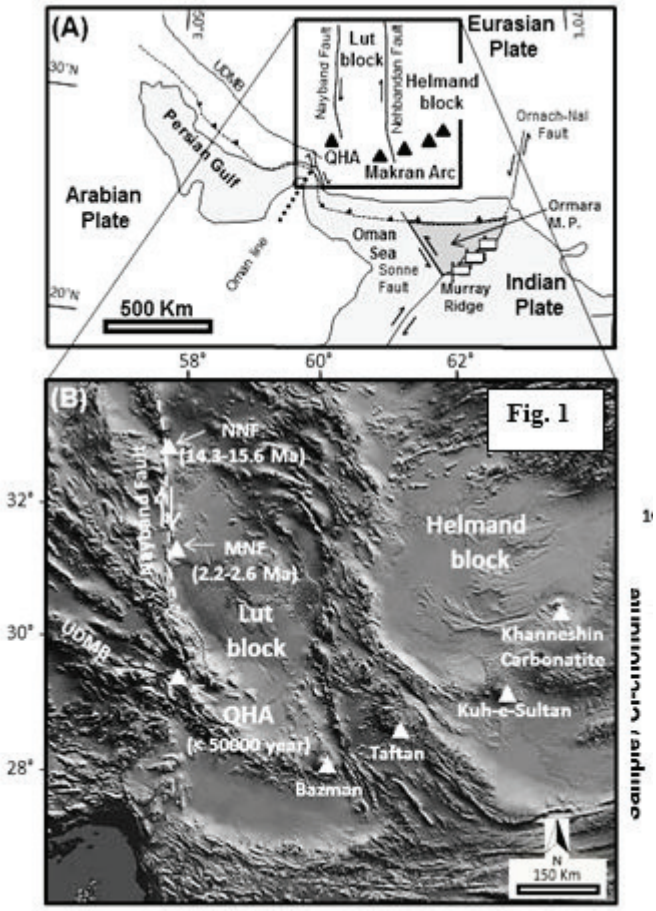

Figure 1: Location of the QHA maars in central Iran.

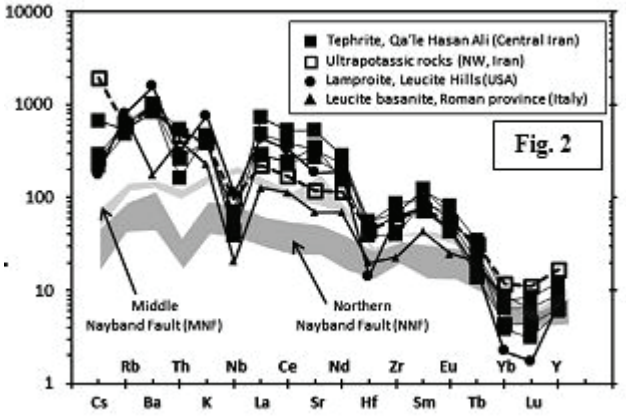

Figure 2: Spider diagrams of trace-element concentrations, normalized to chondritic meteorites for

QHA tephrites and highly potassic rocks from other areas of post-collisional continental arc magmatism.

to both feldspars and aegirine–augite pyroxenes in these rocks, (b) the occurrence of fine grained inclusions of pyroxene and apatite within calcite grains, and (c) the similarity of the isotopic composition of the calcite with the other minerals in this rock (Fig. 4). The high modal proportions of magmatic calcite in some samples suggest that the shallow plutonic complex from which these plutonic xenoliths were derived has affinities with carbonatites. The calcite-bearing plutonic xenoliths have high LREE/HREE ratios and contain ~0.3 wt percent LREE, which may occur in REE-rich allanite, with up to ~20 wt % LREE content that makes up 5 modal % of the most calcite rich samples, and britholite (2).

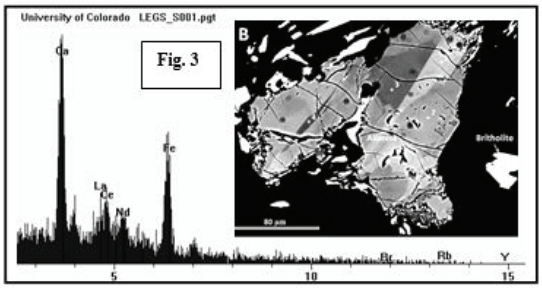

Figure 3: Back-scattered electron image of allanite and britholite in calcite-bearing plutonic xenoliths sample (right) and energy spectrum of the elements in the britholite (left).

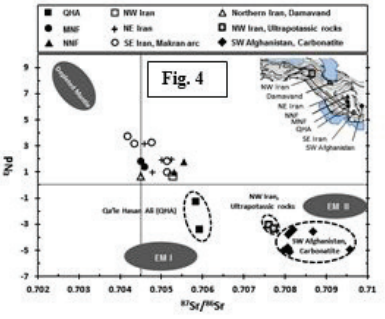

Figure 4: Sr vs Nd isotopes ratios for QHA tephrites and highly potassic rocks from elsewhere in the Alpine-Himalaya belt.

The basanite tephrite of the Quaternary QHA marrs in central Iran are part of an extensive belt of post-collisional highly potassic volcanic rocks associated with the Alpine–Himalayan belt stretching from Spain to Tibet. They formed by melting of a lower lithosphere mantle source metasomatized by fluids derived from subducted crustal sediments, including carbonate-rich sediments, during the closure of the Neotehtys ocean. They occur above an area of mantle with low Pn, consistent with mantle partial melting, and at the intersection of various large crustal structures which allowed the tephrite magmas to reach the surface from the mantle. They may be underlain by a shallow plutonic complex with affinities with carbonatites and potentially economic REE mineralization, similar to other REE-rich carbonatite complexes associated with Alpine-Himalayan collision, including the Quaternary Khanneshin Carbonatite Complex in Afghanistan. We conclude, as did Milton (1), that ''this locality is worthy of further study for its significance in the Quaternary geologic development of Iran and for its petrologic peculiarities.''

References

1. Milton, D.J (1976-77). Qal'eh Hassan Ali Maars, Central Iran. Bull. Volcanol. 40(3), 201-208.
2. Saadat, S, and CR Stern (2014). Petrochemistry of ultrapotassic tephrites and associated cognate plutonic xenoliths from late Quaternary Qa'le Hasan Ali maars, central Iran. Journal of Asian Earth Sciences 89, 108-122.

3. Pang, K.N., Chung, S.L., Zarrinkoub, M.H., Lin, Y.C., Lee, H.Y., Lo, C.H., Khatib, M.M., 2013. Iranian ultrapotassic volcanism at ~11 Ma signifies the initiation of postcollisional magmatism in the Arabia-Eurasia collision zone. Terra Nova 25, 405–413.
4. Saadat, S., Stern, C.R., 2011. Petrochemistry and genesis of olivine basalts from small monogenetic cones of Bazman stratovolcano, Makran arc, southeastern Iran. Lithos 125, 607–619.
5. Mars, J.C., Rowan, L.C., 2011. ASTER spectral analysis and lithologic mapping of the Khanneshin carbonatite volcano, Afganistan. Geosphere 7, 286–289.
6. Tucker, R.D., Belkin, H.E., Schulz, K.J., Peters, S.P., Horton, F., Buttleman, K., Scott, E.R., 2012. A light rare-earth element (LREE) resource in the Khanneshin carbonatite complex of southern Afghanistan. Econ. Geol. 107, 197–208.
7. Shafiei, B., Haschke, M., Shahabpour, J., 2009. Recycling of orogenic arc crust triggers porphyry Cu mineralization in Kerman Cenozoic arc rocks, southeastern Iran. Miner. Deposita 44, 265–283.
8. Agard, P., Omrani, J., Jolivet, L., Whitechurch, H., Vrielynck, B., Spakman, W., Monié, P., Meyer, B., Wortel, R., 2011. Zagros orogeny: a subduction-dominated process. Geol. Mag. 148, 692–725.

SEAMOUNT FRAGMENTS WITHIN THE ANKARA MÉLANGE, CENTRAL TURKEY AND THEIR TECTONIC IMPLICATIONS

Sarifakioglu, E[1]., Sevin, M[1]., Dilek, Y[2].

1 The General Directorate of Mineral Research and Exploration, Geology Department, 06520 Ankara, Turkey
esarifakioglu@mta.gov.tr
2 Department of Geology, Miami University, Oxford, Ohio 4506, USA

The Ankara Mélange, fistly named by Bailey and McCallien [1, 2] is one of the world's major mélanges. The Ankara Mélange representing an ancient subduction-accretion prism in the Mesozoic northern Neo-Tethys ocean, lying between Sakarya Continent in north and Anatolide-Tauride Platform in south contains blocks of ophiolitic rocks, volcanic rocks and/or neritic limestones of seamount and oceanic plateau within serpentinite, mudstone and altered volcanic matrix. In the central Turkey, the chaotic rocks of the Ankara Mélange are found in Ankara, Kırıkkale, Çankırı and Çorum surroundings.

In previous studies, presence of the seamount volcanics in the Ankara Mélange has been described [3, 4, 5, 6]. In these studies, some basalt samples picked from the Ankara Mélange were petrographically and geochemically distinguished and these alkaline and within-plate basaltic lavas were interpreted as oceanic island or seamount characteristics.

We have firstly carried out volcanostratigraphy of the seamount fragments. We made an approaches for the formation and life span of northern Neo-Tethys oceanic crust, using the paleontologic and radiometric age dating of seamount units [7, 8]. The semount volkanostratigraphy is composed of the volcanic, pyroclastic, volkaniclastic rocks, debris flows and nertic limestones. The neritic limestones overlying seamount volcanics give ages Middle-Upper Triassic, Late Triassic to Early Cretaceous paleontologically. Also, the radiolarian cherts associated with alkaline pillow lavas also yield Upper Triassic to Late Cretaceous. Also, we determined 99.6±1.8Ma and 70.0±1.0Ma $^{40}Ar/^{39}Ar$ age dating from seamount volcanic samples. The Ankara Mélange containing the blocks of oceanic rocks unconformably is covered by late Maastrichtian-Lutetian flysh units of marine environment with sandstone-shale alternation, so the oceanic environment in this region lasted before late Maastrichtian.

The alkaline volcanics have high TiO_2 (1.51-3.62wt%), Nb (19.0-96.0 ppm), Y (16.2-49.9 ppm), Yb (1.45-4.42 ppm), Zr (101.3-389.5 ppm) and large-ion-lithophile elements (LILE) such as Ba (135-1241 ppm), Sr (170-1111 ppm), Rb (10-64ppm), Th (2-10.5 ppm). The high Nb/Y ratios (0.93-3.07), TiO_2/Yb (0,57-1,81), Th/Yb (0,93-5,59), Nb/Yb (10.16-54.78) and low Zr/Nb ratios (2.92-7.35) show that these volcanites formed within-plate setting have mainly alkalic to tholeiitic OIB-like geochemical characteristics.

The presence of Middle-Upper Triassic to Late Cretaceous aged seamount volcanics with OIB-like geochemical features within the Ankara Mélange indicate the presence of oceanic lithosphere (northern Neo-Tethys) in pre-Middle-Upper Triassic to Late Cretaceous. Seamount fragments together with other oceanic slices and/or blocks accreted in the trench within intra-oceanic subduction environment, and the trench migrated southward with the time.

References

1. Bailey, E. B. and McCallien, W.J. 1950. Ankara Mélange and Anatolian Thrust. *Maden Tetkik ve Arama Enstitüsü Dergisi* 40, 17-21.
2. Bailey, E. B. and McCallien, W.J. 1953. Serpentine lavas, the Ankara Mélange and the Anatolian Thrust: Transactions of the Royal Society of Edinburg, v.2, part II (no.11), 403-442.
3. Çapan, U.Z. and Floyd, P.A. 1985. Geochemical and petrographic features of metabasalts within units of the Ankara Mélange, Turkey. Ofioliti 10 (1), 3-18.
4. Tankut, A., Dilek, Y. and Önen, P. 1998. Petrology and geochemistry of the Neo-Tethyan volcanism as revealed in the Ankara melange, Turkey. Journal of Volcanology and Geothermal Research 85, 265-284.
5. Rojay, B., Altıner, D., Özkan Altıner S., Önen, A.P., James, S. and Thirlwall, M.F. 2004. Geodynamic significance of the Cretaceous pillow basalts from North Anatolian Ophiolitic Mélange Belt (Central Anatolia, Turkey): geochemical and paleontological constraints. Geodinamica Acta 17 (5), 349–361.
6. Gökten, E. and Floyd, P.A. 2006. Stratigraphy and geochemistry of pillow basalts within the ophiolitic mélange of the Izmir-Ankara-Erzincan suture zone: implications for the geotectonic character of the northern branch of Notethys. International Journal of Earth Sciences (Geological Rundsch). DOI 10.1007/s00531-006-0132-4.
7. Sarifakioglu, E., Sevin, M., Esirtgen, E., Bilgiç, T., Duran, S., Parlak, O., Karabalık, N., Alemdar, S., Dilek, Y., and Uysal, I. 2011. The geology of ophiolitic rocks around Çankırı–Çorum Basen: petrogenesis, tectonics and ore deposits, Mineral Research and Exploration Institute of Turkey (MTA) Report, No. 11449, 196 pp. (in Turkish, unpublished).
8. Sarifakioglu, E., Dilek, Y. and Sevin, M. 2014. Jurassic–Paleogene intraoceanic magmatic evolution of the Ankara Mélange, north-central Anatolia, Turkey. Solid Earth 5, 77–108.

DISTINGUISHING METACARBONATITES FROM MARBLES – CHALLENGE FROM THE CARBONATE-AMPHIBOLITE-EPIDOTITE ROCK ASSOCIATION IN THE PELAGONIAN ZONE (GREECE)

Schenker F. L.[1], Burg J. P.[1], Kostopoulos D.[2], Galli A.[1]

1 Geological Institute, ETH Zurich, Sonneggstrasse 5, 8092 Zürich, Switzerland
andgalli@hotmail.com
2 National and Kapodistrian University of Athens School of Science, Zographou Athens 157 84, Greece

Carbonate rocks were found in association with amphibolites and epidotites in the greenschist- to amphibolite-facies metamorphic basement of the Pelagonian zone (Greece). The mafic rocks both include and are truncated by the carbonates, hinting to a cogenesis of siliceous and carbonatic magmas/fluids. The carbonates have an isotopic signature of $\delta^{13}C$ ranging from -5.18 to -5.56 (‰ vs. PDB) and of $\delta^{18}O$ from 10.68 to 11.59 (‰ vs. SMOW) giving them the geochemical characteristic of carbonatites (magmatic carbonates). Mafic rocks have high Nb and Ta concentrations, typical for alkaline basalts. Therefore, textural relationships and geochemical signals in both the silicate and carbonate rocks hint at a cogenetic, mantle origin. SHRIMP U-Pb zircon ages from a carbonate bearing amphibolite date the intrusion at 278 Ma (magmatic zircon cores), well before the metamorphic event at 118 Ma (metamorphic zircon rims).

However, the concentration of rare earth elements (REE) in the carbonates, amphibolites and apatites is lower than in typical carbonatites, probably because of the interaction with metamorphic fluids during the Cretaceous metamorphism. Since these low REE concentrations raise doubts regarding the carbonatitic origin, other processes altering the $\delta^{13}C$ have to be considered. Skarn metasomatism can fractionate the $\delta^{13}C$ in the carbonates to carbonatitic values, but the absence of a Cretaceous contact metamorphism speaks against that possibility leaving the suggestion that the carbonatite rock association sign the Permian opening of the Tethys Ocean in the eastern Mediterranean.

ALKALI CARBONATES IN MINERALS OF IJOLITE AT THE OLDOINYO LENGAI VOLCANO, TANZANIA

Sekisova V.S.[1-2], Sharygin V.V.[1-2], Zaitsev A.N.[3]

1 Novosibirsk State University, Novosibirsk, Russia, vikasekisova@mail.ru;
2 V.S. Sobolev Institute of Geology and Mineralogy SB RAS, Novosibirsk, Russia, sharygin@igm.nsc.ru;
3 Saint Petersburg State University, Saint Petersburg, Russia, a.zaitsev@spbu.ru

Minerals with high alkalis (mainly carbonates, rarely sulphates, halides and phosphates) are observed in phenocryst-hosted melt and fluid inclusions from olivine-mica ijolite xenoliths [1] in the pyroclastics of the active Oldoinyo Lengai volcano (Gregory rift, Tanzania). They are presented by nyerereite, gregoryite, thenardite, arcanite, neighborite, villiaumite, halite, sylvite, etc. Inclusions with them are occurred in olivine and clinopyroxene phenocrysts and nepheline and apatite microphenocrysts. It should be noted that such minerals are not found in the groundmass of ijolites.

Olivine macrocrystals contain numerous chains of secondary inclusions, which are coexisting melt, fluid and crystal inclusions. Most melt inclusions are completely crystallized, silicate glass occurs rarely. Their phase composition varies strongly. Moreover these inclusions can be divided into two types: inclusions with Na-Ca-carbonates plus sulphates and/or phosphates and inclusions with magnesite. Inclusions with Na-Ca-carbonates consist of fluorapatite, phlogopite, clinopyroxene, Ti-rich magnetite, nyerereite, halite, sylvite, calcite, neighborite, Na-phosphate, Na-rich amphibole, arcanite, witherite, fluorite, thenardite, etc.

Zoned clinopyroxene phenocrysts contain melt, completely crystallized and sulphide inclusions. Completely crystallized inclusions are secondary and form trails in the host. They are carbonate-rich and are composed of nyerereite, gregoryite, fluorapatite, nepheline, phlogopite, Ti-rich magnetite, leucite ?, sylvite, thenardite, Na-Ca-phosphate, etc. Phase composition of primary melt inclusions is silicate glass + gas bubble ± sulphide bleb ± submicron blebs ± daughter/trapped crystals, represented by Ti-rich magnetite, fluorite, etc. They are confined to the central pale-green zones.

Euhedral nepheline phenocrysts contain primary melt inclusions (5-100 μm), comprising green silicate glass + vapor-carbonate globule ± sulphide bleb ± submicron blebs ± daughter/trapped crystals, represented usually by clinopyroxene, rarely alumoakermanite (melilite-group mineral) and Ti-rich garnet. Vapor-carbonate globule (up to 20 μm) consists of gas bubble with Na-Ca-carbonate-rich rim. According Raman spectroscopy and scanning electron microscopy the rim is mainly composed of alkali carbonates such as nyerereite and gregoryite. Heating experiments with inclusions showed that the homogenization of vapor-carbonate globule happened at 900-920 °C, but complete homogenization (disappearance of Na-carbonate melt in silicate liquid) was not achieved.

Carbonate-salt melt inclusions, located in the center of apatite microphenocrysts, are primary. They contain fine-grained aggregate + gas bubble ± daughter crystals. Na-Ca-carbonates (nyerereite, rarely gregoryite) are the most common phases in apatite-hosted inclusions, whereas minor phases are presented by halite, sylvite, fluorite, villiaumite, neighborite, thenardite, bar-

yte, sulphides, Fe-rich spinel-group mineral, Mg-Fe-carbonates and witherite. Silicate phases (haüyne-sodalite, alumoakermanite ?, Ba-Ti-mica and a cuspidine-group mineral) are occasional. Generally mineral composition of inclusions in fluorapatite is similar to that of natrocarbonatite [3]. According to heating experiments homogenization of apatite-hosted inclusions occurs in a wide temperature range from 850 to 1080 °C.

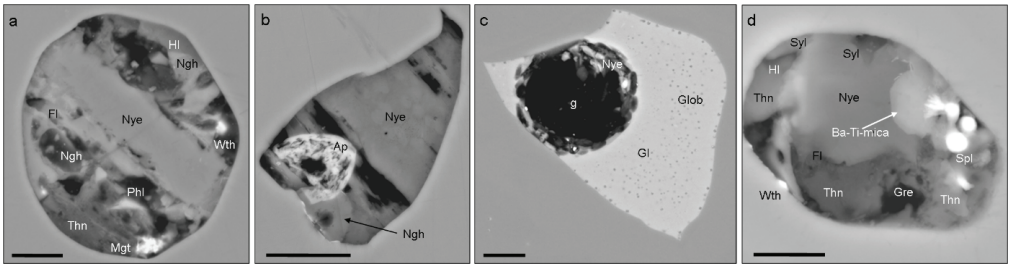

Figure 1: Backscattered electron images (BSE) of Na-Ca-carbonate-rich inclusions: a) secondary melt inclusion in olivine, b) secondary inclusion in clinopyroxene, c) primary melt inclusion in nepheline, d) primary melt inclusion in apatite. Scale bar is 10 μm. Symbols: Gl – silicate glass; g – gas bubble; Nye – nyerereite; Ap – fluorapatite; Fl – fluorite, Hl – halite, Ngh – neighborite, Gre – gregoryite, Thn – thenardite, Wth – witherite, Spl – spinel, Syl – sylvite, Phl – phlogopite, Mgt – Ti-magnetite.

Alkali carbonates were initially studied by means of Raman spectroscopy. These data were obtained for inclusions in olivine and nepheline. Spectra of Na-Ca-carbonates in these two minerals are similar. Their spectra have Raman peaks near 631, 711, 954, 1002, 1047, a weak shoulder at 1077 and the most intensive peak at 1086 cm^{-1}. Spectra of Na-Ca-carbonates, which have Raman bands 711, 1002 and in the region of 1077–1086 cm^{-1}, indicate the presence of nyerereite. Peaks at 631, 954, 1002 and 1077 cm^{-1} suggest that gregoryite can be sited in the inclusions. Other peaks (e.g. 1047 cm^{-1}) do not exclude the presence of other minerals. Studied alkali minerals do not show Raman band in the region of 2800 – 3800 cm^{-1}, indicating the absence of water H_2O or OH^--group.

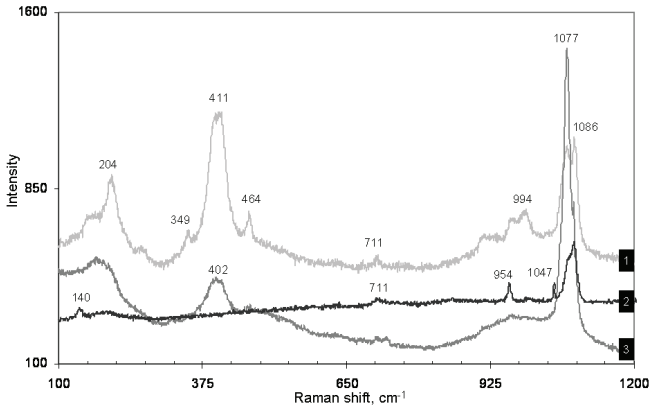

Figure 2: Raman spectra of Na-Ca-carbonates from ijolite: 1, 2 – in nepheline-hosted inclusions, 3 – in olivine-hosted inclusion.

Melt inclusions clearly indicate complex liquid immiscibility between silicate and natrocarbonatite melts, occurring during the crystallization of ijolites. Melt inclusion studies for Lengai ijolite indicated that first stage of separation of initial melt into silicate and Na-Ca-carbonate components is fixed at the fluorapatite crystallization. Melt inclusions with Na-Ca-carbonates in nepheline and lack of coexisting carbonate-rich inclusions show that main stage of immiscibility occurred after their entrapment by minerals. Abundant secondary inclusions in clinopyroxene and olivine are testimony that natrocarbonatite melt separated at lower temperatures. This melt was apparently removed from the system because there are no any signs of subsequent reaction with early minerals, unlike some Lengai nephelinites, in which fluorapatite was rimmed by rim Na-Ca-phosphate and combeite replaced wollastonite [2].

This study was supported by the Russian Foundation of Basic Researches (grant 14-05-00391) and St. Petersburg State University.

References

1. Dawson, J.B., Smith, J.V., Steele, I.M., 1995. Petrology and mineral chemistry of plutonic igneous xenoliths from the carbonatite volcano, Oldoinyo Lengai, Tanzania. Journal of Petrology 36, p. 797-826.
2. Sharygin, V.V., Kamenetsky, V.S., Zaitsev, A.N., Kamenetsky, M.B., 2012. Silicate–natrocarbonatite liquid immiscibility in 1917 eruption combeite–wollastonite nephelinite, Oldoinyo Lengai Volcano, Tanzania: Melt inclusion study. Lithos 152, p. 23-39.
3. Zaitsev, A.N., Keller, J., Spratt, J., Jeffries, T.E., Sharygin, V.V., 2009. Chemical composition of nyerereite and gregoryite from natrocarbonatites of Oldoinyo Lengai volcano, Tanzania. Geology of Ore Deposits 51(7), 608-616.

SULFIDE MINERALS AS NEW SM-ND GEOCHRONOMETERS FOR ORE GENESIS DATING OF MAFIC-ULTRAMAFIC LAYERED INTRUSIONS

Serov P.A., Ekimova N.A., Bayanova T.B., Mitrofanov F.P.

Geological Institute KSC RAS, Apatity, Russia
serov@geoksc.apatity.ru

The Sm-Nd method is one of the most valuable isotope research techniques for dating age of mafic-ultramafic intrusions through main rock-forming minerals, i.e., plagioclase, ortho-, and clinopyroxenes, olivines, etc. It allows employing new minerals to date various frontiers of the rock formation and transformation. Sulphides with which Pt-Pd mineralization is tightly related, may serve as minerals-geochronometers. Sulphide-based rock dating is a direct method since in this case, straight the time of ore genesis is being dated to allow further usage of Sm-Nd systematics as an indicator of ore content or absence for various mafic intrusions.

The available national and international publications devoted to this issue are scarce [2, 3, 4, 8, 11, 12] since studying Sm-Nd system in sulphides is poor. Meanwhile, REE distribution research executed for the sulphides of hydrothermal sources in the mid-ocean ridges reflects probability of REEs to be found in the crystal lattice of sulphides [6, 7, 9]. The influence of crystal-chemical parameters of sulphide minerals on the REE accumulation in monomineral sulphide fractions is studied in [6, 7].

The main method of dating the ore process was the Re-Os method of sulfides [5, 10]. However, studies of Re-Os systematics of sulfide minerals do not always give the correct ages and showing the disturbances of the Re-Os systematics. At the same time, Sm-Nd age of sulfides in good agreement with the U-Pb dating on zircon and baddeleyite and suggests that the Sm-Nd system of sulfides is more resistant to secondary alteration processes. Our studies have shown that along with rock-forming, ore minerals (sulfides) can be used to determine the ore genesis time of industrially important geological sites, since exactly with the sulfides the industry Pt-Pd mineralization is closely connected.

The Sm-Nd investigations steadily employ new minerals-geochronometers. Of these, sulfides of PGE-bearing layered intrusions are quite important in terms of dating the process of ore origin. Studying the REE distribution in the sulfides of MOR hydrothermal sources has shown possible REE presence in the sulfide lattice [9]. These are difficult to carry out because the concentrations of Sm and Nd isotopes in sulfides are much lower than those in chondrites [9].

For the first time in Russia with sulfide and rock-forming minerals and WR in Sm-Nd method have been dated impregnated and brecciform ores of the following objects - Pilguyarvi Cu-Ni deposits, Pechenga (1965±87 Ma, fig. 1); impregnated (2433±83 Ma, fig 2a) and redeposited (1903±24 Ma, fig 2b) ores of Ahmavaara intrusion (Finland). Pt-Pd gabbro-pegmatite ores (2476± 41 Ma, fig 3a) and gabbronorites (2483±86 Ma, Fig 3b) of PGE-bearing Kievei deposit (Fedorovo-Pansky intrusion) [1].

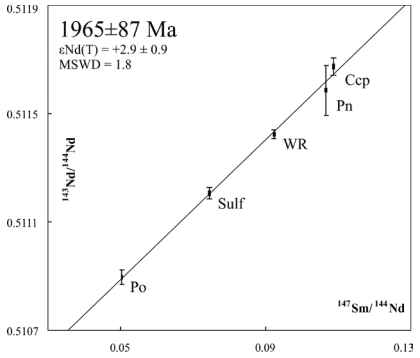

Figure 1: Mineral Sm-Nd isochrones for brecciform ores of Pilguyarvi Cu-Ni deposits, Pechenga

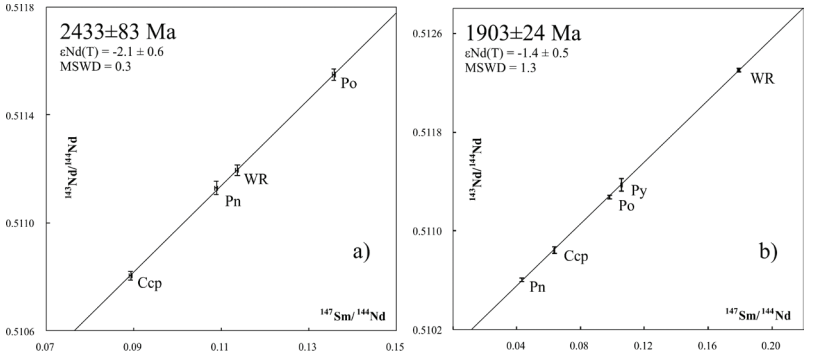

Figure 2: Mineral Sm-Nd isochrones for impregnated (a) and redeposited (b) ores of Ahmavaara intrusion (Finland).

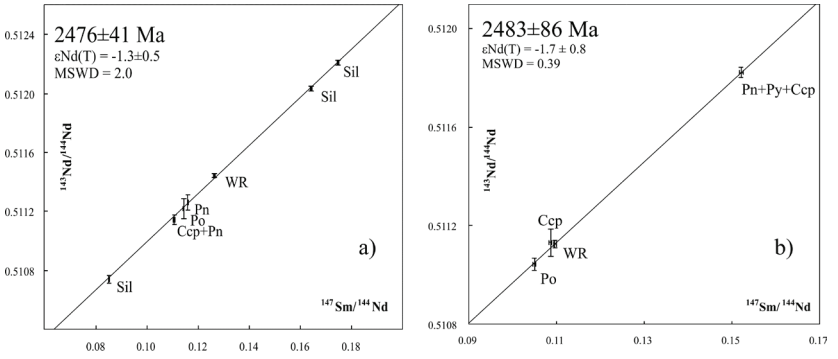

Figure 3: Mineral Sm-Nd isochrones for Pt-Pd gabbro-pegmatite ores (a) and gabbronorites (3b) of PGE-bearing Kievei deposit (Fedorovo-Pansky intrusion).

In [3] sulfides from two metamorphosed chondrites by instrumental neutron activation analysis (INAA) and ion probe were studied. As shown, the level of REE in the sulfide phase determined by the ion probe is quite similar to that obtained by INAA. Although the concentrations of REE in the enstatite and the Fe, Si, Cr-rich inclusions are comparable to those in sulfide, estimates based on mass balance calculations show that the silicate inclusions would not noticeably con-

tribute to the REE budget in sulfides [3].

Main conclusions

Using sulfide minerals as geochronometers in Sm-Nd method were dated syngenetic and epigenetic ore of industrially important geological objects of Fennoscandian Shield;

Studies have shown that sulfides can be used in the Sm-Nd dating of ore-bearing intrusions.

These studies supported by the RFBR 13-05-00493, OFI-M 13-05-12055, State Earth Division Program №4, IGCP-599.

References

1. Ekimova N.A., Serov P.A., Bayanova T.B., Mitrofanov F.P., Elizarova I.R. New data on distribution of REE in sulfide minerals and Sm-Nd dating of ore genesis of layered basic intrusions // Doklady Earth Sciences. 2011. T. 436. № 1. P. 28-31.
2. Jiang S.-Y., Slack J.F., Palmer M.R. Sm-Nd dating of the giant Sullivan Pb-Zn-Ag deposit, British Columbia // Geology. 2000. V. 28.№ 8. P. 751–754.
3. Kong P., Deloule E., Palme H. REE-bearing sulfide in Bishunpur (LL3.1), a highly unequilibrated ordinary chondrite // Earth and Planetary Science Letters. 2000. V. 177. P. 1-7.
4. Li Q.-L., Chen F., Yang J.-H., Fan H.-R. Single grain pyrite Rb–Sr dating of the Linglong gold deposit, eastern China // Ore Geology Reviews. 2008. V. 34. P. 263–270.
5. Luck J.M., Allegre C.J. $^{187}Re/^{187}Os$ systematics in meteorites and cosmochemical consequences // Nature. 1983. V. 302. P. 130-132.
6. Mills R.A., Elderfield H. Rare earth element geochemistry of hydrothermal deposits from the active TAG Mound, 26 °N Mid-Atlantic Ridge // Geochimica Et Cosmochimica Acta. 1995. V. 59, №17, P. 3511-3524.
7. Morgan J.W., Wandless G.A. Rare earth element distribution in some hydrothermal elements: evidence for crystallographic control // Geochimica Et Cosmochimica Acta. 1980. V. 44. P. 973-980.
8. Ni Z.-Y., Chen Y.-J., Li N., Zhang H. Pb–Sr–Nd isotope constraints on the fluid source of the Dahu Au–Mo deposit in Qinling Orogen, central China, and implication for Triassic tectonic setting // Ore Geology Reviews. 2012. V. 46. P. 60–67.
9. Rimskaya-Korsakova M. N., Dubinin A. V., Ivanov V. M. Determination of rare-earth elements in sulfide minerals by inductively coupled plasma mass spectrometry with ion-exchange preconcentration // Journal of Analytical Chemistry. Vol. 58. № 9. 2003. pp. 870–874.
10. Walker R.J., Morgan J.W., Naldrett A.J., Li C., Fassett J.D. Re-Os isotope systematics of Ni-Cu sulfide ores, Sudbury Igneous Complex, Ontario: evidence for a major crustal component // Earth and Planetary Science Letters. 1991. V. 105. P. 416-429.
11. Wan B., Hegner E., Zhang L., Rocholl A., Chen Z., Wu H., Chen F. Rb-Sr geochronology of chalcopyrite from the Chehugou porphyry Mo-Cu deposit (Northeast China) and geochemical constraints on the origin of hosting granites // *Economic Geology.* 2009. V. 104. P. 351-363.
12. Yang J.-H., Zhou X.-H. Rb-Sr, Sm-Nd, and Pb isotope systematics of pyrite: Implications for the age and genesis of lode gold deposits// Geology. 2001. V. 29. № 8. P. 711–714.

GEOCHEMISTRY AND TECTONIC SETTING OF SYENITES OF THE NORTH SHAHREKORD, IRAN

Shabanian N., Jaberi M., Davoudian A.R.

Faculty of Natural Resources and Earth Sciences, Shahrekord University, Shahrekord, Iran
nahid.shabanian@gmail.com

The study area is a part of Sanandaj - Sirjan Zone that is located in the north of Shahrekord, SW Iran. The Sanandaj-Sirjan Zone is a metamorphic belt that was uplifted during late cretaceous continental collision between the Afro-Arabian continent and the Iranian microcontinent [1]. In addition, the Sanandaj-Sirjan zone is a region of polyphase deformation, the youngest one reflecting the collision of Arabia and Eurasia and the subsequent southward propagation of the fold–thrust belt [2]. The syenites are as small bodies that variably mylonitic and shows a foliation and a stretching lineation. Mylonitic fabrics and microstructures in these rocks are visiable in petrographic studies. The most characteristic fabric is an asymmetrical core-and-mantle structure in these rocks.

In the studied area, the mylonitic syenites associated with the predominantly metamorphic rocks such as schist, mica-schist, meta-psammite, metabasite, amphibolite, greenschist, marble and talc-marble have juxtaposed along a ductile shear zone. Their mineralogical composition is K- feldspar, plagioclase and biotite as main minerals and magmatic epidote, sphene, sphalerite, zircon, quartz and magnetite as accessory minerals. The rocks exhibit identical compositional ranges as Table 1. Similarly the trace element compositions exhibit significant variations, particularly in the case of Rb, Sr, Y, Zr and to certain extent in Nb, Cs, Ba, Hf and Ta as also U and Th .All the samples show High K contents (K_2O= 4.5-6.24 wt. %) and plot in the SiO_2 vs. K_2O diagram in the shoshonitic field.

Table. 1. Variation range of major elements of the studied syenites form the North Shahrekord (as %wt)

SiO_2	TiO_2	Al_2O_3	Fe_2O_3	FeO	MnO	MgO	CaO	Na_2O	K_2O	P_2O_5
59.95-63.30	0.24-0.40	17.13-17.54	1.51-2.69	1.02-1.92	0.07-0.12	0.33-0.67	1.45-2.90	5.65-6.48	4.50-6.24	0.02-0.10

They are contain normative diopside (2.18-4.24%) and hypersthene (0.00-0.85%). According to a geochemical classification scheme for the syenites, proposed by [3], the syenites are ferron, alkaline (Fig.1A) and meta-aluminous nature. The syenites show negative slope in Chondrite-normalized spider [4] diagram [$(La/Yb)_N$=17.49-17.64] with negative anomaly Eu (Eu/Eu*=0.51) (Fig. 1B). The MORB normalized patterns of the rocks display enrichment of Zr, Ba, K, and Rb, also they show depletion of Nb, Ti and P in the Primitive Mantle spider diagrams. The ORG-normalized patterns demonstrate enrichment in the LILE and the LREE relative to the HFSE. They have slightly negative anomalies in Nb and display a marked enrichment of the LILE, LREE, and HFSE. The plot of Zr + Nb + Ce + Y vs. 10000*Ga/Al suggest an A-type character for the studied syenites [5, 6]. Their geochemical characteristics, such as negative Eu anomalies, and high Zr + Nb + Y + Ce, are similar to A-type granitoids. [7] subdivided A-type granites into A1 and A2 groups. The genesis and tectonic setting of these two groups are very different from each other. On the ternary plots involving Y-Nb-(3Ga, Ce, 3Th and Zr/4), the syenitic rocks fall in the A2 group. On the tectonic discrimination plot (Y+Nb vs.Rb; Fig. 1D), the rocks show a within-plate granite (WPG) character [8].

The some of syneites contain sphalerite and therefor show enrichment of the Zn. The geochemical analyses show that the rocks have more than 10000 ppm Zn. The sphalerites are mostly associated with biotite. Many of the Zn–Pb deposits in Iran have traditionally been considered to have formed during the Precambrian or Paleozoic, simply based on their spatial association with older country rocks [9].

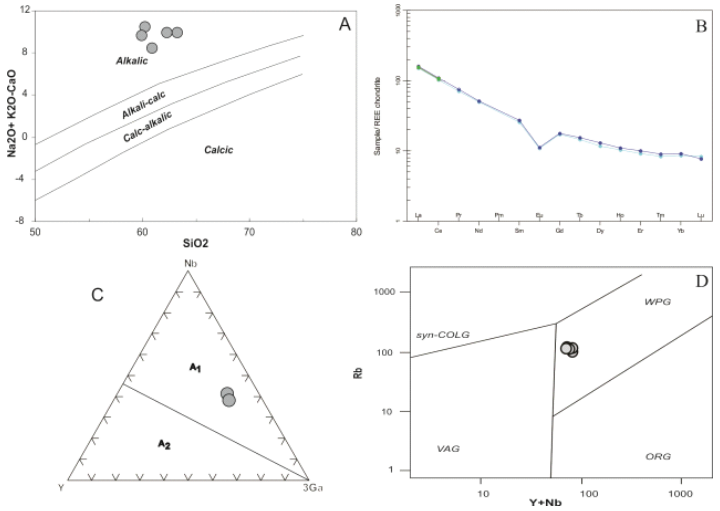

Figure 1: A) Diagrams ($Na_2O + K_2O – CaO$)–SiO_2 (a) for the studied rocks. B) Chondrite-normalized REE patterns for the studied syenite. The data of [4] were used for normalization. C) Diagram Nb–Y–3Ga show A1 and A2 subgroup discrimination of A-type granites [6]. D) Rb vs. (Nb+Y) diagram after [7], showing the fields of syn-collisional granites (SCG), within-plate granites (WPG), volcanic-arc granites (VAG) and ocean-ridge granites (ORG).

References

1. Mohajjel M. & Fergusson C. L., 2000. Dextral transpression in Late Cretaceous continental collision, Sanandaj–Sirjan Zone, Western Iran. J. of Struct. Geol. v. 22, p. 1125–1139.
2. Alavi M., 1994. Tectonics of the Zagros orogenic belt of Iran: new data and interpretations. Tectonophysics. v. 229, p. 211–238.
3. Frost B. R., 2001. A Geochemical Classification for Granitic Rocks. Journal of Petrology. v. 42, P. 2033-2048.
4. Boynton, W. V., 1984. Cosmochemistry of the rare earth elements: meteorite studies. In Rare earth element geochemistry.Loiselle M. C. & Wones, D. R., 1979. Characteristics and origin of anorogenic granites. – Geol. Soc. of America, Abstr. With Programs 11, p.468.
5. Whalen, J. B., Currie, K. L. & Chappell, B. W., 1987. A-type granites: geochemical characteristics, discrimination and petrogenesis. Contrib. to Mineral. and Petrol. v.95, P. 407–419.
6. Eby, G. N., 1992. Chemical subdivision of the A-type granitoids: petrogenetic and tectonic implications. Geology, 20(7), 641-644.
7. Pearce J. A., Harris N. W. & Tindle A. G., 1984. Trace element discrimination diagrams for the tectonic interpretation of granitic rocks. J. of Petrology. v. 25, p. 956–983.
8. Mirnejad, H., Simonetti, A., & Molasalehi, F., 2011. Pb isotopic compositions of some Zn–Pb deposits and occurrences from Urumieh–Dokhtar and Sanandaj–Sirjan zones in Iran. Ore Geology Reviews, 39(4), 181-187.

Y-REE-DOMINANT ZIRCONOLITE-GROUP MINERAL FROM DMITROVKA METASOMATITES, AZOV SEA REGION, UKRAINIAN SHIELD

Sharygin V.V.

V.S. Sobolev Institute of Geology and Mineralogy SB RAS, Novosibirsk, Russia
sharygin@igm.nsc.ru

One of samples of aegirine-quartz-feldspar metasomatite with astrophyllite from the Dmitrovka quarry, Azov Sea region, contains abundant accessory mineralization represented by Y-, REE- and Zr-bearing oxides and silicates (Y-analogue of zirconolite, Y-Yb-Zr-silicate, baddeleyite, Y-titanates and niobates, "seidozerite", Y-rinkite, zircon, Fig. 1).

Unlike zircon, these minerals form fine intergrowths with one another, rarely individual grains (10-15 μm), what sometimes creates a problem in their clear identification. In this sample Y-analogue of zirconolite with composition $(Y,HREE,Ca,Na)Zr(Ti,Nb)_{1.5}(Fe^{2+},Mn)_{0.5}O_7$ was previously documented (wt.%, EDS): TiO_2 – 24-26; ZrO_2 – 26-28; Nb_2O_5 – 4.5-6.5; FeO – 2-3; MnO – 4.0-5.7; ZnO – up to 1; CaO – 1.0-1.5; Y_2O_3 – 15-19; $HREE_2O_3$ – 6-7; Na_2O – up to 0.5 [1]. However, further studies on scanning microscope and microprobe have shown that Na_2O contents are minimal and two types of zirconolite in chemistry occur in the rock: essentially enriched only in HREE and simultaneously enriched in both HREE and LREE (Table 1). There are no any essential differences between two zicronolite types in optical and morphological characteristics: they form elongated crystals (up to 50 μm, Fig. 1); have light or dark brown color; occur as inclusions in microcline and albite or on the boundary between them, rarely on the boundary between grains in aegirine segregations.

In chemical composition the first type of zirconolite has averaged formula $(Y_{0.7}HREE_{0.2}Ca_{0.1})Zr_{1.0}(Ti_{1.3}Nb_{0.2})(Mn_{0.3}Fe^{2+}_{0.2})O_7$, the second type - $(Y_{0.5}HREE_{0.4}LREE_{0.2})Zr_{0.8}(Ti_{1.3}Nb_{0.3})(Mn_{0.3}Fe^{2+}_{0.2})O_7$. In general, chemical and optical zonations are very weak, but elemental maps for some grains indicated the finest (up to 1 μm) individual zones enriched in Ca and in compliance with decreasing in Y and REE. Raman spectroscopy of zirconolite grains did not show any peaks for vibrations of H_2O and (OH)-groups in the 3000-3800 cm^{-1} region.

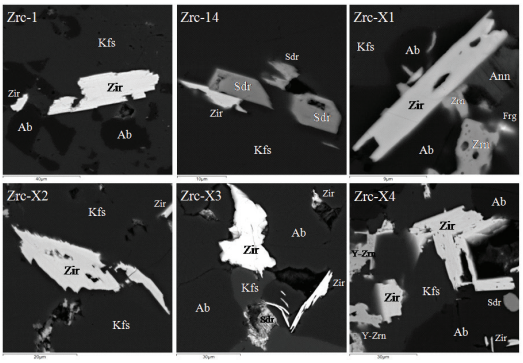

Figure 1: Y-REE-zirconolite in alkaline metasomatites at Dmitrovka, sample DM-11-5-1 (BSE images).

Symbols: Ab – albite; Kfs – microcline; Zir – zirconolite-(Y); Sdr – «seidozerite»; Ann – annite; Zrn – zircon; Frg – fergusonite-(Y); Y-Zrn – Y-Yb-Zr-silicate. Zrc-1 – Zrc-X1 – Y-zirconolite enriched in HREE; Zrc-X2 – Zrc-X4 – zirconolite enriched in both HREE and LREE.

Table 1: Chemical composition (WDS+EDS,wt.%) for Y-REE-zirconolite at Dmitrovka.

Sample	Zrc-1	Zrc-14	Zrc-X1	Zrc-X2	Zrc-X3
n	*13*	*2*	*5*	*16*	*11*
TiO_2	26.04	22.92	25.63	24.08	24.39
ZrO_2	28.89	25.60	27.98	23.78	19.24
HfO_2	0.20	0.41	0.38	0.93	0.87
SnO_2		1.04		0.47	0.34
Nb_2O_5	5.77	5.09	3.54	5.19	7.98
Ta_2O_5	0.19	0.00		0.13	0.10
FeO	2.81	3.79	3.75	4.79	3.11
MnO	5.63	4.45	4.51	3.70	4.70
ZnO	1.00	1.17	1.11	0.91	0.90
CaO	1.24	0.12	0.48	0.59	0.57
Y_2O_3	19.36	19.42	17.93	13.83	12.74
La_2O_3	0.00	0.00		0.16	0.27
Ce_2O_3	0.30	0.12	0.40	1.51	1.96
Pr_2O_3				0.43	
Nd_2O_3	0.02	0.10	0.04	2.13	2.64
Sm_2O_3				1.04	1.60
Gd_2O_3	0.50		0.62	1.86	2.67
Tb_2O_3				0.83	0.82
Dy_2O_3	2.63	2.22	3.08	4.98	6.07
Ho_2O_3	0.69	0.65	0.94	1.18	1.22
Er_2O_3	2.30	3.79	3.61	3.46	3.26
Tm_2O_3	0.66	0.99	0.95	0.74	0.70
Yb_2O_3	2.70	7.21	4.02	3.40	2.41
Lu_2O_3			0.00	0.59	0.61
Sum	100.93	99.08	98.96	100.69	99.12
Formula based on 4 cations					
Ti+Sn	1.33	1.27	1.36	1.32	1.36
Zr+Hf	0.96	0.91	0.97	0.85	0.71
Nb+Ta	0.18	0.17	0.11	0.17	0.27
Fe	0.16	0.23	0.22	0.29	0.19
Mn	0.32	0.27	0.27	0.22	0.29
Zn	0.05	0.06	0.06	0.05	0.05
Sum B	3.00	2.91	2.99	2.90	2.87
Ca	0.09	0.01	0.04	0.05	0.04
Y	0.70	0.74	0.67	0.53	0.50
LREE	0.01	0.01	0.01	0.14	0.17
HREE	0.20	0.33	0.29	0.39	0.42
Sum A	1.00	1.09	1.01	1.10	1.13

ThO_2, UO_2, SrO, Na_2O and F are below detection limits (<<0.01 wt.%).

Thus, zirconolites from the Dmitrovka apogranitic metasomatites represent the compositions maximally enriched in Y and HREE (Table 1). Such compositions are firstly found around the world and this allows saying about possibility to determine a new mineral species within the zirconolite group –"yttrozirconolite". Previously Y-LREE-rich zirconolites were described in the Khibiny massif metasomatites [2-3], but the Dmitrovka zirconolites are richer in Y and HREE. Zirconolite from granite pegmatites at Skalna Brama, Poland [4] seems to be very close in chemistry to the Dmitrovka mineral. It is also extremely rich in Y (0.60 apfu) and REE (0.32 apfu, HREE>LREE). It should be noted that the Dmitrovka zirconolite is also appreciably rich in Mn (up to 0.3 apfu) and has some similarity in its content with laachite $(Ca,Mn)_2Zr_2Nb_2TiFeO_{14}$, another member of the zirconolite group [5].

This work was supported by the project between NAS of Ukraine and SB RAS "Alkaline metasomatites of the Azov Sea and Baikal regions and their ore potential".

References

Sharygin V.V., Krivdyk S.G. New minerals in alkaline metasomatites at Dmitrovka, Azov Sea region, Ukraine // 8th Conference dedicated to E.Lazarenko, 2014, Lviv (in Russian).

Korchak Yu.A. Mineralogy of the Lovozero suite rocks and products of their contact-metasomatic alteration in alkaline massifs // PhD dissertation, Apatity, 2008, 328 p. (in Russian).

Yakovleva O.S., Pekov I.V. Zirconolite family minerals in the alumina-rich fenites of the Khibiny alkaline complex (Kola Peninsula, Russia) // Acta Mineralogica-Petrographica Abstract Series, 2010, v. 6, p. 438-438 (Abstracts of IMA 2010).

Szeleg E., Škoda R., Y, REE-rich zirconolite from the Skalna Brama pegmatite near Szklarska Poręba (Karkonosze Massif, Lower Silesia, Poland) // Mineralogia Polonica - Special Papers, Kraków: Wydawnictwo Naukowe "Akapit", 2008, v. 32, p. 159-159.

Chukanov N.V., Krivovichev S.V., Pakhomova A.S., Pekov I.V., Schäfer C., Vigasina M.F., Van K.V. Laachite, $(Ca,Mn)_2Zr_2Nb_2TiFeO_{14}$, a new zirconolite-related mineral from the Eifel volcanic region, Germany // European Journal of Mineralogy, 2014, v. 26, p. 103-111.

CR-RICH "TIOOXYSPINEL" MINERAL FROM KOSVA DUNITE MASSIF, MIDDLE URALS: POSSIBLE LINK BETWEEN SPINEL- AND TIOSPINEL-GROUP MINERALS

Sharygin V.V.[1], Ivanov O.K.[2]

1 V.S. Sobolev Institute of Geology and Mineralogy SB RAS, Novosibirsk, Russia
sharygin@igm.nsc.ru
2 Ural Institute of Mineral Raw Material, Ekaterinburg, Russia

The active interaction of sulfate rocks and related sulfur-bearing fluids with dunites is very common phenomenon for the Kosva pyroxenite-dunite massif [1-4]. The appearance of Cr-tiospinels (kalininite, daubréelite and their Mn-analogue [1-4]), sulfate-bearing minerals after olivine (previously labeled as "sulfate-olivine" [2]) and exotic pseudomorphs after chromite (Cr-tiospinels + eskolaite + Cr-rich silicates + Cr-rich pyrite + pyrrhotite [4]) is a result of this process. Here we present new mineralogical data for such associations in the Kosva massif, in particular for exotic Cr-rich tiooxyspinel. This phase was found in one sample (M-920) from the contact of dunite with gypsum rock.

The studied specimen is the contact between vein (dike) of gypsum rock (former anhydritite) and serpentinized sulfide-rich dunite with intermediate zone (1-2 cm) of magnesiohastingsite ± phlogopite. The mineralogy of this sample, especially for sulfate and amphibole part, was previously studied [1-2]. The black dunite part contains relics of olivine, its pseudomorphs (sulfate-bearing hydrated Mg-silicate and, possibly, phase $Mg_5(SiO_4)_2(SO_4)$ – Mg-analogue of ternesite), serpentine, chlorite, magnesiohastingsite, Cr-diopside, phlogopite (partially altered by hydromica), sulfides (pyrrhotite, pyrite, Co-rich pentlandite), chromite and Cr-rich "tiooxyspinel".

Cr-rich "tiooxyspinel" mainly forms euhedral crystals, which are commonly mantled by sulfide aggregate (pyrrhotite, Fig. 1). It is seems to be a pseudomorph after chromite. Remarkably, fresh chromite (without sulfide mantle) and "tioxyspinel" may be closely associated in altered rock matrix. Namely, the presence of tiospinels in the Kosva rocks and chemical composition (high content of sulfidic S) of the studied mineral gave us the severe grounds and reasons to consider this phase as an intermediate between the Cr-rich spinel-group and tiospinel-group minerals. BSE images under high magnification indicate that this mineral is homogeneous on submicron level and does not show any solid decay or mixture of some phases. Excepting S, in chemical composition "tiooxyspinel" (especially central part) resembles chromite in the Cr_2O_3, TiO_2 and FeO_t contents, but drastically differs in higher MnO and MgO and in lower Al_2O_3 (Table 1). In general, most "tiooxyspinel" grains show the strong core-to-rim variations: the increase of S and Fe_2O_3 and decrease of Cr_2O_3, FeO and TiO_2. The highest values of Fe_2O_3 and S are most common for thin (10-15 μm) outmost zone near the contact with sulfide mantle (Fig. 1, Table 1); and this is clearly visible on the EDS profiles and elemental maps. Such evolution from the core to rim may be conventionally expressed as a trend from S-containing chromite via "tiooxymagnesioferrite" to Mg-rich greigite (Fig. 2): from $(Mg_{0.5}Fe^{2+}_{0.5})(Fe^{3+}_{1.0}Cr_{1.0})O_{3.5}S_{0.5}$ to $(Mg_{0.5}Fe^{2+}_{0.5})(Fe^{3+}_{1.5}Cr_{0.5})O_2S_2$. In addition, tiooxyspinel contains appreciable CaO and sometimes SiO_2.

Thus, the appearance of "tiooxyspinel" in the Kosva rocks is seems to be a result of impact of hot fluids, containing S^{2-} ions, on chromite. It was one of stages of fluid influence on the Kosva dunitic rocks [4]. At first sight, the finding of "tiooxyspinel", intermediate between the spinel-group and tiospinel-group minerals (between oxides and sulfides in global scale) is very enigmatic and unrealistic for natural environments due to its possible instability. Oxysulfides are very exotic rare phases in natural conditions. For example, layered phases with composition FeS•CaO are sometimes fixed as accessories in combustion metamorphic rocks of the Hatrurim Formation, Israel. However, oxysulfides of different composition are very known phases in ferrous metallurgy [5]. In addition, oxysulfides with the spinel crystal structure (for example, FeS•Fe_2O_3, VS•Fe_2O_3) are successfully synthesized [6-7]; they are stable compounds and with good ferromagnetic properties. Unfortunately, examples for Cr_2O_3-bearing spinel-related oxysulfides are not found yet in literature.

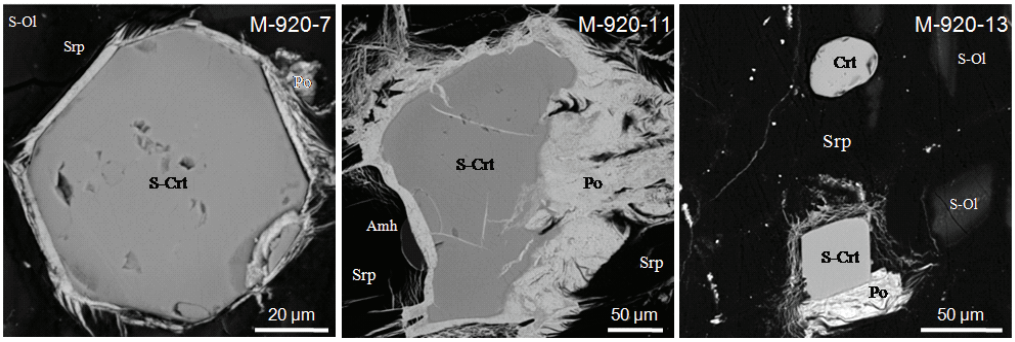

Figure 1: Grains of Cr-rich spinel-tiospinel mineral in altered dunite, sample M-920, Kosva massif (BSE images).

S-Crt – sulfide-containing chromite ("tiooxyspinel"); Crt – chromite; Po – pyrrhotite; Srp – serpentine; S-Ol – sulfate-OH-bearing Mg-silicate ("sulfate-olivine"); Amh – magnesiohastingsite.

Table1: Chemical composition (wt.%, EDS method) of Cr-rich "tiooxyspinel" and chromite from altered dunite, sample M-920, Kosva massif.

	M-920-6 core	M-920-7 core	M-920-9 core	M-920-9 rim	M-920-10 core	M-920-10 rim	M-920-11 core	M-920-11 rim	M-920-13 core	M-920-13 core
SiO_2	0.00	0.32	0.00	0.26	0.28	0.32	0.49	0.28	0.19	0.26
TiO_2	0.82	1.53	1.15	0.22	1.88	0.25	0.83	0.00	0.48	0.82
Cr_2O_3	37.24	35.31	29.71	11.56	26.16	11.41	30.71	10.16	31.54	29.92
V_2O_3	0.00	0.26	0.00	0.00	0.21	0.31	0.15	0.00	0.00	0.00
Al_2O_3	0.26	3.53	0.36	0.00	1.02	0.19	0.25	0.00	0.00	8.98
Fe_2O_3	28.60	24.08	32.36	46.15	31.46	44.12	31.66	47.71	33.55	27.78
FeO	12.71	21.44	12.74	4.94	10.54	7.62	13.69	7.90	8.04	26.62
MnO	3.71	2.08	3.28	4.82	5.50	5.18	4.13	3.99	4.89	0.72
MgO	8.08	4.71	7.79	9.20	7.30	7.30	7.16	7.91	9.90	4.33
CaO	0.59	1.05	0.76	0.80	1.40	0.67	0.53	0.70	0.53	0.00
ZnO	0.57	0.41	0.00	0.00	0.54	0.00	0.41	0.00	0.00	0.00
S	7.46	4.73	11.26	21.85	11.78	21.43	8.92	22.60	10.58	0.00
Sum	100.04	99.45	99.41	99.80	98.07	98.80	98.92	101.25	99.70	99.42

Formula based on 3 cations and 4(O,S)

Si	0.00	0.01	0.00	0.01	0.01	0.01	0.02	0.01	0.01	0.01
Ti+V	0.02	0.05	0.03	0.01	0.07	0.02	0.02	0.00	0.01	0.02
Cr	1.12	1.05	0.94	0.41	0.84	0.41	0.96	0.36	0.97	0.83
Al	0.01	0.16	0.02	0.00	0.05	0.01	0.01	0.00	0.00	0.37
Fe^{3+}	0.82	0.68	0.97	1.55	0.96	1.52	0.94	1.61	0.98	0.73
Fe^{2+}	0.40	0.67	0.43	0.18	0.36	0.29	0.45	0.30	0.26	0.78
Mn	0.12	0.07	0.11	0.18	0.19	0.20	0.14	0.15	0.16	0.02
Mg	0.46	0.26	0.46	0.61	0.44	0.50	0.42	0.53	0.58	0.23
Ca	0.02	0.04	0.03	0.04	0.06	0.03	0.02	0.03	0.02	0.00
Zn	0.02	0.01	0.00	0.00	0.02	0.00	0.01	0.00	0.00	0.00
S	0.53	0.33	0.84	1.83	0.90	1.84	0.66	1.90	0.77	0.00

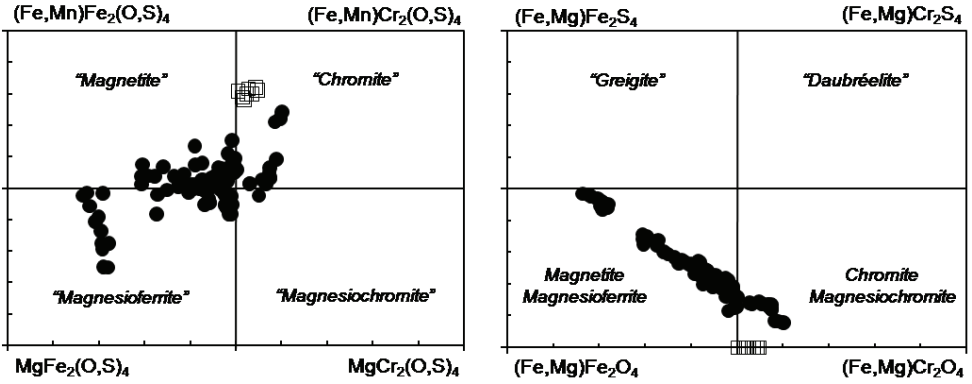

Figure 2: Chemical variations of Cr-rich "tiooxyspinel" and chromite for sample M-920, Kosva massif. Circles – "tiooxyspinel"; squares – chromite.

References

1. Ivanov O.K., Silaev V.I., Filippov V.N. Anhydritites of Kosva massif, Platinumferrous belt of Urals // Ural Geological Journal, 2010, no. 6, p. 3-25 (in Russian).
2. Ivanov O.K., Silaev V.I., Filippov V.N. Sulfate-forsterite from sulfidized dunites of Kosva massif, Urals // Ural Geological Journal, 2011, no. 2, p. 17-32 (in Russian).
3. Ivanov O.K., Filippov V.N. Kalininite ($ZnCr_2S_4$) and eskolaite from contact of carbonatites, Kosvinsky Kamen, Urals // Ural Geological Journal, 2012, no. 3, p. 43-48 (in Russian).
4. Silaev V.I., Ivanov O.K., Filippov V.N. Sulfidization of chromitites at contact of carbonatites with plagioclasites in Kosva dunite massif, Middle Urals // Ural Geological Journal, 2013, no. 5 (95), p. 37-56 (in Russian).
5. Dub A.V., Tsukihashi F., Sano N. Solubilities of Al_2O_3, SiO_2 and Cr_2O_3 in the FeS-containing systems // ISIJ International, 1991, v. 31, no. 12, p. 1438-1440.
6. Loseva G.V., Mukoed G.M., Ovchinnikov S.G, Ryabinkina L.I. Electric and magnetic properties of $MeS•Fe_2O_3$ oxysulfides // Fizika Tverdogo Tela, 1992, v. 34, iss. 6, p. 1765-1769.
7. Loseva G.V., Ovchinnikov S.G., Chernov V.K., Ivanova N.B., Kiselev N.I., Bovina A.V. Correlation between the magnetic and electrical properties of the $(VS)_{(x)}(Fe_2O_3)_{(2-x)}$ oxysulfide system // Physics of the Solid State, 2000, v. 42, iss. 4, p. 730-733.

CHLORINE-BEARING ANNITE FROM KHLEBODAROVKA ENDERBITES, AZOV SEA REGION, UKRAINIAN SHIELD

Sharygin V.V.[1], Kryvdik S.G.[2], Karmanov S.G.[1], Nigmatulina E.N.[1]

1 V.S. Sobolev Institute of Geology and Mineralogy SB RAS, Novosibirsk, Russia, sharygin@igm.nsc.ru
2 N.P. Semenenko Institute of Geochemistry, Mineralogy and Ore Formation NAS of Ukraine, Kyiv, Ukraine

The mica family minerals are the main concentrators of water, F and Cl in crustal acidic rocks. The contents of halogens in micas possibly indicate important information about fluid composition for metamorphic and metasomatic processes, formation of ancient crustal rocks and genesis of ore deposits. The proximity of ion radii for F and OH (1.31 and 1.38 Å) does not create any limitations for the incorporation of F instead of (OH)-group in the mica structure (phlogopite – fluorophlogopite series, etc.). Chlorine has larger ion radius (1.81 Å), what does essentially downrange for the isomorphism (OH) ↔ Cl.

Cl-containing (>0.8 wt.% Cl) annites-biotites rarely occur in nature and are most common of granitoid rocks – granites and their pegmatites, granulites, gneisses and charnokites [1-8] as well as skarns [9]. Ideal "chlorannite" ($KFe_3AlSi_3O_{10}Cl_2$, 12.92 wt.% Cl) and other hypothetical Cl-dominant water-free micas are not yet synthesized and hardly stable in natural conditions. We found Cl-bearing annite (up to 7.3 wt.% Cl) in a large (>15 cm) isolations of gray-blue quartz from enderbite of the Khlebodarovka open pit, Eastern Azov Sea region (Fig. 1). It should be noted that some enderbites of the Khlebodarovka massif may contains primary dark brown mica [10], but its composition is related to Fe-phlogopite – Mg-annite (Mg# - 36-61) with low content of Cl (<0.2 wt.%). Among all studied enderbites, we observed Cl-bearing annite (3.1-5.1wt.%) together with Cl-bearing amphibole (3.4-4.3 wt.%) in one sample only. This association seems to be related to early stage of metasomatism of enderbites and confined to thin veins (fissures) in the rock.

Dark brown annite in the Khlebodarovka quartz forms both individual crystal inclusions and intergrowths with other minerals (Fig. 1), which are related to different stage of formation: from primary enderbitic paragenesises to products of metasomatism and further low-temperature alterations. Most these associations are commonly confined to healed fissures in quartz. The relationships of annite with other phases indicate that mica is hardly primary mineral of enderbite and seems to be a phase of the early metasomatic stage (assemblage hypersthene + Cl-rich annite was not found).

Quartz-hosted annites from Khlebodarovka were studied in detail by scanning microscopy and microprobe technique (Table 1, Fig. 1) as well as Raman spectroscopy. Grains of mica are zoned (Fig. 1) and has variable content of Cl (from 0.0 to 7.3 wt.%). The central zones are richer in Cl and BaO and poorer in FeO than outher zones (Table 1). In general, the positive correlations Fe-Cl and Ba-Cl (Fig. 2) seem to suggest a complex isomorphism scheme $K^{1+} + (OH,F)^{1-} + Mg^{2+} + Si^{4+} \leftrightarrow Ba^{2+} + Cl^{1-} + Fe^{2+} + Al^{3+}$. The Khlebodarovka annites with low Cl (<0.3 wt.%) are associated with minnesotaite and chlorite evidencing about chlorine removal from mica during secondary alteration processes.

Thus, annites with highest contents of Cl (6.5-7.3 wt.%) were firstly found around the world. Such compositions nominally belong to "chlorannite" $KFe_3AlSi_3O_{10}(Cl,OH)_2$ using the 50% rule (Cl>OH, Fig, 2). Previously the high concentrations of Cl in micas of the phlogopite-annite series have been documented in meta-exhalites from Nora, Sweden (Cl - 5.5 wt.%) [4], and in granulites from Black Rock Forest, USA (Cl - 4.6 wt.%) [7].

This work was supported by the project between NAS of Ukraine and SB RAS "Alkaline metasomatites of the Azov Sea and Baikal regions and their ore potential".

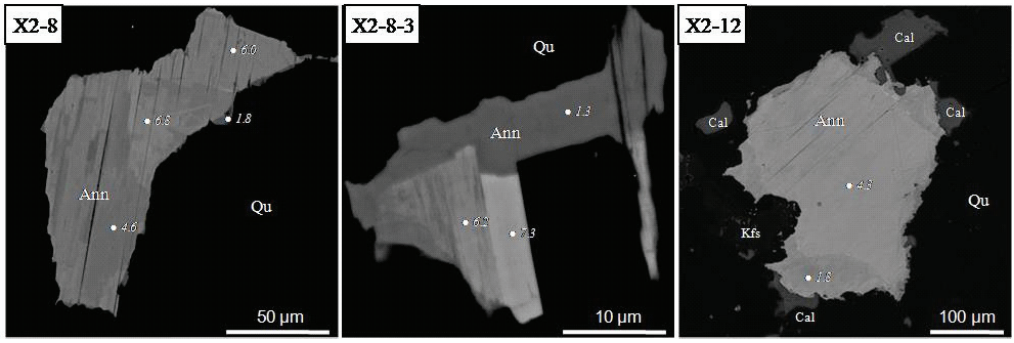

Figure 1: Annite with variable Cl from individual associations in quartz of enderbite, Khlebodarovka (BSE images). Contents of Cl are shown by italic. Symbols: Qu – quartz; Ann – annite; Cal – calcite; Kfs – K-feldspar.

Table 1: Chemical composition (wt.%, WDS method) of Cl-containing annites from individual associations in quartz from enderbite, Khlebodarovka, Azov Sea region.

Association	X2-8			X2-8-3		
	core	middle	rim	core	middle	rim
SiO_2	30.49	32.69	36.22	31.29	33.07	36.13
TiO_2	0.56	0.19	0.46	0.26	0.19	0.58
Al_2O_3	12.00	11.21	10.22	12.04	10.36	9.40
Fe_2O_3	0.00	0.00	0.00	0.00	0.12	1.04
FeO	37.83	37.70	35.52	37.35	38.21	34.84
MnO	0.23	0.20	0.14	0.17	0.21	0.21
ZnO	0.04	0.00	0.10	0.07	0.06	0.10
MgO	1.07	1.22	3.39	0.96	1.25	4.06
BaO	3.62	2.41	0.64	3.72	1.05	0.20
Na_2O	0.00	0.09	0.07	0.10	0.20	0.06
K_2O	7.55	8.02	9.10	7.43	8.27	9.14
Rb_2O	0.00	0.00	0.00	0.00	0.09	0.13

F	0.32	0.39	0.33	0.33	0.41	0.38
Cl	6.85	5.95	1.75	7.32	6.21	1.34
H_2O	1.45	1.71	3.00	1.35	1.62	2.96
Sum	102.01	101.78	100.94	102.38	101.31	100.57
$O=(Cl,F)_2$	1.68	1.51	0.53	1.79	1.58	0.46
Sum	100.33	100.27	100.41	100.59	99.73	100.11
End-members						
Phlogopite	4.71	5.34	14.25	4.25	5.45	16.87
Annite	40.85	46.78	70.26	37.44	44.89	69.67
Fluorannite	4.26	5.05	3.66	4.34	5.40	4.24
Chlorannite	48.92	41.25	10.40	51.62	43.84	8.01

Microprobe analysis. Calculated data (for formula based on 11 oxygens): FeO and Fe_2O_3 – by concentration of tetrahedral Fe^{3+}; H_2O – by charge balance, (OH)=2-Cl-F-O. Positions of spots see Fig. 1.

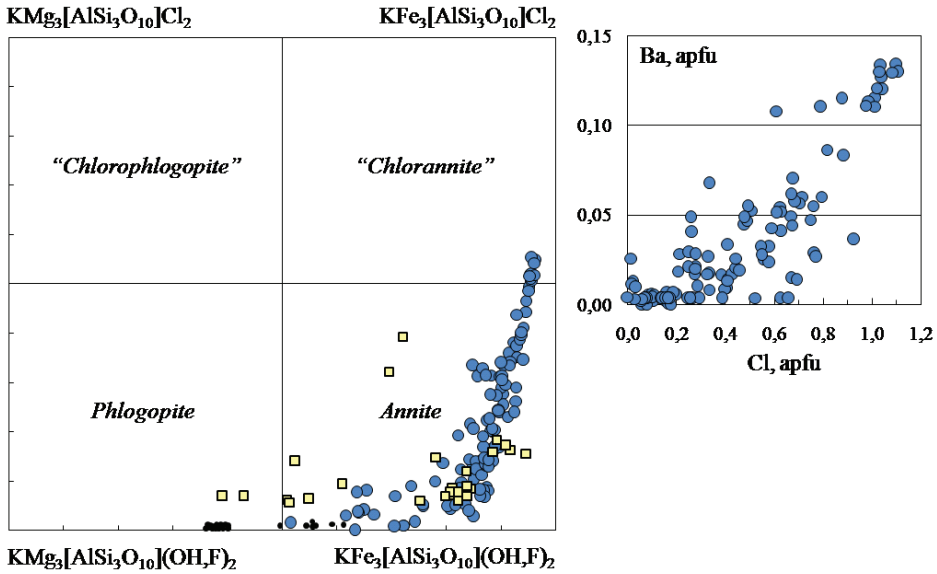

Figure 2: Compositional variations for mica from Khlebodarovka (circles – inclusions in quartz, spots – primary mica in enderbites) in comparison with Cl-containing (>0.8 wt.%) biotites worldwide (squares) [1-8].

References

1. Lee D.E. A chlorine-rich biotite from Lemhi county, Idaho // American Mineralogist. 1958. V. 43. P. 107-111.
2. Bohlen S.R., Peacor D.R., Essene E.J. Crystal-chemistry of a metamorphic biotite and its significance in water barometry // American Mineralogist. 1980. V. 65. P. 55-62.
3. Kamineni D.C., Bonardi M., Rao A.T. Halogen-bearing minerals from Airport Hill, Visakhapatnam, India // American Mineralogist. 1982. V. 67. P. 1001-1004.
4. Oen I.S., Lustenhouwer W.J. Cl-rich biotite, Cl-K hornblende, and Cl-rich scapolite in meta-exhalites: Nora, Bergslagen, Sweden // Economic Geology. 1992. V. 87. V. 1638-1648.
5. Zhu C., Xu H.-F., Ilton E.S. et al. TEM-AEM observations of Cl-rich amphibole and biotite and possible petrologic implications // American Mineralogist. 1994. V. 79. P. 909-920.
6. Jiang S.-Y., Palmer M.R., Li Y.-H. et al. Ba-rich micas from the Yindongzi-Daxigou Pb-Zn-Ag and Fe deposits, Qinling, northwestern China // Mineralogical Magazine. 1996. V. 60. P. 433-445.
7. Leger A., Rebbert C., Webster J. Cl-rich biotite and amphibole from Black Rock Forest, Cornwall, New York // American Mineralogist. 1996. V. 81. P. 495-504.
8. Cesare B., Satish-Kumar M., Cruciani G. et al. Mineral chemistry of Ti-rich biotite from pegmatite and metapelitic granulites of the Kerala Khondalite Belt (southeast India): Petrology and further insight into titanium substitutions // American Mineralogist. 2008. V. 93. P. 327–338.
9. Tracy R.J. Ba-rich micas from the Franklin Marble, Lime Crest and Sterling Hill, New Jersey // American Mineralogist. 1991. V. 76. P. 1683-1693.
10. Kryvdik S.G., Kravchenko G.L., Tomurko L.L. et al. Petrology and geochemistry of charnokitoids of the Ukrainian Shield. – Kyiv: Naukova Dumka, 2011. 216 p.

MINERALOGY OF CRYOLITE ROCKS FROM KATUGIN MASSIF, TRANSBAIKALIA, RUSSIA

Sharygin V.V.[1], Vladykin N.V.[2]

1 V.S. Sobolev Institute of Geology and Mineralogy SB RAS, Novosibirsk, Russia
sharygin@igm.nsc.ru
2 A.P. Vinogradov Institute of Geochemistry SB RAS, Irkutsk, Russia

New mineralogical data were obtained for cryolite-bearing rocks from the Katugin alkaline granite massif, Transbaikalia. These rocks are located in the exocontact part of the massif and some researchers considered them as metasomatic formations [1]. The rocks with high content of cryolite (30-70 vol.%) have been studied in detail (Table 1).

Table 1: Minerals identified in cryolitic rocks of the Katugin massif, Transbaikalia.

Minerals	Formula	K-431-22	K-243	K-243a	K-244
Quartz	SiO_2	+	+	+	+
K-feldspar	$KAlSi_3O_8$	+	+	+	+
Zircon	$ZrSiO_4$	+			+
Thorite	$ThSiO_4$			+	
Fluorannite	$KFe_3AlSi_3O_{10}(F,OH)_2$	+	+	+	+
Lepidolite-Polylithionite	$KLi_{1.5}Al_{1.5}Si_4O_{10}(F,OH)_2 – KLi_2AlSi_4O_{10}(F,OH)_2$	+	+	+	+
Fluoro-arfvedsonite	$(Na,K)Na_2Fe^{2+}_4Fe^{3+}Si_8O_{22}(F,OH)_2$	+	+	+	+
Bafertisite	$Ba_2(Ti,Sn)_2(Fe,Mn)_4(Si_2O_7)_2O_2(OH)_2(F,OH)_2$		+	+	
Pyrochore-group minerals	$(Ca,Na,REE,Y,Pb)_2Nb_2O_6(OH,F)$	+			
Columbite-(Fe)	$(Fe,Mn)Nb_2O_6$	+	+	+	
Ferberite	$(Fe,Mn)WO_4$	+		+	
Ilmenite	$(Fe,Mn)TiO_3$	+	+	+	+
Magnetite	$FeFe_2O_4$		+	+	
Rutile	TiO_2	+	+		
Cassiterite	SnO_2			+	
Cerianite-(Ce)	$(Ce,Th)O_2$		+		
Goethite	$(Fe,Mn)O(OH)$		+	+	
Siderite	$(Fe,Mn)CO_3$		+		
Rhodochrosite	$(Mn,Fe)CO_3$		+	+	
Calcite	$CaCO_3$			+	
Baryte	$(Ba,Sr)SO_4$		+		
Sphalerite	ZnS		+	+	+
Pyrite	FeS_2		+		+
Chalcopyrite	$CuFeS_2$		+		+
Fluorite	$(Ca,Y)F_2$	+	+		
Cryolite	Na_3AlF_6	+	+	+	+
Elpasolite	K_2NaAlF_6	+		+	
Simmonsite	Na_2LiAlF_6	+		+	
Tveitite–(Y)	$Ca_{1-x}Y_xF_{2+x}$, x≈0.3	+		+	+
«Ba-Sr-Tveitite-(Y)»	$(Ba,Sr,Ca)_{1-x}Y_xF_{2+x}$, x≈0.3	+			+
Gagarinite-(Y)	$NaCaYF_6$				+
Fluocerite-(Ce)	$(Ce,La,Nd)F_3$				+

Mafic and opaque minerals in these rocks are represented by Fe-silicates (Na-amphibole, mica, bafertisite), oxides (magnetite, ilmenite, pyrochlore, cassiterite, etc.) and sulfides (sphalerite, pyrite, chalcopyrite). Quartz, K-feldspar, Li-mica and REE-rich fluorides also occurs in the rocks. In general, femic silicates are maximally rich in FeO_t (MgO -< 1 wt.%) and in F; compositional variations are not essential. Microprobe data for Na-amphibole has shown that it is fluoro-arfvedsonite, $(Na,K)Na_2Fe^{2+}{}_4Fe^{3+}Si_8O_{22}(F,OH)_2$, a mineral with the hypothetical IMA status (F - >1 apfu, K - <0.5 apfu). Black mica belongs to fluorian annite – fluorannite. Li-mica (lepidolite-polylithionite) is a common minor mineral in the studied rocks and is mainly localized on the contact between silicates and/or quartz with cryolite. Li-mica is zoned and FeO_t is increased up to 7.5 wt.% from the core to rim; estimated contents of Li_2O are 3.6-5.9 wt.%, and water - <0.7 wt.%. Rare layered titanosilicate, bafertisite $Ba_2Ti_2(Fe,Mn)_4(Si_2O_7)_2O_2(OH)_2(F,OH)_2$, was identified in two rock specimens. This phase is common mineral for apogranitic metasomatites and late alkali granite rocks. The Katugin bafertisite has low hejtmanite content and is rich in SnO_2 (up to 2.7 wt.%).

REE-mineral assemblage is chaotically localized in studied cryolite rocks and mainly represented by fluorides: fluorite + yttrofluorite + tveitite (homogeneous or with solid decay structures) + "Ba-Sr-tveitite" + REE-pyrochlore or gagarinite + tveitite + fluocerite + "Ba-tveitite". It should be noted that Ba-Sr-rich "tveitites" were not mentioned yet in literature and thus are potential new mineral species. "Ba-Sr-tveitite" forms fine intergrowth or solid decay structures of Ba- and Sr-rich individual phases around tveitite, whereas "Ba-tveitite" (Ba>>Sr>Ca) is homogeneous and coexists with fluocerite on the contact between gagarinite and tveitite. Some grains of tveitite are also heterogeneous and now represent oriented solid decay structure (cubic and tetrahedral modifications), which are seem to be originated due to temperature decreasing. In general, chemical difference between two modifications is not essential and expressed in slightly high contents of REE and lower Ca in lamellae at similar values of Y and Na in both phases.

Individual crystallites and their intergrowths in cryolite and fluoro-arfvedsonite are more interesting in mineralogy. Crystal inclusions in fluoro-arfvedsonite occur rarer than in cryolite and are represented by cryolite, Na-Y-Yb-rich fluorite, Li-mica, columbite, REE-pyrochlore, thorite, siderite, rhodochrosite, ilmenite and fluorannite. Cryolite-hosted inclusions do more diverse in mineral set: ilmenite, columbite, pyrite, ferberite, elpasolite, simmonsite, magnetite, cassiterite, bafertisite, Li-mica, siderite, rhodochrosite, rutile and baryte. Elpasolite K_2NaAlF_6 and simmonsite Na_2LiAlF_6 are close to the ideal compositions and firstly discovered in the Katugin massif rocks. Among all minerals identified in cryolite only rutile has broad compositional variations in FeO_t, Nb_2O_5 и WO_3: most grains do not contain WO_3 and differ only in FeO_t (1.2-5.5 wt.%) and Nb_2O_5 (0.0-1.4 wt.%), whereas the central parts of some grains are fairly enriched in these components (WO_3 - 4.6-5.8; Nb_2O_5 – 1.2-1.5; FeO_t – 3.1-3.6 wt.%; Fig. 1). Rutiles with high WO_3 (>2 wt.%, sometimes with high contents of Sb, Ta, V) were previously documented in some ore deposits [2-4].

The mineralogy and study of crystal inclusions in the Katugin massif cryolitic rocks have shown that their formation occurred in high fluorine environment, enriching in other volatiles (CO_2, S, H_2O) and in trace elements (Li, Nb, Th, W, Sn, REE, Y). High fluorine contents are favorable for crystallization of minerals, which maximally concentrated trace elements: Li – lepidolite-polylithionite, simmonsite; Nb – columbite, pyrochlore-group minerals; Th – thorite; REE-Y – fluorides, pyrochlore-group minerals, cerianite; W – ferberite, W-rich rutile; Sn – cassiterite; Ba – baryte, bafertisite, "Ba- and Ba-Sr-tveitite"; Sr – "Ba-Sr-tveitite".

Unfortunately, fluid inclusion study of the Katugin cryolite rocks did not indicate any visible fluid, gas-liquid or melt inclusions, which allowed consider the genesis of the rocks.

This work was supported by the project IP47p "Fluid regime, mantle sources, chemical characteristics and age of the alkaline complexes from framings of platforms, shields and folded zones in respect to their ore potential".

Reference

1. Arkhangelskaya V.V. Rare-metal alkaline complexes of the southern edge of the Siberian Platform. Moscow: Nauka, 1974, 128 p.
2. Urban A.J., Hoskins B.F., Grey I.E. Characterization of V-SB-W-bearing rutile from the Hemlo gold deposit, Ontario // Canadian Mineralogist, 1992, v. 30, p. 319-326.
3. Rice C.M., Darke K.E., Still J.W. Tungsten-bearing rutile from the Kori Kollo gold mine, Bolivia // Mineralogical Magazine, 1998, v. 62(3), p. 421-429.
4. René M., Škoda R. Nb-Ta-Ti oxides fractionation in rare-metal granites: Krásno-Horní Slavkov ore district, Czech Republic // Mineralogy and Petrology, 2011, v. 103, p. 37–48.

Scanning microscope and petrographical data.

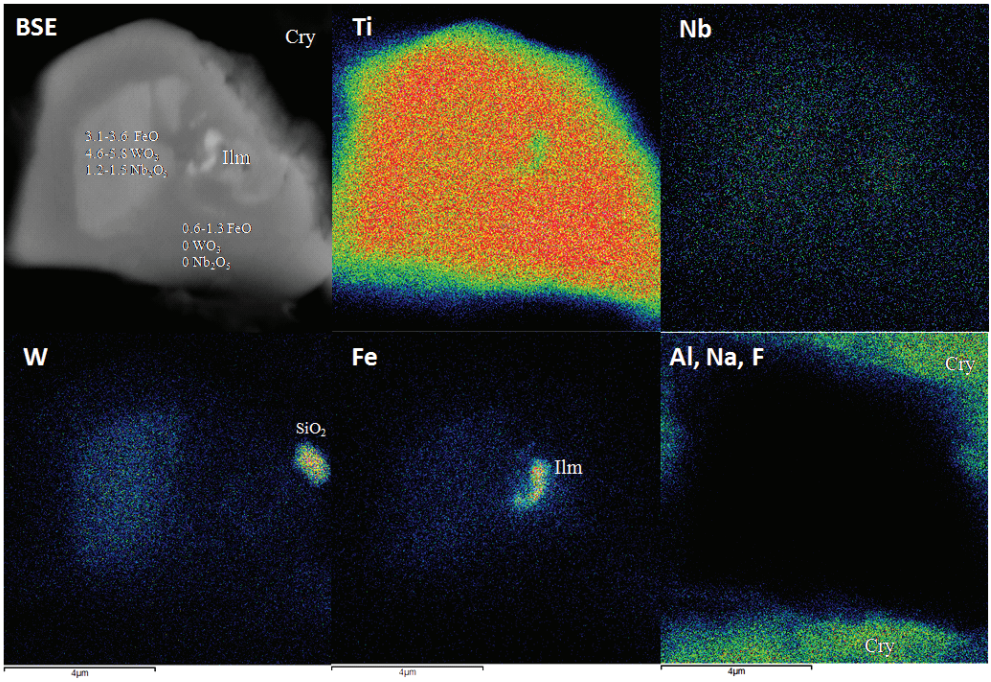

Figure 1: Inclusion of zoned W-Nb-Fe-rutile in cryolite, sample K-243, Katugin massif (BSE image, elemental maps). Cry – cryolite; Ilm - ilmenite.

PHASE RELATIONS IN THE SYSTEMS (K AND NA)2CO3-CACO3-MGCO3 AT 6 GPA AND 900-1400 °C: IMPLICATION FOR INCIPIENT MELTING IN ANHYDROUS CARBONATED MANTLE DOMAINS

Shatskiy A.F.[1,2], Litasov K.D.[1,2] , Ohtani E.[2,3]

1 V.S. Sobolev Institute of Geology and Mineralogy, RAS SB, Novosibirsk 630090, Russia
2 Novosibirsk State University, Novosibirsk 630090, Russia
3 Tohoku University, Sendai 980-8578, Japan
anton.antonshatskiy.shatskiy@gmail.com

Introduction

Alkalis and carbonates play a key role in diamond formation, mantle metasomatism, and deep magma generation. Alkali-carbonates are common components of fluids/melts entrapped by mantle minerals such as diamond and olivine from kimberlite pipes. Numerous peridotitic mantle xenoliths from different localities display the petrographic and geochemical signatures of carbonatite metasomatism. Alkali carbonates would be essential components which control melting in subducting slab and upwelling mantle. Minor amount of alkalis (Na, K) and CO_2 drastically, by ~1000°C, reduces the solidus of lithospheric mantle and subducted rocks (peridotites, eclogites, and pelites). Melting at 3-24 GPa yields alkali-rich Ca-Mg carbonate melts (Grassi and Schmidt, 2011; Litasov et al., 2013). It's shown experimentally that proto-kimberlitic magma, which originates from more than 250 km depth, was essentially alkali-rich carbonatite melt (Sharygin et al., 2013). In this regard, it is essential to know melting phase relations in simple carbonate systems under mantle conditions.

Experimental

In this study we conducted HP-HT experiments at 6 GPa and 900-1450ºC in binary K/Na_2CO_3-Mg/Ca/$FeCO_3$ and pseudo binary K/Na_2CO_3-$CaMgCO_3$ carbonate systems, using large volume multianvil apparatuses Run duration ranged from 2 to 38 hs. Starting materials were loaded in graphite capsules and dried at 300ºC for 2-3 hs. Prior the experiment the cell assemblies were stored at 130ºC in vacuum. Recovered samples were mounted into petro-epoxy and polished in oil using sandpaper and diamond past. Benzine was used to remove oil. Samples were studied using SEM and EDS. EDS was calibrated using experimental samples with known composition and homogeneous texture.

Based on obtained results we plotted binary and ternary phase diagrams for studied systems some of which are shown in Fig. 1.

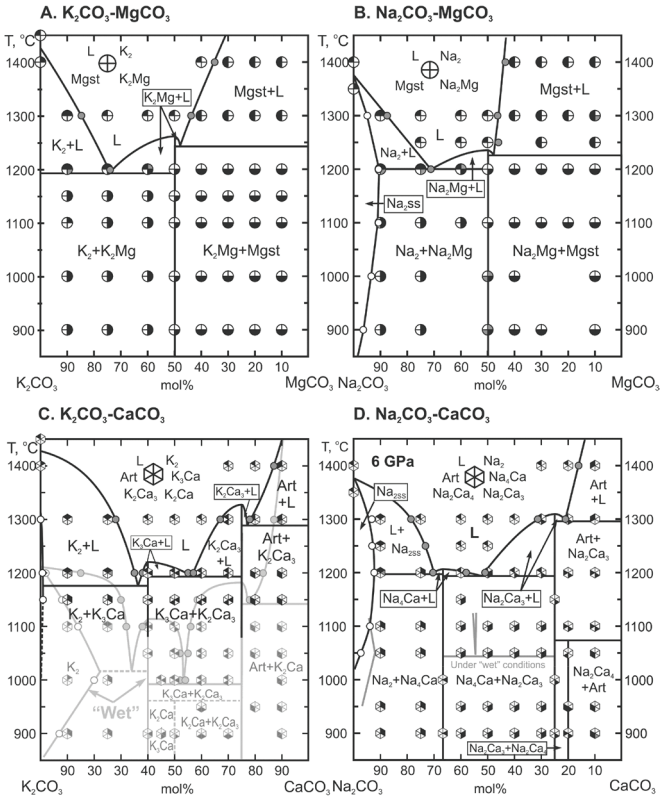

Figure 1: Phase relations at 6 GPa in the binary carbonate systems.

Acknowledgements: This work was supported by the Russian Scientific Fund (proposal No. 14-17-00609) and performed under the project of the Ministry of education and science of Russian Federation (No. 14.B25.31.0032).

References

1. Shatskiy, A., Borzdov, Y.M., Litasov, K.D., Kupriyanov, I.N., Ohtani, E., and Palyanov, Y.N. (2014) Phase relations in the system $FeCO_3$-$CaCO_3$ at 6 GPa and 900-1700 °C and its relation to the system $CaCO_3$-$FeCO_3$-$MgCO_3$. American Mineralogist, 99(4), 773-785.
2. Shatskiy, A., Gavryushkin, P.N., Sharygin, I.S., Litasov, K.D., Kupriyanov, I.N., Higo, Y., Borzdov, Y.M., Funakoshi, K., Palyanov, Y.N., and Ohtani, E. (2013a) Melting and subsolidus phase relations in the system Na_2CO_3-$MgCO_3$+-H_2O at 6 GPa and the stability of $Na_2Mg(CO_3)_2$ in the upper mantle. American Mineralogist, 98(11-12), 2172-2182.
3. Shatskiy, A., Sharygin, I.S., Gavryushkin, P.N., Litasov, K.D., Borzdov, Y.M., Shcherbakova, A.V., Higo, Y., Funakoshi, K., Palyanov, Y.N., and Ohtani, E. (2013b) The system K_2CO_3-$MgCO_3$ at 6 GPa and 900-1450 ºC. American Mineralogist, 98(8-9), 1593-1603.
4. Shatskiy, A., Sharygin, I.S., Litasov, K.D., Borzdov, Y.M., Palyanov, Y.N., and Ohtani, E. (2013c) New experimental data on phase relations for the system Na_2CO_3-$CaCO_3$ at 6 GPa and 900-1400 ºC. American Mineralogist, 98(11-12), 2164-2171.

EFFECT OF CO_2 CONTENT ON MELTING PHASE RELATIONS IN KIMBERLITE GROUP I AT 6.5 GPA AND 1200-1600ºC: IMPLICATIONS FOR THE PARENTAL MAGMA COMPOSITION

Shatskiy A.F.[1,2], Sharygin I.S. [1,2], Litasov K.D.[1,2] , Ohtani E.[2,3]

1 V.S. Sobolev Institute of Geology and Mineralogy, RAS SB, Novosibirsk 630090, Russia
2 Novosibirsk State University, Novosibirsk 630090, Russia
3 Tohoku University, Sendai 980-8578, Japan
anton.antonshatskiy.shatskiy@gmail.com

Introduction

Kimberlite has in several ways attracted more attention than its relative volume might suggest that it deserves. This is because its industrial importance as a source of mined diamonds. Besides, kimberlite is no less important scientifically because it serves as the deepest probe into Earth's interior. However, our understanding of kimberlite petrogenesis is significantly hampered by uncertainty about the compositions of kimberlite magma. It is generally accepted that the last equilibration of kimberlite magma with surrounding mantle (garnet lherzolite) occurred beneath cratons at 6-7 GPa prior its rapid ascent (~70 km/h) to the Earth's surface. This conclusion is based on the following facts. The deepest (170-220 km depths) and hottest (1200-1500ºC) xenoliths entrapped by kimberlites are sheared garnet lherzolites originating from the lower part of lithospheric mantle. The preservation of deformation features in sheared lherzolites indicates that the rock was undergoing dynamic recrystallization just before it was picked up by the magma and that it reached the surface after less than a few days or even hours in magma rising by crack propagation (Green and Gueguen, 1983; Meyer, 1985; Sparks et al., 2006). Based on our resent study (Sharygin et al., 2012) of melting phase relations in an exceptionally fresh kimberlite group I from Udachnaya-East kimberlite (UEK) pipe at 3.0-6.5 GPa and 900-1500°C, the kimberlite melt had essentially Na-K-Ca carbonatite composition <15 wt.% SiO_2, Na_2O + K_2O = 5-18 wt%, Na/K ≈ 2, Cl >1.5 wt%, and Ca/(Ca+Mg) > 0.5. However, the mineral assemblages obtained in these experiments differ from known mantle parageneses. This may be due to unaccounted CO2 budget missed at shallow depth as a result of decarbonation reactions at 1.5-2.5 GPa. Therefore, in present study we examined the effect of CO_2 content on melting phase relations in synthetic UEK kimberlite system at 6.5 GPa and 1200-1600ºC.

Experimental

Experiments were conducted using Kawai-type multianvil apparatuses at Tohoku University (Sendai, Japan). Run duration ranged from 8 to 72 hs. Experimental mixtures were loaded in graphite cassettes. Starting compositions are shown in Table 1. Representative images of recovered samples are shown in Fig. 1. Obtained results are summarized in Fig. 2.

Based on obtained results mineral assemblage equilibrated with kimberlite partial melt gradually changes from peridotite to eclogite paragenesis with increasing its CO_2 content from 13 to 35 mol %. As can be seen at 6.5 GPa kimberlite partial melt (i.e. Na-K-Ca carbonatite melt) becomes equilibrium with garnet lherzolite (i.e. olivine + enstatite + diopside + garnet + FeS + ilmenite assembly) at 1500ºC and 23 mol % (20 wt%) CO_2 (Fig. 1). This value is 10 mol% more

than natural abundance of CO_2 in the Udachnaya-East kimberlite rock (group I kimberlite). In other words, the kimberlite magma lost almost half of the CO_2 budget during the eruption.

Table 1. Starting compositions of UEK kimberlite system.

#	SiO_2	TiO_2	Al_2O_3	FeO	MgO	CaO	Na_2O	K_2O	P_2O_5	SO_3	Cl	F	CO_2	
1	25.0	1.3	1.6	7.3	43.8	13.3	3.3	0.8	0.4	0.2	1.4	1.5	**0**	mol%
	28.9	2.0	3.1	10.0	33.6	14.2	3.8	1.5	1.1	0.3	0.9	0.6	**0**	wt%
2	21.7	1.2	1.4	6.4	38.1	11.6	2.8	0.7	0.3	0.2	1.2	1.3	**13.0**	mol%
	25.7	1.8	2.8	8.9	29.9	12.6	3.4	1.3	0.9	0.3	0.8	0.5	**11.1**	wt%
3	21.2	1.1	1.4	6.2	37.3	11.3	2.8	0.7	0.3	0.2	1.2	1.3	**15.0**	mol%
	25.2	1.8	2.7	8.7	29.3	12.4	3.3	1.3	0.9	0.3	0.8	0.5	**12.9**	wt%
4	20.2	1.1	1.3	5.9	35.5	10.8	2.6	0.7	0.3	0.2	1.1	1.3	**19.0**	mol%
	24.2	1.7	2.6	8.4	28.1	11.8	3.2	1.2	0.9	0.3	0.8	0.5	**16.4**	wt%
5	19.2	1.0	1.2	5.6	33.8	10.2	2.5	0.6	0.3	0.2	1.1	1.2	**23.0**	mol%
	23.1	1.6	2.5	8.0	26.9	11.3	3.1	1.2	0.8	0.3	0.8	0.4	**20.0**	wt%
6	18.2	1.0	1.2	5.4	32.0	9.7	2.4	0.6	0.3	0.1	1.0	1.1	**27.0**	mol%
	22.1	1.5	2.4	7.6	25.7	10.8	2.9	1.1	0.8	0.2	0.7	0.4	**23.6**	wt%
7	17.2	0.9	1.1	5.1	30.3	9.2	2.2	0.6	0.3	0.1	1.0	1.1	**31.0**	mol%
	21.0	1.5	2.3	7.3	24.4	10.3	2.8	1.1	0.8	0.2	0.7	0.4	**27.3**	wt%
8	16.2	0.9	1.0	4.8	28.5	8.6	2.1	0.5	0.3	0.1	0.9	1.0	**35.0**	mol%
	19.9	1.4	2.1	6.9	23.2	9.8	2.6	1.0	0.7	0.2	0.7	0.4	**31.1**	wt%

#1 UEK composition without CO_2 (shown for comparison). #2 UEK with natural abundance of CO_2, #3-8 UEK with additional CO_2.

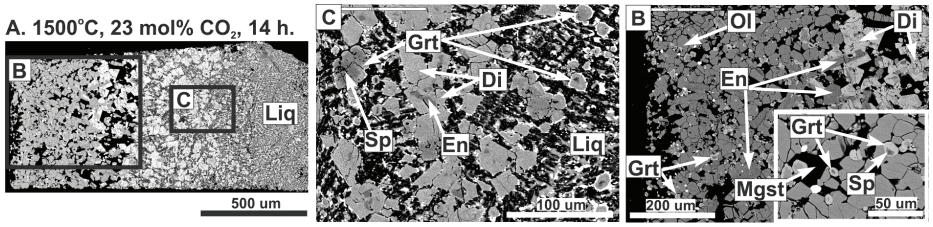

Figure 1: Representative BSE images of kimberlite samples recovered from experiments at 6.5 GPa.

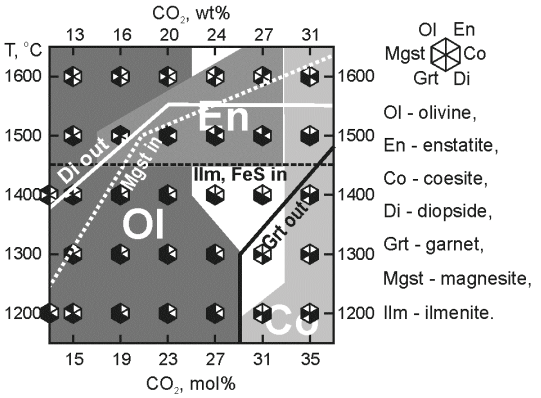

Figure 2: Melting phase relations in Udachnaya-East kimberlite (kimberlite group I) versus temperature and CO_2 content at 6.5 GPa. 13 mol % CO2 corresponds to the natural abundance of CO_2 in UEK rock.

MINERAL AND SPECTRAL REFLECTANCE PROFILE OF HUMID REGION ULTRAMAFIC DIATREMES

Shavers E. J.[1,2], Ghulam A.[1], Encarnacion J.[2]

1 Center for Sustainability, Saint Louis University, St. Louis, U.S.A.
2 Department of Earth and Atmospheric Sciences, Saint Louis University, St. Louis, U.S.A.
eshaver1@slu.edu

The rift zones of central North America feature well distributed yet sparsely identified ultramafic diatreme (UMD) occurrences, valuable for potential economic deposits as well as advancing our understanding of earth's interior and tectonic processes. While discovery of new UMDs is ongoing, it is slowed in this region by overlying sediments as well as vegetation and alteration exaggerated by the humid environment of the US mid-continent. Advances in imaging spectroscopy may offer the ability to increase the rate of UMD discovery in the North American mid-continent. Here we seek to identify mineralogy and spectral reflectance features specific to UMDs in the mid-content environment. The study area is the Avon Volcanic District, a ~200 area of south-east Missouri hosting an ultramafic dike and diatreme complex identified as an olivine melilitite-alnöite-carbonatite assemblage. Outcrop alteration in this area is variable from minimal surface weathering to extensive laterization. X-ray powder diffraction and thin section analysis indicate the dominant mineralogy includes calcite, quartz, clays, Mg and Fe-rich carbonates, Fe and Ti oxides and multiple garnet phases. REE minerals cerianite (Ce O2) and xenotime [(Yb, Tm) P O4] are also indicated. Laboratory Vis-NIR spectral measurements of samples from the study area combined with documented electromagnetic signatures of the identified mineralogy indicate that reflectance and absorption features within the 460-600, 1870-1945 and 2220-2340 nm regions are sufficient to differentiate the variable lithology within the region.

Acknowledgements: We thank the Saint Louis University Center for Sustainability and The Geological Society of America for financial support.

ON THE GENESIS OF KIMBERLITES OF THE UKRAINIAN SHIELD

Sheremet E. M.

Ukrainian State Research and Design Institute of Mining Geology, Rock Mechanics and Mine Surveying, National Academy of Sciences of Ukraine (UkrNIMI), Donetsk, Ukraine
EvgSheremet@yandex.ru

The Ingul and Azov megablocks of the Ukrainian Shield (USh) are known for poor diamond-bearing and diamond-free kimberlite manifestations of Proterozoic age (1.9–1.7 bya). Devonian poor diamond-bearing and diamond-free kimberlite volcanic pipes are found also in the Azov megablock. It appears that their genesis is the same, although they have formed at different times.

Kimberlite manifestations in the Ingul megablock are opened in 14 down holes. Two diamond crystals were found in one of the samples of kimberlite dyke. Proterozoic kimberlite manifestations are known in the West Azov Region – Kolarovka promising area (Mriya Pipe) and are predicted in a number of the promising areas (Demianovka, Andreevka, Uspenovka, Blagoveshchenka and Berezovka).

Judging by carbon dating of 400–350 Ma for alkali-ultrabasic and kimberlite magmatism, tectonic processes in the Azov megablock activated strongly in Devonian. The tensile phase of the coupling of the Azov megablock with the Dnieper-Donets depression (DDD) is characterized by manifestation of magmatism of Devonian alkali-ultrabasic-alkali-basaltoid complex and diamond and diamond-free kimberlite-type volcanic pipes.

The origin of Proterozoic kimberlites is considered in detail in [1, 2]. Under the geodynamic model described in these monographs, diamond-bearing kimberlites, lamproites and their related rocks have occurred due to the pulling down deeply under the Archean shields (down to 200–250 km) of rocks of oceanic crust and Early Proterozoic heavy (ferruginous) marine sediments along the ancient subduction zones. According to Sorokhtin [1,2], lubrication of adjacent plates with heavy sediments, which fell down to the depth, prevented the occurrence of calc-alkaline magmatism of island arc or Andean type in many Early Proterozoic zones. For this reason, very likely, plate subduction zones at the end of Early Proterozoic (during the period of Svecofennian orogeny) and in Middle Proterozoic were mainly amagmatic.

To our opinion, the mentioned model of melt formation at different depths in the process of Proterozoic subduction is completely applicable to the Ukrainian Shield and in particular to the Azov Region. In our previous works [3, 4] we considered geologic-geophysical subduction model of the Azov Region, where areas of granitoid magmatism propagation are from the subduction zone towards the extent of its rear part. Granitoid magmatism is similar to the Andean type zonation but granitoid calc-alkaline magmatism near the subduction zone is not so strongly pronounced in the propagation area of granitoids of calc-alkaline row (Obitochnaya complex) because in this field both subalkalic granitoid magmatism and carbonatite magmatism is developed. The rear subduction zone (East Azov Region) is represented by subalkalic granites (Kamennaya Mogila complex and East Azov complex) and nephelinic syenites, and mariupolites (Oktyabrskoe complex). In this view Sorokhtin's assumption of the absence of calc-alka-

line magmatism of island arc or Andean type due to the effect of falling down to the depth of ferruginous marine sediments in the process of subduction (in our case this is the banded iron formation (BIF) of Orekhov- Pavlograd suture zone – OPSZ), the remains of which preserved in Orekhov-Pavlograd suture zone, discovers substantiation for the Azov megablock subduction model. For the subduction zone under consideration melts were forming at depths of continental lithosphere down to 30–40 km as far as Moho discontinuity. Proterozoic alkali- ultrabasic rocks in the Azov Region, with which kimberlite manifestations are connected, and carbonatite rocks were forming in deep-seated parts, beginning from the depths of more than 50 km, just as derivatives of kimberlite melts were forming.

The examined point of view is confirmed for the Ingul megablock too, taking into account the problem related to the origin of dykes of Proterozoic diamond-free or poor diamond-bearing kimberlites, where, based on geoelectrical survey, high electrical conductance anomaly is recorded within the limits of Kirovograd-Kremenchug suture zone (KKSZ). According to the data from building of the deep geoelectrical model [5], the anomaly is the result of plunging of BIF down to the depth of more than 35 km.

Devonian kimberlite magmatism has developed in the tensile phase over the area of coupling of the Azov megablock with the DDD, which has formed, according to [1, 2], due to the collision of the West Siberian Epi- Paleozoic Platform with the Russian Platform at the end of Carbonic period. It is just this process with which strongly developed magmatism of calc-alkaline and kimberlite rows within the Baltic Shield and the north of the Russian Platform should be connected. In Arkhangelsk region volcanic pipes (Zimneberezhie district) of diamond- bearing kimberlite and melilitite magmatism were found as early as in the beginning of the 80's of the 20th century.

The most probable hypothesis is that subduction mechanism of pulling the pelagic sediments and BIF of deep-sea floor under the continental segments down to different depths is the mechanism of forming melts that led to the formation of plutons of rapakivi-type subalkalic granitoids (at depths of 30–40 km) and melts of carbonatite, alkali-ultrabasic and kimberlite rows (50 km and more).

References

1. Sorokhtin O. G. The origin of diamonds and prospects for diamond content in the east part of the Baltic Shield / O. G. Sorokhtin, F. P. Mitrofanov, N. O. Sorokhtin. — Apatites: KSC RAS edition, 1996. — 144 p. (in Russian)
2. Sorokhtin O. G. Lithosphere plate tectonics and the origin of diamond-bearing kimberlites / O. G. Sorokhtin // Review: General and regional geology, geologic mapping. — Moscow : VIEMS, 1985. — 48 p. (in Russian)
3. Geologic-geoelectric model of Orekhov-Pavlograd suture zone of the Ukrainian Shield / N. Ya. Azarov, A. V. Antsiferov, E. M. Sheremet et al. — Kiev, Nauk. dumka, 2005. — 190 p. (in Russian)
4. Geologic-geophysical criteria for ore bearing and metallogeny of subduction zones of the Ukrainian Shield/ E. M. Sheremet, S. N. Kulik, S. G. Krivdik et al. — Donetsk, Knowledge (Donetsk branch), 2011. — 285 p. (in Russian)
5. Geologic-geophysical model of Krivoi Rog-Kremenchug suture zone of the Ukrainian Shield / N. Ya. Azarov, A. V. Antsiferov, E. M. Sheremet et al. — Kiev, Nauk. dumka, 2006. — 196 p. (in Russian)

HOW TO PRODUCE SODIUM-ALKALINE MAGMA IN THE CRUST? EXPERIMENTAL RECIPE

Simakin A.G.[1,2], **Salova T.P.**[1]

1 Institute of Physics of the Earth, Moscow
2 Institute of Experimental Mineralogy, Chernogolovka
simakin@ifz.ru

Carbonates as carbonatites are often associated with alkaline magmas implying their mutual origin usually attributed to the mantle depths. We explore another possibility of the sodic alkaline rocks formation at the crustal depths due to interaction of a magma, carbonates and sodium chloride.

Key factor in this system is production of sodium carbonate in the exchange reaction

$$CaCO_3 + NaCl = CaCl_2 + Na_2CO_3 \quad (1)$$

Sodium carbonate in contrast to NaCl has high solubility in the silicate melt and is a good solvent for many HFSE and LREE elements. To explore triple magma-$CaCO_3$-NaCl (H_2O) interaction we experimentally study this system at P=2-3 Kbar.

We use andesite and spilitized andesite as the source rocks in experiments. To avoid direct interaction of $CaCO_3$ and NaCl with melt we put these components in a small open capsule pended inside large welded one. Experiments were performed at T=950-1000^oC slightly below liquidus temperature. About 4 wt.% of water presents in the runs. Sphene as a source of the additional REE and HRSF elements was placed into large or small capsules. We vary ratio of $CaCO_3$/NaCl from 3 to 0. After experiment we study partially crystallized glass, fluid precipitates in the large and small capsules and $CaCO_3$ partially transformed into calcium silicates.

Interaction between large and small capsules occurred via H_2O-CO_2 fluid. Some silica with fluid was transferred into small capsule. We find $CaCl_2$ and KCl as the well formed crystals on the surface of the glass and in the micro-spheres of the fluid precipitates at quenching. $CaCl_2$ was formed in the reaction (1) and KCl in the exchange with melt (Ca on K). $NaHCO_3$ was mainly dissolved in the melt and is very rare in the fluid precipitates as well as NaCl spent in reaction (1).

Table 1: Composition of experimental glasses

Run #	Na_2O	MgO	Al_2O_3	SiO_2	K_2O	CaO	TiO_2	MnO	FeO	BaO	Fluid*
35	8.4	2.11	17.7	56.54	1.19	4.91	2.03	0.16	4.80	0	1:1
36	7.81	1.48	18.05	58.09	0.56	6.10	2.30	0.15	3.11	0.06	0:1
37	6.22	1.86	19.41	61.90	1.68	3.46	1.36	0	3.01	0.04	1:0
39	9.60	0.82	18.93	55.55	1.59	4.78	1.77	0.30	4.28	0.13	3:1
42	5.17	0.29	15.64	61.08	1.37	9.69	0.61	0.08	3.13	0.47	3:1
42-2	5.81	1.06	16.54	62.97	1.91	4.83	0.69	0.08	4.53	0.14	3:1
rock1	6.16	4.61	17.50	49.79	1.24	3.14	1.30	0.19	11.84	0.043	-
rock2	2.82	6.73	14.88	57.83	1.80	6.50	0.81	0.13	8.48	0.048	-

*Fluid - ratio of $CaCO_3$ to NaCl in the small capsule. Rock 2 is used in the run42 and rock1 in all other ones. In the run 42 glass gains 3 wt.% Na_2O, and 3.4 wt.% in run39. All runs were performed at P=2 Kbar and T=1000^{O}C.

Due to the fluid-magma interaction the upper part of the glassy sample from the main capsule is enriched with Ca, middle part with alkalis and the near bottom part remains unchanged. In the table 1 we put compositions of the experimental glasses. Maximum alkalis (Na_2O+K_2O) content approaches 11-12 wt.% and can be classified as trachi-phonolites. This maximum is attained for the always alkalis enriched spilite while andesitic composition shifts to the trachi-andesitic one (see table 1). Modification of basalt into spilite (rock1 in table 1) can be attributed to the metasomatic alternation by the similar Na_2CO_3 ($NaHCO_3$) bearing fluid.
In our experiments initially essentially water fluid gains some CO_2 due to the reaction of the $CaCO_3$ transferred by fluid into the contact with melt and SiO_2 moved by fluid into small capsule with calcite:
$CaCO_3 + SiO_2$ (L,F)= $CaSiO_3$ (L,S) + CO_2 (F) (2)
Production of pure CO_2 in the reaction (2) leads to the increase of fO2 in the same way as in the direct $CaCO_3$-Melt interaction [1, 2].
Amphibole and clinopyroxene are prevailing solid phases in the reported experiments. Highly alkaline nature of the melts is reflected in the specific composition of amphiboles enriched in alkalis, LREE and HFSE (Zr, Nb, Ti).

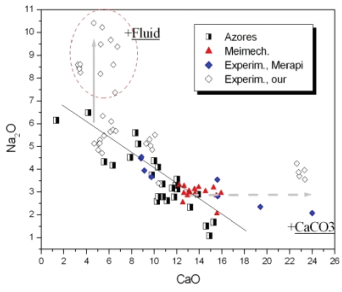

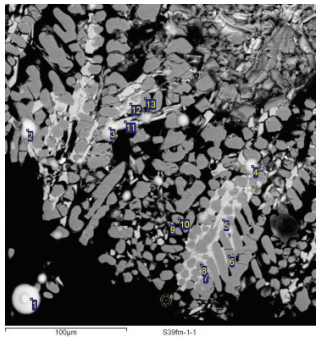

Figure 1: a) Sodium and calcium contents in the magmas and experimental glasses: Meimech.-[3], Azores – [4], Merapi –[2] b) experimental products from the small capsule run 39. Spheres are composed of $CaCl_2$ (contain up to 0.2 wt.% BaO), dark grey – unreacted $CaCO_3$, light grey Ca_3SiO_5

Content of Al in octahedral coordination in amphibole is reducing with rise of alkalinity due to formation of aluminates (such as $NaAlO_2$) where Al is tetrahedral. Similarly Fe^{3+} in alkaline melts shifts to the tetrahedral coordination thus decreasing octahedral Fe^{3+} content in amphiboles. Clinopyroxenes in our runs demonstrates almost totally oxidized iron corresponding to the rather high f_{O2} (NNO+3-4) [1].

Geologic examples. Process of the carbonate- salt – fluid - magma interaction modeled in our experiments can be anticipated in some geologic environments. First of all we expect that evolution of the magmas in the chambers located near the basement of the oceanic islands can occur at such conditions [5]. For example near Tenerife ocean depth is around 3500 m that with 2-3 volcanic load a.s.l. gives around 1.5-2 Kbar at the depth close to the bottom. At such

conditions hydrothermal circulation can get fluid entering into chamber through its bottom. As shown in our experiments such fluid formed at the interaction of NaCl and $CaCO_3$ will carry $NaHCO_3$, Ba, LREE, HFSE into magma. Sea water involvement in the formation of the phonolites on Ua Pou Island is suggested, e.g. in [6].

Similar to the reported interaction between carbonates and sodium chloride may have place deeper in the crust (or upper mantle). Such conditions can arise in the zones of accretion, continental subduction etc. For example currently evaporates (halides and carbonates) had subducted in Mediterranean to the depths of about 40 km [7] probably contributing to the alkaline rocks formation in Italy.

Acknowledgement. This work was supported by RFBR grant № 13-05-00397.

References

1. Simakin A.G., Salova T.P., and Bondarenko G.V., 2012. Experimental Study of Magmatic Melt Oxidation by CO_2. Petrology, v. 20, p.593–606.
2. Deegan F.M., Troll V.R., Freda C., Misiti V., Chadwick J.P.,. Mcleod C.L and Davidson J.P., 2010. Magma- Carbonate Interaction Processes and Associated CO_2 Release at Merapi Volcano, Indonesia: Insights from Experimental Petrology. J. Petrol. v.51, p.1027-1051.
3. A.V. Sobolev, S.V. Sobolev, D.V. Kuzmin, K.N. Malitch, A.G., 2009. Petrunin Siberian meimechites: origin and relation to flood basalts and kimberlites. Russian Geology and Geophysics, v.50, p.999–1033.
4. Genske F.S., Turner S.P., Beier C. and. Schaefer B.F, 2012. The Petrology and Geochemistry of Lavas from theWestern Azores Islands of Flores and Corvo. J. Petrol., v.53, p.1673-1708.
5. Simakin A.G., Salova T.P. and Kovalenko V.I., 2011. Fluid–Magmatic Interactions at Oceanic Islands as a Possible Source for the Sodic Agpaitic Trend. Petrology, v. 19, №. 7, p. 641–652. (in Russian)
6. Legendre C, Maury R. C., Caroff M., Guillou H., Cotten J., Chauvel C., Bollinger C., Hemond C., Guille G., Blais S., Rossi P.and Savanier D. 2005. Origin of Exceptionally Abundant Phonolites on Ua Pou Island (Marquesas, French Polynesia): Partial Melting of Basanites Followed by Crustal Contamination. J. Petrology, v. 46, p.1925–1962.
7. Kagan Y.Y., Jackson D. D., Schoenberg F. P., & Werner M. J,. Linear and Nonlinear Relations between Relative Plate Velocity and Seismicity. 2009. Bulletin of the Seismological Society of America, v. 99, p.3097-3113.

CARBONATITE-RELATED MINERALIZED SYSTEMS, THEIR ORE POTENTIAL, AND RELATED EXPLORATION METHODS.

Simandl G. J. [1,2], **Paradis S.**[3]

1 British Columbia Geological Survey, Ministry of Energy and Mines, Victoria, British Columbia, Canada
2 School of Earth and Ocean Sciences, University of Victoria, British Columbia, Canada,
3 Natural Resources Canada, Geological Survey of Canada, Sidney, British Columbia, Canada,
George.Simandl@gov.bc.ca

Carbonatites are igneous rocks with more than 50% modal carbonate minerals [1]. They range in age from early Precambrian to Recent (Wooley and Kjarsgaard 2008) but in many cases the radiometric age of carbonatite is unreliable because of metamorphic overprint or high Th-U ratios of zircons. Most carbonatites were emplaced in continental extensional settings along large-scale, intra-plate fractures, grabens or rifts. Some are situated in zones of orogenic uplift, due to a post-carbonatite emplacement transition from extensional to compressional tectonic regime. In rare cases, carbonatites are located in oceanic environment [2]. Carbonatites are components of alkaline complexes, or occur as isolated pipes, sills, dikes, plugs, lava flows and pyroclastic blankets. In extensional settings many carbonatite pipe, plugs and carbonatite complexes are characterized by circular, ring, or crescent-shaped aeromagnetic and radiometric anomalies [3, 4] and were discovered by airborne geophysical surveys. Carbonatite-related mineralizing systems may contain economic concentrations of REE (mainly LREE), Nb, Ta, phosphate, vermiculite, Cu, Ti, fluorite, Th, U, Zr, and Fe [5, 6, 7]. Examples of carbonatite-related mineralizing systems are Oka, St. Honoré and Aley carbonatites (Nb; Canada), Mountain Pass (REE; USA), Palabora (Cu, baddeleyite, apatite, vermiculite; South Africa), Bayan Obo (Fe, REE; China), Amba Dongar (fluorite; India). Araxa, Catalao and Tapira (Nb, phosphate, REE, Ti; Brazil). Rock units containing magmatic mineralization within carbonatite complexes and carbonatite pipes are typically circular or crescent-shaped in plan view and steeply-dipping as illustrated by examples from Oka and St. Honoré [8, 9]. Metasomatic mineralization commonly forms irregular zones, veins, or matrix of breccias. Residual, weathering-enriched deposits form blankets overlying protore. Local irregularities within such blankets are caused by variations in the resistance to weathering, intensity and pattern of fracturing (permeability), and the topography. A fenitization halo (typically desilicification with the addition of Fe^{3+}, Na, K, ± Ca) surrounds carbonatites or carbonatite/alkaline complexes [10, 11, 12]. Depending on the size, orientation and the shape of the carbonatite intrusion, and nature of host rock, incorporation of fenitization into deposit model increases the size of the exploration target several fold. Fenitization may manifest itself by the presence of Na- and K-amphiboles, aegerine-augite, wollastonite, nepheline, mesoperthite, antiperthite, pale brown mica, albite, etc. Intensity of fenitization may be used to vector towards a carbonatite [13]. Niobium, REE, P, Ba, Sr, F, U and Th are established pathfinder elements used in geochemical exploration for carbonatites using soils, stream sediments [14, 15, 16], basal tills and vegetation as a sample media; F, Th and U are pathfinders in water. Portable XRF instruments are able to determine concentrations of Nb, LREE, Y, and most pathfinder elements in ores, fenitized zones, and host rocks [17, 18]. Pyrochlore, columbite, Na amphiboles and possibly pyroxenes and fluorite are

useful indicator minerals in stream sediments. Carbonatite systems located in orogenic settings are folded, stretched or truncated and steeply dipping to flat lying. Cross-cutting relationships and igneous or metasomatic textures may be destroyed or obscured by metamorphism; however, they retain high HFSE concentrations and LREE/HREE ratio. Zones of fenitization may be deformed and physically separated from corresponding carbonatites, making exploration challenging. Carbonatites, in both extensional and orogenic settings, are excellent exploration targets.

Acknowledgments: This review was completed under the umbrella of the Targeted Geoscience Initiative 4 spearheaded and supported by Natural Resources Canada.

References:

1. Le Maitre, R. W., *2002. Igneous Rocks. A Classification and Glossary of Terms. Recommendations of the International Union of Geological Sciences Subcommission on the Systematics of Igneous Rocks, 2nd ed.* (Cambridge University Press, New York)
2. Wooley, A.R and Kjarsgaard, B.A., 2008. Carbonatite occurrences of the world; Geological Survey of Canada, Open File 5796
3. Satterly, J., 1970. Aeromagnetic maps of carbonatite-alkalic complexes in Ontario; Ontario Department of Mines and Northern Affairs, Preliminary Map no. P452 (revised).
4. Thomas, M.D., Ford, K.L. and Keating, P., 2011. Exploration Geophysics for intrusion-hosted rare earth metals. Geological Survey of Canada, Open File 6828 (Poster) http://ftpHYPERLINK "http://ftp2.cits.rncan.gc.ca/pub/geott/ess_pubs/288/288092/of_6828.pdf"2HYPERLINK "http://ftp2.cits.rncan.gc.ca/pub/geott/ess_pubs/288/288092/of_6828.pdf".cits.rncan.gc.ca/pub/geott/ess_pubs/HYPERLINK "http://ftp2.cits.rncan.gc.ca/pub/geott/ess_pubs/288/288092/of_6828.pdf"288HYPERLINK "http://ftp2.cits.rncan.gc.ca/pub/geott/ess_pubs/288/288092/of_6828.pdf"/HYPERLINK "http://ftp2.cits.rncan.gc.ca/pub/geott/ess_pubs/288/288092/of_6828.pdf"288092HYPERLINK "http://ftp2.cits.rncan.gc.ca/pub/geott/ess_pubs/288/288092/of_6828.pdf"/of_HYPERLINK "http://ftp2.cits.rncan.gc.ca/pub/geott/ess_pubs/288/288092/of_6828.pdf"6828HYPERLINK "http://ftp2.cits.rncan.gc.ca/pub/geott/ess_pubs/288/288092/of_6828.pdf".pdf
5. Mariano, A.N., 1989. Nature of Economic Mineralization in Carbonatites and Related Rocks. *in* Carbonatites: Genesis and Evolution, K. Bell, Editor, *Unwin Hyman*, London, p. 149-176
6. Mariano, A.N., 1989. Economic Geology of Rare Earth Minerals. in Geochemistry and Mineralogy of Rare Earth Elements, Lipman B.R. and McKay G.A., Editors, Reviews in Mineralogy, Mineralogical Society of America, v. 21, p. 309-338.
7. Birkett, T.C. and Simandl, G.J., 1999. Carbonatite-associated Deposits*; in* Selected British Columbia Mineral Deposit Profiles, Volume 3, Industrial Minerals and Gemstones, G.J. Simandl, Z.D. Hora and D.V. Lefebure, Editors, British Columbia Ministry of Energy and Mines, p. 73-76.
8. Gold D.P., Vallée M. and Charette, J.P., 1967. Economic geology and geophysics of the Oka alkaline complex, Quebec. Transactions of the Canadian Institute of Mining and Metallurgy, v. LLX, p. 245-268Grenier L., Tremblay J.F., 2013. NI 43-101 Technical report, Surface diamond drilling exploration program for rare earth elements, 2012. Niobec Mine Property, IAMGOLD Corporation, _-%
9. Morogan, V., 1994. Ijolite versus carbonatite as sources of fenitization, Terra Nova, v.6, p. 166-176
10. Le Bas, M.J., 2008. Fenites associated with carbonatites; Canadian Mineralogist, v.46, p. 915-932
11. Smith, M.P., 2007. Metasomatic silicate chemistry at the Bayan Obo Fe-REE-Nb deposit, Inner Mongolia, China: Contrasting chemistry and evolution of fenitizing and mineralizing fluids; Lithos, v. 93, p 126-148

12. Simandl, G.J., Reid, H.M., and Ferri, F., 2013. Geological setting of the Lonnie niobium deposit, British Columba, Canada. In: Geological Fieldwork 2012, British Columbia Ministry of Energy, Mines and Natural Gas, British Columbia Geological Survey Paper 2013-1, pp. 127-138.

13. Luck, P. and Simandl, G.J., 2014. Portable X-ray fluorescence in stream sediment chemistry and indicator mineral surveys, Lonnie carbonatite complex, British Columbia. In: Geological Fieldwork 2013, British Columbia Ministry of Energy and Mines, British Columbia Geological Survey Paper 2014-1, p. 169-182.

14. Mackay, D.A.R., and Simandl, G.J., 2014. Portable X-ray fluorescence to optimize stream sediment chemistry and indicator mineral surveys, case 1: Carbonatite-hosted Nb deposits, Aley carbonatite, British Columbia, Canada. In: Geological Fieldwork 2013, British Columbia Ministry of Energy and Mines, British Columbia Geological Survey Paper 2014-1, p. 183-194.

15. Mackay, D.A.R. and Simandl, G.J., 2014. Portable X-ray fluorescence to optimize stream sediment chemistry and indicator mineral surveys, case 2: Carbonatite-hosted REE deposits, Wicheeda Lake, British Columbia, Canada. In: Geological Fieldwork 2013, British Columbia Ministry of Energy and Mines, British Columbia Geological Survey Paper 2014-1, p. 195-206.

16. Simandl, G.J., Paradis, S., Stone, R.S., Fajber, R., Kressall, R., Grattan, K., Crozier, J., Simandl, L.J., 2014. Applicability of handheld X-ray fluorescence spectrometers in the exploration and development of carbonatite-related niobium deposits – a case study of Aley carbonatite, British Columbia, Canada. Geochemistry: Exploration, Environment, Analysis. doi: 10.1144/geochem2012-177, http://geea.geoscienceworld.org/content/early/HYPERLINK "http://geea.geoscienceworld.org/content/early/2014/02/14/geochem2012-177.abstract"2014HYPERLINK "http://geea.geoscienceworld.org/content/early/2014/02/14/geochem2012-177.abstract"/HYPERLINK "http://geea.geoscienceworld.org/content/early/2014/02/14/geochem2012-177.abstract"02HYPERLINK "http://geea.geoscienceworld.org/content/early/2014/02/14/geochem2012-177.abstract"/HYPERLINK "http://geea.geoscienceworld.org/content/early/2014/02/14/geochem2012-177.abstract"14HYPERLINK "http://geea.geoscienceworld.org/content/early/2014/02/14/geochem2012-177.abstract"/geochem-HYPERLINK "http://geea.geoscienceworld.org/content/early/2014/02/14/geochem2012-177.abstract"2012HYPERLINK "http://geea.geoscienceworld.org/content/early/2014/02/14/geochem2012-177.abstract"-HYPERLINK "http://geea.geoscienceworld.org/content/early/2014/02/14/geochem2012-177.abstract"177HYPERLINK "http://geea.geoscienceworld.org/content/early/2014/02/14/geochem2012-177.abstract".abstract

17. Simandl, G.J., Stone, R.S., Paradis, S., Fajber, R., Reid, H.M., Grattan, K., 2013. An assessment of a handheld X-ray fluorescence instrument for use in exploration and development with an emphasis on REEs and related specialty metals. Mineralium Deposita. doi: 10.1007/s00126-013-0493-0, http://link.springer.com/article/HYPERLINK "http://link.springer.com/article/10.1007%2Fs00126-013-0493-0"10HYPERLINK "http://link.springer.com/article/10.1007%2Fs00126-013-0493-0". HYPERLINK "http://link.springer.com/article/10.1007%2Fs00126-013-0493-0"1007HYPERLINK "http://link.springer.com/article/10.1007%2Fs00126-013-0493-0"%HYPERLINK "http://link.springer.com/article/10.1007%2Fs00126-013-0493-0"2HYPERLINK "http://link.springer.com/article/10.1007%2Fs00126-013-0493-0"FsHYPERLINK "http://link.springer.com/article/10.1007%2Fs00126-013-0493-0"00126HYPERLINK "http://link.springer.com/article/10.1007%2Fs00126-013-0493-0"-HYPERLINK "http://link.springer.com/article/10.1007%2Fs00126-013-0493-0"013HYPERLINK "http://link.springer.com/article/10.1007%2Fs00126-013-0493-0"-HYPERLINK "http://link.springer.com/article/10.1007%2Fs00126-013-0493-0"0493HYPERLINK "http://link.springer.com/article/10.1007%2Fs00126-013-0493-0"-HYPERLINK "http://link.springer.com/article/10.1007%2Fs00126-013-0493-0"0

REMARKS ON BEZIER TYPE CURVS AND THEIR APPLICATIONS TO GEOLOGY

Simsek Y.

Akdeniz University Faculty Science Department Of Mathematics 07058 Antalya Turkey
ysimsek@akdeniz.edu.tr

In this paper, we study on the Bezier type curvs. By using genearting functions, the Bernstein type basis functions are defined.The Bernstein basis functions are used to cunstruct the Bezier curves. These curves are related to curves and surfaces. The Bernstein type basis functions and Bezier type curves have been used in Mathematics, in Computer Aided Geometric Design (CAGD), in Engineering and the other scientific areas. Consequently, in this paper, we give some applications of the Bezier type curves in the above areas. We also give some remarks and comments on structural geology, which advantage from design tools. Within the very important of these tools are well-known the Bezier curves which may be used in forward modelling or reconstruction.

Keywords: Bernstein polynomials, Generating function, Bezier curves, Fourier transform, Laplace transform, Partial differential equations, Structural geology

AMS Subject Classification: 14F10, 12D10, 26C05, 26C10, 30B40, 30C15, 42A38, 44A10.

INTERACTION OF THE CARBONATE MELTS AND LHERZOLITE: CONSTRAINTS FROM SANDWICH EXPERIMENTS AT 5.5 GPA AND 1200ºC

Sokol A.G., Palyanov Yu.A., Kruk A.N., Chebotarev D.A.

V.S. Sobolev Institute of Geology and Mineralogy, SB RAS
Novosibirsk, Russian Federation
sokola@igm.nsc.ru

Volatiles-rich carbonate melts are able to separate from the mantle asthenosphere at very low melting degree of sources. To be infiltrated into colder lithosphere these melts percolate upwards and interact with peridotites initiating their metasomatic alteration. Green and Wallace (1984) as well as Kogarko (2006) consider mantle lherzolite and wherlite with secondary clinopyroxene as the products of this type of reactive interaction between asthenospheric carbonatitic melts and depleted lherzolite or harzburgite. It should be noted that xenoliths of metasomatically altered lherzolites hosted by kimberlites are highly oxidized and simultaneously have maximal contents of both phlogopite and clinopyroxene (Creighton et al. 2009). Microinclusions hosted by so-called fibrous diamonds are the most relevant medium recordings and are commonly used for the reconstruction of the compositions of mantle metasomatic agents and protokimberlite melts. During diamond growth K-rich carbonatite or (rarely) hydrous-silicate melts/fluids were encapsulated by fibrous crystals.

The purposes of the present study are (1) to examine the interaction of dry and wet K-rich carbonatitic melts with lherzolite; and (2) to distinguish the rock-forming minerals stability limits and peculiar features of solid phases and melt compositions at the equilibrium conditions. All experiments were carried out at 5.5 GPa, 1200ºC and duration of 150 hours. We have considered as the model carbonatite the compositions of carbonate melts derived by Brey et al. (2011) from melted K-rich carbonatized harzburgite at 6 GPa (Car1, 8 wt% SiO_2) and 10 GPa (Car2, 14 wt% SiO_2) and a temperature of 1400ºC. Peridotite matrix was represented by HZ86 composition (Hart and Zindler, 1986). It was established that at 5.5 GPa and 1200ºC the starting mix of HZ86 composition was transformed into common lherzolite association (in wt%): Ol (52), Opx (19), Cpx (13) и Grt (16). In the system the molar ratios of $CO_2/(CO_2+H_2O)$ vary from 0.57 up to 1. The starting samples were prepared as three-layered sandwich: matrix (HZ86) – carbonatite (Car1 or Car2) – matrix (HZ86). Dry samples were loaded into graphite capsules, whereas samples with (CO_2 + H_2O)- and/or H_2O additive were loaded into Pt capsules lined by graphite. Pt capsules were sealed by arc welding. After the experiments all samples were dried and then impregnated with epoxy resin for SEM examination by Tescan MYRA 3 LMU equipment as well for microprobe examination with Cameca Camebax and Jeol JXA-8100.

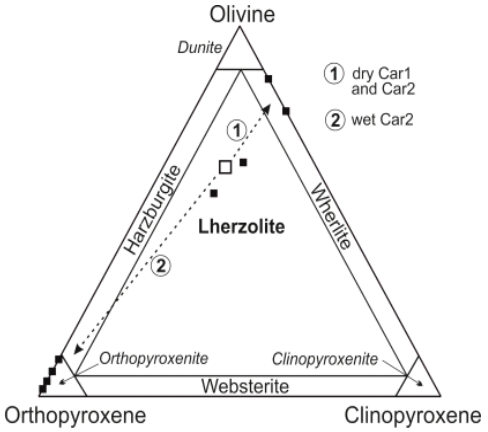

After experiments the phase composition of the peridotite matrix changed depending on the $CO_2/(CO_2+H_2O)$ ratio. Lherzolite interaction with dry Car1 and Car2 melts resulted in total consumption of Opx, owing to lherzolite transformation into magnesite-bearing wherlite. The products of lherzolite alteration contain the more Cpx the higher was silica concentration in carbonatite. After the reaction between lherzolite and wet Car1 (H_2O- or (CO_2+H_2O) additive) we did not fix Cpx consumption. However, extra phases such as magnesite (in the presence of H_2O additive) or magnesite + dolomite (in the presence of CO_2+H_2O additive) occurred in the matrix. Addition of water into Si-richer Car2 composition leaded to total Cpx consumption in lherzolite matrix. Moreover in the system lherzolite + Car2 + CO_2+H_2O the quantity of olivine markedly decrased and it totally disappeared in lherzolite + Car2 + H_2O system. Thus the interaction between lherzolite and SiO_2-, H_2O- and CO_2–bearing carbonatites resulted in its transformation into carbonated garnet-bearing harzburgite or orthopyroxenite (Figure). It should be stressed that phlogopite was not found in the studied samples.

The melts synthesized in the abovementioned sandwiches were quenched (at 150-200˚C/sec) to feather-like aggregates of carbonates and silicate crystals. At the experimental conditions the melt portion varied from 14 up to 40 wt% (according mass-balance calculation). Melt compositions depended on both starting composition of sandwiches and $CO_2/(CO_2+H_2O)$ molar ratios. Silica content in the melt varied from 2 wt% (in the dry Car1 system) up to 9 wt% (in wet Car2 system). The melting degree increased with increasing water content, simultaneously K_2O content in the melt decreased from 14-20 wt% to 1.5-2 wt%.

The main conclusion of the study is that wherlitization of mantle peridotites at P-T conditions of subcratonic lithosphere is the result of their metasomatic alteration by dry carbonatitic melts. Inasmuch as water partitioning coefficients between olivine with OH-defects and carbonatitic melt is as low as 0.001 (Sokol et al., 2013), one can conclude that dry melts had a chance to be percolated upward through the overlying dry (<< 100 ppm H_2O) mantle peridotites only. The characteristics of deep xenoliths transported from the depth of >200 km (Peslier et al., 2010) support this conclusion. Such dry carbonate melts should be maximally enriched in alkalis (with K>>Na). Earlier Thibault et al. (1992) have shown that at 2.0 GPa and 1000ºC wet alkaline dolomitic melts can metasomatize harzburgite to olivine-rich phlogopite wherlite. Does phlogopite remain stable to a depth of 200 km in the presence of carbonate melts? Enggist et al. (2011) based on the phase relations of phlogopite with magnesite from 4 to 8 GPa concluded

that phlogopite + carbonate assemblage is stable in a cold subcontinental lithospheric mantle to a depth 200 km. Moreover Sobolev et al. (2009), finding inclusions of phlogopite in diamonds, have shown that phlogipite was stable under diamond growth conditions. Our new results allow us to suggest that phlogopite becomes unstable in lherzolith in the presence of wet ultra-alkaline carbonate melts. Furthermore the interaction between wet carbonate melts and lherzolite does not markedly change the phase composition of the rocks. Thus phlogopite and clinopyroxene may be considered correspondingly as the products of early and later metasomatic alteration of subcratonic lithospheric mantle (assuming a 40 mW/m^2 geotherm).

Acknowledgement: This work was supported by Russian Found for Basic Researches (grant # 14-05-00203).

References

1. Brey, G.P., Bulatov, V.K. and Girnis, A.V. (2011) Melting of K-rich carbonated peridotite at 6-10 GPa and the stability of K-phases in the upper mantle. Chemical Geology, 281, 333-342.
2. Creighton, S., Stachel, T., Matveev, S., Hofer, H., McCammon, C. and Luth, R.W. (2009) Oxidation of the Kaapvaal lithospheric mantle driven by metasomatism. Contributions to Mineralogy and Petrology, 157, 491-504.
3. Green, D.H. and Wallace, M.E. (1988) Mantle metasomatism by ephemeral carbonatite melts. Nature, 336, 459-461.
4. Hart, S.R. and Zindler, A. (1986) In search of a bulk-earth composition. Chemical Geology, 57 247-267.
5. Peslier, A.H., Woodland, A.B., Bell, D.R. and Lazarov, M. (2010) Olivine water contents in the continental lithosphere and the longevity of cratons. Nature, 467, 78-U108.
6. Sokol, A.G., Kupriyanov, I.N. and Palyanov, Yu.N. (2013) Partitioning of H_2O between olivine and carbonate–silicate melts at 6.3 GPa and 1400ºC: Implications for kimberlite formation. Earth and Planetary Science Letters, 383, 58–67.
7. Enggist, A., Chu, L.L., Luth, R.W., 2012. Phase relations of phlogopite with magnesite from 4 to 8 GPa. Contributions to Mineralogy and Petrology 163, 467-481.
8. Kogarko, L.N., 2006. Alkaline magmatism and enriched mantle reservoirs: Mechanisms, time, and depth of formation. Geochemistry International 44, 3-10.
9. Sobolev, N.V., Logvinova, A.M., Efimova, E.S., 2009. Syngenetic phlogopite inclusions in kimberlite-hosted diamonds: implications for role of volatiles in diamond formation. Russian Geology and Geophysics 50, 1234-1248.
10. Thibault, Y., Edgar, A.D., Lloyd, F.E., 1992. Experimental investigation of melts from a carbonated phlogopite lherzolite – implications for metasomatism in the continental lithospheric mantle. American Mineralogist 77, 784-794.

H2S-BEARING FLUID AND SULFIDE OF THE UPPER MANTLE (EAST ANTARCTIC)

Solovova I.P.[1], Kogarko L.N.[2]

1 Institute of Geology of Ore Deposits (IGEM) of Russian Academy of Sciences, Moscow, Russia
2 Vernadsky Institute of Russian Academy of Sciences (GEOKHI), Moscow, Russia.
solovova@igem.ru

Minerals of garnet lherzolite nodules contain microinclusions of sulfides and fluids. Sulfide inclusions are isolated one- or two phases blebs or spheroids and form clusters. Pentlandite, pyrrhotite, chalcopyrite or other minerals weren't found in the inclusions. As the ratio metal/sulfur (M/S) is one of the most important characteristics of sulfides, their compositions were considered in Ni – M/S coordinates. They form two trends - with positive and negative dependence (Fig. 1). Experimental data allow considering them as Ni-rich *mss* and residual sulfidic melt. Their coexistence within inclusions gives the chance to estimate coefficient of distribution of Ni between *mss* and melt (D*mss*/melt), which varies as 1.01-3.23. Inverse relationship between temperature and DNi allows to estimate temperature of formation of two-phase sulfides' associations as 1060-920oC.

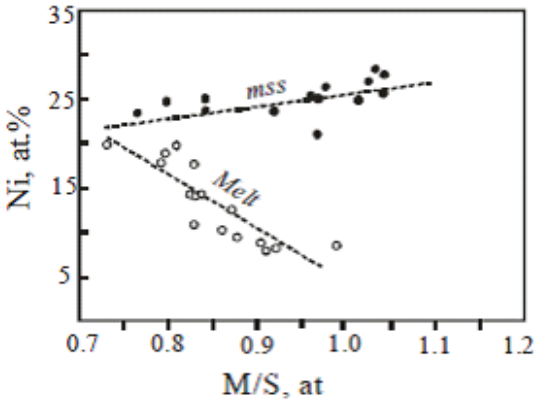

Figure 1: Two trends of compositions of sulfide inclusions.

Olivine and orthopyroxene contain single- (liquid) and two- (liquid+gas) phase CO2-bearing fluid inclusions. The earliest single-phase fluid inclusions coexisting with sulfide inclusions are characterized by abnormally low temperatures of phase transitions in comparison with pure CO2. Phase transition at –151°C is close to the critical point of N2 (–147°C) that conditionally permits to consider of fluid composition within system CO2-N2. According to CO2-N2 system topology a molar proportion of N2 in bulk composition of a fluid reaches 0.2.

The main vibrations of CO2 were observed on the Raman spectra at 1282 cm-1 and 1385cm-1 (Fig. 2). The Raman analyses showed also presence of N2 (2331 cm-1), H2S (2610 cm-1) and H2O (3598-3642 cm-1) dissolved in CO2. The ratio of the integrated squares of N2 and H2S

bands permits to estimate their molar portions in the fluids as 0.2 и 0.1, respectively. H2S-bearing fluids in the presence of H2O are capable to transport Zr, Ti and REE elements, up to crystallization of own minerals, which were found in studied xenoliths.

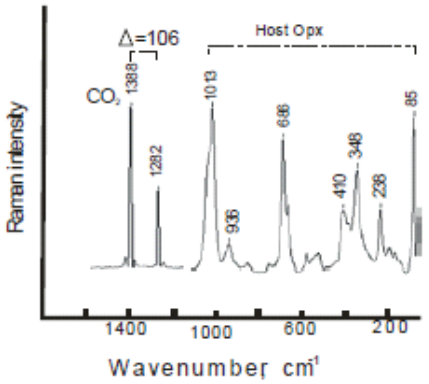

Figure 2: The Raman spectra of fluid inclusions: lines of CO2 and Opx.

Density of primary fluids were estimated by two independent ways, on a ratio of volumes of a crystal CO2 and gas within inclusions (0.8) and on distance between the two main Raman vibrations of CO2 (ν- 1285 cm-1 and ν+ 1388 cm-1, Δ=105.7-106). Density of fluids varies from 1.17 to 1.23 g/cm3. Fluid of such density at 1050-1080oC corresponds pressure >>1.2-1.5 GPa (considering a partial decrepitating of inclusions).

Using combination of experimentally determined of the *mss* + sulfide melt field boundaries, solidus of the peridotite-CO2, H2O and 0.9CO2 + 0.1H2O, and isochors of 0.8CO2 + 0.2N2 - fluid, the initial values of temperature and pressure are 1270-1280oC and ~2.2 GPa (Fig. 3).

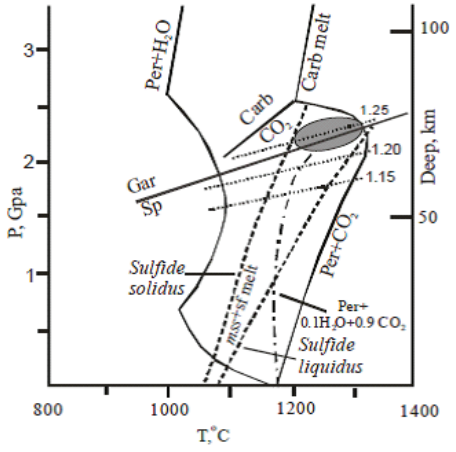

Figure 3: P-T condition of the primary sulfide-fluid associations (grey field)

This study was financially supported by the grants of President and

FLUID AND SULFIDE INCLUSIONS IN THE UPPER MANTLE OF EAST ANTARCTIC

Solovova I.P.[1] , **Kogarko L.N.**[2]

1 Institute of Geology of Ore Deposits (IGEM) of Russian Academy of Sciences
2 Vernadsky Institute of Russian Academy of Sciences (GEOKHI)
solovova@igem.ru

Garnet lherzolite nodules contain microinclusions of sulfides and fluids. Sulfide inclusions are isolated one- or two phases blebs or spheroids and form clusters. Pentlandite, pyrrhotite, chalcopyrite or other minerals weren't found in the inclusions. As the ratio metal/sulfur (M/S) is one of the most important characteristics of sulfides, their compositions were considered in Ni – M/S coordinates. They form two trends - with positive and negative dependence (Fig. 1). Experimental data allow considering them as Ni-rich *mss* and residual sulfidic melt. Their coexistence within inclusions (Fig. 2) gives the chance to estimate coefficient of distribution of Ni between mss and melt (D*mss*/melt), which varies as 1.01-3.23. Inverse relationship between temperature and DNi allows to estimate temperature of formation of two-phase sulfidic associations as 1060-920oC.

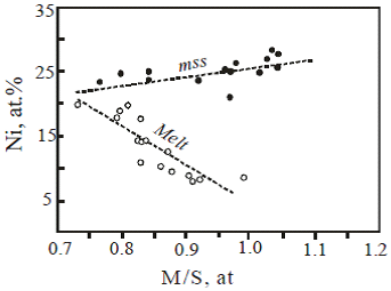

Figure 1: Two trends of compositions of sulfide inclusions.

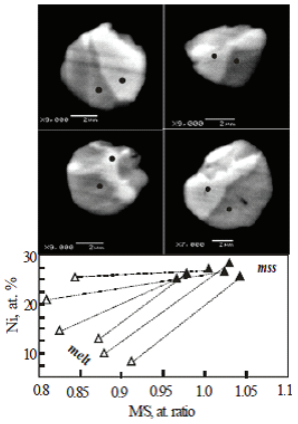

Figure 2: Photomicrographs of two-phase sulfide inclusions (BSE) and its compositions

Olivine and orthopyroxene contain single- (liquid) and two- (liquid+gas) phase CO2-bearing fluid inclusions. The earliest single-phase fluid inclusions coexisting with sulfide inclusions are characterized by abnormally low temperatures of phase transitions in comparison with pure CO2. Phase transition at –151°C is close to the critical point of N2 (–147°C) that conditionally permits to consider of fluid composition within system CO2-N2. According to CO2-N2 system topology a molar proportion of N2 in bulk composition of a fluid reaches 0.2.

The main vibrations of CO2 were observed on the Raman spectra at 1282 cm-1 и 1385cm-1 (Fig. 3). The Raman analyses showed also presence of N2 (2331cm-1), H2S (2610cm-1) and H2O (3598-3642 cm-1) dissolved in CO2 (Fig. 4). The ratio of the integrated areas of N2 and H2S bands permits to estimate their molar portions in the fluids as 0.2 и 0.1, respectively. H2S-bearing fluids in the presence of H2O are capable to transport Zr, Ti and REE elements, up to crystallization of own minerals which were found in studied xenoliths (Kogarko et al., 2007).

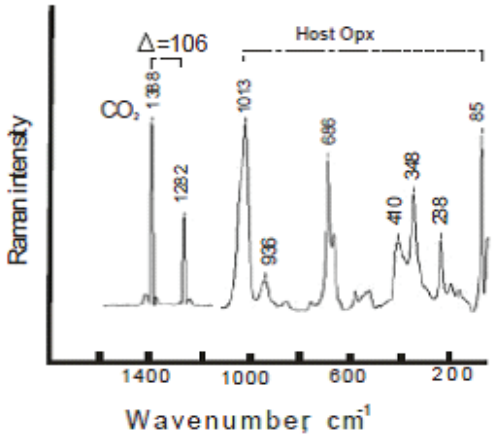

Figure 3: The Raman spectra of fluid inclusions: lines of CO2 and Opx.

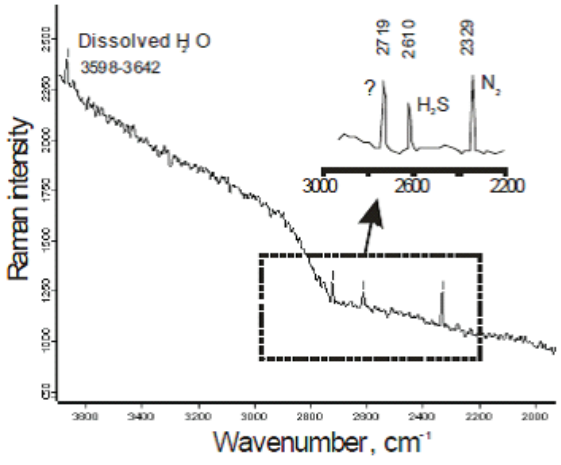

Figure 4: The Raman spectra of fluid inclusions: lines of N2, H2S and H2O

Density of primary fluids were estimated by two independent ways, on a ratio of volumes of a crystal CO2 and gas within inclusions (0.8) and on distance between the two main Raman vibrations of CO2 (ν- 1285 cm-1 and ν+ 1388 cm-1, Δ=105.7-106). Density of fluids varies from 1.17 to 1.23 g/cm3. Fluid of such density at 1050-1080oC corresponds pressure >>1.2-1.5 GPa (considering a partial decrepitating of inclusions).

Thus, the mantle peridotite was affected by CO2-N2-H2S-H2O fluid at a temperature not below 1060oC and pressure >>1.5 GPa, at depths of 45-60 km. The H2S-containing fluid coexisted with the Ni-enriched sulfidic melt and *mss* at temperature from >1060oC up to 920oC.

This study was financially supported by the grants of President and RFBR

CLINOPYROXENE COMPOSITION OF MAFIC-ULTRAMAFIC XENOLITHS IN ALKALINE ROCKS, NORTHWESTERN IRAN: AN EXAMPLE OF COGNATE-TYPE XENOLITHS IN LAMPROPHYRES

Soltanmohammadi A.[1,2], Rahgoshay M.[1], Ceuleneer, G.[2]

1 Geological Department, Faculty of Earth Sciences, Shahid Beheshti University, Tehran, Iran
2 GET. Geoscience Environment Toulouse, CNRS-UMR5563, OMP, University of Toulouse III-Paul-Sabatier, Toulouse, France
azamsoltanmohammadi@gmail.com

The Cenozoic lamprophyres of the Turkish-Iranian high plateau, NW of Iran identified as minette, are associated with a heterogeneous suite of mafic- ultramafic xenoliths. The xenoliths range in composition from mafic to ultramafic, which are ovoid or angular, 1-10 cm in diameter. Mineral assemblages of both xenoliths and host-lamprophyres with calc alkaline affinity [1] consist of mica, clinopyroxene, K-feldspar, apatite, and Fe-Ti oxide. Mafic-ultramafic xenoliths are subdivided in two groups based on mineralogy: (a) ultramafic xenoliths, including clinopyroxenites and accumulations of clinopyroxene- mica, and (b) mafic xenoliths including clinopyroxene-mica-feldspars. There is a number of evidence for magmatic source of xenoliths; they are heterogeneous (variations of grain size and mineralogy) and show disequilibrium and magmatic textures (e.g. oscillatory and sector zoning of the clinopyroxenes).

Clinopyroxenes in ultramafic xenoliths and host lamprophyres show diopsidic character and are same in composition. In contrast, clinopyroxenes in the mafic xenoliths have fassaite-salite in character. Similar to host lamprophyres, clinopyroxenes in xenoliths show relatively moderate to high Mg-numbers (0.63-0.84), variable Al_2O_3 (0.85-8.48 wt.%), low TiO_2 (<1.28) and Na_2O (<1.03) contents and low Al^6/Al^4(mostly <0.25), suggesting clinopyroxenes in igneous rocks and classified as calc alkaline lamprophyre-type. Estimated geobarometric constraints inferred from clinopyroxene composition in xenoliths and host lamprophyres indicate low pressure of pyroxene crystallization. Results reveal that the origin of xenoliths as cumulate from alkaline melts with a shallow level mantle petrogenesis, rather than a deep-stead origin related to mantle convection, and reflecting crystallization in similar conditions for host lamprophyres and classified as cognate type xenoliths which are common in lamprophyres.

References

1. Soltanmohammadi A., RahgoshayM., Ceuleneer G., Gregoire M., Benoit M., 2014. Metasomatism in the subcontinental lithospheric mantle beneath Azarbayjan Magmatic Plateau, NW Iran: Evidance from potassic lamprophyres from the Salavat range: Goldschmidt2014, Sacramento, U.S.A, Abstract 2349.

STABLE ISOTOPE (Δ13C AND Δ18O) COMPOSITION OF CARBONATES OF AURIFEROUS QUARTZ CARBONATE VEINS, CHIGARGUNTA AND BISANATTAM GOLD DEPOSITS, SOUTH KOLAR SCHIST BELTS: IMPLICATION TO SOURCE OF ORE FLUIDS

Swain S.K.[1], Sarangi S.[1], Sarkar A.[2], Srinivasan R.3, Vasudev V.N.[4]

1 Department of Applied Geology, Indian School of Mines, Dhanbad, India
2 Department of Geology and Geophysics, Indian Institute of Technology, Kharagpur, India
3 INSA Senior Scientist, IISC, Bangalore, India
4 Director (Exploration), Geomysore Services Pvt Ltd, India
sagar.swain10@gmail.com

Orogenic gold deposits known from Middle Archaean to Tertiary metamorphic belts are structurally controlled, occur in late syntectonic crustal scale shear zones and quartz carbonate veins (Goldfarb et al., 2005). C and O isotopes of carbonate minerals and silicates of quartz carbonate veins (QCVs) have been studied extensively in many other regions of the world to constrain the source of auriferous fluids. Carbon ($\delta^{13}C_{pdb}$) and Oxygen($\delta^{18}O_{smow}$) isotopic compositions of auriferous quartz carbonate veins (QCVs) of orogenic gold deposits from Chigargunta and Bisanattam mine blocks, South Kolar gold deposit, Kolar Schist Belt, Dharwar Craton, southern India have been examined for the first time to understand the origin of the mineralizing fluids. Isotope compositions of QCVs from Chigargunta mine block (borehole samples: -3.4‰ ±0.8‰) and from Bisanattam mine block (Old workings: -5.0‰ ±2.9‰) are consistent with $\delta^{13}C_{pdb}$ fall in the compositional range of mantle/magmatic derived CO_2 or carbonates.

In contrast, few of the corresponding $\delta^{18}O$ values of the QCVs from Chigargunta mine block (borehole samples: 13.9‰ ±3.3‰) and from Bisanattam mine block (Old workings: 12.1‰ ±3.5‰) are consistent with mantle/magmatic derived CO_2. A very few of these samples show effect of low temperature alteration by meteoric water.

Since the $\delta^{13}C$ values of carbonates of QCVS are well within the $\delta^{13}C$ range of magma (-5 3‰; Ohomotto, 1986) or mantle (-6 2‰; Ohomotto, 1986) derived fluids, we propose that the fluids responsible for gold mineralization at Chigargunta and Bisanattam blocks of South Kolar Schist Belts, have a mantle/magmatic source.

References

1. Ohmoto H (1986) Stable isotope geochemistry of ore deposits. In stable isotopes in high temperature geological processes. Edited by J. W. Valley, H.P. Taylor, Jr and O'Nell. Mineralogical Society of America, Rev Miner 16: 491-560.
2. Goldfarb R.J., Baker T., Dube B., Groves D.I., Hart C.J.R., Gosselin P. (2005) Distribution, character and genesis of gold deposits in metamorphic terrenes. In: Economic Geology 100th Anniversary Volume (2005) 407–450.

DISTRIBUTION OF RARE AND RADIOACTIVE ELEMENTS IN ROCKS AND ORES OF MASSIF TOMTOR

Tolstov A.V.

IGM of the Siberian Branch of the Russian Academy of Science, Novosibirsk, Academician Koptyuga Ave, 3,
tolstov@igm.nsc.ru

Ultramafic alkaline carbonatite magmatism (UACM) with Fe-P-Th-REE mineralization is largely determines minirageny of Northern Siberia . Bright UACM representative is massif Tomtor that located in the NW of Yakutia and characterized by the development of alkaline rocks (syenite), nepheline-pyroxene rocks (foidolite) and rocks of carbonatite complex [1,3,4].

The thick weathering crust (over 200 m) that developed on carbonatites , has binomial structure from the bottom up: oxidized (phosphate and glandular) and restored (siderite and aluminophosphate) zone. Supergene complex is composed of Fe-P-Nb-REE ore whith composition inherited from that of substrate rocks. In the weathering crust author established a clear zonation with universal arrays typical for UACM.. In accordance with this zoning on the ore Fe-P-REE carbonatites from the bottom up sequentially deposited iron-phosphate (limonite-frankolitovy) and gland (limonite and siderite) horizons. Ore column crowned by zone of epigenetic changes - aluminophosphate horizon.

Trace elements are formed industrial concentration within the Tompor massif. Consistent accumulation of Nb and REE from indigenous ores (carbonatites) to supergene (Fe-P) and epigenetically-modified aluminophosphate pyrochlore-monazite-krandallitovym ores are clearly observed. On the background of typical for UAC vfssifs Nb_2O_5 concentrations in silicate rocks (0.05wt. %) higher values are observed in the substrate of weathering crusts - carbonatite ore to 0.2% wt.%.(Table 1). Further growth of concentrations are observed in the supergene zone rocks (0.5-1%), and the absolute maximum - in epigenetically-transformed aluminophosphate species (4%). Concentrations TR2O3 in the described rocks are sequentially increasing from 2.01% to 5.03% and 10%, respectively, and are unique.

Table 1: Chemical compositions of massif Tomtor, in wt.%.

Rocks, number of analyzes	SiO_2	TiO_2	Al_2O_3	Fe_2O_3	FeO	MnO	MgO	CaO	K_2O	Na_2O	P_2O_5	CO_2	TR_2O_3	Nb_2O_5
Silicate rocks														
Foidolite, n = 20	35.81	2.37	17.93	5.61	2.15	0.16	4.66	13.06	3.38	7.65	0.84	н/о	0.05	0.03
Syenite, n = 14	51.90	0.79	21.75	3.12	3.06	0.17	1.45	1.11	11.5	1.06	0.34	н/о	0.07	0.03
Alneity, n = 20	30.97	2.96	8.12	6.85	5.24	0.27	14.0	14.33	3.19	0.87	1.38		0.09	0.04
Picrites, n = 10	26.80	2.67	5.31	8.45	4.77	0.33	15.5	14.64	2.77	0.66	1.17	н/о	0.09	0.04
Carbonatites, n = 335	7.06	0.69	1.54	3.62	4.15	1.49	5.28	36.28	1.07	0.17	2.87	32.26	0.12	0.18
Kamafority, bulk sample	4.00	4.15	1.36	47.35	26.5	1.05	1.14	1.75	0.32	0.40	0.80	н/о	0.09	0.06
Barren group														
Carbonate-silicate rocks, n = 87	29.39	3.04	8.20	5.88	6.80	0.76	6.24	13.28	6.46	0.28	2.59	13.95	0.08	0.05
Carbonatites, n = 103	7.89	0.77	2.08	3.34	4.23	1.32	6.17	35.08	1.06	0.16	1.62	33.62	0.10	0.09
Ore group														

Carbonate-silicate rocks, n = 143 Carbonatites P-TR, n = 194	28.24 6.10	3.43 0.47	9.58 1.17	8.89 3.64	10.5 3.36	1.41 1.26	5.44 4.17	9.30 39.22	5.08 0.90	0.21 0.17	5.58 3.87	5.71 32.43	1.18 1.81	0.18 0.21
Carbonate-silicate rocks, n = 29 Carbonatites TR, n = 37	14.40 9.90	2.20 1.54	4.07 2.00	17.23 3.87	9.72 8.07	3.22 3.20	3.98 8.75	16.14 24.22	0.86 2.08	0.14 0.17	3.81 1.13	13.98 27.71	1.18 1.52	0.33 0.19
Explosive breccia														
Breccia rocks, n = 20	14.83	3.90	14.01	5.44	16.8	1.41	0.53	7.43	1.28	0.15	11.3	8.22	1.50	1.15

Overlying sediments do not contain significant concentrations of ore (rare and radioactive) elements. REE mineral forms represented mainly by monazite (bedrock)hydromonazite and rabdofanite (supergene zones and epigenesis). This resulted in the predominant concentration of La-Ce, which together constitute more than 75%, and with the Nd and Pr – up to 90% of total REE. Average concentrations of yttrium and scandium are, respectively, 0.5 and 0.05%, the concentrations of other REE (Sm-Lu) altogether accounts for less than 10% of total REE. However, in general stable and high ratio of LREE/HREEin several areas significantly disturbed, as on the western flank Burannyi area where concentrations exceed 2% of yttrium and 0.2% of scandium -, which may indicate a shift in the direction of REE spectrum towards HREE (Y-group).[7].

Rock and ore of massif Tomtor have varying degrees of radioactivity due to the presence of appreciable amounts of Th-containing TR minerals (natural radionuclides U, Th, K-40). U content in rocks is low, but it is variable in petrographic varieties [2]. Th / U show even greater variations. Uranium is present in amounts of from 0.0002% to 0.0892%. U content in the richest epigenetically altered ores range from 0.0018 to 0.0892% (average 0,0092%), Th - from 0.019 to 0.304%.

For substrate rocks (carbonatite and syenite foidolite) average contents of U are similar to background. Elevated concentrations of U (up to 0.0072%) observed in the supergene zone bottom (0.0002, 0.025%), as U was removed from the top part of the weathering of ore carbonatites, postponing at the bottom together with phosphorus. U is present in the adsorbed and mineral forms. In epigenetically altered where the content of the U in ores = 0.0065% areas with a noticeable concentration of U to 0.009-0.01% are existed. This does not exclude the possibility of industrial concentration [6].

Table 2. Contents Th and U in the rocks of massif Tomtor

№	Rocks, horizon	Amount of analysis	The average content Th, g\t	U, g\t	**Ratio Th/U**
1	Overlying Jurassic marine sediments	5	15.20	4.0	**3.80**
2	Overlying Permian clastic sediments	52	74.10	13.1	**5.70**
3	Epigenetic kaolinite-krandallitovy horizon	73	1227.60	71.4	**17.18**
4	Lateritic weathering crust on the P-REE carbonatite	108	233.00	14.6	**16.00**
5		109	106.40	7.1	**15.00**
6	Phosphorus-rare metal carbonatites	21	2374.24	3.62	**655.87**
7	Lateritic weathering crust on REE carbonatite	33	738.30	5.94	**124.29**
8	REE (ankerite) carbonatites	20	640.50	13.7	**46.80**
9	Explosive carbonatite breccia	28	132.90	14.1	**9.40**
10	Hydromicaceous weathering crust	50	73.10	7.9	**9.30**
11	Carbonatites barren group	13	36.70	2.8	**13.10**
12	Alkaline and nepheline syenites Foidolite (K-feldspar, carbonatized)	33	39.50	5.6	**7.10**

Thorium is present everywhere in higher concentrations than U. Average Th content in ores

constitute 0.1438% (0.01-0.84%). In the underlying weathering crusts Th forms high concentrations (0.04% -0.08%), comparable with the content in the ore carbonatites (0.074%), which is associated with low migration ability Th at supergene. In the overlying sediments Th is present in concentrations of 0.0221% (variations from 0.0019 to 0.13%), its presence is associated with acuumulation of weathering crusts material in depression with clastic sediments.

Th/U ratio reflects the geochemical characteristics of the behavior of these elements in the endogenous processes and supergene zone [5,6]. Features of uranium, as high-mobile element in an oxidizing and inert - in a reducing environment, determine its removal from the oxidation zone and the accumulation in zone of epigenesis (on reducing geochemical barrier). In this regard, the ratio of Th \ U in primary carbonatites is 124.3 and changed up the supergene zone section in according to geochemical characteristics behavior of Th and U. In the phosphate horizon, lie directly on carbonatites, Th / U = 38.7 (1.5 to 394), and higher in the section, in the limonite horizon, Th / U = 116 (with variations from 4.1 to 621). Within the area of epigenetic ratio Th / U is reduced to 52.3-59.2, while the presence of areas enriched uranium (0.03-0.09%) and spatially discrete areas enriched in Th (up 0.84%), causes a rapid change of Th/U ratio of 0.7 to 1153.8, which is more than 1,500 times [7]. In the overlying coal-bearing sediments averages Th/U is reduced to 14.3 at smaller variations (from 0.7 to 100).

Thus, the particular distribution of Nb, REE, U, Th in rocks and ores of massif Tomtor allow us to ascertain the translational concentration of them from primary carbonatites to supergene and epigenetically modified products. Th/U ratio confirm this character REE concentrations of elements to unique values. Variations of the REE spectrum suggests the presence of local sites with high and abnormal concentrations of heavy REE representing industrial interest within the massif Tomtor.

Referances

1. Lapin AV, AV Tolstov New unique deposits of rare metals in the weathering crusts carbonatites / / Exploration and protection of natural resources, 1993. № 3, p.7-11 (in Russian).
2. Molchanov AV, AV Tolstov Features of uranium ore formation on the boards of the Siberian platform (with the forecasting of high-margin deposits). South Yakutia complex expedition: 50 years of exploration and discovery. Yakutsk, Izd YSU, 2001, p. 130-137 (in Russian).
3. Tolstov AV, Entin AR, Tian OA, AN Orlov Industrial types of deposits in carbonatite complexes of Yakutia, Yakutsk, YSC SB RAS, 1996, 168c (in Russian).
4. Tolstov AV, Tian OA Geology and ore array Tomtor, Yakutsk, YSC SB RAS, 1999, 164 p (in Russian).
5. Tolstov AV Evolution and metallogeny of ore formations (for example, the North Siberian Platform). Materials XI session of the North-East Branch of the WMO "Regional Scientific and Practical Conference" Problems of Geology and metallogeny of Northeast Asia at the Turn of the Millennium ", Magadan, 2001, Volume 2, p. 83-85 (in Russian).
6. Tolstov AV, Konoplev AD Prospects of uranium-bearing North Siberian platform. - Proceedings of the International Symposium on uranium geology. M., VIMS, 2000, p. 65-68 (in Russian).
7. Tolstov AV, Konoplev AD Lithofacies features of localization of complex niobium-rare earth ores of Tomtor massif. - Materials lithological meeting "Lithology and Mineral Resources of Central Russia." Voronezh, 2000, Academy of VSU, p. 84 (in Russian).

PLATINUM PROSPECTS OF ALKALINE ROCKS OF UDZHA PROVINCE (NORTHWEST OF YAKUTIA)

Tolstov A.V.

IGM of the Siberian Branch of the Russian Academy of Science, Novosibirsk,
Academician Koptyuga Ave, 3,
tolstov@igm.nsc.ru

Occurences of placer gold and platinum group minerals (PGM) are widely known on Northern part of the Siberian platform, but their study remains obviously insufficient [1]. Concentration of gold and PGM on some intervals of alluvial placers often make 0,2-0,5 g/m^3, reaching locally economical values (2 and more than a g/m^3) at a ratio of these metals 1:1 – 2:1. In recent years placer gold and platinum are considered as objects of passing extraction at production of diamonds from alluvial placers [3]. The question of a primary source of precious metals in this region still remains open and debatable [4]. Earlier we proved identification prerequisites on an equal basis with a typical primary source – a sulphidic copper-nickel ores of the Norilsk type, a new nonconventional primary source of PGM – cambrian high-carbonaceous shales of kuonamsky bituminous thickness [5]. Results of studying MPGM composition and features of their distribution within the North of the Siberian platform, in detail studied in recent years, points to real possibility of location of their primary source to northeast slope of Anabar anteclise [3,4,5]. Here, within the Udzhinsky raise large massifs of a iyolit-karbonatite formation Tomtor and Bogdo are revealed and studied. However during geological exploration of these massifs the main attention was paid to their unique Nb-TR ores related to their hyper gene complex. Single determination of concentration of platinoids in Tomtor's ultramafic rocks (picrite, alnoite) didn't reveal considerable concentration. In the last decades Russian scientist stated idea about the new primary source of PGM connected with alkaline complexes [1,2]. We consider this direction is very perspective as it considerably expands the expected ore capacity of alkaline massifs whichwere not evaluated for their possible PGM concentrations. Due to the renewal of studying of the massif Tomtor we consider this task as the most actual. Prime objects for PGM evaluation are massifs Tomtor and Bogdo. Existence of the meso-Cainozoic deposits of the alkaline-carbonatite massives that is covered by sediments (to Chuempe, Uele) multiply the chances to find primary PGM deposits in the North of Siberia [6].

Referances

1. Dodin D. A. Metallogeniya of the Taymyro-Norilsky region (North of the Central Siberia). // "Science", S-Pb. 2002, page 618-621 (in Russian).
2. Kogarko L.N. Ukhanov A.V. Nikolskaya N. E. New data on the maintenance of elements of group of platinum in rocks of an iyolit-karbonatitovy formation (massifs Babble also Kugd, the Maymecha-Kotuysky province, Polar Siberia). // Geochemistry. 1994 . No. 1, page 1568-1577 (in Russian).
3. Okrugin A.V. Zaytsev A.I. Borisenko A.S. Zemnukhov A.L. Ivanov of P. O. Zolotoplatinonosnye of a scattering of the basin of the Anabar River and their possible communication with the alkaline and ultramain magmatite North of the Siberian platform. // Domestic geology, 2012, No. 5, S. 11-20 (in Russian).

4. Tolstov A.V. Mineralogiya and geochemistry of SZ gold of Yakutia and prospect of a zolotorudnost of the Anabarsky board//VGU Bulletin, Voronezh, 1999, No. 8, page 194-197 (in Russian).
5. Tolstov A.V. Prospects of a platinonosnost of Anabarskaya антеклизы//Goskomgeologiya's Messenger (Materials on geology and minerals of the Republic of Sakha (Yakutia), Yakutsk, 2001, No. 1, page 82-87 (in Russian).
6. Tolstov A.V. Main ore formations of the North of the Siberian platform. M.: IMGRE, 2006, 212 pages (in Russian).

ULTRAPOTASSIC ROCKS OF THE LOWER PART OF THE BASALT COVER (MIDDLE TIMAN)

Udoratina O. V.[1], Varlamov D. A.[2]

1 Institute of Geology of Komi SC UB RAS, Syktyvkar, Russia,
2 Institute of Experimental Mineralogy RAS, Chernogolovka, Russia
udoratina@geo.komisc.ru

In two open pits of the Vezhayu-Vorykva group of bauxite deposits (Middle Timan, headwaters of Verkhnya Vorykva Rivers) during their development the sole of the Verkhne-Vorykva basalt cover was opened and in it unusual high-potassium rocks of problematic (most possibly – magmatic) genesis were found.

In ground part of a cover (opened here on all power thickness – about 10-12 m) accurately traced layer of the 40-50 cm (Fig.1) alkaline high-potassium rocks (presumably basaltoides) separated by a thin (5-10 cm) layer of loose disintegrated basalts from above-located rocks is found. The top contact everywhere is grass-covered, and the bottom contact is traced on a big extent, thus it is possible to observe overlapping of cover on bauxites. In "Basalt" open pit these rocks (alkaline "basalts") are observed in secants in relation to blanket basalts a dyke-like body (sample 13-5/11).

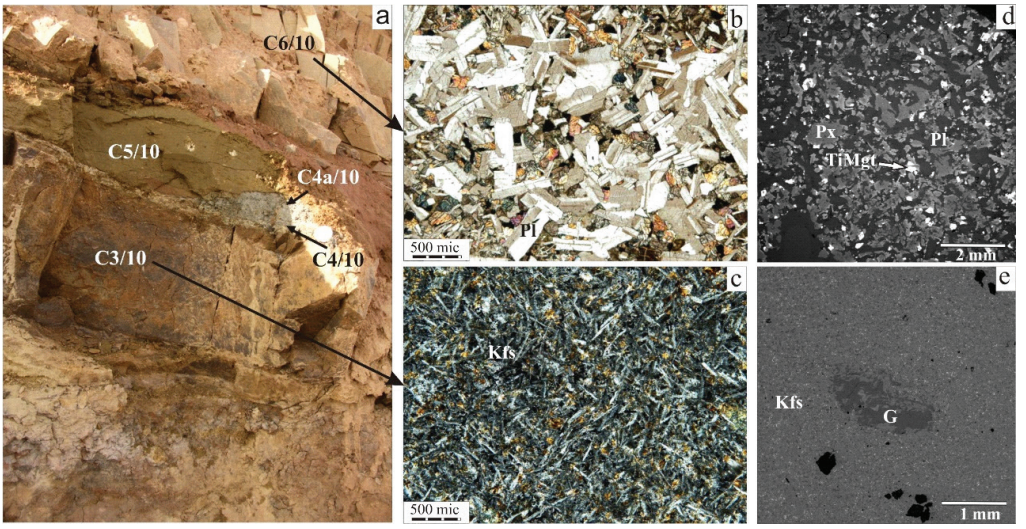

Figure1: Structure of the lower part of a cover. (a) – the location of samples in a pit section, (b-c) – examples of microstructures of basalts (b) and alkaline "basalts" (c), d-e – images of basalts (d) and alkaline "basalts" (e) in back-scattered electrons (BSE)

The rock (sample C3/10) in the bottom part of a cover has light brown color and is fine-grained or aphyric. Under a microscope the porphyritic structure is observed, the phenocrysts are stacked by thin needle laths of difficult diagnosed salic mineral. The groundmass of rock is

presented by microliths of the same mineral. According to microprobe researches and data of the Raman spectroscopy this mineral – the potassium feldspar immersed in a matrix of glass of similar composition. On a chemical composition these rocks considerably differ from other rocks of a cover. The content of SiO_2 is 53 wt.%, rock is moderately high-titanian and high-aluminous, content of K_2O reaches up to 11 wt.% that allows to attribute studied rock to alkaline type (Table 1).

Table 1: Chemical composition of rocks (typical samples, wt.%)

№	SiO_2	TiO_2	Al_2O_3	Fe_2O_3	FeO	MnO	MgO	CaO	Na_2O	K_2O	P_2O_5	ППП
C6/10	50.64	1.89	12.24	3.81	8.13	0.20	6.86	10.14	2.04	0.43	0.15	0.68
C5/10	44.58	2.47	19.36	9.70	0.85	0.11	4.64	3.38	1.10	2.04	0.20	12.31
C4a/10	51.34	2.92	23.05	4.32	0.25	0.44	2.18	1.47	0.42	2.88	0.24	11.05
C4/10	49.78	3.09	23.33	5.07	0.69	0.25	1.16	1.35	0.29	4.49	0.26	10.12
C3/10	53.06	2.54	18.36	6.73	0.25	0.13	1.87	0.79	0.32	**10.84**	0.21	4.34
13-5/11	51.64	1.56	18.36	5.50	0.36	0.07	3.99	1.28	0.28	**9.07**	0.18	6.8

Remark: The chemical composition is determined by a method of "wet" chemistry in IG Komi SC UB RAS (Syktyvkar).

However, the absence of typical alkaline minerals (salic and femic) in the rock possibly indicates its intensive post-magmatic changes caused by an arrangement in a bottom of a cover. On all diagrams the positions of points of composition are abnormal. Content of REE is relatively high. Spectra of REE distribution strikingly differ from REE spectra of overlying basalts and have a negative slope and weakly expressed negative Eu minimum. Depletion of LREE relatively HREE is observed. Genesis of the found rock while isn't clear.

Samples (C4/10, S4a/10, C5/10) from an intermediate zone between the rocks of bottom part and basalts of a cover are presented by bulk material of different colors and dimensions, representing mixture of sand from the minerals composing basalt and fragments actually of basalt. On the chemical composition they also correspond to basalts (Table 1).

Overlying basalts (C6/10) are presented is incomplete-crystalline rock of dark gray color with a greenish shade. Texture is massive, structure is porphyritic. Phenocrysts are presented by a clinopyroxene of 0.1-0.3 mm (in the diameter) and a plagioclase – elongated, 0.3-0.5 mm in length, up to 1 mm. Under a microscope the porphyritic structure of rock caused by existence of phenocrysts of a plagioclase and pyroxene, intersertal structure for groundmass is observed. Phenocrysts of a plagioclase make 15-45 vol.% of rock and pyroxenes – 5-30 vol.%); the matrix is presented by microliths of a plagioclase and pyroxenes, an ore mineral (titanomagnetite (?)), glass (palagonite). The structure of rock is defined by the plagioclase phenocrysts located both in the form of single crystals, and in the form of clusters. They are immersed in mikrolitic matrix, created from small laths of plagioclase and near-isometric crystals of pyroxene. Volcanic glass makes 7-30 vol.% of the rock and composes intergranular spaces between plagioclase and pyroxene crystals. Ore minerals take up to 10 vol.% of the rock, shapes of their allocations is various: angular, irregular, frequent skeletal growth forms, "fir-tree" shape and the other, the size of 0.3-0.5 mm. Ore minerals (magnetite and ilmenite) are products of disintegration of primary titanomagnetite. Basalts of normally alkali series, silica (SiO_2) content at the level of

50 wt.%, the total content of $Na_2O + K_2O$ is 2 wt.%. Basalts belong to moderately low-titanous and low-aluminous. In the diagrams for separating calc-alkaline and tholeiitic series points of compositions of the studied basalts fall in the tholeiitic rocks field. On diagrams used for the reconstruction of geodynamic conditions of formation, the composition of the studied basalts fall into different fields, and generally to the fields of development of basalts from continental rifts.

Covers of basalts and a dykes of dolerite are considered as a part of Kanin-Timan complex with Medium-Upper Devonian age (D_{2-3}). In earlier works of predecessors in the bottom part of complex it wasn't noted presence of high-alkaline basalts which are found by us. High contents of potassium mineralogical are confirmed by availability of exclusively potassium feldspar and potassium glass. Their existence, and also lack of signs of substitution, in our opinion doesn't allow telling about imposed potassium metasomatism of basalts.

Possible options of genesis of such rocks: (1) it is the first portion of the basalt melt enriched with alkalis, from the top part of the magmatic chamber; (2) these are rocks (bottom) near-contact zone where there is a vitrification (roasting), a potassium source – probably bedrock (bauxites). On different authors the content of potassium oxide in bauxites of the Vezhayu-Vorykva deposit group strongly varies, generally is at the level of 0.01–0.3 wt.%, but can be up to 5 wt. %.

ALKALINE PICRITES FROM THE CHETLASSKY COMPLEX IN MIDDLE TIMAN: AR-AR DATA

Udoratina O.V.[1], Travin A.V.[2,3]

1 Institute of Geology Komi SC UB RAS, Syktyvkar, Russia
2 IGM SB RAS, Novosibirsk, Russia
3 Tomsk State University, Tomsk, Russia
udoratina@geo.komisc.ru

Dyke complex of alkaline picrites is developed in Middle Timan, in the south-eastern part of Chetlassky Kamen. The dykes mark faults of NE strike and form Kosyuskoe, Mezenskoe, Bobrovskoe and Oktyabrskoe dyke fields. The rocks transect Riphean sediments of Chetlasskaya and Bystrinskaya series.

Picrites, carbonatites, various phenites, both melanocratic and leucocratic ones, and also vein formations were developed. Chetlassky complex of dyke ultrabasic rocks is close to early and middle stages of autonomous picrite-lamprophyric series associated with ultrabasic alkaline complexes and is specified by the absence of feldspatolites and presence of kimpicrites and aikilites [4]. Generally the rocks are altered by secondary processes.

Phlogopite is one of rock-forming minerals of alkaline picrites of Chetlassky complex. It forms poikilocrystals (often zonal) in the rocks composed of olivine and clinopyroxene inclusions, bulk minerals and accessories. There are several generations of phlogopite discerned by color and chemical composition and formed by different processes. Magmatic phlogopite is characterized by pale yellow-brown color, autometasomatic one is greenish brown, hydrothermal-metasomatic one is green. Optical refraction indices of different generations vary insignificantly. The chemical composition shows decreasing content of alumina, increasing iron content and increasing silica at the metasomatic transformation of magmatic phlogopite [2].

The chemical composition of alkaline picrites from V. I. Stepanenko's collection was studied (Kosyuskoe dyke field), and also Ar-Ar isotope-geochemical data were obtained (IGM SB RAS, Novosibirsk) for the monofraction of magmatic phlogopite to determine the age of alkaline picrites.

Microprobe studies confirm trends marked by V. I. Stepanenko (Fig. 1, a-b, points of phlogopite compositions from different Chetlassky magmatic rocks are presented for comparison). K_2O content (wt %) varies insignificantly from 9.5 to 11.

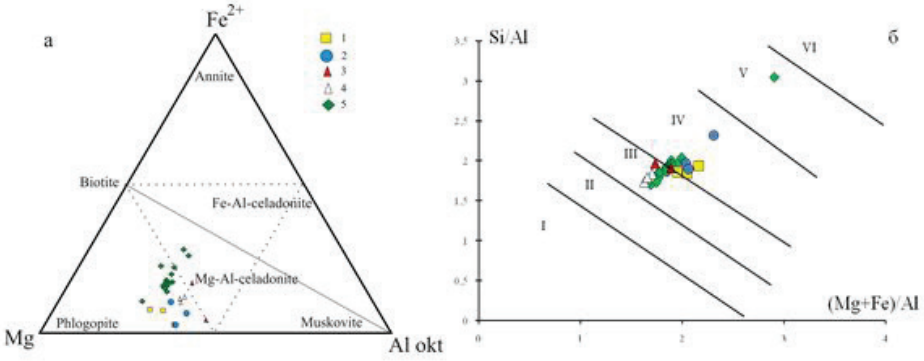

Figure 1: Phlogopite of Chetlassky magmatic rocks. a – octahedral cation ratio in micas [6], b – phlogopites from A. A. Marakushev and I. A. Tararin [3]. 1-4 phlogopite composition [2]: 1 – alkaline picrites (magmatic stage), 2 – alkaline picrites (autometasomatic stage), 3 – phlogopite mikaites, 4 – carbonatite, 5 – phlogopites under study.

The correlation dependence in $^{40}K/^{40}Ar$ isochronous positions was determined by K-Ar method for the phlogopites from this complex (picrites, phlogopite mikaites and carbonatites) that had been done previously in Institute of Geology of Komi SC UB RAS, which fixes the age 600±15 Ma [1].

$^{40}Ar/^{39}Ar$ dating was done (IGM SB RAS, Novosibirsk) by the method [5] of stage heating of phlogopite monofraction from alkaline picrites of sample 1308. The plateau is determined in the age spectrum with the age 598.1± 6.2 Ma (Fig. 2). The obtained data conform with the data for Chetlassky complex [1].

The isotope-geochemical researches confirmed that the magmatic rocks, namely alkaline picrites of alkaline-ultrabasic complex with carbonatites, were formed 598.1±6.2 Ma. The age level of complex formation is also supported by previous K-Ar researches of phlogopites of this complex.

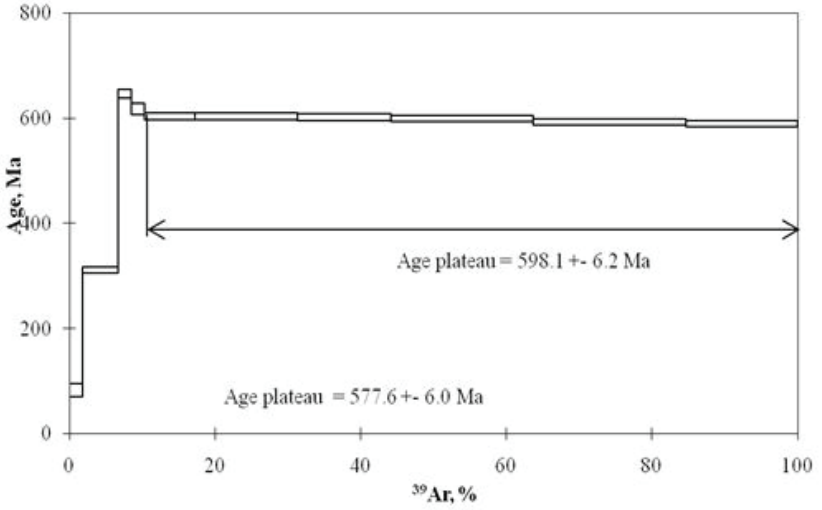

Figure 2: Age spectrum of phlopite (sample 1308).

In Middle Timan the impulse of plume (riftogenic) magmatism on Timan passive margin of East-European continent was reconstructed for this period. The generation of melts occurred in mantle conditions. The magmatic activity is connected to deposition of progressively abyssal magma-controlling fault structures.

This work is supported by Program of Fundamental researches UB RAS, project 12-П-5-2015.

References

1. Andreichev V. L., Stepanenko V. I. Age of carbonatite complex of Middle Timan // Works of Institute of geology of Komi branch of AS of the USSR. Issue 41. Syktyvkar: 1983. Ore formation and magmatism of Northern Urals and Timan. P.83-87.(in Russian)
2. Kostyukhin M. N., Stepanenko V. I. Baikal magmatism of Kanin-Timan region. Leningrad: Nauka, 1987. 232 pp. (in Russian)
3. Marakushev A. A., Tararin I. A., About mineralogical criteria of granitoid alkalinity//Izvestiya AS USSR. Geol. 1965. No 3. pp 20-37. (in Russian)
4. Nedosekova I. L., Udoratina O. V., Vladykin N. V., Pribavkin S. V., Gulyaeva T.Ya. Petrochemistry and geochemistry of dyke ultrabsites and carbonatites form Chetlassky complex (Middle Timan) / Ezhegodnik-2010, IGG UB RAS, issue 158, 2011, pp. 122-130. (in Russian)
5. Travin A. V., Yudin D. S., Vladimirov A. G, Khromykh S. V., Volkova N. I., Mekhonoshin A. S., Kolotilina T.B. Thermochronology of Chernorudskaya granulite zone (Olkhonsky region. Western Baikal region)//Geochemistry. 2009. V 11. pp. 1181-1199. (in Russian)
6. Vasilyev N. V., Udoratina O. V., Skorobogatova N. B., Borodulin G.P. Micas from Taykeu deposit (Polar Urals): structure and classification questions / Vestnik of Institute of geology of Komi SC UB RAS. Syktyvkar, 2012. No 1. (205). P.9-14. (in Russian)

GEOCHEMICAL PATTERNS OF THE BUYUKKIZILCIK (KAHRAMANMARAS) FLUORITE DEPOSITS

Uras Y., Caliskan V.

Kahramanmaraş Sütçü İmam University, Faculty of Engineering and Architecture, Department of Geological Engineering, 46050-9, Kahramanmaraş, Turkey; yuras@ksu.edu.tr

The aim of this study is to demonstrate the origin of fluorites that are located near the Dinari area in Buyukkizilcik (Kahramanmaras). Buyukkizilcik fluorites are spatially associated with the altered portion of the Permian Yoncayolu Formation and are also commonly hosted by the syenitic intrusions. Geochemical properties of the Buyukkizilcik fluorites have been investigated by characterizing their rare earth element (REE) compositions. The fluorite samples are poor in terms of their REE contents with REE abundances of the analyzed samples ranging between 0.45 and 11.99 ppm, whereas REE concentrations of the associated host-rocks vary between 0.01 and 17.30 ppm. When plotted on a Tb/La vs. Tb/Ca diagram, the fluorites lie within the field of hydrothermal stage indicating that they are likely formed by the contribution from hydrothermal fluids. The relative depletion of high-field strength elements (HFSE) and REE in the fluorites relative to their host-rocks indicates the influence of hydrothermal fluids on these elements. The negative anomalies observed in Eu and positive anomalies observed in Ce indicate low temperature (T) and low fO_2 conditions during formation. In addition, Sc/Eu vs Sr, (La/Yb)n–(Eu/Eup)n, Sc–SREE, (Tb/Yb)n–(La/Yb)n, Tb/Ca–Tb/La diagrams also provide important information regarding the origin of the Buyukkizilcik fluorites. As a result, the geochemical data and related plots presented in this study imply that the fluorites were formed from hydrothermal fluids within an alteration zone of an intrusion.

Keywords: Fluorite, REE, Buyukkizilcik, Geochemistry, Kahramanmaras, Turkey

THE ACCOUNTING POLICY PRACTICED BY THE MINING FIRMS IN THE COST OF MINING EXCAVATION

Utku Demirel B.

Akdeniz University, Department of Business Man., 07058, Antalya, Turkey

Mining is one of important engineering works. Mining and Geological Engineers' technical research and studies are very important for business profitability. However, when losses and gains balance in mining operations are emphasized, there is important financial condition has to be considered. The most important issue to be considered in the calculation of the cost is the distinction between the costs made until reaching the ore and starting to get the ore.

The excavation work is one of the studies made until reaching the ore is one of the factors that determine the balance of profit and loss. Correct use of cost accounting to be done here determines the profitability of the companies. Therefore, the costs of excavation should not be commentated with the cost of ore extracted from mine otherwise; seeming to be out of pocket is inevitable when it might be a profit for the firm.

Keywords: IFRS 6, Mining Enterprises Accounting, Excavation Costs

Introduction

Ore deposits have great importance in human life and in the development of countries. Most of the tools and materials we use in our daily lives are made from the ores that are dug out of the Earth's crust. Mining industry relies on the extraction of all kinds of ore, mineral and petroleum and considering its structural characteristics mining industry brings along different accounting practices.

When mining industry is considered from accounting practices point of view, it is apparent that, there has never been an accounting standard that is oriented to mining industry until recently. When considered from international accounting standards, until 2004 the accounting policies that entities, which operate in this industry, are to carry out were issued in International Accounting Standard 38 (IAS 38), Intangible Assets and International Accounting Standard 16 (IAS 16), Property, Plant and Equipment. Having been issued in 2004 and been in practice since 2006, Standard 6, Exploration for and Evaluation of Mineral Resources (IFRS 6) embodies regulations for this purpose and therefore shed light on accounting practices in mining industry.

Exploration for and Evaluation of Mineral Resources: IFRS 6 – VUK (Tax Procedure Law)

Standard 6, Exploration for and Evaluation of Mineral Resources (IFRS 6) came into force with the purpose of setting the reporting fundamentals related to the exploration and evaluation of mineral resources. For this purpose, it has focused on concepts such as exploration and evaluation assets and expenditures, processes of exploration and evaluation of mineral resources. According to the Standard, "cost price" should be used in the measurement of exploration and evaluation assets. Moreover, it is stated that the expenditures incurred before obtaining legal rights to explore and the expenditures incurred after proving the technical feasibility and commercial viability of extracting a mineral resource will not be considered as exploration and evaluation expenditures.

When Turkish tax legislation and general communique on accounting system application are analyzed in respect thereof, it can be seen that regulations related to the charging or capitalizing the expenditures arising from the exploration and development of ore and petroleum are not included. It only states to charge expenditures with *cost price.* According to tax laws, expenditures incurred while obtaining rights to explore petroleum, development costs and operational expenses are capitalized as *Intangible Assets.* According to VUK (Tax Procedure Law), it is of no importance whether the capitalized expenditure is ore exploration, development costs or entity expenses. All the expenditures incurred during the exploration and developments are capitalized as *Intangible Assets.* Expenses incurred by the purpose of obtaining the right to explore and capitalized with cost price are amortized by depreciation as long as the right to explore is retained. According to tax laws, it is also possible to charge the expenditures arising from mine businesses as direct expenditures.

The advantage of the expenditures incurred for the preparations for drilling an oil-well or removing vegetation for digging out the ores is that because the expenses are limited with the amount of oil or ore that can be dug out of that area, they are subject to depletion and they are reported as "Depletable Assets" in the Uniform System of Accounts that is in practice in our country. According to the Uniform System of Accounts, "Exploration Cost" is the sum with which the expenditure incurred for determining whether the ore deposit is suitable for business and the expenditure for petroleum exploration are monitored. If ore or oil reserve is found as a result of the exploration works, the expenditure can be amortized. Otherwise, these expenditures are charged as direct loss. Another sum among depletable assets is "Preparation and Development Expenses" with which the expenditures arising from the necessary processes that prepare the ore and oil for excavation such as removing the vegetation off of the mine, digging through the mine and dividing ore deposits into suitable parcels are monitored. Both sums are amortized by deprecation. The depreciation rate that will be applied to oil exploration and development expenses are separately determined by the Ministry of Finance considering the reserve condition (Karapınar et al., 2010, 65).

Cost Elements of Exploration and Evaluation Assets

According to IFRS 6, entities should develop an accounting policy for recognition of exploration and evaluation expenditures as assets and apply it consistently. While developing this policy, the entity should consider the point that to what extent expenditures can be related to the extraction of the mine resources. Examples of expenditures that can be included in the recognition of exploration and evaluation assets for the first time, which is also called cost elements, are as follows:

(a) Obtaining the rights to explore,

(b) Topographical, geological, geochemical and geophysical works,

(c) Exploratory drilling,

(d) Excavation,

(e) Sampling and

(f) Activities related to the determination of technical feasibility and commercial viability of extracting a mineral resource.

However, expenditures incurred for the development of mine resources shouldn't be recognized as exploration and evaluation assets. In the recognition of assets acquired as as result of devel-

opment activities, "Conceptual Framework Related to the Preparation of Financial Tables and Presentation Fundamentals" and "TMS (Turkish Accounting Standards) 38 Intangible Assets" should be taken as basis.

Classification of Exploration and Evaluation Assets

According to IFRS 6, entities should classify their exploration and evaluation assets as tangible or intangible assets considering their qualities and apply it consistently. While some exploration and evaluation assets are considered as intangible (rights to explore/drill), some are considered as tangible (vehicles and exploring/drilling equipment). When tangible asset is used to the extent of the development of intangible asset, the amount representing this usage becomes a part of intangible asset costs. Additionally, the use of tangible asset in the development of intangible asset does not make tangible asset an intangible asset.

Creation of Exploration and Evaluation Assets

In the determination of whether intangible asset created within the structure of an entity meets the criteria to be placed in financial tables; whether it can be defined as an asset that will probably be of benefit and if so when it was created and the reliable determination of asset's cost are evaluated within the framework of provisions related to intangible assets. The exploration and evaluation asset should be measured by cost price.

Expenditure incurred by the interim exploration activities should be monitored in 7/A option in "750 Costs of Exploration and Development" account. This account can be classified based on cost types and what it was spent on (Sağlam et al., 2009, 1285).

Example 1:

Entity X paid 2000 TL+ 360 TL VAT mining permit warrant fee as part of costs of exploration and development.

A; The entity did not find a useful reserve in that period. Accordingly the accounting record is;

750 RESEARCH AND DEVELOPMENT EXPENSES 2000

191 DEDUCTIBLE VAT 360

102 BANKS 2360

31.12

630 RESEARCH AND DEVELOPMENT EXPENSES 2000

751 REFLECTION ACCOUNT FOR RES. AND DEV. EXP. 2000

31.12

751 REFLECTION ACCOUNT FOR RES. AND DEV. EXP. 2000

750 RESEARCH AND DEVELOPMENT EXPENSES 2000

B; The entity found a useful reserve in that period. Accordingly the accounting record is;

271 RESEARCH EXPENSES 2000

751 REFLECTION ACCOUNT FOR RES. AND DEV. EXP. 2000

The Creation of Preparation and Development Costs

General communique on accounting system states, "Expenditures that activities such as removing the vegetation odd of the mine in open entities or digging down the underground ore deposits, establishing a constant contact between the deposit and above ground until the general mass is used up and separating the ore deposit into productive segments, vertical, horizontal and inclined path, course require; drilling wells, cleaning, deepening, completion or labor, fuel, repair and maintenance, shipping, supply, material etc. expenditures in petroleum operations are monitored in 272 Preparation and Development Costs account." According to aforementioned communique, when entities have such expenditures they should be monitored by being charged in 272 numbered account and once started production these expenditures must be included in inventoriable cost by means of amortization.

Example 2:

Entity X found 200.000 ton ore that can be dug out in the mine they were examining. In order to dig out the whole ore 300.000 m^3 earth need to be removed. A contractor charges 15,00 TL / m^3 for 300.000 m^3 pickling work. At the end of the year, 25.000 ton ore is dug out. (Inspired by http://www.mercekdenetim.com/makale/makale/5/)

Earth to be removed: 300.000 m^3

Ore to be extracted: 200.000 tons

Earth coefficient: 300.000 m^3 / 200.000 tons = 1,5 m^3 / tons

Accounting record of contractor's progress payment

272 PREPARATION AND DEVELOPMENT EXPENSES	4.500.000	
191 DEDUCTIBLE VAT	81.000	
102 BANKS		5.310.000

300.000 m^3 X 15,00 TL / m^3

Actual cost: 300.000 m^3 X 15,00 TL / m^3 = 4.500.000 TL

Average cost: 4.500.000 TL / 300.000 m^3 = 15 TL/ m^3

Depletion allowance: 25.000 tons x 1,5 m^3 / tons x 15 TL/ m^3 = 1.125.000 TL (4 year of amortisation)

730 GENERAL PRODUCTION EXPENSES	1.125.000	
278 ACCUMULATED DEPLETION		1.125.000

If the entity in question carried out the pickling itself, expenses related to preparation and development activities would have been collected in account 750 and be transferred to account 272 at the end of the period.

Depreciation (Amortization)

According to Tax Procedure Law, "upon the appeals of those who are concerned, cost prices or franchise fees of mines and quarries that lost material value resulting from the decrease in ore because of the entity are depleted at rates to be jointly determined by the Ministry of Finance and the Ministry of Industry considering the size of entities and qualities and differently for mines and quarries (VUK Article 316)".

Amortization rate can be found by the average of total reserve and useful life/annual processing capacity in the operating license. For example, if the total reserve is 50.000 tons and the annual processing capacity is 5000 tons the amortization rate is 5000 / 50.000 = %10 (Sağlam et al., 2009, 1293).

Example 3:

Mine entity X bought a mine for 50.000 TL and started production. It determined its annual amortization rate as %10. So the accounting record is;

730 GENERAL PRODUCTION EXPENSES	5000	
268 ACCUMULATED AMORTIZATION		5000

Conclusions

One of the biggest mistakes that entities operating in mine industry make in their accounting practices is that excavations carried out before finding the reserve are put in income table as interim expenditure and therefore transferred to interim loss. Such records reflect badly on the reliability of financial tables; and cause people who use these tables to make wrong decisions. Moreover, it results is misconceptions in the notion of periodicity which is the basic concept in accounting and cause entities to be subject to penal assessments by resulting in tax losses. For this reason, in mine entities, 271 Research Expenses and 272 Preparation and Development Expenses need to be recognized as expenditure by amortization with 278 Accumulated Depletion. Otherwise records that are kept as direct interim expenditure will result in unreal interim losses and therefore it may appear to be resource loss.

References

1. http://www.mercekdenetim.com/makale/makale/5/, "Maden İşletmelerinde Özellikli İtfa Yöntemi ve Muhasebe Kayıtları" (erişim tarihi: 08.09.2014) (in Turkish).
2. Karapınar, A, Zaif, F., Torun, S., (2010), "Maden İşletmelerinde Uygulanan Muhasebe Politikaları ve Uluslararası Finansal Raporlama Standardı 6'nın Getirdiği Düzenlemeler", *Gazi Üniversitesi İktisadi ve İdari Bilimler Fakültesi Dergisi 12/3 (2010). 43-68* (in Turkish).
3. Sağlam, N., Şengel, S., Öztürk B., (2009), TMS Türkiye Muhasebe Standartları Uygulaması, Maliye ve Hukuk Yayınları (in Turkish).
4. TFRS-6: Maden Kaynaklarının Araştırılması ve Değerlendirilmesine İlişkin Türkiye Finansal Raporlama Standardı, 2006, Resmi Gazete Tarihi: 31.01.2006 ve Resmi Gazete Sayısı: 26066 (in Turkish).
5. TMS-16: Maddi Duran Varlıklar Standardı, 2005, Resmi Gazete Tarihi: 31.12.2005 ve Resmi Gazete Sayısı: 26040 (in Turkish).
6. TMS-38: Maddi Olmayan Duran Varlıklara ilişkin Türkiye Muhasebe Standardı, 2006, Resmi Gazete

Tarihi: 17.03.2006 ve Resmi Gazete Sayısı: 26111 (in Turkish).

7. Vergi Usul Kanunu Madde: 316, 2003, Resmi Gazete Tarihi: 28.05.2003 ve Resmi Gazete Sayısı: 25121 (in Turkish).
8. 1 Seri no MSUGT, 1992, Resmi Gazete Tarihi: 26.12.1992 ve Resmi Gazete Sayısı: 21447(in Turkish).

THE GEOCHEMISTRY OF CHROMITITES IN ELDIVAN OPHIOLITE, ÇANKIRI (CENTRAL ANATOLIA, TURKEY)

Uner T.[1], Oghan F.[1], Cakır U.[2]

1Department of Geological Engineering, Yuzuncu Yil University, Van, Turkey (tcakici@yyu.edu.tr)
2Department of Geological Engineering, Hacettepe University, Ankara, Turkey

The Eldivan Ophiolite, exposed around Ankara and Çankırı cities, is located at the central part of the Izmir- Ankara-Erzincan Suture Zone (IAESZ). It represents fragments of the Neotethyan Oceanic Lithosphere emplaced towards the south over the Gondwanian continent during the Albian time [1]. It forms nearly complete series by including tectonites (harzburgites, rare dunites and pyroxenite), cumulates (dunites, wherlites, pyroxenites, gabbro and plagiogranites) and sheeted dykes from bottom to top. Imbricated slices of volcanic-sedimentary series and discontinuous tectonic slices of ophiolitic metamorphic rocks are located at the base of tectonites.

Tectonites constitutes the most important parts of Eldivan Ophiolite. Tectonites are generally formed by harzburgite with dunite and pyroxenite levels. In tectonites which have traces of plastic deformation (foliation, lineation and folding), the minerals display a distinct orientation as a result of intra crystallographic dislocation and grinding mechanism. The deformation degree represents gradually decreasing to the upwards. Ophiolitic chromitites originated from mantle peridotites in the form of veinlets, nodular and irregular bodies. Cr composition of Alpine Type chromitites show a wide variation of Cr composition (Cr # 33-85). The chromitite content show negative correlated with some major oxides such as Al_2O_3 and MgO. Chemical composition in Eldivan Ophiolite chromitites are two different origins. high content Cr# are crystallized out of boninitic melt in a subduction environment and thought to crystallized either low content Cr# from the MORB type melt in mid ocean ridge setting or back arc environment.

References

1. Akyürek, B., Bilginer, E., Dağer, Z., Soysal, Y., and Sunu, O., 1979. Evidences for the ophiolite emplacement around Eldivan-Şanabözü. Chamber of Geological Engineers, 9, 5-11 (in Turkish)

MINERALOGICAL-PETROGRAPHIC CHARACTERISTICS OF ULTRABASITE MASSIF IN THE NORTHERN KRYVBAS.

Velikanov Y.F., Velykanova O.Y.

M.P. Semenenko Institute of geochemistry, mineralogy and ore formation of NASU, Kiev, Ukraine
olgavelikanova1@rambler.ru

Reconnaissance and exploration programs of the "Kryvbasgeologia" Enterprise resulted in discovery of the lense-like ultrabasic body, about 1 km × 80-100 m in size, invaded the metamorphic rocks of the Kryvy Rig series 8 km west from the Pervomaysk iron mine. The body strikes submeridionally, dips steeply and intersects bedding of the host strata.

The host rocks are composed by quartz-biotite, quartz-biotite-chlorite and two mica schists, quartzites and quartz-calcareous rocks of the Gdantsi suit of the Kryvy Rig series.

The ultrabasic body consists of antigorite serpentines, and serpentine-tremolite, actinolite-tremolite and chlorite schists.

The antigorite serpentinites macroscopically represent green-grey to dark-green rocks locally spotted with circlelike and streaky pattern. Microscopically, the rocks consist of relics of olivine (10-40 %), antigorite (20-65 %), chrysolite (5-10 %), carbonates (3-8 %), chlorite (8-10 %) and magnetite (5-7 %). The serpentinites are intersected by veinlets of light-green serpophite and carbonates. Structurally the rocks are needle-, leaf-like and lamellar, fine- to middle-crystalline.

Serpentine-tremolite schists are green-grey middle- to fine-crystalline schistose rocks consisting of relic olivine (10-15 %), and tremolite (30-35 %), antigorite (15-20 %) and chlorite (20-30 %). Rarely, they include thin sulfides (pyrite and pyrrhotite) and magnetite, and thin carbonate veinlets and nests.

Actinolite-tremolite schists are macroscopically fine- to middle-crystalline dark-green schistose rocks consisting of lamellar actinolite and tremolite. Pyroxenes, carbonates and magnetite form scarce microscopic mineralization. Irregularly, the schists are chloritized.

Chlorite schists represent dark-green lamellar slightly schistose rocks, composed by chlorite lamellas, 2-3 mm in size. Microscopically, the rocks are composed by chlorite with a minor amount of actinolite, tremolite and carbonates. The rocks include scarce magnetite crystals.

5 samples of the ultrabasic rocks of the massif were investigated using chemical analysis. In ACFM diagram the described rocks are scattered in the frame of peridotite field. A relic structures of the rocks show that primarily the rocks consisted of olivine and pyroxene that suggest that the primary rocks were represented by peridotites and pyroxenites.

5 rock analyses are insufficient amount to provide complete conclusion on petrochemical characteristics of the rocks studied. However they demonstrate several important petrochemical characteristics which were used to generate several preliminary conclusions.

M/F petrochemical coefficients from 5.7 to 5.3 are near those characterizing the peridotite rock composition. A femic index b of 60.2 and 60.5 is also close to the values typical to the ultrabasic

rocks of the peridotite formation. The virtual characteristics z, y, x show the presence of olivines, ortho- and clinopyroxenes. Other petrochemical characteristics have the values as follow: the magnesium index – 72 and 75 %, alkalinity index – 0.9 and 1.0 %, TiO2 content – does not exceed 1 %. These and mineralogical composition of the rocks are a basis to relate the ultrabasites studied to the derivatives of the peridotite magma.

Semiquantitative spectral analyses of the ultrabasic rocks of the massif demonstrate increased concentrations of Ni, Co and Cr. In average, antigorite schists contain from 0.22 to 0.64 % Ni, 0.02 % Co, 0.3 % Cr; serpentine-tremolite schists: 0.16 % Ni, 0.01 % Co, 0,2 % Cr; actinolite-tremolite schists: 0,14 % Ni, 0,01 % Co, 0,4 % Cr; chlorite schists:

0,07 % Ni, 0,003 % Co, 0.2 % Cr. Cu is detected at negligible concentrations.

Ni is accumulated in pentlandite, millerite and nikeline. Cobaltite and Co-pyrite concentrate both Co and Ni. Summarizing, the ultrabasic rocks of the massif may represent a prospective interest for Ni, Co and Cr.

COMPARATIVE CHARACTERISTICS OF ULTRABASITES OF THE DEVLSDIVSKA FAULT ZONE AND VYSOKOPILSKA STRUCTURE (FORE-MIDDNIEPRIAN)

Velykanova O.Y., Velikanov Y.F.

M.P. Semenenko Institute of geochemistry, mineralogy and ore formation of NASU, Kiev, Ukraine
olgavelikanova1@rambler.ru

Ultrabasic rocks in the Kryvy Rig structure are widely found along the Devladivska fault zone and Vysokopilska structure. Ultrabasic bodies are also known in the Pervomaysk and Lenin mines.

A strike of the Devladivska crustal-scale fault zone is latitudinal. It represents a 5 km wide system of latitudinal faults striking east from the Kryvy Rig – Kremenchug meridional structure over 50 km. The zone controlled an invasion of 9 different in size massifs of the ultrabasic rocks in the area studied.

Starting from mineralogical composition, the ultrabasic rocks include dunites, olivinites, peridotites (harzburgite, lherzolite, and verlite), plagioclase-bearing peridotites and olivine peridotites.

From geological-structural signatures and petrological-geochemical characteristics, 2 groups of the Devladivska zone rocks are divided.

The first group ultrabasic rock (the Ternovka area) composes the Veseloternovsky, Pryvorotnensky, Promezhutochny and Kodaksky massifs. This group ultrabasites is intensively altered during later metamorphic events to serpentinitized and talcifcated peridotites interlayered by serpentinites serpentine-talc, actinolite-tremolite and chlorite schists and talc-carbonate rocks.

This group rocks are of low magnesia at low content of alkalis, titanium, calcium and alumina, suggesting about their derivation from picritic magma (hypermagbasites by N.D. Sobolev classification).

The second group (Devladivsky area) includes the rocks of Vod'ansky, Devladivsky and Krasnoyarsky massifs, and a group of small massifs named as the Gulaypolsky massifs. They consist of peridotites, olivine gabbro, pyroxenites, gabbro-norites and amphibole schists.

These rocks are insignificantly altered during late postmagmatic processes. The ultrabasic rocks include high concentration of titanium, calcium, alumina, alkalis at low magnesia, suggesting the rock derivation from subalkaline gabbro-peridotite magmas (ultraferbasites).

The Vysokopilska structure consists of the ultrabasite-metabasite formation shaped as the band extended 35 km length at 1.5-2.5 km wide. Plenty and steeply dipping ultrabasite bodies, from 100 m to 2.5 km length and up to 300 m wide, form two parallel ranges.

Large ultrabasite bodies are well zoned and composed by antigorite serpentinites in central parts and serpentinecarbonate-talc, antigorite-actinolite-tremolite and chlorite schists in the peripheries. A small ultrabasite bodies commonly intensively altered to talc, actinolite-tremolite-talc,

antigorite-actinolite-chlorite and chlorite schists. Generally, the ultrabasic rocks contain significant concentrations of Ti, Al, Ca, increased alkali and low magnesia, suggesting about their ultraferbasite composition.

A comparison of the alterations of ultrabasites of the Ternovsky, Devladivsky and Vysokopilsky fields show that the Ternovsky and Vysokopilsky massifs intensively serpentinized, chloritized, carbonatized and talcificated. The Devladivsky massif is less altered, and in part amphibolitized and phlogopitized. These type of alterations almost not occur in the Ternovsky and Vysokopilsky massifs.

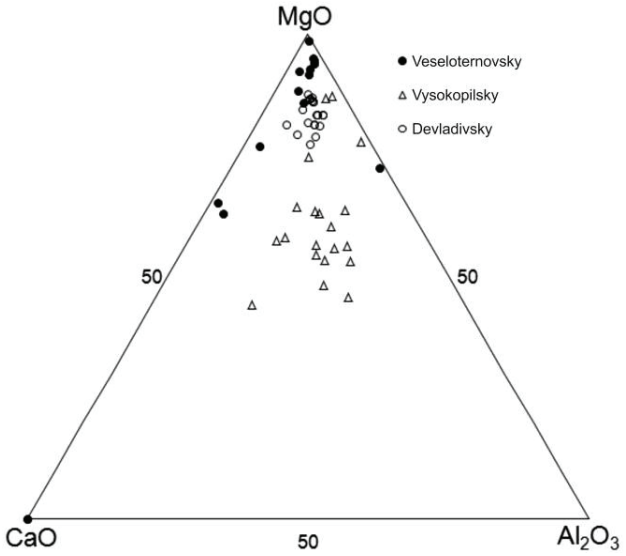

Figure 1: Distribution of the figurative points of chemical compositions of the ultrabasites in the discrimination diagram CaO-MgO-Al_2O_3.

Captions: 1 – Veseloternovsky; 2 – Devladivsky; 3 – Vysokopilsky.

Comparison of petrochemical characteristics was performed for the Veseloternovsky, Devladivsky and Vysokopilsky massifs (Table 1).

Chemical compositions, discrimination diagram CaO-MgO-Al_2O_3 (Fig.1) and chemical indices (Table 1) show that the Vysokopilsky ultrabasites are highly ferrous and siliceous. The Ternovsky ultrabasites have much lower values of these parameters whereas the Devladivsky rocks have the intermediate position. Magnesia is decreased from Ternovsky to Vysokopilsky ultrabasites. The alkalinity is different, but the lowest values demonstrate the Ternovsky ultrabasites, whereas in the Vysokopilsky and Devladivsky rocks it always exceeds 1.

Calculated petrochemical indices of the ultrabasic rocks

Table 1:

Veseloternovsky massif											
	M/F	b	2c	s	h	x	y	z	Km	Kf	Ka
from	6.4	44.2	0.5	27.6	12.4	0.8	0.0	30.7	90.4	5.3	0.0
to	13.4	71.2	3.4	54.3	46.5	15.9	34.4	96.2	94.7	9.6	1.5
average	9.7	61.7	1.7	36.6	31.0	8.8	12.9	78.3	92.6	7.4	0.6
D evladivsky massif											
	M/F	b	2c	s	h	x	y	z	Km	Kf	Ka
from	4.3	46.7	2.5	36.2	3.4	0.3	11.6	18.8	83.4	9.2	0.0
to	7.5	59.8	12.6	43.6	47.1	31.3	70.7	71.1	90.8	16.6	2.89
average	5.4	54.9	5.1	39.9	19.1	15.1	37.7	47.2	86.7	13.3	1.1
Vy sokopilsk y massif											
	M/F	b	2c	s	h	x	y	z	Km	Kf	Ka
from	2.2	40.3	4.5	37.6	5.5	2.72	10.3	6.28	72.9	10.5	0.1
to	6.3	57.8	17.4	45.3	42.38	68.4	89.9	63.7	89.5	27.1	2.6
average	3.2	48.0	10.1	41.7	24.0	32.07	47.06	20.87	79.2	20.79	1.02

Thus, the Vysokopilsky ultrabasites are petrologically similar to the Devladivsky ultrabasites whereas the Ternovsky ultrabasites are significantly different, suggesting difference of the magma composition.

The ultrabasites studied contain increased concentrations of Ni, Co, Cr, Cu and Au, which may represent a prospective significance.

Residual soils of the Ternovsky, Devladivsky and Krasnoyarsky massifs represent the largest deposits of Ni composed by Ni-silicates. All the deposits are complex-type, with economic concentrations of Co.

Geochemical analyses may suggest a presence of Ni-Co sulfide ores connected with the massif studied, which represent a future prospective interest.

RARE EARTH ELEMENT AND NIOBIUM ENRICHMENTS IN THE ELK CREEK CARBONATITE, USA

Verplanck, P.L.[1], Kettler, R.M. [2], Blessington, M.J. [2], Lowers, H.A. [1], Koenig A.[1], E., Farmer, G.L. [3]

1 US Geological Survey, Denver, Colorado, USA
2 Department of Earth and Atmospheric Sciences, University of Nebraska, Lincoln, Nebraska, USA
3 Department of Geological Sciences, University of Colorado, Boulder, Colorado, USA
plv@usgs.gov

The multilithologic Elk Creek carbonatite and associated alkaline intrusive units are located in southeastern Nebraska, USA. The carbonatite, reported to be the largest niobium resource in the United States, contains zones enriched in rare earth elements (REEs). This intrusive complex is buried by more than 200 m of Pennsylvanian marine sedimentary rocks and Quaternary glacial till. Alkaline intrusive units associated with the carbonatite include syenites and subordinate mafic dikes. The carbonatite and alkaline intrusives intrude into Precambrian granite and gneiss on the eastern margin of the Mid-Continent rift where the rift has been offset by one of a series of southeasterly trending structures. Age determinations of the carbonatite range from ~ 500 to 570 Ma.

In 1970, a geophysical anomaly associated with the carbonatite was identified, and the following year the carbonatite was discovered when drilled by the state of Nebraska. Between 1973 and 1986, Molycorp undertook an extensive exploration program at the site, including over 100 drill holes that amassed ~46,800 m of core. Our study utilizes a subset of the archived Molycorp drill cores to evaluate REE enrichment in carbonatites. Molycorp geologists divided the carbonatite into three primary lithologies: apatite beforsite, barite beforsite, and magnetite beforsite; beforsite is a dolomite-rich carbonatite [1, 2]. Brecciated carbonatite is also present in some of the cores, and much of the carbonatite was overprinted by various fluids. Zones of ferruginous alteration resemble "rodbergite" as described at the Fen complex, Norway.

The apatite beforsite is the most voluminous carbonatite unit in the Elk Creek complex; it consists of dolomite and apatite with variable amounts of quartz, fluorite, phlogopite, pyroxene, chlorite, feldspar, magnetite, sulfides, barite, and REE-rich phases. Zones enriched in pyrochlore (the primary Nb host mineral) or REE-phases occur quite sporadically. Apatite is either disseminated or occurs in narrow bands. The magnetite beforsite consists of dolomite, magnetite, ilmenite, hematite, barite, and quartz, with variable amounts of rutile, apatite, fluorite, phlogopite, pyroxene, sulfides and pyrochlore. Much of the magnetite beforsite is brecciated, with magnetite beforsite occurring as clasts and/or as the matrix. The barite beforsite is the least voluminous lithology; it consists of dolomite, barite, and quartz with minor or variable apatite, fluorite, phlogopite, pyroxene, feldspar, chlorite, sulfides, and contains the highest abundance of REE phases. The barite beforsite primarily occurs as veins and dikes, a few millimeters to meters in width, but thicker zones (tens of meters thick) have been identified in a few cores.

Recent work has documented a range in REE concentrations and patterns within the carbonatite. The chondrite-normalized REE patterns of apatite beforsite samples display a typical carbonatite pattern (Fig. 1) with moderate light REE enrichment (La 118-1780 ppm), no Eu anomaly, and a negative slope. Samples of apatite beforsite with the highest LREE content (> 500 ppm

La) contain late-stage fluorocarbonates (parasite, synchysite, and bastnäsite) and phosphates (monazite). The fluorocarbonates occur as clusters of fine needles, sometimes in a radiating morphology, which were first identified during the Molycorp exploration studies. Similarly, the monazite occurs as fine needles, in radiating or random orientations. The barite beforsite contains the most REE-rich zones within the Elk Creek carbonatite with La as much as 53,100 ppm, Ce as much as 66,900 ppm and Nd as much as 13,100 ppm; their chondrite-normalized REE patterns display typical carbonatite REE patterns (Fig. 1). Similar to the apatite beforsite, samples of barite beforsite with the highest LREE content contain late-stage fluorocarbonates and phosphates. The magnetite beforsite, the carbonatite unit that contains much of the Nb mineralization, has an anomalous REE pattern displaying enrichment of the more valued middle and heavy REEs (Eu, Gd, Tb, and Dy) relative to lower mass La, Ce, and Nd, and higher mass Tm, Yb, and Lu (Fig. 1). Studies are underway to determine the hosts of these elements in the magnetite beforsite.

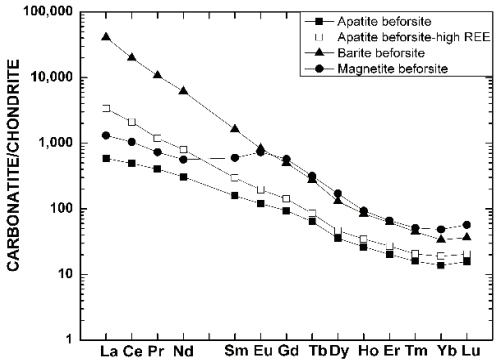

Figure 1: Chondrite normalized rare earth element diagram displaying various carbonatite lithologic units of the Elk Creek carbonatite. Median values used for apatite beforsite, apatite beforsite-high REE, barite beforsite, and magnetite beforsite.

The primary Nb mineral phase is pyrochlore, and three generations of pyrochlore have been identified based on size, morphology, and composition [2]. The first generation primarily occurs in the apatite beforsite and consists of large (0.1mm-2mm diameter), euhedral grains that display complex concentric zoning controlled by substitution of Ta for Nb. The second generation pyrochlore, occurring in most of the carbonatite lithologies, consists of euhedral to subhedral, unzoned grains ranging from 10-50 μm in longest dimension. The third generation of pyrochlore is associated entirely with a magnetite beforsite unit and occurs as an accessory phase in nearly all intercepts of this rock. These pyrochlore grains are typically less than 10μm in longest dimension, occurring as anhedral inclusions and aggregates in ilmenite, rutile, and magnetite or as subhedral-to-anhedral disseminations.

In our study, the chemical compositions of 25 samples of various carbonatite lithologies were determined to characterize general features of the carbonatite. The samples were integrated pulps from ten-foot core intervals. The apatite beforsite has the highest P_2O_5 concentrations (up to 3.7%), but La is not correlated with P_2O_5, suggesting that apatite concentration does not control the high REE abundance. This is consistent with the observation of fluorocarbonates in high

REE zones. Fluorine concentrations are variable (up to 39,100 ppm), and do not correlate with La or Ce. Fluorite likely controls the fluorine budget and masks the presence of fluorocarbonates. In the magnetite and barite beforsite, barium concentrations are higher (24,800 to 83,400 ppm) than in the apatite beforsite (500 to 34,200 ppm). From our limited samples, the highest Nb concentration (12,400 ppm) was found in an apatite beforsite sample, and the magnetite beforsite samples (n=5) had the highest median Nb concentration (6800 ppm, compared to 470 ppm for the apatite beforsite). Further work by utilizing microanalytical methods is underway to better constrain which minerals control the REE budget in each carbonatite lithology.

Acknowledgements: This work was supported by the US Geological Survey's Mineral Resources Program, in part through the MRP External Research Program. We greatly appreciate the effort of Matt Joeckel, University of Nebraska-School of Natural Resources, for providing access to the archived core and to Tony Mariano for lively discussions of carbonatite petrology.

References

1. Mariano, A.N., 1975, Descriptive of petrography of selective drill core from ST-2, Elk Creek, Nebraska: confidential report to Molycorp Inc. May, 1975, 22 p.
2. Mariano, A.N., 1978, A summary of petrology and niobium mineralization in drill core from EC-11 and EC-15, Elk Creek, Nebraska: confidential report to Molycorp Inc. December, 1978, 64 p.

GEOCHEMISTRY AND GENESIS OF KATUGIN COMPLEX OF RARE-METAL ALKALINE GRANITES

Vladykin N.V.

Institute of Geochemistry, SB RAS, Irkutsk, Russia
vlad@igc.irk.ru

The Katugin complex of alkaline granites is located in the south part of the Western Aldan (Eastern Siberia) in the Kalar Ridge. The complex is small, it consists of two outcrops – Western and Eastern (Bykov et al., 1989). The Eastern massif is subdivided into two blocks. The zircon age of the complex (data by A.B. Kotov) is estimated as 2 Ga. Close to the Katugin complex there is a vast Kalar complex that includes rapakivi granites covering over 1000 km^2. There is the Ulkan complex of rapakivi granites with an area of over 1000 km^2 in the Amur Region. The second phase of alkaline granites (1728 Ma) that is that is genetically related to rapakivi granites and mineralization being similar to the Katugin complex is found inside the complex of rapakivi granites (Nedashkovskyi, 2003). We suggest that the Katugin alkaline granites are genetically related to the rapakivi granites. However, these granites are younger.

The Katugin rare-metal alkaline granites include medium-grained rocks with the massive texture. The porphyry-like varieties with potassium feld spar phenocrysts are found as well. The granites are composed of quartz, microcline, albite and dark-color minerals (aegirine and arfvedsonite). Rare metal zircon and pyrochlore occur as accessory minerals. In terms of the chemical composition the granites are agpaitic with the agpaitic coefficient (Ka) being up to 1.4. The varieties demonstrating Ka=1 are observed as well. The mica of lepidomelane composition occurs here.

The earlier researchers (Bykov et al., 1989) believed that the rare-metal occurrence was associated to near-fault metasomatites. The recent petrologic-geochemical and thermobarogeochemical studies confirmed the magmatic genesis of ore-bearing alkaline granites. Alkaline granites are enriched in volatile components (fluorine), alkalies and rare elements, thus their magma is active and fenites up to 1 m are produced at the contacts with host gneisses. As opposed to granites proper the accessory mineralization of fenites includes thorite and fluorite.

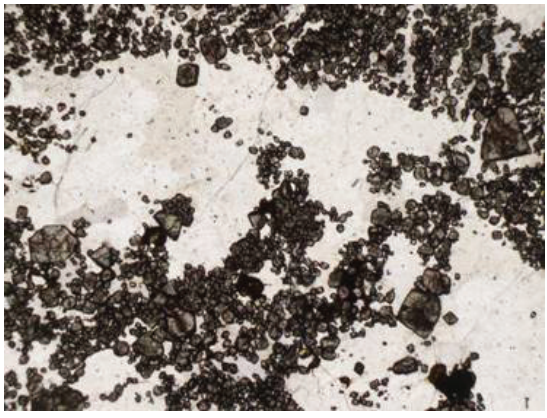

Figuer 1: Cumulate zircon crystals in the Katugin granite (thin-section, magnification 3X).

The melt-fluid that is residual from crystallization of alkaline granites forms the schieren-like body in the apical part of the Eastern complex and is composed of cryolite, gagarinite, other alkaline fluorides and feld spars while the dark-color minerals include arfvedsonite and lepidomelane. The early magmatic origin of zircon and pyrochlore confirm the magmatic genesis of granites. The Katugin complex shows an anomalous phenomenon: cumulate of early crystals of zircon and pyrochlore. In the pile of the adit we have found fine-banded granites; their bands are composed of separate zircon grains (to 50% of the rock) (Fig. 1).

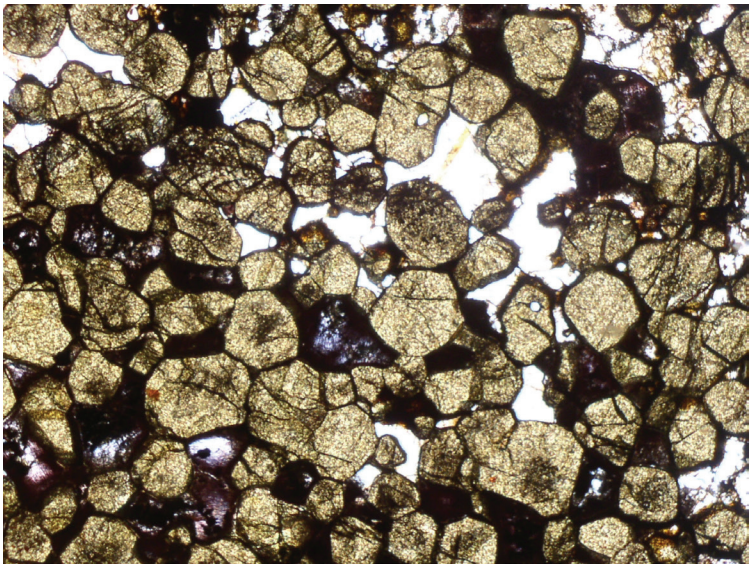

Figuer 2: Aggregates of the cumulate cuboctahedron pyrochlore crystals in the Katugin granite (thin-section, magnification 3X).

Those bands were generated when early zircon crystals were cumulate. In addition to zircon the ilmenite and pyrochlore grains are found as well. We have also found a horizontal body (up to 1 m) consisting of separate pyrochlore grains (cuboctahedrons). Their share reaches as high as 95% (Fig. 2). In addition to pyrochlore separate zircon grains are also observed. We can observe here the separation of early faceted pyrochlore crystals. Similar unites composed of brown zircons - cytrolite are found in Ukraine in the South-Kalchik (Azov deposit), layered Yastrebetsk complex (Azov rare-metal deposit, 2012). They compose the significant ore occurrences. As opposed to the Katugin granites the zircons were separated in those complexes from the alkaline syenite magma.

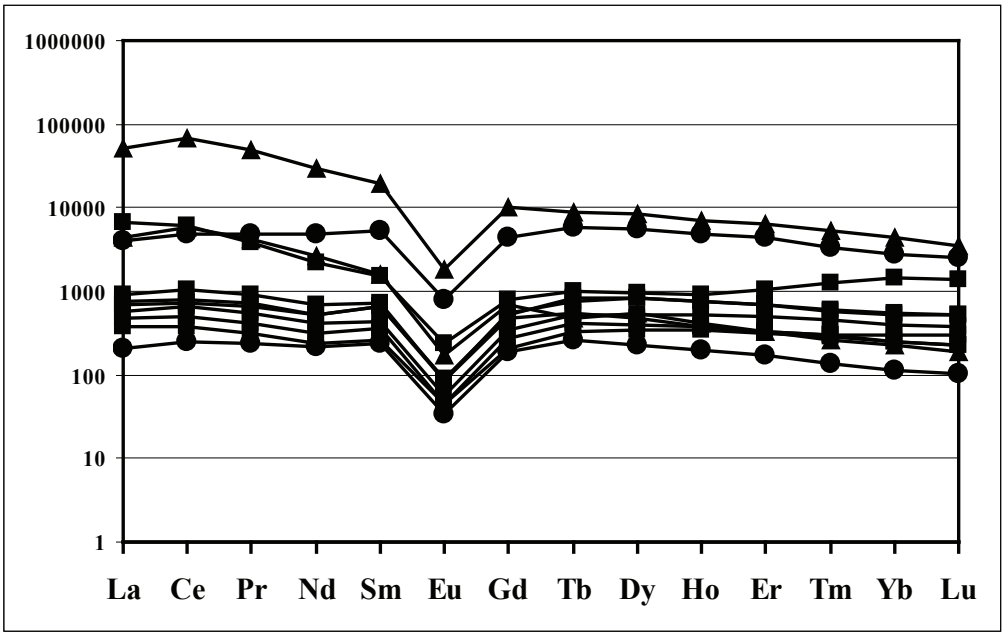

Figuer 3: TR spectra of rare-metal granites

Figure 3 indicate that TR spectra of rare-metal granites are almost uniform. A slight slope of the spectrum curves and a characteristic Eu-minimum are typical of them. The host non-altered amphibolites and syenite porphyries show almost a chondrite-like TR spectrum without Eu fractionation. The highest TR contents are typical of the pyrochlore occurrence and fluid-hydrothermal rocks with cryolites and gagarinite (two upper plots). The near-contact fenites show lower TR contents as compared with granites (three lower plots). However, their spectrum curves are similar to those of granites that evidences that the granites served as TR source.

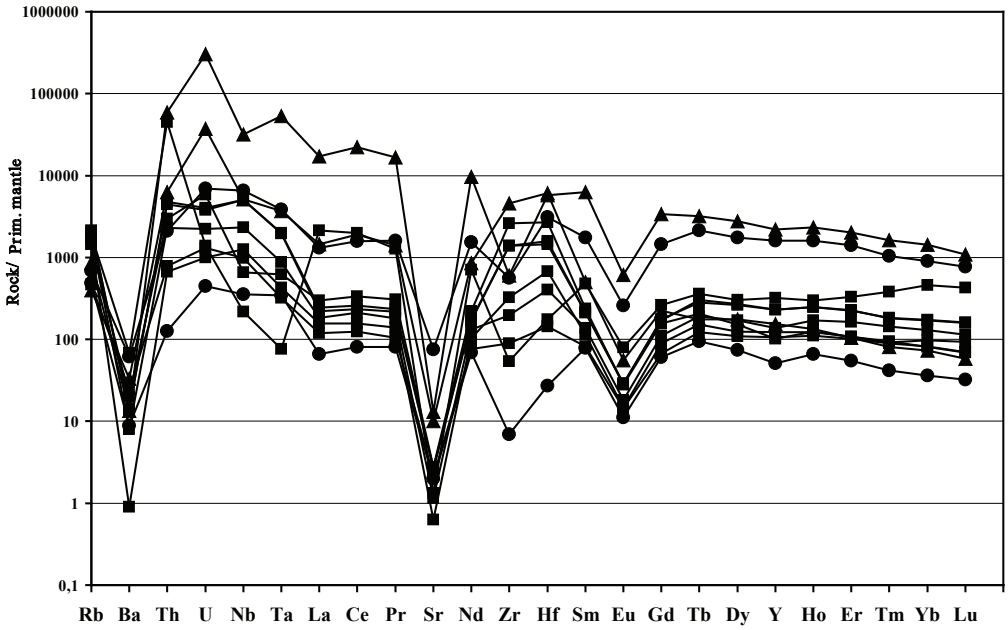

Figure 4: Spider diagrams of rare-metal granites.

Spider diagrams (Fig. 4) of rare-metal granites and near-contact metasomatites (fenites) (three lower spectra) are significantly different. They demonstrate lower concentrations of rare elements with negative and positive yttrium anomalies and different U, Th, Nb, Ta etc. variations. The spectrum curves of the non-altered host rocks are almost horizontal.

Geologic, geochemical and thermobarogeochemical data confirm the magmatic genesis of rare-metal rocks and ores of the Katugin deposit.

THE NGUALLA RARE EARTH ELEMENT DEPOSIT, TANZANIA

Witt W.K.[1], Hammond D.P.[2], Townend R.[3]

1 The Walter Witt Experience, 122 Edward Street, Bedford WA 6052, Australia
2 Peak Resources Limited, 2/46 Ord Street, West Perth, WA 6005, Australia
3 Roger Townend and Associates, 4/40 Irvine Drive, Malaga, WA 6090, Australia
wittww@iinet.net.au

The Ngualla carbonatite complex in southwest Tanzania contains Proven and Probable Reserves of 20.7 million tonnes at 4.54% total rare earth element oxides at a 3% cut-off (Peak Resources, 2014), contained within the Bastnaesite Zone. The resource is one of the world's largest and highest grade rare earth deposits. The REE resource has low Th and U contents and is amenable to further concentration through acid leaching and solvent extraction processes. The carbonatite complex also contains concentrations of phosphate and niobium that are being assessed for their economic viability. Rare earth elements were concentrated in two stages. In-situ fractionation concentrated rare earths as bastnaesite and synchesite in miarolitic cavities achieving grades of 1 to 2% TREO. Further upgrading to >3% TREO resulted from weathering during which $CaCO_3$ and $MgCO_3$ were leached from the host rock leaving a porous rare earth-enriched mass of goethite and barite.

The Ngualla carbonatite complex has a circular outline with a diameter of approximately 4 km by 3.5 km and is probably pipe-like in form. The age of the intrusive complex is uncertain but a K-Ar age of 1,040 (±40) Ma for igneous biotite was determined by Cahen and Snelling (1966). Surrounding Precambrian country rocks (gneisses, quartzites and rhyodacitic volcanics) have been hydrothermally altered to alkali feldspar, biotite and riebeckite by K- and Na-rich fluids expelled by the crystallizing carbonatite magmas. The resulting "fenite" alteration zone produced by this process is up to 1km wide, is relatively resistant to erosion and therefore forms a ring of hills surrounding the carbonatite intrusion.

The complex comprises a central plug of magnesiocarbonatite that intruded an annular calcite carbonatite. Calcite in the calcite carbonatite, and is accompanied by variable phlogopite, richteritic amphibole, magnetite, apatite and minor to trace ilmenite, monazite and sulphides (mainly pyrhhotite). Magnesiocarbonatite is predominantly ferroan dolomite with miarolitic cavities containing quartz, calcite, barite, fluorite and rare earth fluorocarbonate minerals (synchesite, bastnaesite). The abundance of these minerals appears to increase inwards from the margins of the magnesiocarbonatite plug. Segregations of hematite – barite form ovoid to irregular bodies up to several metres within the central part of the magnesiocarbonatite plug. Sulphides, where present, are minor and pyrite is dominant. The calcite carbonatite and magnesiocarbonatite can be distinguished by their Ba/P ratio (Ba/P >77 in magnesiocarbonatite). In addition to the carbonatite phases, several silicate-rich phases have been distinguished within the complex. These are generally poorly exposed but can be recognised as strong magnetic anomalies. Silicate-rich phases are olivine-bearing ultramafic rock and mica-rich glimmerite. Exploration drilling and outcrops present extensive structural and textural evidence for mingling between carbonatite and silicate-rich magmas.

Rare earth elements (REE) are concentrated in the magnesiocarbonatite as fluorocarbonate minerals (synchesite and bastnaesite). Within the unweathered magnesiocarbonatite, %TREO increase inwards from about 0.5% or less in the outer plug to 1 to 2% in the centre. In addition to synchesite and bastnaesite, the central magnesiocarbonatite contains one or more of quartz, calcite, fluorite and barite in miarolitic cavities that are interstitial to ferroan dolomite crystals. Rare earth elements, along with other chemical components rejected by ferroan dolomite (Si, Ba, F), were enriched by *in situ* fractional crystallization of the magnesiocarbonatite magma. Local, very high primary %TREO grades (3 to 5%) are found in proximity to some ultramafic units; however, this rare earth element enrichment is not present in proximity to all ultramafic units. The magnesiocarbonatite is characterised by lower HREE/LREE compared to the calcite carbonatite. Phosphate concentrations in the central magnesiocarbonatite plug are characteristically <0.5% although there is minor enrichment (to about 1%) where the carbonatite contains inclusions of the same ultramafic unit associated with TREO enrichment (see above).

The calcite carbonatite is the main source of phosphate, as apatite and monazite. Total rare earth oxide (REO) concentrations in the calcite carbonatite are generally <0.25% and are concentrated in monazite. Aggregates of water clear, colourless to pale yellow crystals of apatite formed at contact zones between carbonatite and phlogopite-rich glimmerite where these two magmas mixed and mingled, resulting in concentrations as high as 6% P_2O_5.

Economic mineralisation at Ngualla is closely related to weathering, for all commodities. Different modes of weathering highlight compositional differences between calcite carbonatite and magnesiocarbonatite. Outcrops of calcite carbonatite are relatively fresh since weathering proceeds mainly by dissolution of calcite, and calcite carbonatite is recessive in outcrops where calcite carbonatite and "ferrocarbonatite" occur together. The central magnesiocarbonatite plug is partly obscured by ferricrete, which now forms a ridge as a result of topographic inversion. Where exposed to erosion, magnesiocarbonatite weathers through oxidation of $FeCO_3$ and dissolution of $MgCO_3$ and $CaCO_3$ components of ferroan dolomite. This process results in significant mass reduction and a porous goethite-rich regolith unit with very low S.G. (1.84). Quartz, barite and rare earth minerals are unaffected by weathering and are residually enriched in the goethite-rich regolith. Further oxidation of goethite to hematite involves a volume reduction of 27% and a more compact, higher density rock (S.G. ~2.28) but does not seem to result in further upgrading of rare earths. Weathering of the Ngualla magnesiocarbonatite is concentrated in several north- to northeast-trending zones that probably reflect structurally weak fracture or fault zones, and is also apparently concentrated along some contacts between carbonatite and ultramafic units.

The *Bastnaesite Zone* is located within a broader volume of magnesiocarbonatite, known as the*Southern Rare Earth Zone.* It is centred on Mount Ngualla where rare earth mineralisation is hosted by *in situ* iron oxide and barite-rich weathered magnesiocarbonatite and underlying fresh magnesiocarbonatite. The depth of weathering is extremely variable. Grades of >3% total REO are common within the iron oxide-rich material, which extends from surface to depths of up to 140 metres. Petrographic studies of the iron oxide-rich material indicate that rare earths are present as bastnaesite and synchesite and that *in situ* weathering of the magnesiocarbonatite has not significantly modified the rare earth mineralogy relative to the primary source. Upgrading of rare earth content in the regolith by up to 300% is caused by residual concentration of rare earth minerals (bastnaesite, synchesite) resulting from the mass reduction following dissolution of $CaCO_3$and $MgCO_3$ and conversion of $FeCO_3$ to goethite (hydrated iron oxide). RC drill

chips recovered from the iron oxide-rich ore zone typically comprise residual goethite dust and insoluble barite with characteristic negative crystal shapes produced by the breakdown of ferroan dolomite. East of the Bastnaesite Zone but within the broader *Southern Rare Earth Zone*, a relatively minor rare earth resource is hosted by colluvium deposited in an erosional channel incised into the outer margin of the magnesiocarbonatite. In contrast to the mineralogy in the central "ferrocarbonatite" plug and its overlying regolith, rare earths in the colluvium are hosted by monazite and lesser cerianite, as well as bastnaesite. This colluvium was probably formed partly by erosion of adjacent calcite carbonatite. Rare earths are also concentrated in the *Southwest Alluvial*s, a Recent alluvial deposit derived from the central "ferrocarbonatite" plug and adjacent areas of calcite carbonatite. Consequently, rare earths in the alluvial channel are hosted by variable proportions of bastnaesite, monazite and cerianite.

No phosphate resource has yet been estimated but primary apatite in calcite carbonatite has been upgraded by weathering in the *Northern Zone*. Residual mineral concentration following dissolution of calcite resulted in upgrading of primary apatite concentrations from about 6% $P_2O_5$to produce residual phosphate concentrations of >20% P_2O_5. Apatite is accompanied by fine-grained goethite and variable amounts of other insoluble minerals (phlogopite, amphibole, magnetite) but coarse, idioblastic magnetite (commonly pseudomorphed by hematite) is the most consistent additional mineral. Triangular (mCaO – mMgO – mFeO+mMnO) plots support field and petrographic observations that many drill intervals within this residual apatite mineralisation consist of essentially apatite and magnetite and the P_2O_5 grade can be directly related to %CaO. Two generations of apatite can be recognised: residual primary apatite and secondary apatite infill. Secondary apatite, re-deposited from downwardly percolating groundwater, is tentatively identified as stafflerite, the low-temperature form of the mineral. The residual apatite – magnetite unit is partly overprinted by near surface ferricrete resulting in the introduction of secondary goethite and hematite from groundwater and an increase in the concentration of iron at the expense of the P_2O_5grade. Rare earth grades in the residual apatite – magnetite unit are generally in the range 0.5 to 3% REO. Residual primary apatite contains approximately 0.5% rare earth oxides and is probably the main source of rare earths but grades additionally reflect the presence of monazite (residual from calcite carbonatite), minor synchesite (derived from nearby magnesiocarbonatite?), and secondary rare earth-bearing minerals, including cerianite and florencite. These secondary rare earth-bearing minerals may have been introduced during the ferricretisation process.

Percent Nb_2O_5 is generally <0.15% and Ta_2O_5 <20 ppm in all Ngualla rock types, below the weathering interface. The Ta_2O_5 and Nb_2O_5 concentrations are well correlated. The *Northern Zone* residual apatite – magnetite regolith unit is enriched in niobium and tantalum, in addition to rare earths and phosphate. Background values of generally <0.25% Nb_2O_5 in fresh calcite carbonatite are upgraded to >0.75% in the residual apatite – magnetite regolith unit. Niobium in fresh calcite carbonatite is present as trace amounts of pyrochlore. By comparison, the residual apatite – magnetite unit in the Northern Zone contains accessory to trace ferrocolumbite and pyrochlore as the main source of niobium. These minerals are probably also the source of tantalum, which however does not achieve economic levels over significant widths. In detail, the three commodities are slightly offset vertically from one another. These displacements suggest variations in the relative roles of residual enrichment and supergene enrichment for each commodity.

Acknowledgements: This abstract is published with the permission of Peak Resources Limited. The authors would like to acknowledge the support provided by Peak in the period leading up to this publication.

References

1. Cahen, L. and Snelling, NJ. 1966. The geochronology of Equatorial Africa. Elsevier (North-Holland Publishing), Amsterdam.
2. Peak Resources Limited, 2014, Release to Australian Stock Exchange, March, 2014.

MULTIVARIATION STATISTICS DETERMINATION OF THE HAMIT ALKALINE PLUTONIC ROCKS (KIRSEHIR-TURKEY)

Yalcin F[1]., Ilbeyli N[2].

1 Akdeniz University, Deparment of Mathematics, 07058, Antalya, Turkey
2 Akdeniz University, Deparment of Geological Engineering, 07058, Antalya, Turkey
fusunyalcin@akdeniz.edu.tr

The alkaline-peralkaline Hamit pluton is located in the Central Anatolian Crystalline Complex, Turkey. It is made up of nepheline syenite, pseudoleucite syenite, alkali feldspar syenite and quartz syenite (Ilbeyli 2004).

Nepheline syenite is medium-grained with a hypidiomorphic granular texture, whereas pseudoleucite syenite is porphyritic with a hypidiomorphic granular texture (Ilbeyli 2004). The alkali feldspar syenite and quartz syenite are medium-grained, equigranular with a hypidiomorphic granular texture. For these rock types, the dominant mineral is perthitic K-feldspar.

We have chosen this pluton since it contains different kind of rock types. Therefore we have made analyses on 63 whole-rock samples, 20 elements (ppm) and 11 chemical compounds (wt.%) which were analyzed by X-Ray Fluorescence (XRF) (Ilbeyli 1998).

We have used SPSS 21 program and have evaluated the results using multivariate statistical analyses. Factor analyses "Extraction Sums of Squared Loadings" indicate that the results' rates are high as 82.490 % cumulatively. The component analyses show that there are three components: (i) first group is Fe_2O_3, CaO, P_2O_5, TiO_2, MgO, and MnO; (2) second group is Al_2O_3 and LOI; and (3) third group is Na_2O. The interpretation of rock contents using by Multivariate statistical procedures have shown positive results (Tables 1-3).

Keywords: Hamit, alkaline-peralkaline, multivariation statistics, SPSS 21 program

Table 1: Correlations analyses of the Hamit plutonic rocks

		SiO_2	TiO_2	Al_2O_3	Fe_2O_3	MnO	MgO	CaO	Na_2O	K_2O	P_2O_5	
SiO_2	Pearson Correlation	1										
	Sig. (2-tailed)	.000										
	N	63										
TiO_2	Pearson Correlation	-.772**	1									
	Sig. (2-tailed)	.000										
	N	63	63									
Al_2O_3	Pearson Correlation	-.380**	-.199	1								
	Sig. (2-tailed)	.002	.117									
	N	63	63	63								
Fe_2O_3	Pearson Correlation	-.858**	.969**	-.083	1							
	Sig. (2-tailed)	.000	.000	.515								
	N	63	63	63	63							
MnO	Pearson Correlation	-.789**	.799**	-.055	.814**	1						
	Sig. (2-tailed)	.000	.000	.671	.000							
	N	63	63	63	63	63						
MgO	Pearson Correlation	-.728**	.886**	-.178	.928**	.650**	1					
	Sig. (2-tailed)	.000	.000	.162	.000	.000						
	N	63	63	63	63	63	63					
CaO	Pearson Correlation	-.807**	.929**	-.193	.962**	.812**	.903**	1				
	Sig. (2-tailed)	.000	.000	.129	.000	.000	.000					
	N	63	63	63	63	63	63	63				
Na_2O	Pearson Correlation	.076	-.427**	.271*	-.361**	-.010	-.422**	-.301*	1			
	Sig. (2-tailed)	.552	.000	.031	.004	.937	.001	.017				
	N	63	63	63	63	63	63	63	63			
K_2O	Pearson Correlation	.149	-.353**	.300*	-.404**	-.219	-.506**	-.451**	-.130	1		
	Sig. (2-tailed)	.244	.005	.017	.001	.085	.000	.000	.309			
	N	63	63	63	63	63	63	63	63	63		
P_2O_5	Pearson Correlation	-.782**	.933**	-.159	.965**	.700**	.962**	.940**	-.384**	-.465**	1	
	Sig. (2-tailed)	.000	.000	.214	.000	.000	.000	.000	.002	.000		
	N	63	63	63	63	63	63	63	63	63	63	
L.O.I	Pearson Correlation	-.528**	-.020	.802**	.131	.149	.056	.116	.226	.123	.048	1
	Sig. (2-tailed)	.000	.874	.000	.306	.243	.660	.364	.075	.338	.707	
	N	63	63	63	63	63	63	63	63	63	63	63

**. Correlation is significant at the 0.01 level (2-tailed). : *. Correlation is significant at the 0.05 level (2-tailed).

Table 2: Rotated component matrix of the Hamit plutonic rocks (Extraction Method: Principal Component Analysis. Rotation Method: Varimax with Kaiser Normalization.a a. Rotation converged in 5 iterations)

	Component		
	1	2	3
Fe_2O_3	.995	.018	-.046
CaO	.976	-.046	.038
P_2O_5	.971	-.086	-.033
TiO_2	.963	-.107	-.123
MgO	.944	-.116	-.034
SiO_2	-.849	-.507	-.007
MnO	.822	.135	.134
$A_{12}O_3$	-.110	.936	-.010
L.O.I	.131	.910	.080
Na_2O	-.333	.320	.817
K_2O	-.442	.367	-.673

Table 3: Total variance of the Hamit plutonic rocks

Component	Initial Eigenvalues			Extraction Sums of Squared Loadings			Rotation Sums of Squared Loadings		
	Total	% of Variance	Cumulative %	Total	% of Variance	Cumulative %	Total	% of Variance	Cumulative %
1	7.594	39.967	39.967	7.594	39.967	39.967	6.780	35.686	35.686
2	5.506	28.980	68.948	5.506	28.980	68.948	5.604	29.495	65.181
3	1.472	7.747	76.695	1.472	7.747	76.695	1.842	9.696	74.877
4	1.101	5.795	82.490	1.101	5.795	82.490	1.447	7.614	82.490
5	.827	4.350	86.841						
6	.541	2.846	89.687						
7	.438	2.308	91.994						
8	.385	2.025	94.019						
9	.301	1.584	95.603						
10	.213	1.121	96.724						
11	.199	1.046	97.769						
12	.152	.802	98.571						
13	.080	.420	98.991						
14	.062	.326	99.317						
15	.050	.263	99.580						
16	.028	.149	99.729						
17	.021	.113	99.842						
18	.019	.098	99.940						
19	.011	.060	100.000						

Extraction Method: Principal Component Analysis.

References

1. Ilbeyli, N. 1999. *Petrogenesis of collision-related plutonic rocks, Central Anatolia (Turkey).* Ph.D. Thesis, University of Durham, Durham, UK.
2. Ilbeyli, N. 2004. Field, Petrographic and Geochemical Characteristics of the Hamit Alkaline Intrusion in the Central Anatolian Crystalline Complex, Turkey. Turkish Journal of Earth Sciences, 13, 269-286.

RARE EARTH ELEMENTS (REE) CONTENTS OF BAUXITE DEPOSITS OF BOLKARDAGI (AYRANCI – KARAMAN)

Yalcin M.G., Paksu E.

Akdeniz University, Deparment of Geological Engineering, 07058, Antalya, Turkey

Nowadays fast-growing technology brought about a need for alternative mane such as rare earth elements. Rare Earth Elements (REE) refer to the part of which atomic numbers are between 57 (Lanthanum- La) and 71 (Lutetyum- Lu). They chemically resemble to between each other and symbolize totally 15 (+2) elements (La, Ce, Pr, Nd, Pm, Sm, Eu, Gd, Tb, Dy, Ho, Er, Tm, Yb, Lu). These elements are known as lanthanide group. In addition to those 15 elements, Yttrium (Y) and Scandium (Sc) of which atomic numbers are respectively 39 and 21 are included into lanthanide group because of their ionic calibers and small atomic calibers. Rare Earth Elements (REE) is increasing in importance day by day because of their luminous quality, the quality acting as catalyzer and their unique magnetic features related with their physical features.

To specify the potential of rare earth elements which are rarely available and to confirm their formation conditions is extremely important in our country. Within this framework, rare earth element ingredients on the samples obtained from Bolkardag region (Ayranci- Karaman) were analyzed, and the results obtained were interpreted by graphic and static techniques.

In the study area where Bolkardag bauxite stratums exist, respectively Dedekoy Formation, Gerdekesyayla Dolomite Member, Bulgarian limestone Member, Saraycik Formation, Kasir Diabase, the Berendi Formation, Karamanoglu Ophiolite, Mazi Formation, Divrek Formation and alluvium are located.

In the study conducted on Dolomite which is one of the base rocks, the concentrations of 32 trace elements and 15 rare earth elements were analyzed and sum of their averages is calculated as 183 pmm. Fifteen of 58 chemical components such asAl_2O_3, Fe_2O_3, TiO_2, K_2O, Ag, Cs, Cu, Ga, Pb, Rb, Sc, Th, W, Zn, Zr and REE (except Pr) are strong all the time and give a meaningful positive correlation at the level of $p>0.99$. Likewise, the sum of the average of REE and trace elements on limestone is calculated as 194 pmm. Fifteen of 58 chemical components such as Al_2O_3, Fe_2O_3, TiO_2, Ag, As, Bi, Mo, Nb, Sb, Sc, Se, V, Zn, Zr, Y and REE (except Pr) are strong all the time and give a meaningful positive correlation at the level of $p>0.99$.Considering to the average geochemical correlation of limestone and dolomites, we can see that only La of REE differs and gives a little bit bigger results in dolomite.

Data's negative relations are specified at the level of 0.99 meaning fullness between Terra Rossa on the cretaceous old limestone and CaO (calcium oxide) and REE values. According to oxide and trace element concentrations, it shows meaningful correlations with both of the groups but REE (except Ce) provide strong positive correlations between each other. According to conducted chemical analysis, the REE (Sc, Y, La, Ce, Pr, Nd, Sm, Eu, Gd, Tb, Dy, Ho, Er, Tm, Yb, Lu)'s average values existing in Dolomite are determined as respectively 0.8, 6.4, 2.7, 4.7, 3.8, 2.5, 0.5, 0.13, 0.65, 0.10, 0.60, 0.12, 0.34, 0.04, 0.27, 0.04 (Table 1).

As a consequence, during the occurring of bauxite it is thought that firstly Terra Rossas are formed and some of REE are preserved, the others move to other elements and behave like

them. While land conversion from Terra Rossa is happening, REE remain and flourish as a motionless element.

Table 1: The statistical parameters of the REE included in the dolomites belonging to Dedekoy formations and forming the base of the bauxite

REE	Sc	Y	La	Ce	Pr	Nd	Sm	Eu	Gd	Tb	Dy	Ho	Er	Tm	Yb	Lu
1	1.0	4.6	3.6	7.5	0.9	3.5	0.8	0.18	0.71	0.11	0.64	0.12	0.36	0.05	0.27	0.05
2	1.0	14.8	4.6	8.9	1.2	4.8	0.9	0.24	1.33	0.20	1.27	0.26	0.78	0.09	0.64	0.09
3	0.5	3.3	1.8	2.0	32.0	1.6	0.2	0.08	0.44	0.05	0.29	0.06	0.17	0.02	0.12	0.02
4	1.0	4.4	2.6	4.7	0.6	2.4	0.4	0.09	0.46	0.07	0.58	0.10	0.29	0.02	0.29	0.06
5	1.0	7.6	2.9	4.9	0.7	2.6	0.5	0.12	0.59	0.10	0.62	0.12	0.33	0.02	0.26	0.03
6	1.0	6.1	2.7	4.6	0.6	2.1	0.5	0.13	0.53	0.09	0.52	0.10	0.25	0.02	0.19	0.04
7	0.5	4.8	1.9	3.0	0.4	1.5	0.4	0.11	0.49	0.07	0.42	0.08	0.26	0.02	0.14	0.03
8	0.5	4.8	1.9	2.6	0.4	1.5	0.4	0.13	0.57	0.08	0.50	0.08	0.23	0.02	0.18	0.03
9	1.0	11.5	4.5	8.1	1.1	4.1	1.0	0.22	1.21	0.19	1.03	0.25	0.66	0.08	0.56	0.07
10	0.5	2.0	0.6	1.0	1.0	0.5	0.1	0.02	0.13	0.01	0.09	0.02	0.06	0.02	0.07	0.01
11	1.0	9.7	4.1	8.2	1.0	4.2	0.9	0.21	1.02	0.16	0.96	0.19	0.57	0.07	0.46	0.07
12	0.8	3.9	2.2	3.4	16.3	2.0	0.3	0.09	0.45	0.06	0.44	0.08	0.23	0.02	0.21	0.04
13	1.0	6.9	2.8	4.8	0.6	2.4	0.5	0.13	0.56	0.10	0.57	0.11	0.29	0.02	0.23	0.04
14	0.5	4.8	1.9	2.8	0.4	1.5	0.4	0.12	0.53	0.08	0.46	0.08	0.25	0.02	0.16	0.03
15	0.8	6.8	2.6	4.6	0.6	2.3	0.6	0.12	0.67	0.10	0.56	0.14	0.36	0.05	0.32	0.04
Mean	0.8	6.4	2.7	4.7	3.8	2.5	0.5	0.13	0.65	0.10	0.60	0.12	0.34	0.04	0.27	0.04
Stan. Dev.	0.3	3.9	1.3	2.7	9.9	1.3	0.3	0.07	0.36	0.06	0.34	0.08	0.22	0.03	0.19	0.02

LA, CE, Y, AND SC (RARE EARTH ELEMENTS) CONTENTS OF COASTAL SANDS BETWEEN ALANYA AND MANAVGAT (WESTERN MEDITERRANEAN) AREAS

Yalcin M.G.[1], Paksu E.[1], Kilic S.[2]

1 Akdeniz University, Deparment of Geological Engineering, 07058, Antalya, Turkey
2 Akdeniz University, Food Security and Agricultural Research Center, 07058, Antalya, Turkey

REE are included in many minerals including halides, carbonates, oxide and phosphates. REE are mostly included in the minerals which form rocks and change place with. To form their own minerals, the concentrations of REE must be higher (Möller, 1986). Stratums getting rich as REE are divided into two categories such as primary (resulted from metamorphic and magmatic processes) and secondary (resulted from sedimentation process and weathering) stratums. Because of some unclear genetical relations and/or more than one geologic processes happen inter bedded categorizing some stratums is complicated. (Orris, G. J. AndGrauch, R. I., 2008). Samples containing Monazite samples observed at 0.1% -0.046 values and accumulated along the coastline as result of coast activities of some durable and heavy minerals are available.

The study area located between Alanya-Manavgat is located in approximately 60 km coastline. Among the samples belonging to 45 locations from the coastline, La (Lanthanum), Ce (Cerium), Y (Yttrium) ve Sc (Scandium) were analyzed and their anomaly values were taken out. When we look at the minimum and maximum values, Lanthanum is 4.9-22.3, Cerium is 9-45, Yttrium is 3.9-25.6, Scandium is 0-9 and their averages are observed as respectively8.39, 16.06, 8.6and 2.6 pmm. Maximum value for Lanthanum and Cerium is observed in 15 numbered location, for Yttrium in 24 numbered location and for Scandium in 45 numbered location (Table 1,2). Those locations and the existence of minerals such as monazite must be controlled.

Table 1: Chemical analysis contents of some REE

REE	La	Ce	Y	Sc
1	6,2	11	7,3	1
2	6,4	11	7,5	2
3	7,4	13	9,3	2
4	6,9	12	8,1	2
5	8,0	15	9,6	2
6	7,3	12	8,4	2
7	7,8	15	9,2	3
8	7,8	15	8,9	3
9	7,6	16	8,1	2
10	7,1	11	6,5	2
11	6,2	10	6,2	2

12	6,5	11	6,6	2
13	5,9	11	6,2	2
14	5,4	11	6,6	2
15	22,3	45	11,3	4
16	7,4	14	6,8	2
17	6,9	13	5,9	2
18	7,2	13	6,7	2
19	10,1	19	10,8	0
20	7,4	14	6,9	2
21	6,2	11	6,0	2
22	5,6	11	5,9	2
23	16,9	32	13,7	5
24	11,3	23	25,6	2
25	10,7	18	14,0	1
26	4,9	9	3,9	1
27	8,1	16	5,9	2
28	9,9	19	11,0	1
29	9,1	19	11,2	1
30	11,1	22	8,5	3
31	9,8	19	7,1	4
32	8,8	18	4,7	3
33	8,6	22	4,9	3
34	10,8	22	5,3	3
35	8,1	16	5,3	2
36	6,3	12	5,3	2
37	6,2	12	4,9	2
38	7,0	14	10,3	4
39	8,3	15	16,6	6
40	8,5	17	7,0	3
41	7,1	14	6,1	3
42	6,1	12	11,0	4
43	5,4	10	4,9	2
44	11,5	23	12,6	6
45	13,6	25	18,4	9

Table 2: Statistic evaluations of chemical analysis results

		La	Ce	Y	Sc
N	Valid	45	45	45	45
	Missing	0	0	0	0
Mean		8,39333	16,06667	8,60000	2,60000
Std. Error of Mean		,468647	,973591	,612702	,232249
Median		7,40000	14,00000	7,10000	2,00000
Mode		6,200	11,000	4,900[a]	2,000
Std. Deviation		3,143782	6,531045	4,110132	1,557971
Variance		9,883	42,655	16,893	2,427
Skewness		2,546	2,398	2,126	2,032
Std. Error of Skewness		,354	,354	,354	,354
Range		17,400	36,000	21,700	9,000
Minimum		4,900	9,000	3,900	,000
Maximum		22,300	45,000	25,600	9,000
Sum		377,700	723,000	387,000	117,000
Percentiles	25	6,35000	11,50000	5,95000	2,00000
	50	7,40000	14,00000	7,10000	2,00000
	75	9,45000	19,00000	10,55000	3,00000

a. Multiple modes exist. The smallest value is shown

References

1. Möller, P., 1986, Physical factors and biological interactions regulating infauna in shallow boreal areas. Mar. Ecol. Prog. Ser., 30, pp. 33–47.
2. Orris, G. J. and Grauch, R. I., 2002, Rare earth element mines, deposits and occurrences. US Geological Survey, Tucson, Open-File Rep., 189, 167.
3. Grauch, R.I. and Mariano, A.N., 2008, Ion-adsorption type lanthanide deposits [abs]: Society of Mining, Metallurgy and Exploration Annual Meeting and Exhibit Preliminary Program, p. 40.

MINERALOGY AND GEOCHEMISTRY OF BAUXITE DEPOSITS OF KARAMAN AREA (TURKEY)

Yalcin M.G., Nyamsari D.G., Paksu E.

Akdeniz University, Deparment of Geological Engineering, 07058, Antalya, Turkey

This study was carried out in the Bauxite region of the Karaman city and its around. In this study, we investigated and compared the mineralogy and the geochemistry of the 3,5 million bauxite deposited and their Wall Rock (dolomite and Limestone).

In this study region, bauxite deposits were respectively found in the following areas: Dedekoy Formation, Gerdekesyayla dolomite member, Bulgarian limestone member, Saraycik Formation, Kasir Diabase, Berendi Formation, Karamanoglu Ophiolite, Mazi Formation, Divrek Formation and alluvium.

The bauxite deposit is identified to consist of different amounts of diaspore, hematite, and clay minerals. The paragenesis ore has been determined as diaspore, hematite, kaolinite, anatase, rutile, sphene, calcite, muscovite, magnetite, quartz, goethite, chlorite, amorphous iron- and aluminum-hydroxide, gibbsite, boehmite, illite, specularite, epidote, chalcedony, amphibole and psilomelane. In bauxite, different ore types with different appearance can be noticed, depending on the abundance of diaspore, hematite and clay minerals, as they pass into vertical and horizontal transitions to each other. These ore types are black bauxite, brown bauxite, oolitic bauxite and clayey bauxite.

According to laboratory analysis, the dolomite of Gerdekesyayla is composed of 31% CaO, 20% MgO, 1.03% SiO2 and less than 1% other oxides, indicating that the rock is made up of 81% dolomite and 16% calcite. While the limestone of the Bulgardede Member is composed of 55% CaO, 0.33% MgO and less than 1% other oxides and rock contains 97% calcite and 1% dolomite. The chemical composition of bauxites in average is 54% Al2O3, 26% Fe2O3, 5% SiO2, 3% TiO2 and less than 1% other major oxides. With their module values ranging between 1.4 and 91.2, and with an average of 34.66, they are accepted as the first quality bauxite.

MANTLE CONDITIONS AND GEOCHEMICAL ENVIRONMENT AS CONTROLS OF DIAMOND SURVIVAL AND GRADE VARIATION IN KIMBERLITIC DIAMOND DEPOSITS: LUNDA PROVINCE, N.E. ANGOLA

Yambissa M.T, Bingham P.A., Forder S. D.

Materials and Engineering Research Institute
Sheffield Hallam University, City Campus, Howard Street, Sheffield, S1 1WB, UK
tshivangulula@hotmail.com

Diamondiferous kimberlites and the geology of Lunda Province (NE Angola) have been studied by Ganga et al. (2003) and White et al. (1995) among others. However, a clear understanding of diamond survival and preservation conditions within Lunda Province (LP) has not yet been formed. Determination of diamond preservation conditions in the lithospheric mantle/kimberlite pipes is a crucial parameter for diamond exploration. Factors such as oxygen fugacity (fO_2), oxidation state, speed of kimberlite emplacement and variations in temperature and pressure can impose conditions sufficiently oxidised for diamond to break down into carbonate or carbon dioxide / resorption (Gurney and Zweistra 1995; Nowicki et al. 2007). Understanding these processes is important for diamond exploration and assessing the potential diamond grade of kimberlites. The principal aim of this research is to investigate the mantle conditions and geochemistry of diamondiferous kimberlites located on the Congo Kassai Craton (NE Angola). Conditions of formation and preservation of diamonds before and during emplacement of the kimberlitic magma, and the causes of variations in diamond abundance (including resorption) and grades observed between pipes, are being considered.

Results from petrography and geochemistry of peridotite, eclogite and kimberlite rocks suggest that the Lunda lithospheric mantle experienced several processes of metasomatic episode. The most studied diamond indicator minerals (olivine **-ol**, garnet **-gnt**, pyroxene **-cpx, opx** Figure 1, spinel, ilmenite, and perovskite) reflect these redox reactions. These alteration/oxidation processes may have affected the original diamond structure, resorption or may impose conditions sufficiently oxidised within LP kimberlites to cause diamond breakdown. In addition, the model of this study (Figure 2) and the calculated diamond carats per hundred tonnes of rock that each pipe produce, and possible percentages of diamond brought to surface by kimberlite, reveal that the observed variations in diamond grade or abundance within LP is associated with the heterogeneous mantle, consequently each kimberlite pipe has transported different amount of diamond in the mantle to the surface.

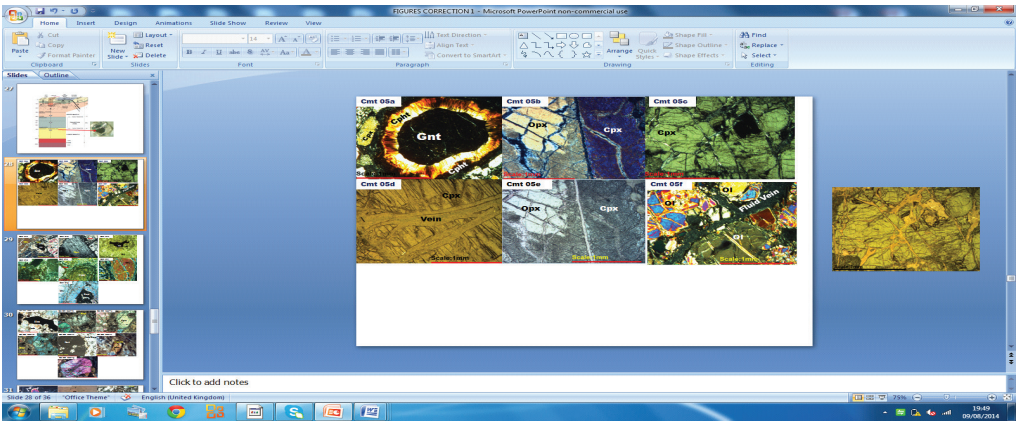

Figure 1: Textures (thin section analysis & interpretation) of CMT - 05 mantle xenoliths, P-types (LP)

Despite having ~70% of deficient diamond and sampled more diamond than any other pipe in LP, our preliminary geochemistry results place Catoca kimberlite in a no-diamond preservation zone, according to the work of Gurney and Zweistra (1995) and Nowicki et al. (2007), which indicated crystallization under relatively high oxygen fugacity (fO_2) and hence relatively oxidising redox conditions.

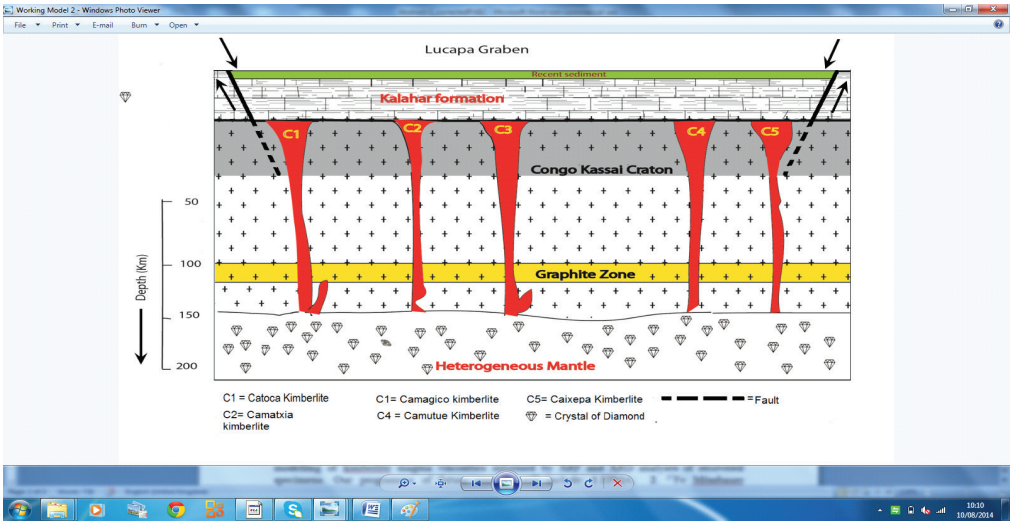

Figure 2: Developed model for diamondiferous kimberlites, Western Africa (NE Angola) showing relative locations of 5 principal pipes investigated in this study.

Here we will report on our findings to date in from this ongoing project, and a brief discussion of future work will also be given. This involves a systematic structural and chemical analysis of geological samples taken at several depths from the 5 pipes shown in Figure 2, coupled with modelling of kimberlite magma viscosities informed by XRF and XRD analyses of recovered specimens. Our programme of future research will include: 1- A systematic petrographic study of mantle xenoliths and kimberlite rocks, 2. EPMA analysis; **3**. ^{57}Fe Mössbauer

spectroscopy; **4.** SEM analysis**; 5.** XRF and XRD**; 6.** Viscosity modelling of kimberlite magma; **7.** Geothermobarometry.

Conclusions

Initial results show that the observed variation in diamond grade and abundance within Lucapa graben (NE Angola) is associated with metasomatism event/poor diamond preservation conditions and the heterogeneous mantle (each kimberlite pipe has transported different amounts of diamond in the mantle to the surface). Preliminary geochemistry studies place LP kimberlite in a no-diamond preservation zone and further analysis is underway to enable a more detailed understanding of diamond transport and preservation conditions in LP.

References

1. Correira, E. A. and Laiginas, F. A. (2006). Garnets from the Camafuca-Camazambo kimberlite (Angola), Annals of the Brazilian Academy of Sciences, pp: 309-315.
2. Ganga J., Rotman, A.Y. and Nosiko. S. (2003). *Pipe Catoca, an example of the weakly eroded kimberlites from North-East of Angola, Proceedings of the* 8th International Kimberlite Conference.
3. Gurney, J.J. and Zweistra, P. (1995). The interpretation of the major element compositions of mantle minerals in diamond exploration, Journal of Geochemical Exploration 53 (1–3), p. 293–309.
4. Nowicki, T. E., Moore, R.O., Gurney, J.J. and Baumgartner, M.C. (2007). Diamonds and associated heavy minerals in kimberlite: review of key concepts and applications, Developments in Sedimentology 58, p. 1235–1267.
5. White, S.H., de Boorder, H. and Smith, C.B. (1995). Structural controls of kimberlites and lamproite emplacement, Journal of Geochemical Exploration 53, p. 245-264.

GEOCHEMISTRY OF THE ALKALINE IGNEOUS ROCKS IN THE SOUTHWESTERN MARGIN OF ORDOS BASIN, NORTH CHINA CRATON

Wang Y.

School of Earth Science and Resources, China University of Geosciences, Beijing, China
allen_thalassa@sina.com

Located in the southwest margin of Ordos Basin, Taoshaoshan porphyry and Longmen buried alkaline complex exist in dikes or sills intruded into the Lower Jurassic Yanchang Group and the underlying strata. According to their mineral association, Taoshaoshan porphyry belongs to leucite syenite, and Longmen alkaline complex is made up of leucite syenite, nepheline syenite, monzodiorite, aegirine-bearing monzonite, and alkaline feldspar syenite. Geochemically, these rocks have high K_2O, Al_2O_3, CaO and low SiO_2, MgO, TiO_2 and P_2O_5 content. The basic rocks (SiO_2 < 56%, i.e., leucite syenite and nepheline syenite) have more than 7% K_2O content and very high K_2O/Na_2O ratio (13 ~ 52), and they belong to the ultrapotassic rocks. Meanwhile, the intermediate rocks with SiO_2 content over 56% (monzodiorite, monzonite and alkaline feldspar syenite) exhibt lower K_2O content and much lower K_2O/Na_2O ratio. In the spider diagrams, all of the alkaline rocks are enriched in K, Rb, Sr, Ba, and Th, but depleted in Nb, Ta; meanwhile, these rocks have total REE from 96 ppm to 620 ppm, and $(La/Yb)_N$ values between 8.7 to 251, with moderate to very slightly negative Eu anomalies (Fig. 1). The leucite syenites exhibit $^{143}Nd/^{144}Nd$ ratios of 0.511711 to 0.511901, and $^{87}Sr/^{86}Sr$ ratios of 0.70814 to 0.70863, and $^{206}Pb/^{204}Pb$ ratios of 18.829 to 18.978, $^{207}Pb/^{204}Pb$ ratios of 15.646 to 15.655, $^{208}Pb/^{204}Pb$ ratios of 39.151 to 39.266. The characteristics of major elements, trace elements as well as Sr-Nd-Pb isotopes of these alkaline rocks indicate that they were generated from the metasomatic lithospheric mantle. Accordingly, the lithospheric mantle beneath Ordos basin had been modified during the pre-Cenozoic tectono-thermal event, and does not preserve the petrological and geochemical characteristics of the stable lithospheric keel as suggested by our previous study [1].

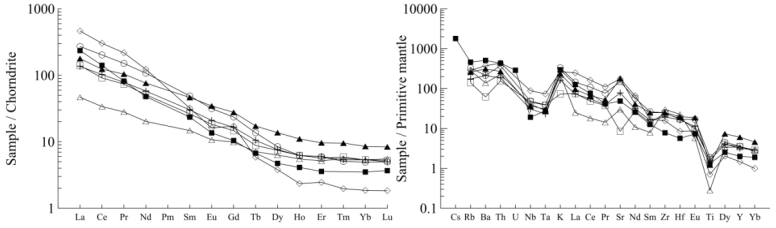

Figure1: The REE (left) and spider (right) diagrams for the representative samples of ultrapotassic rocks in SW Ordos basin. The filled square and open diamond are leucite syenite, the circle is nepheline syenite, the open triangle is aegirine-bearing monzonite, the open square is alkaline feldspar syenite, the filled triangle and cross are monzodiorite.

Acknowledgement: This study is financially supported by the Fundamental Research Funds for the Central Universities, grants No.2652013021 and No.2010ZD15.

References

1. Wang Y., Cheng S.-H., 2012. Lithospheric thermal structure and rheology of the eastern China. Journal of Asian Earth Sciences. v. 47, p. 51–63.

KONTAY LAUERED SUBALKALINE INTRUSION (POLAR SIBERIA)

Zaitsev V.A.

Vernadsky Institute of Geochemistry and Analytical Chemistry RAS, Moscow, Russia. va_zaitsev@geokhi.ru

Kontay intrusion located very close the Krestovsky alkaline-ultramafic intrusion 30 km WSW from Guli massif. Geophysical data show that both intrusions cut upper Triassic volcanogenic sequence. The intrusion has form of laccolite with diameter ~7.5 km and thickness ~ 2.5 km (Kushnir, 2005). Intrusion is fully overlaid by Jurassic and Cretaceous marine and continental sediments and Quaternary glacial and fluvio-glacial sediments. The first data about intrusion was provided by G.G. Lopatin and N.N. Kalashnik (2004) who studied drill core and describe lower part of intrusion as "gabbro-anortosite and anortositic gabbro" and higher part – as "leucocratic granophyric anortosites". We sampled the same drill core.

Drill core section is build up of three parts:

- **lower part** (below 1100 m) consists of layered sequence with alternation of leucocratic and melanocratic layers of biotite- and ortopyroxene-bearing gabbro with pseudomorphoses after olivine. Biotite overgrow and replace pyroxene crystals. Accessory minerals: titanomagnetite, apatite.

- **medium part** (1100-700m) consists of biotite- and K-feldspar bearing gabbro and monzonites. Accessory minerals: zoned titanomagnetite-magnetite, ilmenite, apatite. Interstitial space often contains micrographical structures. Biotite overgrow and replace pyroxene crystals clinopyroxene and form interstitial crystals. Sometime, in titanomagetite dissolution structures ilmenite is replaced by secondary minerals, including biotite.

- **upper part** (700-214 m) consists of monotone rocks with dacite-trachydacite composition and porphyrytic texture. Phenocrysts of plagioclase, magnetite, clinopyroxene and biotite (the last two minerals often fully replaced), the matrix with micrographic structure formed by quartz and feldspars .

Rocks of the lowest part if intrusion contain low SiO_2 (40-46% up to 35.5%), strongly variable content of TiO_2 (2-8.5%), Al_2O_3 (9-20%) FeO (10-25.5%), MgO (2.5-6.5%), CaO (8.5-12%), Na_2O (2-3.5%) and low concentration of K_2O (usually 0.6%) and P_2O_5 (0.3%). Was found relatively high concentrations of sulphur (up to 0.36%) and halcophyle elements Ni (40-230 ppm), Co (45-100 ppm), Cu (80-370 ppm), and low concentrations of non-coherent lithophile elements (10-20 ppm Nb, 100-150 ppm Zr, 20-25 ppm Y). TiO2 content is not correlated with P2O5.

In the medium part of sequence SiO_2, Na_2O and K_2O concentrations linearly increase, while TiO_2, FeO, MgO, CaO and P_2O_5 concentrations linearly decrease upward from concentrations typical in the lower part of intrusion to concentrations, typical in the upper part. Al_2O_3 content is practically constant (15%). Interesting, that highest concentration of P_2O_5 (up to 2%) was found in the bottom of this part of intrusion. Co and Cu concentrations decrease upward while S and Ni concentrations are low (below 10 and 100 ppm respectively) Nb, Zr, Y, Rb, Ba concen-

trations increase upward. Sr-content in this part of intrusion is highest (900-1200 ppm).

In the highest part of intrusion concentrations of main elements slight vary: SiO_2- 66-68%, Al_2O_3 13%, TiO_2- 1%, FeO 4.7-6.5%, MgO 0.7-0.8%, CaO 2-3%, Na_2O – 3.4-3.9%, K_2O 3.1-4.4%, P_2O_5 – 0.2-0.3%. Concentrations of sulfur and chalcophile elements are low, while concentrations of non-coherent lithophile elements are high practically similar (Rb~70 ppm, Y~50 ppm, Zr~600 ppm, Nb~45 ppm, Ba~ 800 ppm) but the highest concentration of all these elements (119, 57, 890, 62 and 1150 ppm respectively) located in the bottom of these part of intrusion.

On the total alkalis vs SiO_2 and K_2O vs SiO_2 –diagrams (Fig 1) rocks form single trend in sub-alkaline (calc-alkaline) fields. They are slightly less alkaline then country trachybasalt-trachyandesit-trachydacites and much more alkaline then intrusions of Norilsk district and much less alkaline then alkaline-ultramafic intrusions of Maymecha-Kotuy province.

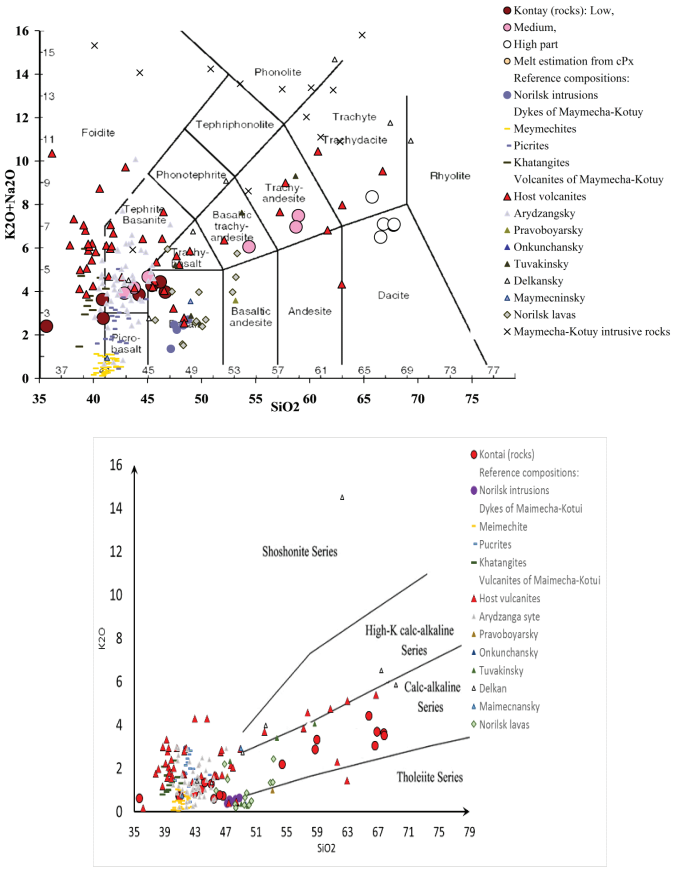

Figure 1: Kontay rocks on total alkalis and K2O vs. silica classification diagrams. Also shown literature data: average composition of Norilsk-type intrusions (Krivolutskaya, 2009), higly evolved rocks of Maymecha-Kotuy province (Egorov, 1991) dykes of Maymecha-Kotui region (Ryabcikov et al., 2002), volcanic country rocks samples near Krestovskaya intrusion (Platinum-bearing… 2001) and stratigraphically characterized volcanic rocks of region (Fedorenko et al., 2000)

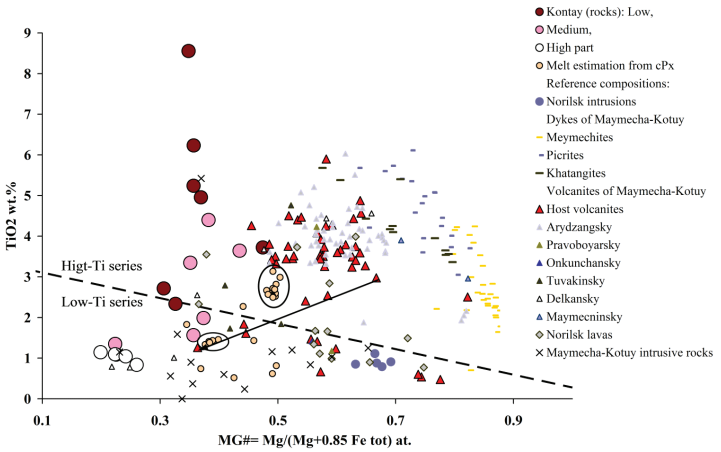

Figure 2: Classification by titanium content and Mg-number =[Mg/(Mg + 0.85Fe_{total})], where elements are presented in atomic units. Subdivisions to high- and low-Ti series after Ivanov and Balyshev (2005). Arrow show evolution on country trachybasalt-trachyandeite-trachydacite rocks.

Microprobe analyses show two group of clinopyroxene compositions, both are diopside-hedenbergite. The high-titanium pyroxene (1-1.2% TiO_2 2-2.5% Al_2O_3 0.2-0.3 % MnO, 0,3-0,35% Na_2O) present only in the lower part of intrusion. Low-titanium pyroxene present overall, Mg/(Mg+Fe) in low-titanium clinopyroxen decrease from 0.7 to 0.63, concentration of Al_2O_3 increase from 0.7 to 1.3, TiO_2 increase from 0.4 to 0.6, MnO from 0.4 to 0.7 and Na_2O decreace from 0.32 to 0.28 wt%.

Estimations of melt composition in equilibrium with clinopyroxen are shown in the Figure 2. Two groups of estimated compositions are clearly seen: high-Ti, located near the composition of the rock with highest Mg# from the lower part of intrusion, and low-Ti, with less MG#, located near the composition of rocks from the medium part of intrusion. Formally, melts composition as well as compositions of rocks of Kontay intrusion and belong two distinct (high-titanium and low-titanium) series, typically present in large igneous provinces, but mass-balance modeling show, that low-titanium trachyandesute melt (composition of sample form depth 815m) might be a produced by crystallization of association cPx+Pl+Ti-Mt (probably accompanying with crystallization of biotite and oPx dissolution) from high-titanium alkaline basaltic melt (composition of sample from depth 1230.5 m).

Analyses of volcanic country rocks chemically divided into three groups: high-Ti foidites, tephrite-basanites, trachybasaltes, low-Ti basalts, chemically similar to lavas and intrusions of Norilsk district, and clearly distinct from low-Ti trachyandesites and trachydacites. The lasts can be believed to be a result of magmatic differentiation of the Ti-high trachybasaltic magma. So we can suppose that magmatic chamber of Kontay intrusion responsible the formation of these volcanic rocks.

These observations show that Kontay intrusion present first for Polar Siberia sample of differentiated subalkaline-gabbroic intrusion, clearly distinct both from the alkaline-ultramafic intrusions of Maymecha-Kotuy province and from Norilsk-type intrusion. We can suppose existing

of similar type intrusions in this region, basing on reported (Fedorenko et al., 2000) trachyte and trachyriodacite analyses in Delcansky suite.

Work supported by Program of RAS presidium «Basic scientific research for development of Russian arctic zone»

References

1. Egorov L.S. Iolite-carbonatite plutonism (the sample of Maymecha-Kotuy complex). // Leningrad, Nedra, 1991, 260 pp.
2. Fedorenko V., Czamanske G., Zen'ko T., Budahn J., Siems D. Field and Geochemical Studies of the Melilite-Bearing Arydzhangsky Suite, and an Overall Perspective on the Siberian Alkaline-Ultramafic Flood-Volcanic Rocks s // International Geology Review. Vol. 42. 2000. P. 769-804. Kushnir D.G. Geological structure of transitional zone between Enisey-Khatangski forebelt and Siberian platform between rivers Kheta and Kotuy by geophysical data. Ph.d. thesises, 25.00.10 Ekatirenburg, 2005, 154pp.
3. Ivanov A V and Balyshev S V 2005 Mass flux across the lower-upper mantle boundary: vigorous, absent, or limited?; In: Plates, plumes and paradigms (eds) Foulger G R et al (Princeton: Geological Society of America Special Paper) 388 327–346.
4. Lopatin G.G. and Kalashnik N.N. (2004) The new source of platinum-group metals in Maymecha-Kotuy province. // Mineral recourses of Taimyr autonomy district and they perspectives. Materials of science-practical conference 25-28 October 2004, Sankt-Pererburg
5. Platinum-bearing alkaline-ultramafic intrusions of Polar Siberia. Sazonov A.M., Zvagina E.A., Leont'ev S.I. // Tomsk, CNTI, 2001, - 509 p.
6. Ryabchikov I.D., Solovova I.P., Kogarko L.N., Bray G.P., Ntaflos Th., Simakin S.G. Thermodynamic Parameters of Generation of Meymechites and Alkaline Picrites in the Maymecha–Kotuy Province: Evidence from Melt Inclusions // Geochemistry International 2002. Vol. 40, No. 11, p. 1031-1041.

STRUCTURE OF UPPER CRUST OF THE KHIBINY AREA ON THE BASIS OF THE GEOLOGICAL AND GEOPHYSICAL DATA AND THE RESULTS OF 3D SEISMIC AND DENSITY MODELING

Zhirov D.V.[1], Glaznev V.N.[2], Zhirova A.M.[1]

1 Geological Institute Kola Science Centre of Russian Academy of Science, Apatity, Russia,
2 Voronezh State University, Voronezh, Russia
zhirov@geoksc.apatity.ru

The area considered is located in the central part of the Kola Peninsula and represents a part of tectonically compound terrane, consisting of the AR, PR and PZ geological structures of the East of Fennoscandian shield. One of the most important stages in the evolution history of this crust block became the Neo Archaean (?) ÷ Paleoproterozoic rifting, which began a fracturing of deep faults. The rifting together with the ancient plume controlled the formation of the PGE-bearing layered mafic-ultramafic massifs [1]. On modern geological map the northern border of the rift is well-marked by a chain of quasiconformal layered intrusions from Fedorovo-Pansky intrusion on SE of the Imandra-Varzuga belt to the General Mountain massif in the Pechenga structure on the NW of the region through massifs (Main ridge, Monchetundrovsky, Monchepluton and others) of Monchegorsk ore area. Zone of the Paleozoic tectonic activation of NE-extension is discordantly located to the Paleoproterozoic and Archean structures. This zone controls the formation of central-type massifs: from the Sokle massif in Finland to the Barents sea coast (close by the Ivanovsky armlet) through the Mavragubsky, Khibiny, Lovozero, Kurgansky, Kontozersky massifs. Discussed in the article the largest Khibiny massif of the nepheline syenites upthrusts the Archean complexes (the northern contact) and the Paleoproterozoic volcanogenic-sedimentary Imandra-Varzuga complex (southern and SW-contacts) [2].

According to the results of numerous researches [2, 3, 12, 16, 17 and others] the massif is an ellipse-shaped in plan multiphase pluton, elongated in the latitudinal direction along the 82^{o} azimuth, with shifted to the east the root (Fig. 1). The shape of the Khibiny pluton is close to the asymmetrical lopolit, characterized by the steep eastern and northern contacts and the gentler south and west contacts. The eastern contact in zone of carbonatite stock is sub vertical to the depths of 3 ÷ 4 km and tends to a sharp flattening at the depth of 4 ÷ 5 km. The western and southern contacts are falling towards the center at 65 ÷ 70 angle to the depth of 4 km. In the range of 4 ÷ 6 km the position of the contact is gently sloping (30), but the angle of incidence increases up to 50 ÷ 60 at the depth more than 7 km.

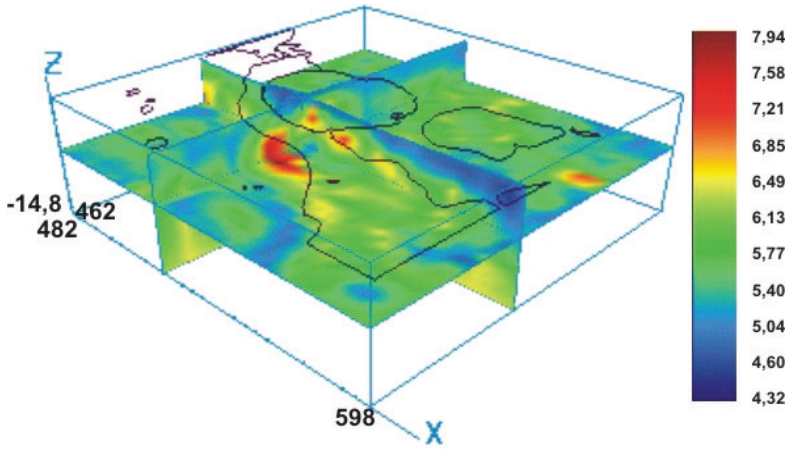

Figure 1: - Sections of 3D velocity model (values in km / sec) by [6].

The results of the 3D seismic and density modelling [5] refined the structure of the pluton and its contact with Imandra-Varzuga sedimentary-volcanic complex. In accordance with the obtained model the massif is allocated by the low-velocity anomaly at depth from 5 km to 11 km and characterized by average velocity below the background velocity at these depths (Fig. 1, 2). In the upper part the velocity model has two local high-velocity anomalies with dimensions of 5 x 10 km approximately. The intensity of the first anomaly which detected at the depth of 1.5÷2.0 km and the spatial coincide with the central part of the massif is increased to the depth of 3 km (Fig. 2).Within the anomaly the value of Vp-velocity reaches 6.8÷7.0 km/s relative to the value of the background velocity of approximately 5.5 km/s. The velocity structure of the Khibiny massif, which expressed in the alternation of the anomalies of the positive and negative signs in the middle of the massif, evidence the more complex structure than the currently existing representations formulated in predictive geological model. According to the density model derived from the complex modeling of structure of the central part of Kola Peninsula the density anomalies correlate with the revealed velocity anomalies very well. The second high-velocity anomaly, discovered southeast of the first anomaly at a depth of about 3 km, more clearly is revealed at a depth of about 4 km, where the intensity of the first anomaly begins to decrease. This high-velocity anomaly as a first approximation coinciding with the boundaries of Imandra-Varzuga complex - Archean country rocks is traced up to the depth about 9-10 km (Fig. 2) and reaches the maximum intensity (7.0÷7.5 km/s) at a depth of 4÷7 km.

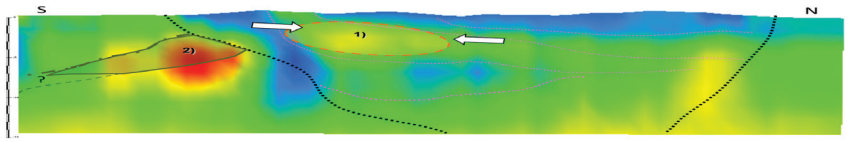

Section 2, density model

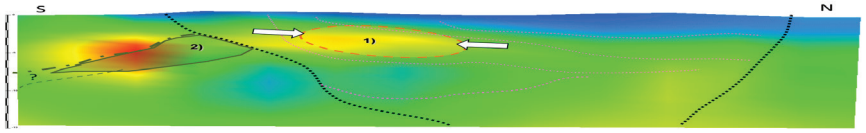

Section 2, velocity model

Figure 2: - Sections of the velocity and density models with the marked and proposed: 1) - zone of concentration of the anomalous tectonic stresses and 2) - probable layered mafic-ultramafic intrusion.

Variants of the interpretations of these anomalies were analyzed in terms of the correspondence to principal features: "substance" and "state / rheology of the rock massif." The first group conditionally unites interpretations of the anomalies by mafic-ultramafic rocks with various morphology and position in the upper crust, and the second group - explains the anomalies by status / rheology of substance (consolidation due to abnormally high tectonic stress). The first anomaly cannot be explained by "substance" factor only (titanomagnetite-apatite ore bodies), as it has a structural disconformity to general structure of the pluton (see Fig. 2). Therefore, to interpret it, we involved the results of researches of stress and strain of the Khibiny massif [8-10]. According to the numerous instrumental measurements the actual (measured) values of stress are significantly greater than values calculated by weight of rocks. It is important the main normal axis of compressive stress has usually quasi-horizontal position. Thus, the zone of abnormally high tectonic stress is the best explanation for this anomaly. The partial contribution to anomalies in this block due to localization of the apatite-titanomagnetite ore bodies is also possible. The quick isostatic uplift of the massif after the digression of the last glacier, during which the rocks did not have time to unload, can be a source of the increased horizontal stress.

Based on the properties of typical rocks and geological structure of the region the second anomaly is well interpreted by large layered intrusion of Fedorova-Pana type, subsurface of which is cut by Khibiny massif (see Fig. 2). Taking into account the current level of erosion the upper part of the layered intrusions is 2 ± 0.5 km of about surface. The lower boundary is defined on the basis of loss of contrast in the density and velocity models in the range of 7÷9 km of about surface. These boundaries well corresponds to regional features of localization of the layered

intrusions of Fedorovo- Pana type, which are always agreed with the northern and north-eastern tectonic boundary of the Imandra-Varzuga paleorift and have the fall to the south at different angles in the range of 15º to 70º. Thus we forecast big "blind" (not outcropping) PGE-bearing layered intrusion, the upper part of which was cut during the magma intrusion of the Khibiny pluton. This massif is interesting from the point of view of possible generation the non-traditional hybrid rocks and the secondary offset PGE and copper-nickel ores in the near-contact area during alkaline magmatism. The occurrence of the pyrrhotite ores (Pyrrhotite ravine) in the hornfels of south contact of Khibiny rocks with the Imandra-Varzuga zone is indirect confirmation of this hypothesis. This study was supported by the Russian Foundation for Basic Research (project nos. 13-05-12055).

References

1. Mitrofanov F.P. Correlation of composition and ore-forming stages in early Proterozoic mafic-ultramafic layered intrusions of Finland and the Kola Peninsula (Russia) / Collection of materials of the Project INTERREG-TASIS: Strategic mineral resources of Lapland - the basis of sustainable development of the North. - Apatity: KSC RAS. - 2008. - P. 13-18.
2. Arzamastsev A.A., Arzamastseva L.V., Belyatsky B.V. Alkaline volcanism of the initial stage of the Paleozoic tectono-magmatic activization of the north-east Fennoscandia: geochemical peculiarities and petrological consequences // Petrology. - 1998. - V.6. - № 3. - P. 316-336.
3. Pozhilenko V.I., Gavrilenko B.V., Zhirov D.V., Zhabin S.V. Geology of mineral area of the Murmansk region. (Edited by MitrofanovF.P., Bichuk N.I.). - Apatity: KSC RAS, 2002. -359 p.
4. Seismological model of the lithosphere of the northern Europe: Barents region / Edited by F.P. Mitrofanov and N.V. Sharov. - Apatity: KSC RAS. - 1998. - Part 1, 237 p. - Part 2, 205 p.
5. Structure of lithosphere of the Russian part of the Barents region / Edited by N.V. Sharov, F.P. Mitrofanov, M.L.Verba, K. Gilen. - Petrozavodsk: KRC RAS. - 2005. - 318 p.
6. Glaznev V.N., Zhirova A.M., Raevsky A.B. New data concerning the deep structure of the Khibiny and Lovozero massifs, Kola Peninsula / Reports of the Russian Academy of Sciences. - 2008. - V.422. - №3. - P.391-393.
7. Glaznev V.N., Zhirova A.M. Working out and applying technique of the studying velocity properties of intrusive massifs in constructing a complex model of earth's crust of the Khibiny and Lovozero massifs of the Kola Peninsula // Geophysical Bulletin. - Moscow: EAGS. - №6. - 2007. - P. 15-19.
8. Seismicity in mining / Edited by Melnikov N.N. – Apatity: KSC RAS. - 2002. - 325 P.
9. Markov G.A., Savchenko S.N. Stress state of rocks and rock pressure in the structures with mountainous relief. - Leningrad: Science. - 1984. - 140 p.
10. Kurlenya M.V. (editor). Management of rock pressure in tectonically stressed massifs. - Apatity: KSC RAS. - 1996. – Part 1, 162 p. - Part 2, 165 p.

MINERALOGICAL SPECIFIC FEATURES OF ALTERED KIMBERLITES

Zinchuk N.N.

West-Yakutian Scientific Centre of the Sakha Republic (Yakutia) Academy of Sciences, Mirny, Russia
nnzinchuk@rambler.ru

Kimberlite new formations in our understanding are all minerals, having formed from thermal solutions, which mean not only postmagmatic juvenile ones, but also solutions generated both in the period of diatreme formation and at much later stages of their establishment. Quite often the border between primary and secondary minerals of kimberlites in a number of cases to some degree is provisional. Carried out by us investigations revealed that serpentine and carbonates are the basic secondary minerals of kimberlites, of which these rocks are mostly composed. All other minerals, generated at various stages of kimberlite pipes' formation, should be referred to subordinate ones. During complex investigation of kimberlite rocks of the Siberian, African, East-European and other platforms of the world we identified and studied: silicates (serpentine, phlogopite, chlorite, vermiculite, talk, montmorillonite, saponite, sepiolite, thaumasite), carbonates (calcite, dolomite, aragonite, pyroaurite, shortite, strontianite, magnesite, hydromagnesite, hantite), oxides and hydroxides (magnetite, hematite, goethite, amakinite, quartz, chalcedony, brucite), sulphides (pyrite, sphalerite, galenite, millerite, pyrrhotite, pentlandite, chalcopyrite, tochilinite), sulphates (gypsum, andradite, celestine, barite, epsomite, metabasaluminite, brochantite), halogenides (halite), phosphates (francolite), borates (yekaterinite, ferroszaibelyite) and bitumens. Basing on the morphology study of identified minerals, physical properties and chemical composition analysis of their formation conditions was given. In spite of irregular in whole distribution of secondary minerals row (both by lateral and vertical of the pipes), some regularities in their allocation are defined, that is possibility of certain zones' revelation arises. This zonality emerged mainly as a result of postmagmatic transformation of initial rocks and is the product of mineral-formation processes, which could be not synchronous in time and occurred in various physical-chemical conditions, as a result of which much later stages of secondary mineral formation superimposed on occurrence of much earlier ones. Accessible for research part of kimberlite pipes underwent repeated alterations during the process of its formation. Depending on certain conditions of mineral formation regularities of secondary minerals distribution at various stages of pipes' formation were different and were defined by several factors. *In geological structure of kimberlite pipes* inherited zonality can be defined, emerged in the process of diatremes establishment. Heterogeneity of kimberlites proper generates zonality, conditioned by various degree of initial material reprocessing. Thus, much deeper alterations of rock-forming minerals than in dense rocks take place in kimberlite breccias, and on the sites infilled by breccias processes of hypergene transformation occur more intensively. *Composition of kimberlites* is also of important significance because pipes are infilled by various rocks. Investigation of deep levels of pipes Mir, Udachnaya, Sytykanskaya, Yubileynaya and others indicates that with depth other (non-kimberlite) rocks originate without any regularity. Enrichment of near-contact parts by xenoliths of country rocks (especially in upper levels of bodies) may be considered as general regularity in infilling pipes. Consequently, mineral composition of kimberlites, their structural and textural specific features define the course of secondary alterations to exogenous ones inclusively in many respects. Alternation of various rocks of a pipe to

depth is the cause of secondary zonality origination, in the first place, in distribution of silicate minerals. Influence of *country rocks composition* on kimberlite zonality occurs, on one part, in enrichment of kimberlite magma by xenoliths, which are more available in near-contact sites of upper levels, on the other part – in supply of fissure solutions into kimberlites. Influence of xenoliths of terrigenous-carbonate and carbonate rocks is reflected on specific features of kimberlites in various ways. Xenoliths of silicate rocks define stability in relation to the processes of secondary kimberlite alteration, while carbonate rocks usually contribute to intensive transformation of latter ones, in particular to dissolution. Since carbonate and terrigenous-carbonate sediments most often are hosting sedimentary rocks of Phanerozoic, edge parts of pipes are not less susceptible to leaching processes than kimberlite. Soluble salts, being part of country rocks composition, and which redeposit in kimberlites, significantly effect the formation of secondary mineralization. Water, carbonic acid, petroleum bitumens and methane also go out from country rocks. *Hydrodynamic and climatic conditions of kimberlite magmatism development regions* greatly effect generation of secondary formations. Since the size of pipes is usually not large, their hydrodynamic conditions are close to those which are typical of hosting sedimentary rocks. Influence of fissure waters exhibit not only in near-surface conditions but in depth as well. *Permafrost* greatly influences hydrodynamic conditions in pipes of the northern part of the Siberian platform. Cryosolic weathering is mainly limited by physical transformation of rocks and deposition of soluble compounds in upper parts of pipes, which unfreeze in summer. Permafrost serves as a screen, below which alteration of kimberlites takes place. That is why this process obviously should be referred to weathering. As opposed to usual weathering, processes in the frozen part of the section run in rehabilitation environment out of direct dependence on climatic conditions. Degree of deep emanation penetration exerts sufficient effect on alteration of kimberlites, as deep gas emanations not only cause stagnant fissure waters to move but impact chemical transformation of rocks as well. Water solutions heat at this, which increases their reactivity. Gases, being under pressure, dissolve in water with formation of acids. Rock-forming minerals of ultrabasic magma (olivine, pyroxenes, micas, etc.) had time to alter in fine debris in the process of explosion and ejection of magma, and large blocks suffered only partial alterations which continued into postmagmatic stage of diatremes formation. High-temperature, hydrothermal metasomatism was going on, in the process of which basic silicates were replaced predominantly by serpentine and chlorite. Further alteration of rocks occurred while they were cooling. At average and low temperatures initial silicates area replaced. In these conditions garnets and micas are stable silicates. At average temperatures sulphides, quartz, strontium and barium sulphates, magnetite, abundant calcite isolations are generated. Thus, in the result of complex investigation of secondary minerals and their associations new data were received on conditions of their formation and regularities of distribution in kimberlite pipes. Processes of secondary mineral formation took place in a large interval of temperatures and caused by their decline alteration of medium reaction from alkaline to acidic with subsequent neutralization, which was fixed in forms of dissolution, final growth and emergence of new generations of minerals. Deep emanations and vadose thermal solutions took part at hydrothermal stage of mineral formation. Formation of kimberlites at different stages not everywhere occurred identically. In the process of serpentinization of large masses fluids were poor in carbonic acid and rich in water. Even less carbonic acid was contained in solutions from which brucite was forming. The process of mass brucitization did not coincide with general serpentinization in spatial relation and in time. Leaching of carbonates and magnesia silicates was most intensive in upper apical parts of pipes. The reason of this is in strong watering of these parts, as well as in solution

composition of carbonic, hydrosulphuric, and may be more strong acids and their salts (halite), caused by temperature decline. Rock leaching process in upper parts of bodies took place in rehabilitation conditions and completed in oxidizing ones. The whole course of secondary mineral formation is in general characterized by sharp oxidizing conditions and increased hydrosulphuric contamination. Most of secondary processes took place in rehabilitation or neutral in relation to iron (and even to sulfur) medium.

SPECIFIC FEATURES OF ORE-MAGMATIC KIMBERLITE SYSTEMS IN CONNECTION WITH DIAMOND-PROSPECTING WORKS

Zinchuk N.N.

West-Yakutian Scientific Centre of the Sakha Republic (Yakutia) Academy of Sciences, Mirny, Russia
nnzinchuk@rambler.ru

Kimberlite rocks, infilling diatremes, veins and sills, are known on all ancient platforms of the World, but in most detail they have been studied on the Siberian, African, East-European, Chinese, Australian and North-American platforms. Complex research of specific features of geological structure and development of the Siberian platform, material composition, facial features, formation conditions of ancient sedimentary thick layers and distribution of kimberlite minerals in them made it possible to carry out mineragenetic zonation of territories and basing on it to determine the lines and methods of diamond-prospecting works, and in the first turn within developed by diamond-mining industry areas of Central-Siberian diamondiferous sub-province, covering Daldyn-Alakit, Malo-Botuobinsky, Markoka and Sredne-Markhinsky diamondiferous regions, the greater part of diamond raw material reserves being in the first two at this. *Daldyn-Alakit* diamondiferous region is one of the main regions of "ALROSA" OJSC diamond mining, since the basic part of diamond reserves on the Siberian platform is concentrated here. That is why compensation of mineral-raw material base is a paramount task for operating in this region mining and processing complexes. Stock gain of diamonds in the considered region is related only with discovery of new primary diamond deposits mainly in its south-western part, within *Alakit-Markhinsky* kimberlite field, where terrigenous sediments of Upper Paleozoic are widely developed, intruded by tabular bodies of dolerites, since due to insignificant erosion cut of kimberlites Upper Paleozoic placers of diamonds were not formed here. At the same time, kimberlite-hosting rocks of Lower Paleozoic outcrop to modern surface in its north-eastern part (*Daldyn* kimberlite field), and carried out in such simple geological situation complex of structural-tectonic, heavy concentrate mineralogical and geophysical prospecting methods promoted discovery of all kimberlite pipes, including large diamond deposits Udachnaya and Zarnitsa. In the sequel discovery of only small in size nonmagnetic and poorly diamondiferous kimberlite pipes and dykes of no practical interest is possible here. Diamond finds in sand-pebble levels (mainly of continental facies of Upper Paleozoic formations), with accessory minerals of predominantly good integrity and poor grain-size sorting, which differ from those related to known here kimberlite bodies, are direct indication of possible discovery of high-diamondiferous kimberlite pipes within Alakit-Markhinsky field. This possibility is strengthened by the presence of about sixty kimberlite pipes within this field. Five of these pipes are diamond deposits (Aykhal, Komsomolskaya, Krasnopresnenskaya, Sytykanskaya and Yubileynaya). Various state of exploration of Alakit-Markhinsky kimberlite field territory should be noted at this. Insufficient state of exploration is typical of its south-western and western parts. Central part of the field is most explored, though there are sites here (in the region of local dispersion haloes of diamond associated minerals) with irregular prospecting grid of boreholes where skipping of even average in size kimberlite diatremes of complicated configuration are

possible. In connection with this it should be emphasized that south-western and western wings of this field are a transition zone to the territory of *Markoka* kimberlite field with the only so far kimberlite pipe Markoka (it is already in north-western part of Markoka diamondiferous region). In whole all this territory is prospective on discovery of kimberlite pipes, since it is within Daldyn-Oleneksky kimberlite-controlling fault zone, to which a whole number of kimberlite fields gravitate (Alakit-Markhinsky, Daldyn, Verkhne-Munsky, Chomurdakhsky, West- and East-Ukukitsky, Ogoner-Yuryakhsky, Merchimdensky, Toluopsky, Kuoysky and other fields), and in Upper Paleozoic sediments finds of diamonds and dispersion haloes of their paragenetic associated minerals (AMD) were discovered. The fact of only one kimberlite pipe occurrence in Markoka field also enhances the forecast to some degree. In terms of this it follows that central part of Alakit-Markhinsky field needs additional prospecting of sites with not completely studied high-contrast local dispersion haloes of kimberlite minerals aiming realization of residual prospects of its primary diamondiferousness. At the same time it is necessary to carry out prospecting works in south-western and western parts of this field, including the region of pipe Markoka (within the areas of dispersion halo development of AMD, in the zone of Daldyn-Olenekskaya system faults and where summarized thicknesses of Upper Paleozoic sediments and traps do not exceed 200m), with the goal of finding diamondiferous kimberlite pipes. Within the rest of Markokinsky diamondiferous region middle course basin of r. Ygyatta is most prospective on discovery of diamondiferous kimberlite pipes. Here haloes (Ozerny and others) of dispersion of increased pyrope and picroilmenite concentrations, often with magmatogene new surface, were established in Upper Paleozoic sediments, together with finds of diamonds. These haloes are located in the zone of kimberlite-controlling faults of Vilyuy-Markha system, to which Mirny and Nakyn kimberlite fields are confined. In connection with this it should be noted that the said area of fault zone in the basin of r. Ygyatta middle course, where AMD dispersion haloes and finds of diamonds proper were established in Upper Paleozoic sediments, deserves being prospected with the goal of finding primary sources of diamond. Diamonds found there differ from those of Malo-Botuobinsky and Daldyn-Alakit regions by a complex of indications. All these together testify about real perspectives of discovering here a new diamondiferous kimberlite field, and coarse proluvium-alluvial facies of basal levels of Upper Paleozoic sediments may contain placers of diamonds. *Malo-Botuobinsky region*, where kimberlite pipes Mir, Sputnik, International, Dachnaya, Amakinskaya and Tayezhnaya were discovered, is an important region of diamond mining. However for compensation of decreasing diamond resources it is necessary to discover here new primary and placer deposits, because available reserve deposits are characterized by limited resources. Analysis of established mineralogical indications, structural-tectonic and lithology-facial premises of prospecting forecasting, as well as degree of prospecting, testifies about possibility of finding diamondiferous kimberlite pipes in this region. Thus, its central part (Mirny kimberlite field) is most studied. However it is possible to discover here nonmagnetic and small in size diamondiferous kimberlite bodies within distinguished and still not completely studied local perspective sites gravitating to fault zones of Vilyuy-Markha system. On the rest (basic) north-western and north-eastern parts of the region, where sedimentary deposits of Upper Paleozoic are well developed, diamond-prospecting works of different detail were carried out. So far kimberlite pipes have not been found here. At the same time, in sediments of Lapchanskaya (P_1l), Botuobinskaya (P_1b) and Borulloyskaya (P_2br) suites two spacious mineralogical fields (*Kuelyakhsky* and *Bakhchinsky*) were established, stretching from Mirny kimberlite field in north-western and north-eastern directions, correspondingly, with haloes of mixed (continental and basin) type and with poorly sorted dia-

mond-pyrope-picroilmenite association of these minerals. These haloes are characterized by high concentrations of AMD (to several thousand grains per 10 l heavy concentrate sample), which have traces of mechanical wear and availability of up to 2 mm size grains (with relicts of kelyphite rims on some grains of pyrope) is noted. Besides, finds of diamonds are noted in these haloes, and in *Kuelyakhsky* mineralogical field two placers were registered (Eastern and Western) and Sylaginsky placer occurrence of diamonds. Detailed and complex investigation of physiographic, morphological and chemical specific features of these kimberlite minerals indicated that their basic quantity has similarity with those from high-diamondiferous pipes of Mirny field (pipes Mir and International) and suffered significant wear due to repeated rewashing and redeposition in Pre-Late Paleozoic time, and smaller part is characterized by distinct from them indications. To the west of placer Zapadnaya picroilmenite association of minerals of relatively good integrity was established and it is assumed that the minerals originated from an unknown kimberlite body located in western part of Verkhne-Irelyakhsky heave. Similar contrast haloes were also registered in rudaceous sediments of Botuobinskaya and Borulloyskaya suites within *Bakhchinsky* mineralogical field (haloes Dalberginsky and Medvezhiy), where shallow paleohollow is infilled within the fault zone of Vilyuy-Markha system. It is in the region of these haloes that local primary sources of these minerals are supposed to be. Considering insufficient degree of site prospecting of the three specified haloes it is necessary to additionally explore them with the goal of finding own diamondiferous kimberlite pipes here. In connection with this it should be also noted that diamond reserve increment is possible at the expense of revealing new Upper Paleozoic placers within development areas of high-contrast AMD dispersion haloes of Kuelyakhsky mineralogical field, though with complicated structure of productive stratum and at significant thickness (to 80 m) of overburden. Occurrence of diamondiferousness of southern, south-western edges of Tungusskaya syneclise (*Chuno-Biryusinsky, Muro-Kovinsky, Ilimo-Katangsky, Nizhne-Tungussky* and *Tychansky* diamondiferous regions), as well as north-eastern part of the Siberian platform (southern edge of Lena-Anabar and western – of Predverkhoyansky saggings and region of Kyutyungdinsky trough) should be assessed in some other way. Here finds of single spark diamonds and their associated minerals (mainly pyropes, seldom chrome-spinellids and picroilmenites), characterized by high degree of wear (to balls, especially pyropes), have been established in terrigenous sediments (predominantly of basin Carboniferous and Permian sediments). On individual sites concentration of such worn-out pyropes and chrome-spinellids reaches tens, sometimes hundreds of grains per heavy concentrate sample of 30 l volume. Degree of exploration of listed regions is different but insufficient in whole. Analysis of all available material on them testifies about expediency of carrying out here at present full scale prospecting works, because it leads only to mapping of dispersion haloes of rather worn-out and repeatedly redeposited and cut off from primary sources of kimberlite minerals in basin sediments. At this stage of prospecting complex analysis of all available material should be performed and probable areas of washdown be determined, which later should be prospected by applied modern complex of methods depending on geologic-landscape conditions. In the first turn similar works should be done in the region of Kyutyungdinsky trough and Tychansky diamondiferous region, where diamonds of predominantly octahedral habit, usually typical of rich kimberlite pipes, were established. In connection with this broad development of basin, mainly fine-grain facies should be noted. Formation of these facies is conditioned by general sinking of the territory at basin ingression in the central part of Tungusskaya syneclise.

LOW-TEMPERATURE ZR-REE-Y-NB-TH MINERALIZATION FROM EL'OZERO DEPOSIT, KOLA PENINSULA, NW RUSSIA

Zozulya D.[1], Macdonald R.[2], Bagiński B.[2], Lyalina L.[1], Kartashov P.[3], Dzierżanowski P.[2]

1 Geological Institute, Kola Science Centre, Russian Academy of Sciences, Apatity, Russia
2 Institute of Geochemistry, Mineralogy and Petrology, University of Warsaw, Warsaw, Poland
3 Institute of Ore Deposits, Russian Academy of Sciences, Moscow, Russia
zozulya@geoksc.apatity.ru

The El'ozero rare metal deposit is confined to a linear tectonic zone at the contact between the Keivy terrane and Central Kola composite terrane, in the NE Fennoscandian shield. The zone strikes in a SE-NW direction for ca. 12 km and has an outcrop width varying from 200 to 1500 m. A few hundred peralkaline A-type granite and aplite veins are confined to this zone and are concordant with the faults. The length of the veins is 50-500 m, with thicknesses of 3-50 m. The granites, whose age is 2.65-2.67 Ga [1], intruded and metasomatically altered a range of rocks in the Keivy complex, namely, gabbro-anorthosites, gabbro-amphibolites and gneisses. All the rocks of the terranes were metamorphosed during Svekofenian regional metamorphism at 1.7-1.8 Ga.

The granite veins were altered autometasomatically and are represented by two types. The first type, intruded into amphibole-biotite gneiss, has the mineral association biotite-magnetite, aegirine-biotite-magnetite and aegirine-arfvedsonite. Rare-metal mineralization related to this type is represented by small irregular linear bodies 0.2-0.5 m thick and comprises zircon-allanite-titanite-magnetite assemblages. The second type intrudes gabbro and amphibolites and shows albite-amazonite and magnetite-amazonite associations. The related mineralization is confined to lenses and oval and linear bodies of 0.1-2 m thickness and is represented mainly by zircon. Both types of mineralization in the granites are accompanied by minor monazite, thorite, fergusonite-(Y), chevkinite-(Ce), and accessory yttrialite-(Y), thalenite-(Y), gadolinite-(Y) and danalite. Rare-metal mineralization in the granites formed during albitisation (zircon-allanite-monazite association) and later silicification (fergusonite-yttrialite-thalenite-gadolinite association). Fluorite is common in all types of mineralized granite veins; it is most abundant in contact zones of the veins. Our study sample of autometasomatic rock of quartz-albite-zircon composition was taken from a granite vein. The zircon has features of a hydrothermal genesis (numerous mineral and fluid inclusion and pores (lightest in BSE)) and later (metamorphic?) recrystallization (darker patches in BSE images).

Metasomatic alteration of gabbro-anorthosite due to intrusion of the granite veins ranges from unaltered rocks to more intensively altered types as follows; massive gabbro-anorthosite – plagioamphibolite – amphibole-biotite metasomatite – mineralized garnet-biotite metasomatite – mineralized biotite-albite metasomatite with quartz – (epidotic metasomatite). Rare-metal mineralization is confined to small linear and lensoid bodies, nodules and pods 0.5-2 m in size. The study sample was taken from a small, oval (0.2 x 0.5 m), heavily mineralized pod in a basic metasomatite. The rock is characterized by extremely high REE (85000 ppm), Y (42000 ppm), Nb (62000 ppm), Zr (67000 ppm), Th (17000 ppm). Rare-metal mineralization is repre-

sented by thorite, chevkinite-(Ce), ferriallanite-(Ce) and allanite-(Ce), zircon, monazite, fergusonite-(Y), samarskite-(Y), aeschynite-(Y), pyrochlore, Nb-bearing titanite and rutile, ilmenite, magnetite, cassiterite, REE-carbonates, uraninite and gadolinite-group minerals. It is assumed that rare-metal minerals crystallized under medium- to low-temperature conditions as the earliest rare-metal mineral phase - zircon - is of hydrothermal genesis (porous, numerous mineral inclusions, high content of Y, REE, Hf, as shown in Fig. 1). Moreover chevkinite-(Ce) and samarskite-(Y) also underwent extensive alteration (Figure 2).

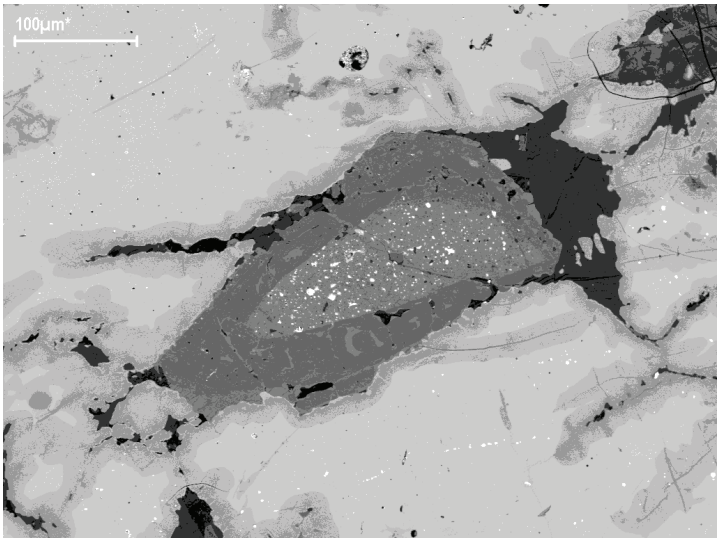

Figure 1: Zircon (centred) with porous core (bright white inclusions are thorite and galena) and uniform rim in a matrix of Y, Nb, Ti oxides (sample is from apobasic metasomatite).

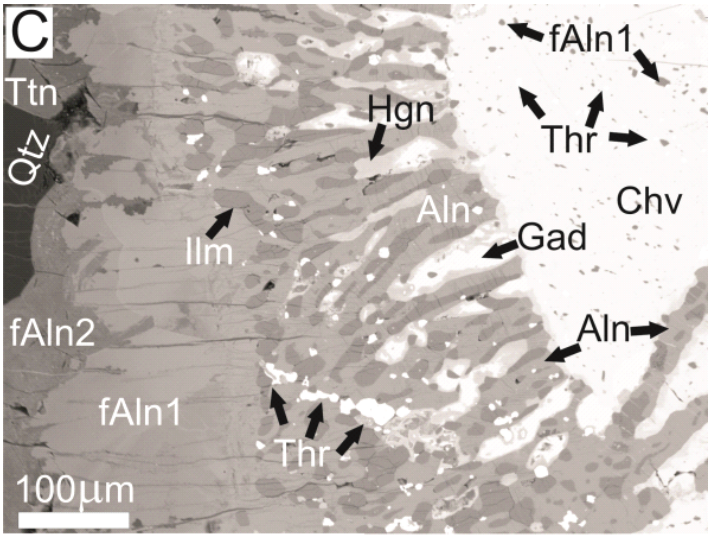

Figure 2: Chevkinite-(Ce) (brightest phase in top right corner) and its alteration products in apobasic metasomatite.

The sequence of events involving the major and minor rare-metal minerals is: (1) crystallization of chevkinite-(Ce) and included thorite and zircon; (2) fluid-driven replacement of chevkinite-(Ce) by ferriallanite-(Ce), alteration of large zircon, with formation of some thorite, uraninite and Nb,Ti oxides; (3) patchy replacement of ferriallanite by ilmenite + titanite ± magnetite, further growth of thorite; (4) formation of fingers of gadolinite in ferriallanite zone, followed by hingganite and thorite; (5) ferriallanite-(Ce) zone mantled by allanite-(Ce) zone containing samarskite; (6) all zones cut by veins (and rarer patches) of quartz and REE-carbonate; (7) possible recrystallization (refinement) of zircon during later metamorphism.

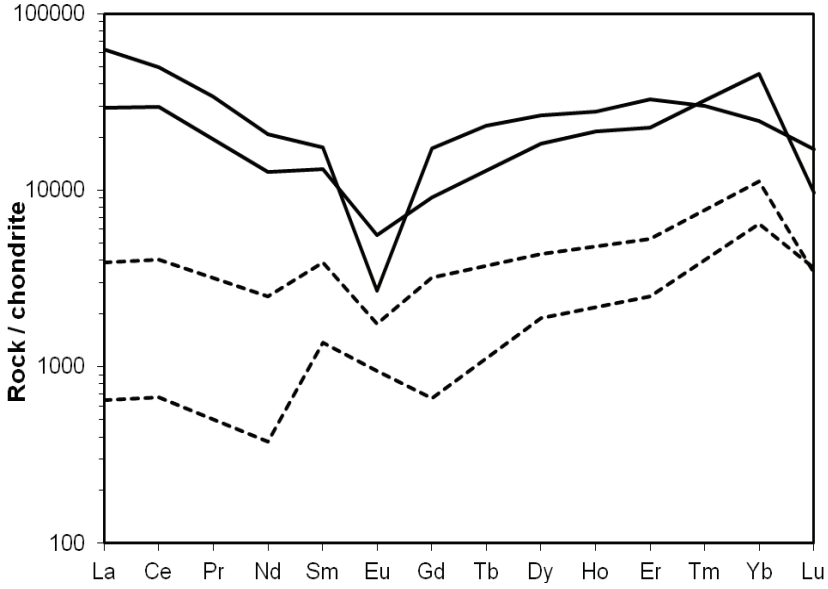

Figure 3: Chondrite-normalized REE patterns for different metasomatic rock of the El'ozero deposit (solid line - apobasic metasomatite; dotted line – autometasomatic mineralized granite vein).

Chondrite-normalized REE patterns for the different metasomatic rocks of the El'ozero deposit strictly confirm their major rare-metal mineral specialization (chevkinite-allanite-zircon-fergusonite type in basic metasomatites and mainly zircon type in mineralized granite vein) (Fig. 3). The REE patterns for some metasomatite samples are of V-shape form, which is a characteristic of hydrothermal alteration.

It is inferred that the metasomatic fluid was alkaline and fluorine-rich for the autometasomatic mineralized granite veins and of alkaline-fluorine (?)-carbonate composition for basic metasomatites.

The study is supported by the Earth Science department of Russian Academy of Sciences (Program 9).

References:

1. Zozulya D.R., Bayanova T.B., Eby G.N., 2005. Geology and age of the Late Archean Keivy alkaline province, Northeastern Baltic Shield. Journal of Geology, v. 113, p. 601-608.

SPONSORS AND SUPPORTERS

for

the 30thInternational Conference on "Ore Potential of Alkaline, Kimberlite and Carbonatite Magmatism

30th International Conference on "Ore Potential of Alkaline, Kimberlite and Carbonatite Magmatism"

Alkaline, Kimberlite and Carbonatite Magmatism"

ABSTRACT BOOK